Apoptosis in haematopoietic progenitors

Sophia Catherine Rossouw

(RSSSOP001)

Submitted to the University of Cape Town
In fulfilment of the requirements for the degree of
Master of Science in Medicine
in the Department of Clinical Laboratory Sciences
Faculty of Health Sciences

October 2009

For my mother, my ever fixed mark
and the strongest person I know

TABLE OF CONTENTS

PREFACE

This research project was supervised by Dr Karen Shires of the division of Haematology in the Department of Clinical Laboratory Sciences at the University of Cape Town. It is hereby declared that this thesis, submitted for the degree of Master of Science in Medicine, is the result of my own investigation, except where the work of others are acknowledged.

DECLARATION

I, Sophia Catherine Rossouw, hereby declare that the work on which this dissertation is based is my original work (except where acknowledgements indicate otherwise) and that neither the whole work nor any part of it has been, is being, or is to be submitted for another degree in this or any other university. I have used the American Psychological Association (APA) referencing system.

Signature: ……

Date: …….

ACKNOWLEDGEMENTS

I would like to thank Prof. Sturrock's lab (Division of Medical Biochemistry at UCT) for the use of their Cary Eclipse fluorimeter and advice on the caspase activity assays. I would also like to thank the Cardiovascular Research Unit (MRC/UCT Cape Heart Centre) for the use of their microscope. And especially Melanie Black for her assistance and advice on cell staining procedures and using the microscope. I am also grateful to Marcia Watkins and the Division of Clinical Immunology (at UCT) for their generous donation of the Jurkat cell line, without which I would not have been able to complete this project. I would also like to thank Prof. Jacquie Greenberg for her time spent advising me and overseeing the post-examination corrections required on this thesis. I really struggled financially throughout this project and I would like to thank the Postgraduate funding office at UCT for their service and financial assistance, without which I would not have been able to complete my studies. I am also very grateful to Prof. Uliana at the Fees Office (UCT) for his assistance and tuition fees relief for 2009.

LIST OF ABBREVIATIONS

% (v/v)	Percentage volume solute per 100 ml
% (w/v)	Percentage gram(s) solute per 100 ml
% (w/w)	Percentage gram(s) solute per 100 grams
β	Beta
µg	Microgram
µl	Microlitre
µM	Micro-Molar
°C	Degrees Celsius
AMC	7-Amino-4-methylcoumarin
ANT	Adenine nucleotide transporter
Apaf-1	Apoptotic protease activating factor-1
APS	Ammonium Persulphate
ASK1	Apoptosis-signal-regulating kinase
ATF4	Activating transcription factor 4
ATF6	Activating transcription factor 6
AV	Annexin V
Bcl-2	B-cell lymphoma-2
BFA	Brefeldin A
Bip	Immunoglobulin heavy chain-binding protein
bp	Base pair (s)
BSA	Bovine serum albumin
CARD	Caspase recruitment domains
CHAPS	3- ((3-cholamidopropyl) dimethylammonio)-1-propane sulfonate
CHOP	CEBP homologous protein
CO_2	Carbon dioxide
CypD	Cyclophilin D
Da	Dalton
DD	Death domain
DED	Death effector domains
dH_2O	Distilled water
ddH_2O	Double distilled water
DIABLO	Direct IAP-binding protein with low pI
DISC	Death-inducing signalling complex
DMSO	Dimethylsulphoxide
DNA	Deoxyribonucleic acid
DTT	Dithiothreitol
EDTA	Ethylenediamine-tetra-acetic acid
eIF2	Eukaryotic initiation factor 2
ER	Endoplasmic recticulum
ERSE	ER stress response element

FADD	Fas-associated death domain protein
FasL	Fas ligand
FBS	Foetal bovine serum
Fig(s).	Figure(s)
FITC	Fluorescein isothiocyanate
FLIPs	FADD-like interleukin-1 β-converting enzyme inhibitory proteins
GADD153	Growth arrest- and DNA-damage-inducible gene 153 (CHOP)
GRP	Glucose-regulated protein
GRP78	Glucose-regulated protein 78
HEPES	N-(2-hydroxyethyl)piperazine-N'- (2-ethanesulfonic acid)
hr(s)	Hour(s)
H_2O	Water
H_2O_2	Hydrogen peroxide
HCl	Hydrochloric acid
IAPs	Inhibitor of apoptosis proteins
IMDM	Iscoves Modified Dulbecco Medium
IRE1	Inositol-requiring enzyme 1
JAB1	Jun activation domain-binding protein 1
JIK	c-Jun N-terminal inhibitory kinase
JNK	c-Jun N-terminal kinase
KCl	Potassium Chloride
kDa	Kilo Dalton
KH_2PO_4	Potassium dihydrogen phosphate
L	Litre
MDS	Myelodysplastic syndromes
$MgCl_2$	Magnesium chloride
MGG	May-Grünwald-Giemsa
min	Minute(s)
ml	Millilitre
mM	Milli-Molar
ms	Milli-second
MTP	Mitochondrial transmembrane potential
MW	Molecular weight
Na	Sodium
NaCl	Sodium chloride
Na_2HPO_4	Di-sodium hydrogen phosphate
NaOH	Sodium hydroxide
nm	Nanometre(s)
nM	Nano-Molar
O/N	Over night
PAGE	Polyacrylamide gel electrophoresis

PBR	Peripheral benzodiazepine receptor
PBS	Phosphate-buffered Saline
PE	Phycoerythrin
PERK	Pancreatic eIF2 ER protein kinase
pH	Hydrogen ion concentration
PI	Propidium iodide
PIPES	1,4-piperazinediethanesulfonic acid
PMSF	Phenylmethylsulphonyl fluoride
POD	Peroxidase
PP1	Protein phosphatase 1
PVDF	Polyvinylidene difluoride
RFUs	Relative Fluorescence Units
RIPA buffer	Radioimmunoprecipitation buffer
ROS	Reactive oxygen species
RPM	Revolutions per minute
RPMI 1640	Roswell Memorial Park Institute culture medium
s	Second(s)
SAB	Sample Application Buffer
SDS	Sodium dodecyl sulphate
sFasL	soluble FasL
Smac	Second mitochondria-derived activator of caspases
TBS	Tris buffered saline
TBST	Tris buffered saline with Tween-20
TEM	Transmission electron microscopy
Tris	2-Amino-2-(hydroxylmethyl)-1,3-propanediol
TNF	Tumor necrosis factor
TNFR	Tumor necrosis factor receptor
TRAF2	Tumour-necrosis-factor receptor-associated factor 2 protein
U	Enzymatic units
UPR	Unfolded protein response
UV	Ultraviolet light
V	Volt(s)
VDAC	Voltage dependant anion channel
XBP1	X box-binding protein 1

LIST OF FIGURES

LIST OF TABLES

ABSTRACT

This study has investigated three caspase-dependent apoptotic pathways using HL60 and Jurkat cells as haematopoietic models. The three apoptotic pathways studied were the Fas death receptor pathway, the mitochondrial-mediated apoptosis pathway and the endoplasmic reticulum (ER)-stress induced apoptosis pathway. These pathways were induced in the cells via pathway-specific drug treatment.

The first part of the study involved obtaining and testing for markers specific to each pathway (after pathway-specific drug treatment). HL60 cells were treated with Brefeldin A (BFA), to induce the ER-stress induced apoptotic pathway, and hydrogen peroxide (H_2O_2), to induce the mitochondrial-mediated apoptotic pathway. Jurkat cells were treated with FLAG-tagged FasL and ANTI-FLAG® antibody to induce the death receptor pathway. The assays used to analyse the pathway-specific markers were optimised to ensure that each technique was sensitive and reproducible. In addition, the drug concentrations required to induce a low (5-15%) and high (20-50%) percentage of early apoptosis were established for each pathway. In the final part of this study, these drug concentrations were used to induce apoptosis in the cells, which were subsequently tested for all the pathway-specific markers.

It was found that the flow cytometry assays were sensitive to detect changes within the cells. Both Annexin V-FITC (AV)-propidium iodide (PI) labelling and MitoCapture™ assays could be used to determine the apoptotic status (early or late) of the cells. There was evidence of changes in mitochondrial transmembrane potential (MTP) for all three drug treatments. Therefore it was concluded that the mitochondrial-mediated apoptotic pathway was activated, to some extent, in all three pathways. The western blot assays were not as sensitive as desired, since a large amount of protein and volume of cells were required. In addition, it was not quantitatively reproducible in all instances. The caspase assays were sensitive and appeared to be reproducible, however, the assay seemed to be sensitive to sample reagents like H_2O_2, which affected readings. The caspases appeared to be specifically activated for each pathway and caspase activity was generally elevated at the higher drug concentrations for all three pathways.

The results suggested that the Fas death receptor and ER-stress induced apoptosis pathways interact, to some extent, with the mitochondrial-mediated apoptosis pathway. Hence, the mitochondria seem to play central roles in amplifying and transmitting the death signal between apoptotic pathways.

CHAPTER ONE

LITERATURE REVIEW

1.1 General Introduction

Apoptosis is a strictly controlled, natural form of programmed cell death. It is an important regulatory process, which allows multicellular organisms to tightly control and maintain cell numbers and tissue size and to safeguard against dysfunctional and defective cells (Greenberg, 1998).

Apoptosis signalling pathways exist in inactive states in viable cells and are activated in response to apoptotic stimuli. Various amplification steps and positive feedback loops within the apoptosis signalling pathways ensure that a cell either completely commits to apoptosis or totally refrains from it (Hengartner, 2000). Apoptosis can be initiated by external stimuli such as ligation of cell surface receptors, cytokines, cytotoxic drugs, lack of survival signals, growth factor withdrawal and developmental death signals (Fig. 1). In addition, various internal signals such as DNA damage, the formation of reactive oxygen species (ROS) and defects in protein production can also initiate apoptosis (Fig. 1). Survival signals like growth factors, nutrients, and hormones continuously inhibit apoptosis by enhancing the activity and/or expression of anti-apoptotic regulatory molecules. In so doing it represses the activity of pro-apoptotic molecules (Hellström-Lindberg, 2005) (Fig. 1).

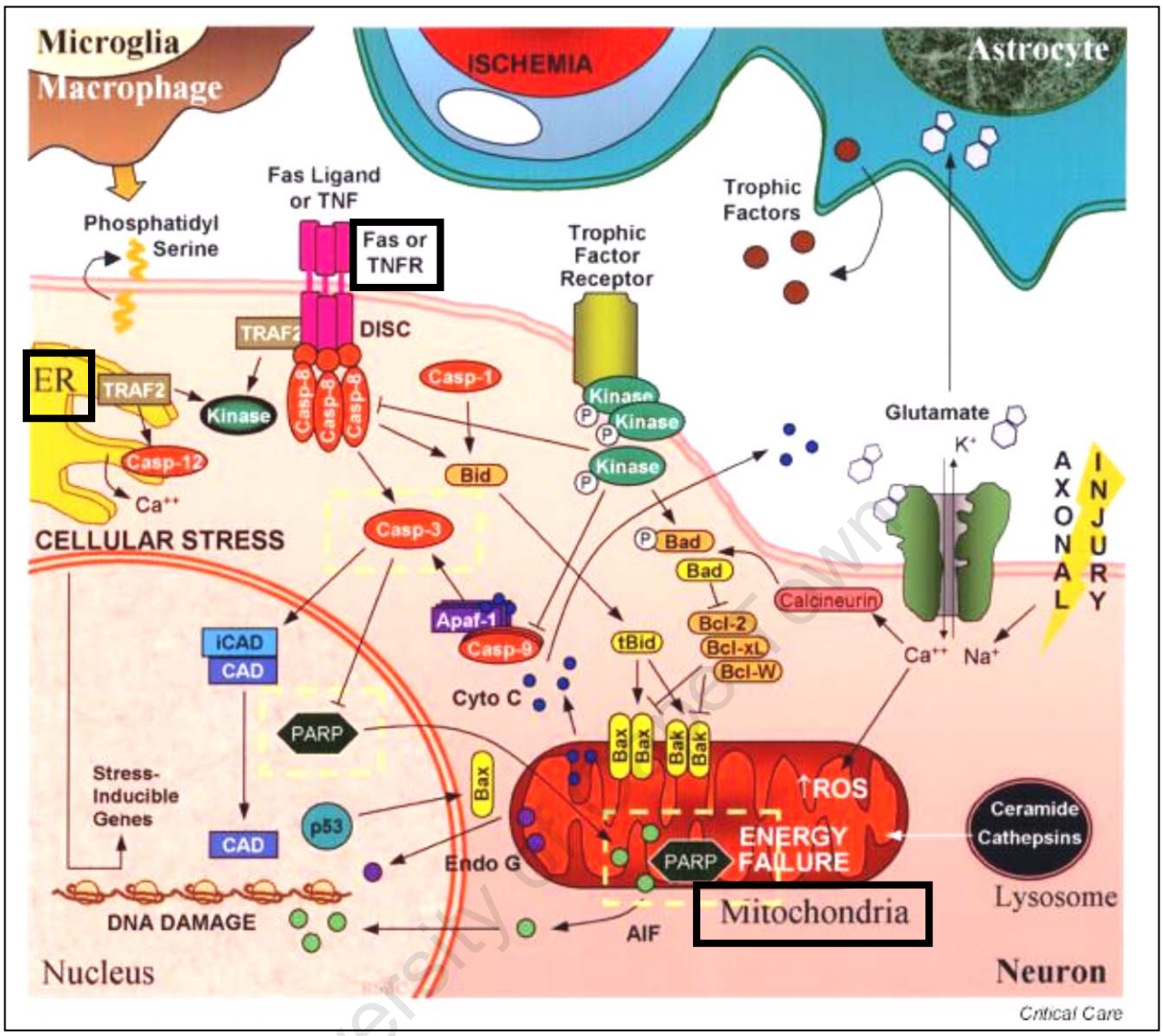

Fig. 1. Various apoptosis pathways within a nerve cell. The figure shows a schematic representation of the death receptor, mitochondrial-mediated and ER-stress induced apoptotic pathways, with the specific molecules and caspases activated for each pathway (modified from Zhang *et al*., 2005).

Apoptotic cells share morphological features, which include cell shrinkage and deformation, loss of contact to neighbouring or supportive structures, chromatin condensation and cell membrane blebbing or budding (Kerr *et al*., 1972). These changes occur as a result of proteolysis, by proteolytic enzymes known as caspases. Caspase activity affects the integrity of cellular organelles and the cytoplasm and induces DNA cleavage into oligonucleosomal pieces by nucleases (Zhang *et al*., 2005). In the final stages the cell ruptures and is compacted into membrane-bound apoptotic bodies, which contain cytoplasm, organelles and condensed chromatin. These apoptotic bodies are subsequently removed by macrophages without eliciting an inflammatory response. These features are in contrast to cells that undergo necrotic cell death, which is usually

caused by mechanical injury to the cells. Depending on the severity of damage suffered, the cell membrane either bursts upon impact or, after injury, the cell swells and eventually its membrane ruptures. Therefore necrotic cell death causes the uncontrollable leakage of cell contents into the extracellular environment. This, in turn, leads to the damage of neighbouring cells and an inflammatory response in the affected tissue (Gewies, 2003).

Defective apoptotic signalling, which either causes disproportionate cell proliferation or apoptosis, plays an important role in the pathogenesis of several diseases, including the myelodysplastic syndromes (MDS) (Hellström-Lindberg, 2005). MDS are a set of pre-leukaemic myeloid clonal haemopathies, characterized by a high incidence of intramedullary apoptosis. This brings about the symptoms of peripheral cytopenias, ineffective haematopoiesis and refractory anaemia observed in these disorders (Mundle, 2003). There are many controversies surrounding the incidence of both apoptosis and proliferation and the potential of clonogenic expansion in MDS (Parker *et al.,* 2000). The fundamental mechanisms that cause progenitor cell abnormalities are still poorly characterised (Tehranchi *et al.,* 2003). Multiple intrinsic and extrinsic factors influence the stem cells. These factors can cause increased apoptosis, abnormalities within the signalling pathways and changes in the bone marrow stroma and stromal cell cytokine production. How these factors contribute to bring about accelerated proliferation and accelerated apoptosis simultaneously still remains unclear (Liesveld *et al.,* 2004). Understanding apoptosis signalling in haematopoietic cells is fundamental in unravelling the underlying disease mechanisms of conditions like MDS and leukaemia.

The three caspase-dependent apoptosis pathways reviewed here are the death receptor pathway, in particular the Fas (CD95) apoptotic pathway, the endoplasmic reticulum (ER)-stress induced and mitochondrial-mediated apoptosis pathways (Fig. 1). The death receptor pathway forms part of the extrinsic apoptosis pathway, whereas the ER-stress induced and mitochondrial-mediated apoptosis pathways are part of the intrinsic cell death pathways (Bredesen *et al.*, 2006).

1.2 The role of caspases in caspase-dependent apoptosis

The set of cysteine proteases, known collectively as caspases, play a central role in the apoptosis signalling network, since they activate, execute and amplify the apoptotic signal (Thornberry *et al.*, 1997). Caspases are cysteine-dependent aspartate-specific proteases, which specifically cleave their substrates after aspartate residues (Alnemri *et al.*, 1996; Chowdhury *et al.*, 2008).

Caspase substrates are a tightly regulated set of protein targets, which are either activated or rendered inactive after cleavage. For example, by cleaving off a negative regulatory domain or inactivating a regulatory subunit on a substrate, the caspases can regulate the apoptosis signalling cascade (Hengartner, 2000). The caspases are responsible for cleaving many cellular proteins. Cleavage of cytoskeletal and structural proteins (like fodrin and gelsolin) causes cell shrinkage and deformation, whereas cleavage of nuclear lamins are essential for nuclear shrinking and budding (Rao *et al.*, 1996; Takahashi *et al.*, 1996). Other caspase substrates include transcription factors, protein kinases, proteins involved in the cell cycle and cell replication, as well as B-cell lymphoma-2 (Bcl-2) protein family members, like Bid (section 1.3.4) (Stroh and Schulze-Osthoff, 1998).

Caspases are synthesized intracellularly as inactive zymogens (procaspases) that possess three domains: an N-terminal prodomain and one large and one small subunit, the p20 and p10 domains, respectively (Fig. 2). The procaspases are activated by proteolytic cleavage between the large and small subunits, since all of the cleavage sites have aspartate residues, and the prodomain may or may not be removed in the process (Thornberry *et al.*, 1997). The active caspase is a hetero-tetramer consisting of two p20/p10 hetero-dimers, with two active sites (Nicholson and Thornberry, 1997) (Fig. 2).

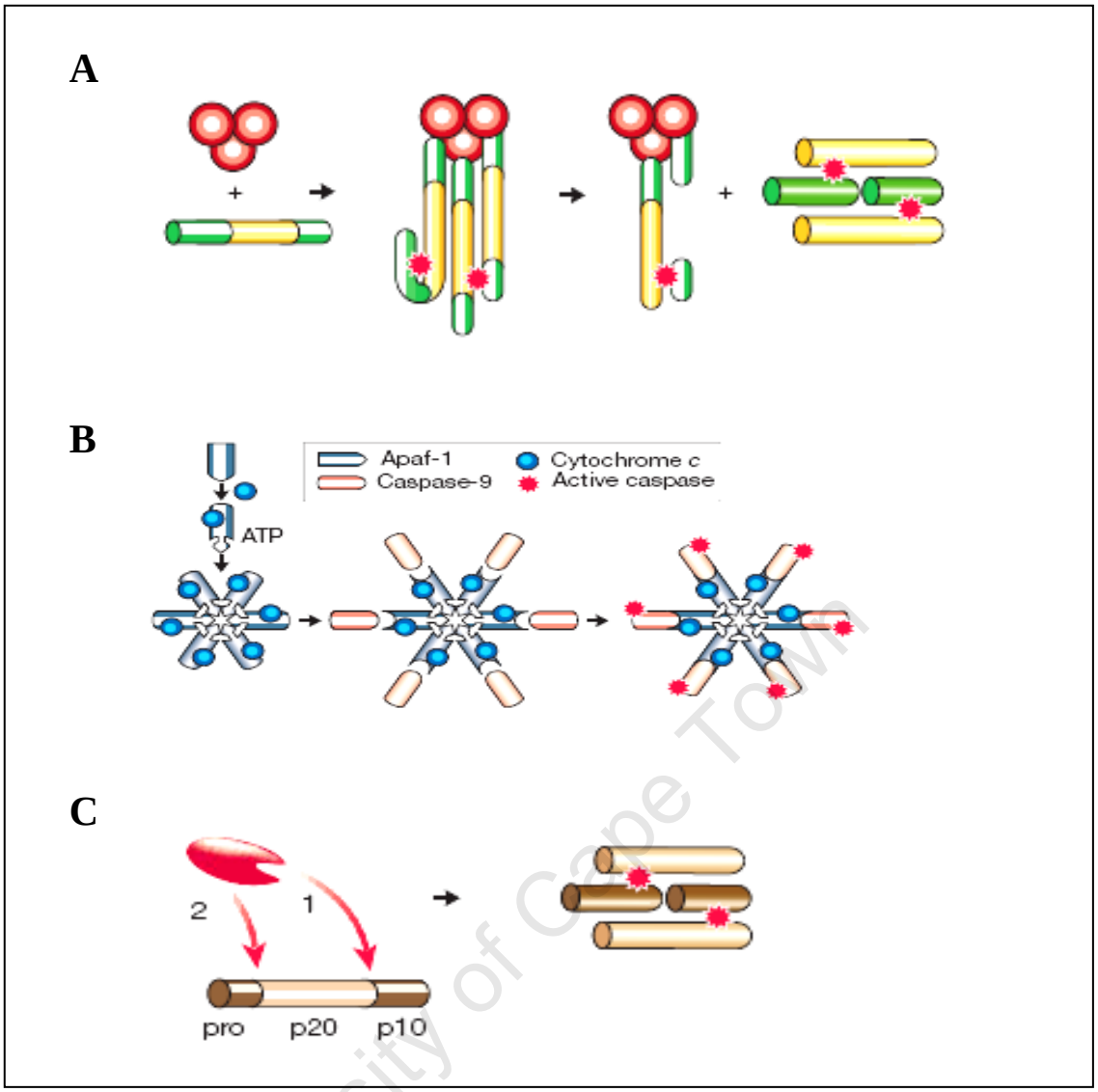

Fig. 2. Three mechanisms of caspase activation. Procaspases are activated by induced proximity (**A**), holoenzyme formation (**B**), and/or proteolytic cleavage by an upstream initiator caspase (**C**). Activated initiator caspases proteolytically cleave downstream effector procaspases to initiate a caspase cascade resulting in cell death. Initiator procaspases can be activated through recruitment by apoptosis inducing signalling complexes resulting in cross activation of caspases in close proximity or via holoenzyme formation like the apoptosome complex (modified from Hengartner, 2000).

The caspases can be divided into two groups. A group of initiator caspases that include caspase-2, -4, -12, -8, and -9 and a group of executioner or effector caspases that include caspase-3, -6 and -7 (Thornberry *et al.*, 1997). The initiator caspases possess long prodomains, containing death effector domains (DED) or caspase recruitment domains (CARD), whereas the executioner caspases possess short prodomains (Li, P *et al.*, 1997; Liu *et al.*, 2005). The initiator and effector caspases are activated via different mechanisms and so far three mechanisms of caspase activation have been elucidated (Fig. 2 A-C) (Hengartner, 2000).

Initiator procaspases can be activated through induced proximity by oligomerization, aided by adapter proteins, and subsequent recruitment to apoptosis inducing signalling complexes (such as the death-inducing signalling complex) (Budihardjo *et al*., 1999) (Fig. 2 A). The formation of holoenzyme complexes, such as the apoptosome complex, is another mechanism of initiator caspase activation (Fig. 2 B). These holoenzyme complexes recruit various molecules to facilitate in procaspase cleavage and activation (Rodriguez and Lazebnik, 1999; Stennicke *et al*., 1999). The activated initiator caspases, like caspase-4, -8 and -9, subsequently bring forth a downstream caspase cascade, by proteolytic cleavage, which leads to the activation of executioner caspases such as caspase-3 (Earnshaw *et al*., 1999).

The group of executioner caspases are generally activated through proteolytic cleavage by an upstream initiator caspase (Fig. 2 C) via a caspase cascade, which integrates and amplifies the apoptotic signals (Liu *et al.*, 2005). Executioner caspase activation occurs during the late stages of apoptosis and results in proteolysis. This affects the integrity of the cell's organelles and cytoplasm and leads to cellular breakdown and eventual cell lysis (Cohen, 1997).

1.3 The Fas death receptor apoptotic pathway

1.3.1 The Fas ligand (FasL)

FasL is a cytokine, which is primarily expressed in activated T lymphocytes and Natural Killer cells of the immune system (Suda *et al*., 1995; Oshimi *et al*., 1996). Expression of FasL during stressful conditions is dependent on activation of the MEKK1 and c-Jun N-terminal kinase (JNK) pathways, which results in binding of c-Jun and ATF2 to the promoter region of the FasL gene (Faris *et al.*, 1998).

FasL is synthesized as a membrane-bound protein, sharing a well conserved extracellular region of approximately 150 amino acids with the other members of the tumor necrosis factor (TNF) family (Suda *et al*., 1993). Although membrane-bound FasL is active in initiating apoptosis, a soluble trimeric form of FasL (sFasL) can be produced when membrane-bound FasL is proteolytically cleaved by a metalloproteinase

at its extracellular domain (section 1.6.3) (Kayagaki *et al*., 1995; Tanaka *et al*., 1996). This cleavage of FasL from its membrane was found to significantly decrease its activity in inducing apoptosis. It was also found that membrane-bound FasL was more active in inducing apoptosis than its soluble form (Suda *et al.*, 1997; Tanaka *et al*., 1998). This indicates that circulating cells, which express membrane-bound FasL, can interact with other cells and are therefore powerful inducers of apoptosis and systemic tissue damage. Schneider *et al*. (1998) found that although sFasL was less active, it still maintained its capacity to bind to Fas and its cytotoxicity could be restored by addition of cross-linking antibodies.

1.3.2 The Fas/CD95 receptor

Apoptotic signalling via the death receptor pathway is mediated by activation (through ligation) of the death receptors, which are situated on the external cell membrane surface (Zhang *et al*., 2005). These receptors are members of the tumour necrosis factor receptor (TNFR) family, which includes TNFR-1, Fas/CD95, and TRAIL receptors DR-4 and DR-5 (Gewies, 2003). TNFR, a monocyte/macrophage-derived transmembrane protein, is the prototype receptor of the TNF family and was found to be responsible for the cytotoxicity in tumour cells (Old, 1985; Beutler and Cerami, 1986).

The death receptors are composed of cysteine rich extracellular subdomains, which recognize specific ligands, and a cytoplasmic death domain (Boldin *et al*., 1996) (Fig. 3). Fas and TNFR1 share a homologous cytoplasmic death domain, which consists of approximately 80 amino acids. This death domain is essential for relaying the apoptotic signal (Itoh *et al*., 1993; Tartaglia *et al*., 1993).

X-ray diffraction analysis has shown that the TNFα ligand, in its trimerized form, binds to three TNF receptor molecules (Banner *et al*., 1993). Upon ligation, the death receptor trimerizes and becomes activated (Boldin *et al*., 1996) (Fig. 3). Both TNFR1 and Fas are only activated upon oligomerization (Dhein *et al*., 1992; Takahashi, 1996). FasL shares similarities in structure to TNFα, and likewise the Fas receptor shares similarities in structure to TNFR. Therefore it was deduced that in the same way as TNFα activates TNFR, so too FasL induces trimerization and activation of Fas. This activation leads to

the transfer of the apoptotic signal through the trimerized cytoplasmic regions of the Fas receptor to downstream effector molecules in the death receptor pathway (Banner *et al*., 1993) (Fig. 3).

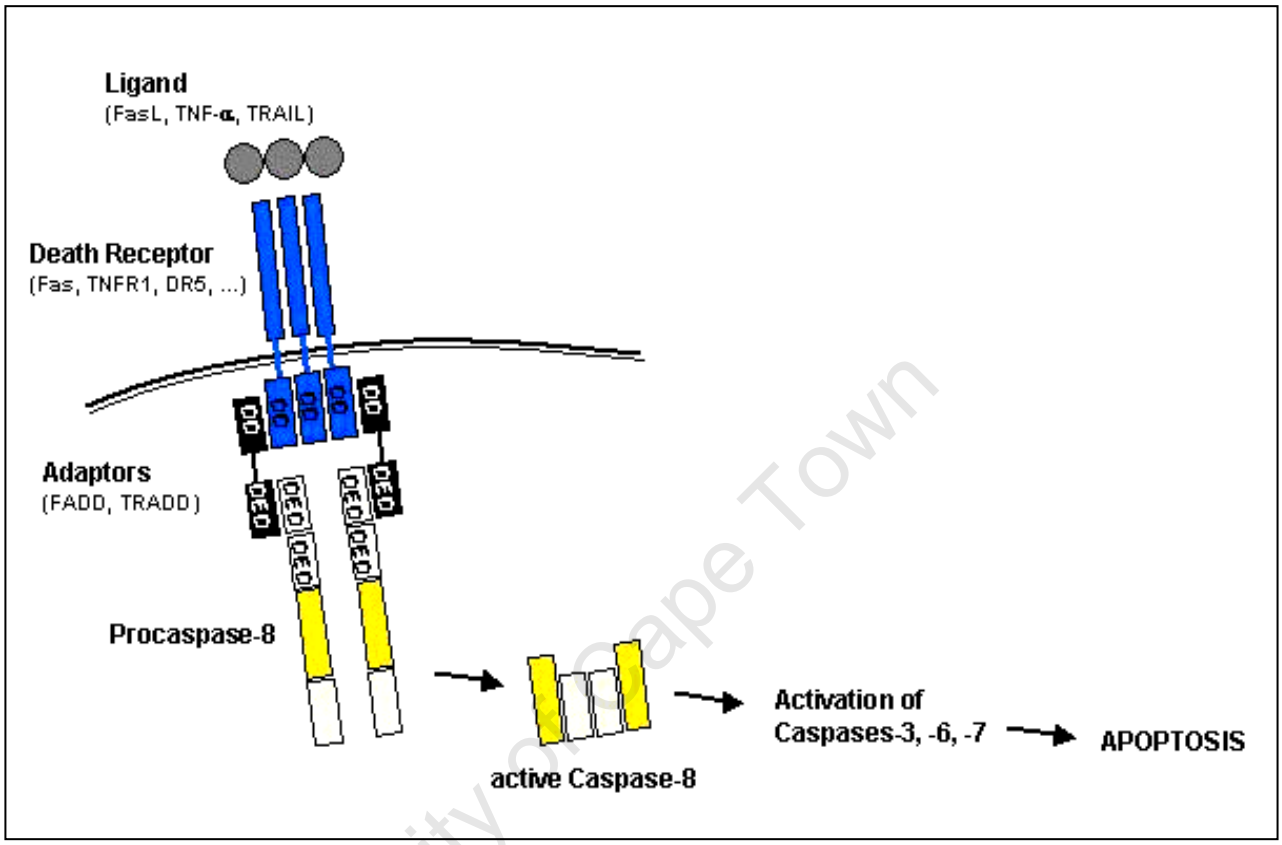

Fig. 3. Caspase-8 activation at the death-inducing signalling complex (DISC). Trimerization of the death receptor occurs upon ligand binding, followed by the recruitment of adaptor proteins via death domain (DD) interactions. The adaptor proteins subsequently recruit procaspase-8 molecules through death effector domains (DED) to the DISC. Active caspase-8 is produced by autoproteolytic cleavage of procaspase-8 molecules in close proximity. The active caspase-8 consists of two small and two large subunits forming a hetero-tetramer. Caspase-8 induces a caspase cascade by cleaving and activating effector caspase downstream leading to the execution of apoptosis (Gewies, 2003).

Some researchers have found alternative ways of activating the death receptor pathway. Yonehara *et al*. (1989) found that anti-Fas antibody exerts identical cytotoxic effects as TNFα. Studies have also found that cross-linking of Fas by agonistic antibodies, in Fas-bearing cells, can induce apoptosis (Trauth *et al*., 1989; Yonehara *et al*., 1989; Itoh *et al*., 1991).

1.3.3 FADD and Caspase-8

After FasL binds to the Fas receptor, the activated trimeric Fas receptor recruits the adapter protein FADD (Fas-associated death domain protein) (Kischkel *et al*., 1995; Barnhart *et al*., 2003) (Fig. 3).

FADD contains a death domain at its C-terminal region and a death effector domain at its N-terminus (Fig. 3). Its death domain allows complex formation with the death domain of the activated Fas receptor. The resultant complex that is formed is known as the death-inducing signalling complex (DISC) (Boldin *et al*., 1996) (Fig. 3). Studies have shown that cells that are deficient in FADD or possess mutations in FADD are resistant to death receptor-mediated apoptosis, either by Fas, TNFR1 or DR-3. This infers the importance and necessity of FADD in the Fas-mediated apoptosis pathway (Yeh *et al*., 1998; Zhang *et al*., 1998).

Caspase-8 possesses two death effector domains at its N-terminus, which interacts with FADD's death effector domains and in so doing is recruited to the DISC (Martin *et al*., 1998) (Fig. 3). Due to the weak intrinsic protease activity of procaspase-8, it is able to cleave and activate other procaspase-8 molecules upon oligomerization (Ashkenazi and Dixit, 1998; Yang *et al*., 1998). As more procaspase-8 molecules associate with the DISC, they oligomerize and undergo autoproteolytic cleavage and cross-activation due to their high local density and close proximity (Thornberry and Lazebnik, 1998). This mechanism used for procaspase-8 activation is called the induced proximity model, and requires a high concentration of procaspase molecules to be in close proximity to each other (Muzio *et al*., 1998; Salvesen *et al*., 1999).

1.3.4 The two pathway model: Type I and Type II cells

There are two Fas-mediated apoptotic pathways, which diverge after caspase-8 activation. The two pathways exist based on the ability of the type of cell to execute apoptosis independently of the mitochondria (Type I cells) or in a dependent manner, relying on amplification of the death signal by the mitochondria (Type II cells) (Strasser *et al*., 1995; Li *et al*., 1998; Luo *et al*., 1998) (Fig. 4). Examples of Type I cells include the B lymphoblastoid cell lines, SKW6.4 and CH1 (murine), as well as the T lymphoma

cell line, H9 (Scaffidi *et al*., 1998; Huang *et al*., 1999). Examples of Type II cells include the T cell lines, CEM and Jurkat and the human myeloid cell line, HL60 (Scaffidi *et al*., 1999).

In Type I cells, the amount of caspase-8 activated at the DISC is sufficient to bring forth a downstream caspase cascade (Scaffidi *et al*., 1998) (Fig. 4). The activated caspase-8 molecules activates procaspase-3 and/or procaspase-7, which in turn activates procaspase-6 thereby transmitting the apoptotic signal to bring about cell death (Hirata *et al*., 1998).

In Type II cells, however, the amount of activated caspase-8 is insufficient to elicit a caspase cascade. Therefore the apoptotic signal needs to be amplified via the mitochondria, thereby significantly delaying activation of the caspase cascade (Kuwana *et al*., 1998; Scaffidi *et al*., 1998). In Type II cells, the Fas death receptor pathway therefore converges with the mitochondrial-mediated apoptosis pathway to initiate apoptosis (Fig. 4). A pro-apoptotic member of the Bcl-2 family of proteins, Bid, forms the link between the death receptor- and mitochondrial-mediated apoptosis pathways. Activated caspase-8 cleaves Bid to produce its truncated form, tBid, which translocates to the outer mitochondrial membrane where it initiates the mitochondrial-mediated apoptosis pathway (as described in sections 1.5.2.2 and 1.6.1.2). Here tBid interacts with other pro-apoptotic members of the Bcl-2 family, Bax and Bak, to induce the release of pro-apoptotic factors from the mitochondria. These released molecules further amplify and execute the apoptotic cascade (Li *et al*., 1998; Luo *et al*., 1998). One of the released apoptotic molecules, cytochrome *c*, activates procaspase-9 in the apoptosome complex (described in section 1.5.3), leading to the activation of caspase-3 (Li, P *et al*., 1997) (Fig. 4).

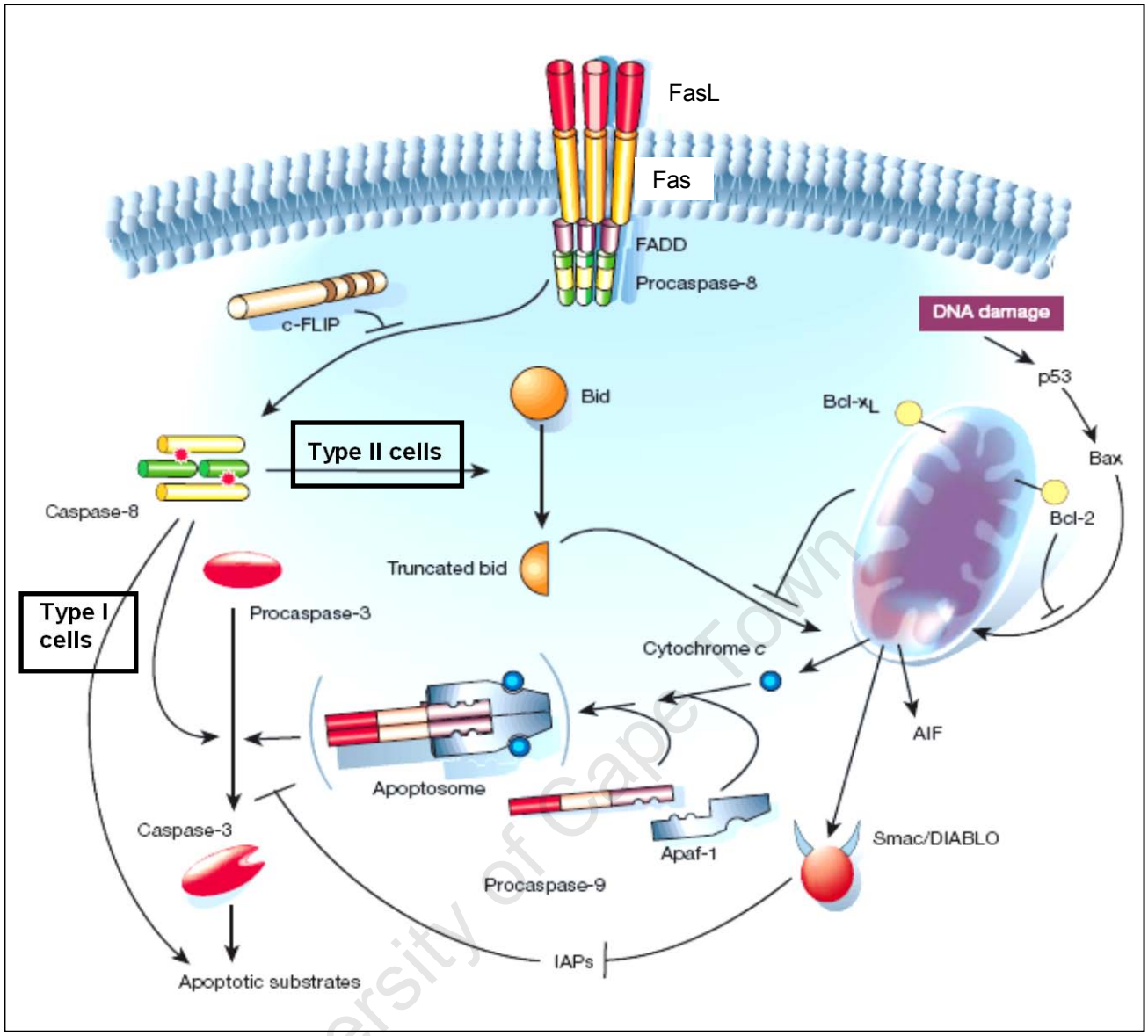

Fig. 4. The two different Fas/CD95 pathways involved in Type I and Type II cells. Type I cells are able to execute apoptosis independently of the mitochondria, however Type II cells rely on amplification of the apoptotic signal by the mitochondria (modified from Hengartner, 2000).

1.4 ER-stress induced apoptosis

Cellular stress is defined as conditions in which the homeostatic balance is disturbed and cells encounter and react to abnormal states. Cells are very capable of maintaining homeostasis through various stress responses. Transient levels of cellular stress occur regularly, however, more severe stress signalling may be too challenging to overcome. Therefore the best option for the organism, as a whole, would be programmed cell death for these affected cells (Cullinan and Diehl, 2006).

Healthy proficient functioning of the ER is vital for maintaining cellular homeostasis and survival. The ER-stress induced apoptotic pathway forms part of the intrinsic apoptosis machinery (Morishima *et al*., 2002; Rao *et al.*, 2002 a). The malfunctioning of this apoptosis pathway is implicated in the pathology and disease progression of numerous neurodegenerative and cardiovascular diseases (Szegezdi, *et al*., 2006).

The ER is the site of protein synthesis and folding (Gaut and Hendershot, 1993). For optimum protein processing and folding, a number of factors are important, including ATP, calcium and an oxidizing environment to allow the formation of disulphide bonds (Imaizumi *et al*., 2001). Stress conditions that negatively affect the functioning of the ER, reduce its protein folding ability, which leads to the accumulation and aggregation of unfolded proteins inside the ER lumen (Kaufman, 2002). This, in turn, activates the unfolded protein response (UPR) (Lee, 1992; Forman *et al*., 2003). However, if the stress is too severe or prolonged to overcome and the UPR fails, the ER-stress induced apoptotic pathway is initiated and cell death ensues (Wu and Kaufman, 2006).

1.4.1 The Unfolded Protein Response (UPR)

The UPR is a pro-survival stress response that attempts to restore normal ER function. It does this by inhibiting further accumulation of misfolded proteins, initiating the degradation of aggregated proteins and improving the folding capacity of nascent proteins (Haze *et al*., 1999; Bertolotti *et al*., 2000).

The UPR is initiated and mediated by three ER transmembrane receptors, which detect the onset of ER stress (Harding *et al*., 1999; Forman *et al*., 2003). These transmembrane receptors are Pancreatic eIF2 ER protein kinase (PERK), Activating transcription factor 6 (ATF6) and Inositol-requiring enzyme 1 (IRE1). The receptors are maintained in an inactive state via their association with Immunoglobulin heavy chain-binding protein (Bip) (Haze *et al.*, 1999; Ma *et al*., 2002 a) (Fig. 5).

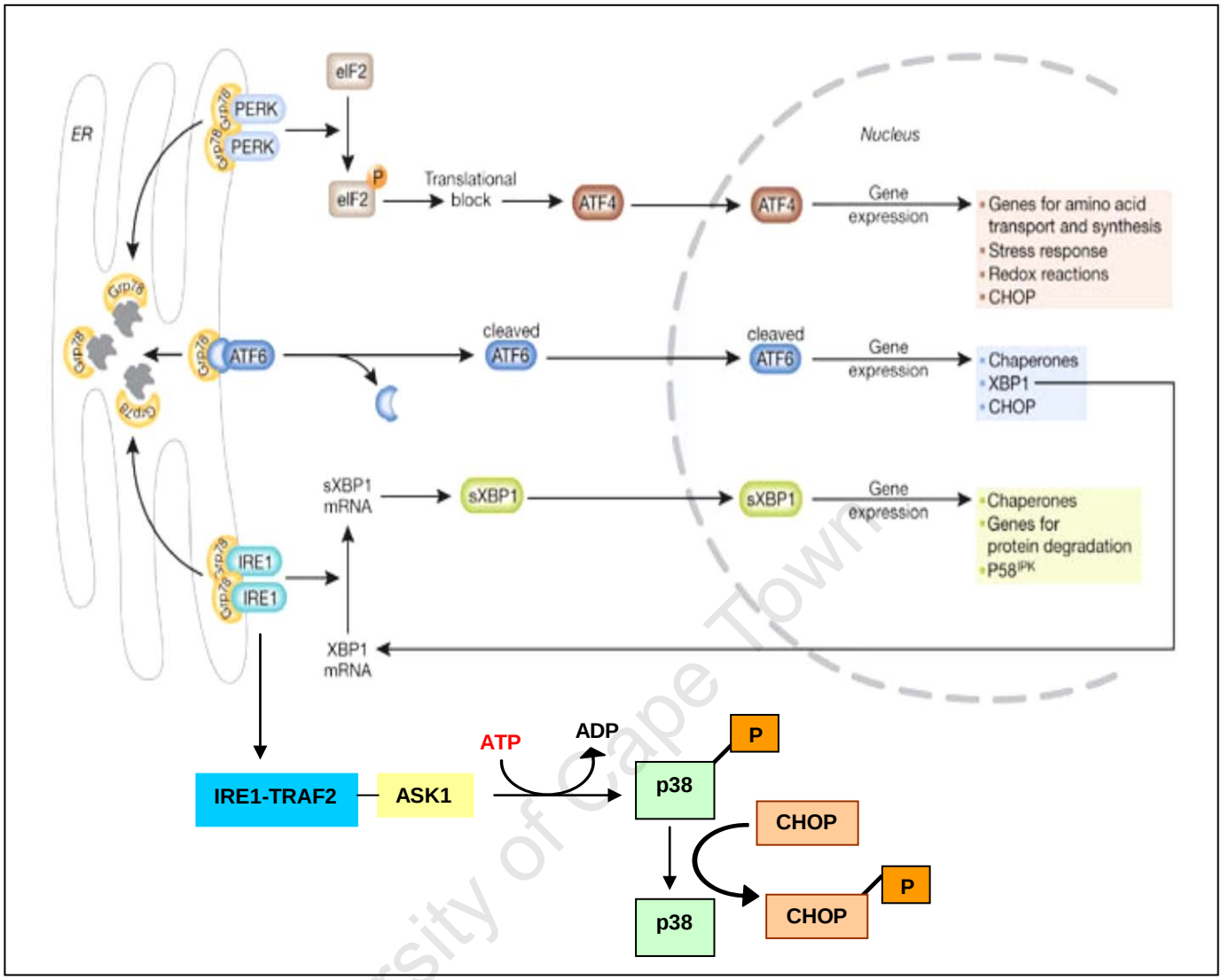

Fig. 5. Schematic representation of the UPR and initiation of ER-stress induced apoptosis pathway. During resting (unstressed) conditions the three ER transmembrane receptors are maintained in an inactive state via their association with Bip. At the onset of ER stress, Bip dissociates from the receptors resulting in their sequential activation and the induction of the UPR. PERK is activated first, then ATF6 and lastly IRE1 (modified from Szegezdi, *et al.*, 2006).

1.4.1.1 Bip

Bip, also known as glucose-regulated protein 78 (GRP78), is an ER membrane protein and chaperone (Haas and Wabl, 1983; Munro and Pelham, 1986). Bip and other GRPs are constitutively expressed in all cells and their expression is upregulated when ER function is disrupted (Kozutsumi *et al.*, 1988; Chang *et al.*, 1989; Li *et al.*, 1994). This increase in Bip transcription is an attempt by the UPR to prevent the accumulation of cytotoxic misfolded protein aggregates in the ER. Bip molecules, that have dissociated from the ER receptors and/or are newly synthesized, act as protein chaperones by

binding unfolded or misfolded proteins. Therefore Bip becomes directly involved in protein folding and translocation, and in so doing increases the protein folding capacity of the ER (Dorner *et al*., 1989; Flynn *et al.*, 1991).

In addition to its chaperone function, Bip also serves as a negative regulator of the three ER transmembrane receptors (Fig. 5). Induction of the UPR leads to the dissociation of Bip from the three ER stress receptors allowing for their sequential activation and dimerization (Fig. 5). This results in their autophosphorylation and subsequent increase in activity, allowing them to act on their substrates (Ma *et al*., 2002 a). PERK is activated first, followed by ATF6 and lastly IRE1 (Fig. 5). This sequence of activation allows time for the PERK and ATF6-mediated pathways to resolve the stress before IRE1 is activated (Szegezdi, *et al.*, 2006).

1.4.1.2 The three ER transmembrane receptors

1.4.1.2 A) PERK

PERK dimerization and autophosphorylation occurs when Bip dissociates from it, generating the active form of PERK (Shi *et al*., 1998). Activated PERK phosphorylates the eukaryotic initiation factor 2 (eIF2), which inhibits protein synthesis and translation. In so doing, the load of emerging proteins at the ER is decreased, thereby promoting cell survival (Kimball and Jefferson, 1992; Sood *et al*., 2000).

Cell survival, during ER stress, depends on the UPR's ability to block the accumulation of unfolded nascent proteins. However, a number of genes, which are involved in the UPR, carry specific regulatory sequences in their 5' untranslated regions. These regulatory sequences enable them to bypass the PERK-mediated eIF2-dependent translational block, thereby allowing these proteins to be synthesized to mediate the UPR and stress response (discussed in section 1.6.2) (Miller and Hinnebusch, 1990; Harding *et al.*, 2000 b).

1.4.1.2 B) ATF 6

Upon dissociation from Bip, ATF6 translocates from the ER to the Golgi apparatus (Li *et al*., 2000) (Figs. 5 and 6). AFT6 is proteolytically cleaved and activated in the Golgi compartment by the site-1 and site-2 proteases (S1P and S2P) to produce ATF6DC, which is a transcription factor (Haze *et al*., 1999; Ye *et al*., 2000). ATF6DC translocates to the nucleus where it induces and regulates genes with an ER stress response element (ERSE) that code for proteins involved in protein folding (Figs. 5 and 6). The transcription factors CEBP homologous protein (CHOP) and X box-binding protein 1 (XBP1), as well as the ER chaperones Bip, GRP94 and protein disulphide isomerase are among these genes that are induced. XBP1 is important in the IRE1 pathway signalling, as described in section 1.4.1.2 C (Yoshida *et al*., 2001; Okada *et al*., 2002). The ATF6-mediated signalling pathway is entirely pro-survival and has not yet been linked to ER-stress induced apoptosis but rather the prevention of ER stress (Szegezdi, *et al*., 2006).

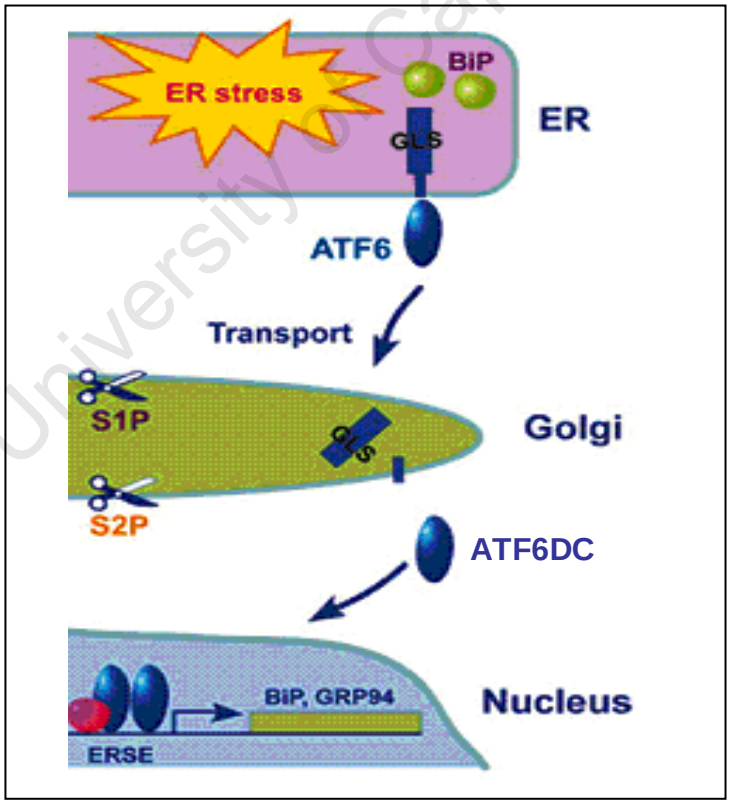

Fig. 6. ATF6 activation in response to ER stress. Upon induction of ER stress, Bip releases ATF6, which is then transported into the Golgi where cleavage by S1P and S2P follows. Cleaved and activated ATF6DC then translocates to the nucleus. Here it binds and activates ER-stress inducible target genes, which code for proteins involved in protein folding (modified from Shen and Prywes, 2005).

1.4.1.2 C) IRE1

During resting conditions, inactive IRE1 is bound to Bip by its ER-lumenal domain (Bertolotti *et al*., 2000). Bip releases IRE1 during conditions of ER stress, thereby allowing for its activation. IRE1 is a type I transmembrane protein that has both anti-apoptotic and pro-apoptotic functions. It is an enzyme that possesses a serine-threonine kinase domain, as well as an endoribonuclease domain, presenting it with dual activity (Tirasphon *et al*., 1998; Wang *et al*., 1998).

As an endonuclease, IRE1 splices XBP1 mRNA, thereby rendering it competent for translation (Yoshida *et al*., 2001) (Fig. 5). The translated protein, XBP1, is an active transcription factor. XBP1 attaches to the promoters of numerous genes involved in ER-induced protein degradation and retrograde transport of misfolded proteins (out of the ER into the cytoplasm) to counteract apoptosis (Yoshida *et al*., 2001; Lee *et al*., 2003). However, XBP1 also regulates genes such as $P58^{IPK}$, which bind and inhibit PERK thus creating a negative feedback loop that lifts the PERK-mediated translational block (section 1.6.2) (Yan *et al*., 2002; van Huizen *et al*., 2003). This occurs several hours after the activation of PERK and eIF2 and represents the point of termination of the UPR and initiation of apoptosis. Therefore, during the initial stages of IRE1 activation it aids the UPR by splicing XBP1 mRNA. However, later on it becomes important for initiating pro-apoptotic signals by inducing genes such as $P58^{IPK}$ and removing the translational block. If the UPR was successful in counteracting ER stress, the ER will return to its normal functioning and the cell will survive. However, if the UPR failed and/or the stressful conditions persist, removal of the translational block allows for the synthesis of pro-apoptotic proteins leading to cell death (Yan *et al*., 2002).

IRE1 also initiates apoptosis by recruiting and activating caspase-12 through its complex with Tumour-necrosis-factor receptor-associated factor 2 protein (TRAF2) (Yoneda *et al*., 2001). The IRE1-TRAF2 complex releases procaspase-12 from the ER membrane, thereby allowing for its cleavage and activation.

The IRE1-TRAF2 complex also recruits Apoptosis-signal-regulating kinase (ASK1) (Fig. 5). ASK1 is a mitogen-activated protein kinase kinase kinase (MAPKs), which transmits various stress signals to downstream MAPKs like c-Jun N-terminal kinase

(JNK) and p38 (Nishitoh *et al*., 1998; Urano *et al*., 2000). The activated JNK pathway subsequently allows for the activation of pro-apoptotic factors that transmit the apoptotic signal to the mitochondria (section 1.6.1.2). Here the apoptotic signal is amplified and relayed via the mitochondrial apoptosis pathway (discussed in section 1.5) (Leppa and Bohmann, 1999; Nishitoh *et al*., 2002). Activated p38 regulates pro-apoptotic molecules, such as CHOP, through phosphorylation, thereby increasing their activity and enhancing the apoptotic signal (Wang *et al*., 1996; Harding *et al*., 2000 a; Harding *et al*., 2002) (Fig. 5).

1.4.2 CHOP

CHOP, also known as Growth arrest- and DNA-damage-inducible gene 153 (GADD153), is involved in ER-stress induced apoptosis and serves as an important switch from the pro-survival to pro-death signalling pathways (Marciniak *et al*., 2004). Under normal unstressed conditions CHOP is not constitutively expressed, unlike the ER chaperone genes, which include Bip (Brewer *et al*., 1997).

CHOP is a pro-apoptotic basic leucine zipper-containing transcription factor that is induced with the commencement of the ER-stress induced apoptosis pathway (Ron and Habener, 1992; McCullough *et al.*, 2001). CHOP is involved in all three arms of the UPR, namely the PERK, ATF6 and IRE1 signalling pathways (Carlson *et al*., 1993; Wang *et al*., 1996; Ma *et al*., 2002 b) (Fig. 5). In addition to controlling levels of CHOP transcription and translation, the UPR is also involved in its post-translational modification and activation (Fig. 5). Activation of CHOP mediates and enhances apoptosis by inducing gene expression of apoptotic molecules and inhibiting the expression of the anti-apoptotic Bcl-2 gene (discussed in section 1.6.1.2) (Zinszner *et al.*, 1998; Oyadomari *et al*., 2002).

1.4.3 Caspase-4/12

Initiation of the ER-stress induced apoptotic pathway also leads to the specific activation of caspase-4. In humans ER stress is mediated by caspase-4, however, in rodents caspase-12 takes on this role (Nakagawa *et al.*, 2000; Hitomi *et al.*, 2004). Human caspase-12 protein cannot be produced. A frame shift and premature stop codon

interrupts this gene, in addition to a loss of caspase function caused by amino acid substitution in the critical site (Fischer *et al*, 2002). Therefore human caspase-12 does not mediate ER-stress induced apoptosis. Studies have found that human caspase-4 could functionally substitute the function of murine caspase-12 in human systems (Nakagawa *et al.*, 2000). Human colon cDNA libraries were screened using the murine caspase-12 gene as probe and it was found that caspase-4 is the homologous gene to murine caspase-12 (Hitomi *et al.*, 2004).

Caspase-4 is predominantly localized to the ER membrane in its inactive form. This allows it to sense ER stress signals and changes in ER homeostasis, making it a central player in the ER-stress induced apoptotic pathway. Hitomi *et al.* (2004) also showed that caspase-4 is also found on the mitochondrial outer membrane. Bcl-2, which was found to completely inhibit the downstream mitochondrial apoptotic signal, did not inhibit ER-stress induced cleavage and activation of caspase-4. It was therefore concluded that mainly caspase-4 localized to the ER is activated upon ER-stress induced apoptosis and not mitochondrial caspase-4 (Hitomi *et al.*, 2004).

Karki *et al.* (2007) found that caspase-4 activation requires both oligomerization and proteolytic cleavage for activation. It was found that caspase-12, in murine systems, could be activated by calcium-activated cysteine endopeptidases (proteases similar to caspases) called calpains (Nakagawa and Yuan, 2000). Other studies have shown that caspase-7 activates caspase-12 after prolonged ER stress (Rao *et al.*, 2001). Yoneda *et al.* (2001) found that caspase-12 activation is mediated by TRAF2 and regulated by IRE1. Studies have also found that caspase-12 activates caspase-9 in a cytochrome *c*-independent (Morishima *et al*., 2002) and Apaf-1-independent (Rao *et al*., 2002 a) manner, thereby bypassing the apoptosome pathway (section 1.5.3).

The exact mechanism of caspase-4 activation, the function of mitochondrial-localized caspase-4 and the group of caspases linked or activated upon ER-stress induced apoptosis are, however, still not fully elucidated (Yoneda *et al.*, 2001; Rao *et al.*, 2002 a; Rao *et al.*, 2002 b; Karki *et al*., 2007).

1.5 Mitochondrial-mediated apoptosis

The mitochondria are responsible for cellular metabolism and producing most of the cellular ATP. In cells that are undergoing apoptosis, the mitochondria function as central executioners and/or regulators. The mitochondrial-mediated apoptosis pathway can amplify and intercede in the extrinsic and intrinsic apoptotic pathways. In addition, it can also initiate and propagate death signals that originate within the cell. DNA damage, radiation, chemotherapy, oxidative stress, nutritional deprivation and cytotoxic drugs are all stimuli that induce the mitochondrial-mediated apoptotic pathway (Skommer *et al*., 2007).

1.5.1 The structure of the mitochondria

Mitochondria possess double membranes, which form two compartments, namely the intermembrane space and the matrix (Fig. 7). The intermembrane space exists between the inner and outer mitochondrial membranes, whereas the matrix is the space enclosed by the inner mitochondrial membrane (Fig. 7). The matrix contains powerful pro-apoptotic molecules. Under physiological circumstances these molecules are used in the processes of oxidative phosphorylation, whereby energy from food molecules are converted into usable forms of chemical energy (Solomon *et al*., 1999).

The outer mitochondrial membrane is quite permeable and contains many aqueous channels, which allow small molecules to pass through it. These aqueous channels are made up of the transport protein called Voltage dependant anion channel (VDAC) (also called porin) (Beutner *et al*., 1998). The inner mitochondrial membrane is selectively permeable and folded into numerous cristae (Solomon *et al*., 1999). The cristae contain the transport proteins necessary for oxidative phosphorylation, including Adenine nucleotide transporter (ANT), which controls the exchange of ADP and ATP across the membrane (Bauer *et al*., 1999).

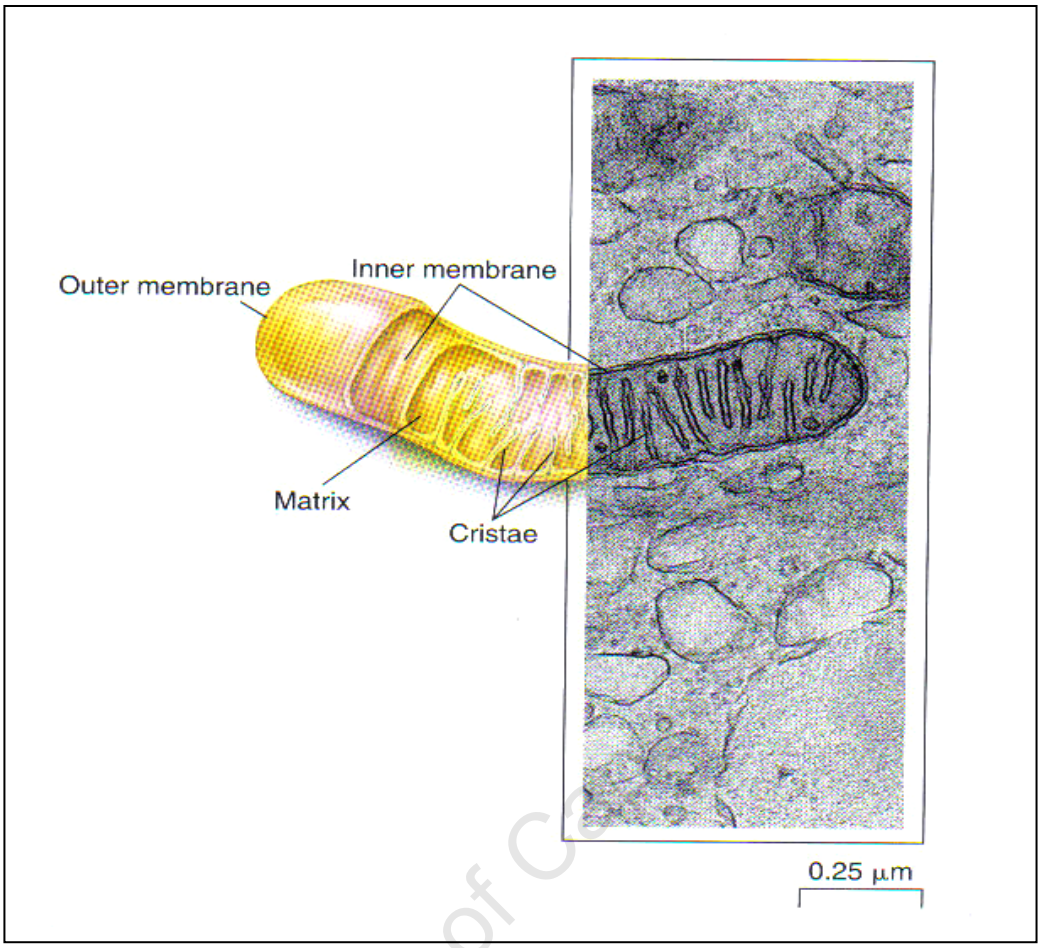

Fig. 7. Drawing and transmission electron microscopy (TEM) of a mitochondrion. The drawing shows the different compartments and membranes of the mitochondrion. The double membranes, matrix and cristae can also be seen in the TEM (drawing by D.W. Fawcett taken from Solomon *et al.*, 1999).

1.5.2 Mitochondrial membrane depolarisation and outer membrane permeabilization

The mechanisms responsible for mitochondrial membrane depolarisation and outer membrane permeabilization include the opening of the permeability transition pore and the interaction of pro-apoptotic members of the Bcl-2 family (also discussed in section 1.6.1) (Crompton, 1999; Harris and Thompson, 2000).

1.5.2.1 The permeability transition pores

A permeability transition pore, also known as a mitochondrial megachannel or multiple conductance channel, is made up of a complex of proteins situated at contact sites

between the inner and outer mitochondrial membranes (Bernardi, 1996; Lohret *et al*., 1996). A permeability transition pore consists of several proteins, which include VDAC, ANT, cyclophilin D (CypD), and peripheral benzodiazepine receptor (PBR) (Beutner *et al*., 1998; Bauer *et al*., 1999) (Fig. 8). Due to their location, the permeability transition pores form important sites of metabolic coordination between the mitochondrial matrix, intermembrane space and the cytoplasm (Fig. 8). They function as regulators of the matrix's pH and volume, as well as intracellular calcium concentration. This allows it to act as voltage and redox-gated channels, with different levels of conductance (Zoratti and Szabò, 1995; Ichas *et al*., 1997; Marzo *et al*., 1998).

Following apoptosis-inducing stress conditions, the mitochondrial inner transmembrane potential is disrupted (Bras *et al*., 2005). This change in inner mitochondrial membrane potential causes permeability transition pores to open. As a result, due to an influx of water molecules, the matrix and outer mitochondrial membrane expands. This distension causes depolarisation of the outer membrane, which also becomes more permeable (Kantrow and Piantadosi, 1997; Petit *et al*., 1998). The increased permeability of the outer mitochondrial membrane results in further osmotic swelling of the mitochondrion and eventual rupture of the outer membrane. When the mitochondrion ruptures, it releases pro-apoptotic proteins, which were sequestered in the matrix and intermembrane space, into the cytoplasm (Loeffler and Kroemer, 2000). As a result, the synthesis of ATP stops, levels of ROS increase and redox molecules, such as NADH, NADPH and glutathione, are oxidized. A positive feedback loop is produced as ROS oxidizes the cell's lipids, proteins and nucleic acids. This further enhances the death signal and reinforces the cell's fate towards apoptosis (Kroemer *et al*., 1997; Marchetti *et al*., 1997; Ricci *et al*., 2003). Studies have shown that pharmacological inhibition of the permeability transition pores safeguards the cell against apoptosis (Marchetti *et al*., 1996; Zamzami *et al*., 1996).

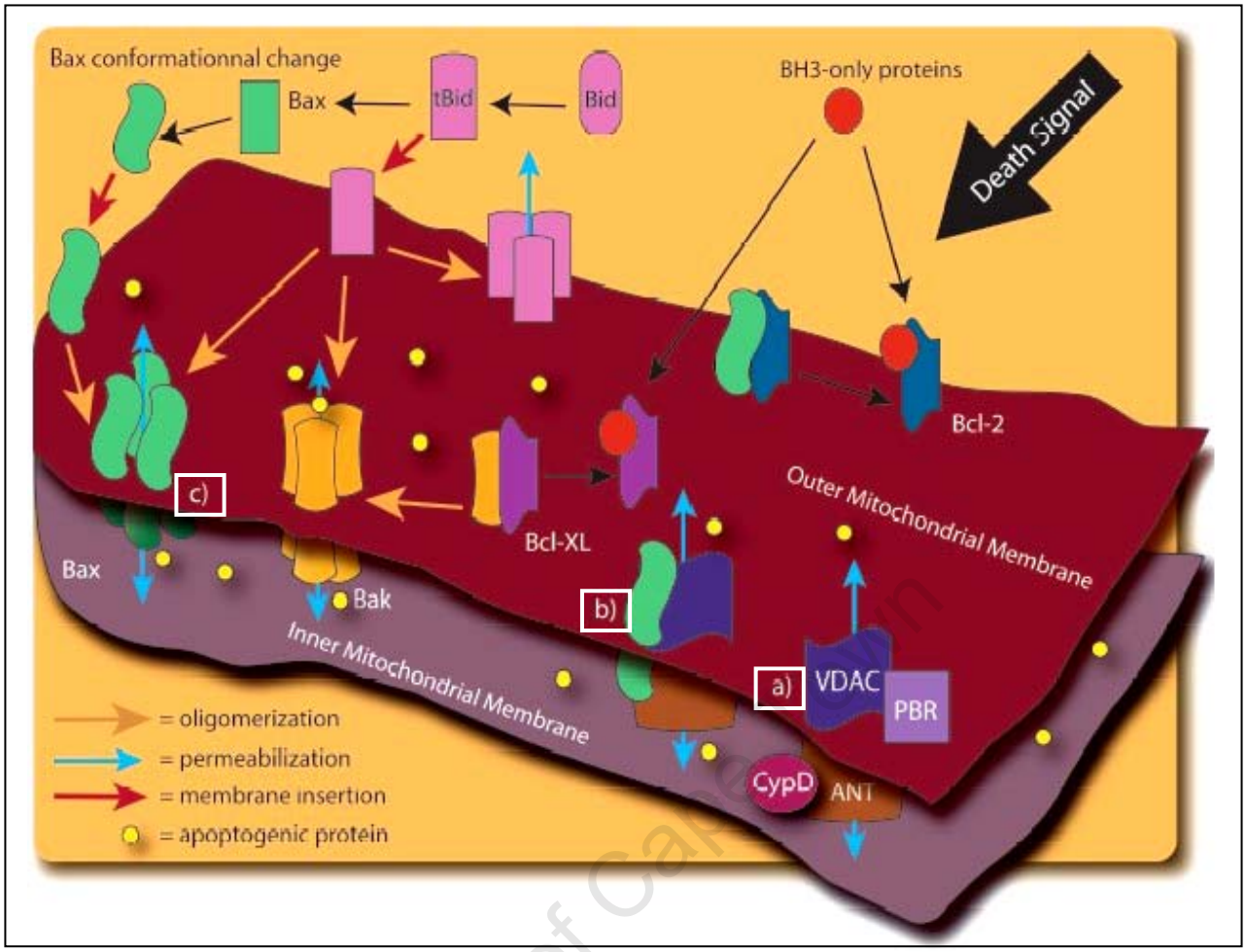

Fig. 8. The different mechanisms involved in mitochondrial outer membrane permeabilization. It is proposed that release of the pro-apoptotic mitochondrial factors can result from either permeability transition pore opening (**A**) or mitochondrial permeabilization due to the interaction of pro-apoptotic members of the Bcl-2 family (such as Bax) with VDAC and/or ANT (**B**). Another mechanism proposes that the release of pro-apoptotic proteins depends on the balance between the pro- and anti-apoptotic Bcl-2 family members (**C**) (modified from Bras *et al.*, 2005).

1.5.2.2 Involvement of the Bcl-2 family proteins in outer mitochondrial membrane permeabilization

The Bcl-2 family of proteins directly affect mitochondrial homeostasis and play a crucial role in regulating the mitochondrial mediated apoptotic pathway (as discussed in section 1.6.1) (Antonsson *et al.*, 1997; Kuwana *et al.*, 2002). The Bcl-2 proteins can form channels in the mitochondria, or facilitate channel formation by interacting with other family members or mitochondrial proteins. In so doing, the Bcl-2 proteins increase the outer mitochondrial membrane's permeability, which leads to its eventual rupture (Crompton, 1999; Harris and Thompson, 2000).

Central pro-apoptotic members of the Bcl-2 family are truncated Bid, Bax and Bak, as they can directly interact with outer mitochondrial membrane proteins (Shimizu *et al*., 1999; Wei *et al*., 2001). As mentioned in section 1.3.4, Bid provides a link between the death receptor and mitochondrial-mediated apoptosis pathways. Activated, truncated Bid relocates to the mitochondria where it is required to activate the pro-apoptotic function of Bax and Bak (Li *et al*., 1998; Luo *et al*., 1998) (Fig. 8). Oligomerised Bax and Bak molecules initiate or contribute to the permeability of the outer membrane by forming channels themselves or by interacting with other mitochondrial proteins, like VDAC and ANT (of the permeability transition pores) (Fig. 8). A number of Bcl-2 family members can bind to VDAC, causing it to undergo conformational change and in so doing, regulate its channel activity. These Bcl-2 proteins therefore modulate mitochondrial homeostasis by regulating channel activity, in addition to producing pores to increase outer mitochondrial membrane permeability (Shimizu *et al*., 1999; Wei *et al*., 2001) (Fig. 8).

1.5.3 The apoptosome pathway

The powerful mixture of pro-apoptotic proteins that are released from a mitochondrion (when it ruptures) include cytochrome *c*, Apoptosis-inducing factor (AIF), Smac/DIABLO, several procaspases such as procaspase-2, -3 and -9, Omi/HtrA2 and the endonuclease endoG (Susin *et al*., 1999; Li *et al*., 2001; Verhagen *et al*., 2002). Upon release, these proteins ensure that the apoptosis cascade rapidly progresses to the end. The release of cytochrome *c* into the cytosol is a key event in mitochondrial-mediated apoptosis (Liu *et al*., 1996).

Cytochrome *c* is situated between the outer and inner mitochondrial membrane. It is strongly linked with complex IV of the respiratory chain and functions mainly to mediate the electron transport between complex III and IV (Skommer *et al*., 2007). In the cytoplasm, the released cytochrome *c* oligomerises with Apoptotic protease activating factor-1 (Apaf-1) and ATP to form the apoptosome complex (Li, P *et al*., 1997; Cain *et al*., 1999) (Fig. 9).

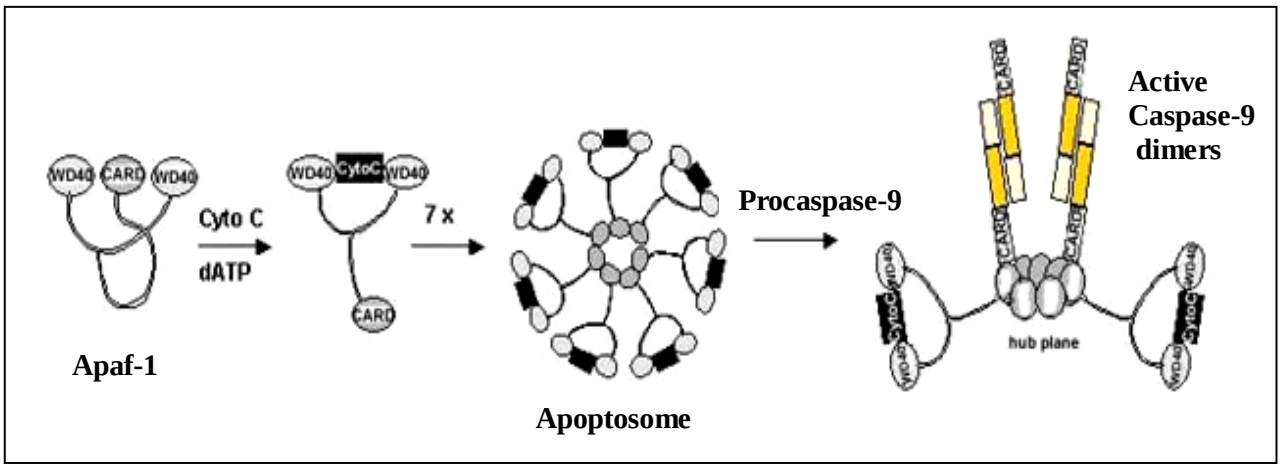

Fig. 9. Formation and activation of the apoptosome complex. Mitochondrial release of cytochrome *c* leads to the formation of the apoptosome complex and subsequent activation of procaspase-9 (modified from Gewies 2003).

The apoptosome is a cytosolic apoptosis signalling protein complex. To form the apoptosome complex, cytochrome *c* requires dATP to bind to monomeric Apaf-1 (Fig. 9). The cytochrome *c*-Apaf-1 complex undergoes a conformational change and oligomerizes to form a wheel-like structure with 7-fold symmetry (Fig. 9). Apaf-1 contains a caspase recruitment domain, which binds procaspase-9, and it also possesses multiple WD-40 repeats that allows for self-oligomerization and auto-activation of caspase-9 (Zou *et al*., 1997; Cain *et al*., 2000) (Fig. 9). The apoptosome complex is seen as the true active form of caspase-9, forming a caspase-9 holoenzyme. Cytochrome *c* and Apaf-1 are therefore not just activators of caspase-9 but are essential regulatory subunits of this holoenzyme (Rodriguez and Lazebnik, 1999). Activated caspase-9 in turn activates downstream effector caspases like caspase-3, relaying and amplifying the caspase cascade towards cell death (Slee *et al*., 1999; Acehan *et al*., 2002).

1.6 Regulation of the apoptosis signalling pathways

The apoptotic pathways have various regulatory molecules and mechanisms in place to prevent healthy cells from apoptosing under normal unstressed conditions.

1.6.1 The Bcl-2 family of proteins regulate all three apoptotic pathways

Bcl-2 was identified by Vaux *et al.* (1988) as an oncogene, which inhibits apoptosis instead of promoting cell proliferation. Homologues of Bcl-2 were categorized by the

presence of highly conserved sequence motifs, which were identified as Bcl-2 homology domains. These proteins are grouped together as the "Bcl-2 family of proteins" and are divided into two groups, namely the pro-apoptotic and anti-apoptotic members. Some anti-apoptotic members are Bcl-2, Bcl-X_L, Bcl-w, A1 and Mcl-1. Two subgroups of pro-apoptotic members exist, namely the Bax-subfamily, which include the proteins Bax, Bak and Bok, and the BH3-only protein subgroup, which include Bid, Bim, Bik, and Bad (Gross *et al*., 1999; Cory and Adams, 2002; Willis and Adams, 2005).

The highly conserved Bcl-2 homology domains are vital for homo-complex and hetero-complex formation between pro- and anti-apoptotic family members (Muchmore *et al*., 1996; Borner, 2003). This enables the Bcl-2 proteins to interact with each other and neutralize the effect of each one on the other. Therefore, cells with more pro-apoptotic proteins will apoptose, whereas cells with more anti-apoptotic members will survive or are resistant to apoptosis (Rosse *et al*., 1998; Harris and Thompson, 2000).

1.6.1.1 Regulation of the Fas death receptor pathway via Bcl-2 proteins

Fas-induced apoptosis that occurs via the mitochondria in Type II cells can be inhibited by Bcl-2 (Strasser *et al*., 1995). Overexpression of anti-apoptotic members of the Bcl-2 family, Bcl-2 and Bcl-x_L, were found to block mitochondrial apoptotic activity in both Type I and II cells. However, caspase-8 and -3 activity was only blocked in Type II cells, followed by inhibition of apoptosis (Scaffidi *et al*., 1998). The death receptor pathway, in Type II cells, can therefore be regulated by events that control the mitochondrial apoptosis response (section 1.2.5).

1.6.1.2 Regulation of the ER-stress induced and mitochondrial-mediated apoptotic pathways via Bcl-2 proteins

The ER-stress induced apoptosis pathway is regulated by CHOP, JNK and the Bcl-2 family of proteins, which also regulates the mitochondrial-mediated apoptotic pathway. In this way the apoptotic signal is passed on from the ER to the mitochondria (Boya *et al*., 2002; Giorgi *et al*., 2009) (Fig. 10).

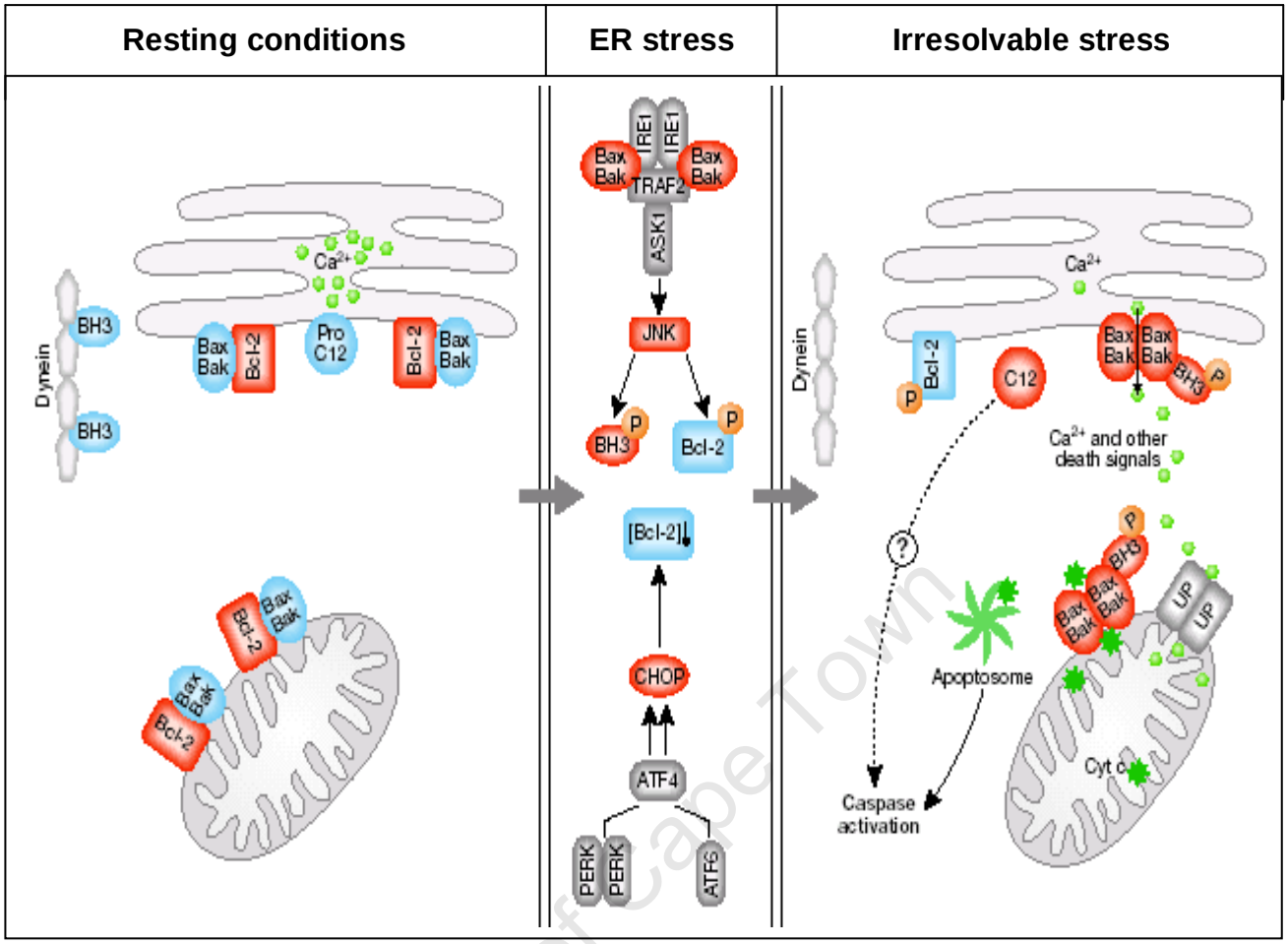

Fig. 10. Regulation of the ER-stress induced and mitochondrial-mediated apoptosis pathways. In unstressed conditions, the pro-apoptotic Bax and Bak are kept inactive by their association with Bcl-2 on the mitochondrial and ER membranes. By binding to cytoskeletal dynein, the pro-apoptotic member, Bim, is kept inactive. Stressful conditions in the ER cause the activation of JNK and induction of CHOP, both of which remove the anti-apoptotic effect of Bcl-2. JNK phosphorylates Bcl-2 and CHOP blocks its expression. JNK also activates Bim by phosphorylation, leading to its release from the cytoskeleton. Through the activation of Bax and Bak the unresolved stress results in the transmission of the apoptotic signal from the ER to the mitochondria where death signal is amplified. Subsequently caspases are activated both on the ER membrane (caspase-4/12) and through the apoptosome (caspase-9) (modified from Szegezdi, *et al.*, 2006).

In resting conditions, the pro-apoptotic proteins Bax and Bak are kept in an inactive state by their association with Bcl-2 on the mitochondrial and ER membranes (Krajewski *et al.*, 1993; Zong *et al.*, 2003) (Fig. 10). When stressful conditions in the ER develop, it leads to the activation of the JNK pathway and induction of CHOP, both of which remove the anti-apoptotic effect of Bcl-2 (McCullough *et al.*, 2001; Bassik *et al.*, 2004) (Fig. 10).

The phosphorylation of Bcl-2 by JNK, at the ER, abolishes the anti-apoptotic effect of Bcl-2. This allows for the activation of pro-apoptotic factors, Bax and Bak, which relays

the apoptotic signal to the mitochondria where it is amplified (Hacki *et al.*, 2000) (Fig. 10). CHOP blocks the expression of Bcl-2 and in so doing reduces the amount of Bcl-2 protein able to prevent apoptosis (McCullough *et al.*, 2001) (Fig. 10). Consequently caspases are activated both on the ER membrane (caspase-4/12) and through the apoptosome (caspase-9), although this mechanism is still unclear (Nakagawa *et al*., 2000; Hitomi *et al*., 2004) (Fig. 10).

JNK also regulates BH3-only members through phosphorylation, thereby increasing their pro-apoptotic potential. The pro-apoptotic member, Bim (BH3), is kept inactive by its association with the cytoskeletal protein dynein (Fig. 10). JNK phosphorylates and activates Bim, leading to its release from the cytoskeleton. Activated Bim translocates to the mitochondria were it acts as a pro-apoptotic protein on the outer mitochondrial membrane (Lei and Davis, 2003; Morishima *et al*, 2004) (Fig. 10).

1.6.2 General regulation of the ER-stress induced apoptotic pathway

The ER transmembrane receptors, IRE1 and PERK (sections 1.4.1.2 A and 1.4.1.2 C), are also regulated during ER stress. Regulatory proteins such as c-Jun N-terminal inhibitory kinase (JIK) and Jun activation domain-binding protein 1 (JAB1), interacts with IRE1, thereby controlling its function (Urano *et al*., 2000; Yoneda *et al*., 2001). During resting conditions JAB1 associates with IRE1 and the interaction is increased upon mild ER stress. However, severe ER stress causes JAB1 to dissociate from IRE1, which can then be activated. JIK can also bind to TRAF2, and in that way regulate the recruitment of TRAF2 by IRE1, as well as the activation of the MAPK pathway (section 1.4.1.2 C). More research into the regulatory activities of JIK and JAB1, and how exactly they provide the switch between pro-survival and pro-apoptotic signalling via IRE1, is still required (Oono *et al*., 2004).

Activating transcription factor 4 (ATF4) is one of the proteins that are able to bypass the eIF2-dependent translational block (PERK pathway) (section 1.4.1.2 A). ATF4 induces genes involved in the stress response, amino-acid metabolism, redox reactions, and protein secretion to promote cell survival and to restore ER homeostasis (Harding *et al*., 2003). However, ATF4 also induces pro-apoptotic genes such as the transcription factor CHOP, which promotes apoptosis (Ohoka *et al*., 2005) (Fig. 10).

PERK is inhibited by $P58^{IPK}$, thereby releasing the PERK-mediated translational block (section 1.4.1.2 A) (Yan *et al*., 2002; van Huizen *et al*., 2003). The translational block is also lifted when the protein phosphatase 1 (PP1)-interacting protein, GADD34, mediates the dephosphorylation of eIF2 by PP1 (Connor *et al*., 2001; Brush *et al*., 2003). GADD34 expression is associated with apoptosis induced by a variety of signals and its overexpression can induce or augment apoptotic cell death (Adler *et al.,* 1999). The release of the translational block acts as a positive feedback loop, creating more unfolded proteins and also allows for the synthesis of pro-apoptotic proteins, which drives the cell towards apoptosis (Novoa *et al*., 2001; Ma and Hendershot, 2003).

1.6.3 General regulation of Fas-mediated apoptosis

The shedding of membrane-bound FasL and formation of sFasL is one way in which the death receptor pathway is regulated. Soluble FasL, which has decreased activity, retains its binding affinity to the Fas receptors and can thereby act as a competitive inhibitor (Suda *et al*., 1997; Schneider *et al*., 1998; Tanaka *et al*., 1998). Decoy receptors, which are part of the TNF family, have also been discovered (Nagata, 1999). One such decoy receptor, DcR3, is secreted from cells and can bind FasL with almost the same affinity as Fas, even though these two receptors do not share similar primary structures. It was found that the DcR3 gene is amplified in more than 50% of colon and lung carcinomas, which express high levels of DcR3 mRNA. Since FasL would bind the decoy receptors, this could explain why these defective cells, having an increased expression of DcR3, cannot die via Fas-mediated apoptosis (Pitti *et al*., 1999).

There are also regulatory and/or inhibitory steps involved once the Fas receptors have been activated and start recruitment of FADD and formation of the DISC. Once the DISC is assembled for caspase-8 activation, the degenerate caspase homologues, FADD-like interleukin-1 β-converting enzyme inhibitory proteins (FLIPs), can be recruited by FADD instead of caspase-8 molecules. FLIPs therefore act as decoys by binding to FADD and in so doing prevents caspase-8 activation (Irmler *et al.*, 1997; Shu *et al*., 1997).

1.6.4 Regulation of the caspase cascade by the Inhibitors of apoptosis proteins (IAPs)

The apoptosis pathway is also regulated once the caspase cascade is initiated. The Inhibitor of apoptosis proteins (IAPs), are powerful inhibitors of caspases. The IAPs are a family of anti-apoptotic proteins that are essential for their interaction with caspases. IAPs regulate caspase activity by acting as caspase substrates and can therefore directly inhibit caspase function and regulate the caspase cascade (Miller, 1999; Uren *et al*., 1999).

Human IAP homologues that have been identified are NAIP, c-IAP1, c-IAP2, XIAP and survivin (Deveraux *et al*., 1997; Takahashi *et al*., 1998). XIAP, c-IAP1 and c-IAP2 also contain a greatly conserved domain with E3 ubiquitination activity at their C-terminal ends. Proteins that interact with IAPs are therefore targeted for ubiquitination and degradation by the proteasome (Huang *et al*., 2000; Yang *et al*., 2000; Huang *et al*., 2001).

An important negative regulator of IAP activity is the protein Second mitochondria-derived activator of caspases (Smac), which is also known as Direct IAP-binding protein with low pI (DIABLO). Smac/DIABLO is one of the pro-apoptotic factors released from the mitochondria during apoptosis. It possesses a conserved tetrapeptide motif, which enables it to bind to IAPs. In so doing, it displaces bound caspases, thereby neutralising the inhibitory effect of IAPs on caspase activation (Du *et al*., 2000; Verhagen *et al*., 2000; Srinivasula *et al*., 2001).

1.7 Aim and objectives of the investigation

The aim of this investigation was to study and monitor three caspase-dependent apoptotic pathways (death receptor, mitochondrial-mediated and ER-stress induced) in a defined haematopoietic cell population (HL60 cells).

The objectives were as follows:

- To establish appropriate drug concentrations and exposure times required to induce different levels (low and high) of early apoptosis in the cells.

- To find pathway-specific markers for each pathway during the initial (Bip and FADD), intermediate (changes in mitochondrial transmembrane potential) and later (CHOP, cytochrome *c* release and caspase activation) stages of apoptosis.

- To optimise the assays and techniques required to detect these pathway-specific markers.

- To determine if the techniques are sensitive and reproducible and if the cell models are reliable.

- To determine if each marker is specific to its pathway or if there is cross talk between the pathways.

CHAPTER TWO

MATERIALS AND METHODS

2.2 Cell culture

2.1.1 Cell lines and culture conditions

The promyleocytic leukaemic HL60 (passage number 2; 01/11/1985), as well as the Jurkat (passage number unknown; gift from Division of Clinical Immunology at UCT) cell lines, were cultured in accordance with American Type Culture Collection (ATCC) protocol (ATCC: Cell Biology Collection, 2007). The HL60 cells were maintained at approximately 10^5-10^6 viable cells per ml in suspension in Iscoves Modified Dulbecco Medium (IMDM) (Gibco^{TM}, Invitrogen), which was supplemented with 20% (v/v) heat inactivated Foetal bovine serum (FBS) (Gibco^{TM}, Invitrogen). The Jurkat cell line was maintained at approximately 10^5-10^6 viable cells per ml in suspension in Roswell Memorial Park Institute (RPMI 1640) culture medium (Gibco^{TM}, Invitrogen), which was supplemented with 10% (v/v) FBS (Gibco^{TM}, Invitrogen). All cells were cultured in the absence of antibiotics. The cells were sustained at 37°C in a humidified (approximately 80-90% relative humidity) atmosphere with 5% carbon dioxide (CO_2).

2.1.2 Quantification of cells

2.1.2 A) Determination of cell viability

Cell viability was determined via Trypan blue (0.4% (w/v) Trypan blue in 1x PBS) staining and cell counting using a light microscope (Zeiss, West Germany) at 10x magnification. A drop of cell suspension, from the same sample of cells to be counted (section 2.1.2 B), was placed on a microscope slide. A drop of Trypan blue was placed on top of the cells and covered with a cover slip. Cell viability was expressed as %viable cells (unstained cells per 100 cells counted).

2.1.2 B) Determination of cell number

The cell number was determined using an automated cell counter, Coulter Counter® model ZF (Beckman Coulter, Florida USA). The Coulter Counter® settings were: amplification at ½, threshold at 60 units and aperture current at 1 mA. The average cell number calculated by the Coulter Counter® was multiplied by the %viability of the cells (section 2.1.2 A) to reflect the number of viable cells in the culture.

2.1.3 Culture initiation and maintenance

The cells (HL60 or Jurkat) were thawed and washed with pre-warmed (37°C) medium (IMDM and 20% (v/v) FBS), to remove the dimethylsulphoxide (DMSO) cryopreservant (Doyle *et al*., 1998). The cells were collected by centrifugation (MSE, UK) at 1500 revolutions per minute (RPM) for 10 min at room temperature. The supernatant was removed and the pellet resuspended in 2 ml fresh pre-warmed medium. The cell number and viability was determined as described in section 2.1.2.

Cells were plated at 10^5-10^6 cells per ml in 100mm x 20mm tissue culture dishes (Corning® Inc.). The growth medium was changed every 2-3 days to prevent depletion of nutrients and medium constituents. To maintain approximately 10^6 cells per ml of medium, the cells were collected through centrifugation (1500 RPM for 10 min at room temperature), the medium removed, and the pellet resuspended in fresh pre-warmed medium. The cell counts and viabilities were determined (as described in section 2.1.2) and the cells were plated at 10^5-10^6 cells per ml in 100mm x 20mm tissue culture dishes (Corning® Inc.).

2.1.4 Storage of cells

The cells were cryopreserved for future use in freezing solution (for HL60 cells: 70% (v/v) IMDM, 10% (v/v) DMSO, 20% (v/v) FBS and for Jurkat cells: 80% (v/v) IMDM, 10% (v/v) DMSO, 10% (v/v) FBS) according to Doyle *et al*. (1998) with some modifications. The freezing solution was kept on ice before addition to the cells. Cells were collected through centrifugation (1500 RPM for 10 min at room temperature), the medium removed, and the pellet resuspended in fresh medium. The cell counts and

viabilities were determined as described in section 2.1.2. The cells were then diluted with medium so that the final concentration of cells, after addition of the freezing solution, would be approximately 10^6 to 10^7 cells per ml. The freezing solution was added to the cell suspensions in a ratio of 1:1. Cells were frozen at -20°C over night (O/N) then placed at -80°C for short-term storage (at passage number 5 or 7 for HL60).

2.1.5 Drug treatment of cells over different exposure times (initial optimisation experiments)

The HL60 cells (passage number 14-16) were treated with Brefeldin A (BFA) (0.5 µg/ml - 30 µg/ml) for 6, 24 and 48 hrs to induce the ER-stress induced apoptotic pathway (Guillemain and Exton, 1997; Li *et al*., 2006). The HL60 cells (passage number 8-34) were treated with hydrogen peroxide (H_2O_2) (0.005 mM - 1.5 mM) for 6, 15 and 24 hrs to induce the mitochondrial-mediated apoptotic pathway (Hosokawa *et al*., 2005). FLAG-tagged FasL with ANTI-FLAG® M2 antibody (Sigma®-Aldrich, 2008) was used to induce the death receptor pathway via Fas receptor for both HL60 (passage number 35-37) (0.5 - 500 ng/ml FLAG-tagged FasL, 4 and 24 hrs) (Li, W. *et al*., 2006; Sigma®-Aldrich, 2008) and Jurkat (0.04 ng/ml - 5 ng/ml FLAG- tagged FasL for 4 hrs) (Huang *et al*., 1999; Sigma®-Aldrich, 2008) cells in the presence of 0.25 µg/ml or 0.5 µg/ml ANTI-FLAG® M2 antibody. The FLAG-tag (FLAG octapeptide: N-DYKDDDDK-C) is a polypeptide protein tag, which can be attached to a recombinant expressed protein to facilitate, for example, recognition by an antibody. For drug treatment, the drugs (BFA, H_2O_2, FasL) were always added with fresh medium (with FBS) to the cells.

2.1.6 Drug treatment of cells for analysis of all three apoptosis pathways (final experiments)

HL60 cells (passage number 11-19) (10^6 viable cells per ml, approximately 15-20 ml volume) were treated with BFA (5 µg/ml or 30 µg/ml) for 24 hours to induce the ER-stress induced apoptosis pathway (Guillemain and Exton, 1997). HL60 cells (passage number 16-20) (10^6 viable cells per ml, approximately 15-20 ml volume) were also treated with H_2O_2 (0.4 mM or 1 mM) for 24 hours to induce the mitochondrial-mediated

apoptotic pathway (Hosokawa *et al.*, 2005) (as determined in section 3.1.1.3). Jurkat cells (10^6 viable cells per ml, approximately 15-20 ml volume) were treated with FLAG-tagged FasL (0.2 ng/ml or 0.4 ng/ml) for 4 hrs, in the presence of 0.25 μg/ml ANTI-FLAG® M2 antibody, to induce the Fas-mediated death receptor pathway (Huang *et al.*, 1999; Sigma Aldrich, 2008) (as determined in section 3.1.1.3 D). The drugs (BFA, H_2O_2, FasL) were added to the cells with fresh medium (with FBS) each time. These drug-treated cells were used for the final experiments of section 3.2

2.2 Annexin V (AV) and Propidium Iodide (PI) labelling and flow cytometry

The percentage of apoptosing cells, after induction, was determined with Annexin V-fluorescein isothiocyanate (AV-FITC) and propidium iodide (PI) labelling using flow cytometry.

2.2.1 AV/PI labelling procedure

Following drug treatment, the cells were collected by centrifugation (Beckman GS-15R, Beckman Coulter, USA) (1500 RPM for 10 min at room temperature) and labelled with AV and PI according to the manufacturer's recommendations (Annexin V-FITC Apoptosis detection kit, Beckman Coulter). The cell pellets were washed once with ice-cold 1x PBS (Oxoid Dulbecco A Tablets, Typical formula: 140 mM NaCl, 2.7 mM KCl, 10 mM Na_2HPO_4, 1.8 mM KH_2PO_4) (pH 7.2), to remove culture medium and/or drug and centrifuged for 10 min, at 1500 RPM and 4°C. Following the removal of the PBS wash, the cells were resuspended in ice-cold 1x Binding buffer to $5x10^5$ - $5x10^6$ cells per 500 μl. From each cell suspension, 100 μl (of the 500 μl sample) was transferred to a new microcentrifuge tube and placed on ice. AV-FITC solution (1 μl of a 0.025 μg/μl stock solution) and PI solution (5 μl of a 0.25 μg/μl stock solution) were added to each tube, and mixed gently. The samples were subsequently incubated on ice, in the dark, for 15 min to allow for cell labelling. After the incubation period, 400 μl of 1x Binding buffer was added to each sample and the samples transferred to flow cytometry tubes for analysis on the flow cytometer (FC 500, Beckman Coulter, USA).

2.2.2 AV/PI flow cytometry analysis protocol

A flow cytometry protocol was first established using HL60 cells (passage number 16) treated with 10 μg/ml BFA for 24 hrs (Guillemain and Exton, 1997; Li *et al*., 2006). The cells were either labelled with AV or PI, or both, to allow for colour compensation of the small signal overlap between the two fluorochromes, AV (detected in the FL1 channel) and PI (detected in the FL4 channel). The experimental controls included: untreated cells (negative control), unlabelled cells (to test for auto-fluorescence) and cells treated with drug solvent (DMSO) only (to determine if it had an effect on fluorescence of the cells). All samples were prepared and analysed in triplicate.

The flow cytometry protocol was set up by adjusting the voltages of the FL1 (AV-FITC) and FL4 (PI) channels to obtain clear positive or negative peaks in each channel using the untreated and/or drug-treated cells. The protocol was set up so that there was a clear increase in fluorescence (positive peak) detected in the FL1 (AV-FITC) and FL4 (PI) channels for the drug-treated cells. Colour-compensation was also performed to obtain distinct cell populations in the colour-coded density plots (PI vs. AV plots). The resultant flow cytometer protocol, used to analyse both cell lines, incorporated the cytometer settings shown in Table 1.

Table 1: Flow cytometer settings for the AV and PI labelling protocol

	FS	**SS**	**FL1**	**FL2**	**FL3**	**FL4**	**FL5**	**AUX**
Voltage	189	663	318	337	402	295	530	300
Gain	2.0	5.0	1.0	1.0	1.0	1.0	1.0	1.0
	FS	**SS**	**FL1**	**FL2**	**FL3**	**FL4**	**FL5**	**AUX**
Discriminator	100	OFF	OFF	OFF	OFF	OFF	OFF	OFF
	FL1	**FL2**	**FL3**	**FL4**	**FL5**			
FL1		0	0	2.5	0			
FL2	0		0	0	0			
FL3	0	0		0	0			
FL4	0	0	0		0			
FL5	0	0	0	0				

2.2.3 Flow cytometer laser alignment verification

To ensure that the optical and fluidics systems were aligned for maximal detection of fluorescence signals, a flow cytometer laser alignment verification was performed on a regular basis. Beckman Coulter FLOW-CHECK^{TM} fluorospheres were used for this purpose according to manufacturer's instructions.

2.3 Western blot analysis

After drug treatment, levels of FADD, Bip and CHOP proteins (with β–actin as the invariant positive control) were determined by immunodetection. Proteins in whole cell extracts were immobilized on microporous polyvinylidene difluoride (PVDF) membrane and each specific protein was detected using the BM Chemiluminescence Western Blotting Kit (Mouse/Rabbit) (Roche, Germany).

2.3.1 Protein Extraction

HL60 cells (passage number 14-34) (10^6 cells per ml) were treated with 30 μg/ml BFA for 24 hrs to induce the ER-stress induced apoptotic pathway, after which they were collected via centrifugation (at 1500 RPM for 10 min at room temperature). The cell pellets were subsequently pooled to a density of approximately 10^7 cells per ml and washed once with ice-cold 1x PBS (pH 7.2) to remove any remaining culture medium and/or BFA. The cells were collected by centrifugation (Beckman GS-15R, Beckman, USA) at 1500 RPM for 10 min at 4°C and the PBS removed.

Ice-cold radioimmunoprecipitation (RIPA) buffer (0.05 M Tris-HCl, 1 mM EDTA, 15 mM NaCl, 1% Triton X-100, 1% NP-40, 0.1% SDS, 1x Protease inhibitors cocktail (Complete protease inhibitor cocktail tablets, Roche, Germany)) was added to each sample (approximately 100 μl of RIPA buffer to 10^7 cells). The samples were incubated on ice for 20 min to allow for complete cell lysis according to Pae *et al.* (2007) with some modifications. The samples were centrifuged (Beckman GS-15R, Beckman Coulter, USA) at 14000 RPM for 30 min at 4°C to pellet the cell debris, after which the

supernatant was transferred to new tubes (kept on ice). The protein lysates were stored in aliquots at -80°C.

Protein concentration was determined using the BCA™ protein assay kit (Pierce Biotechnology, USA) according to manufacturer's instructions. Briefly, protein standards were prepared using bovine serum albumin (BSA) diluted in RIPA buffer. The microplate procedure for preparing the samples was followed whereby 10 µl of each standard and unknown sample was added to the microplate wells followed by 200 µl of the BCA™ working reagent. The contents were subsequently mixed on a plate shaker for 30 sec, followed by incubation at 37°C for 30 min. The plate was cooled to room temperature, after which the samples' absorbances (562 nm) were measured using a NanoDrop® ND-1000 spectrophotometer (NanoDrop® Technologies, LLC, USA). A standard curve was drawn for the BCA™ protein standards and the equation of the curve was used to determine the protein concentrations of the unknown samples from their absorbance values.

2.3.2 Sodium dodecyl sulphate polyacrylamide gel electrophoresis of protein

Protein samples were resolved by discontinuous sodium dodecyl sulphate polyacrylamide gel electrophoresis (SDS-PAGE) according to the method described by Laemmli (1970). A Hoefer electrophoresis system (Hoefer, USA) and 12.5%T/3%C Glycine-SDS polyacrylamide gels were used. The Glycine-SDS polyacrylamide separating gels (12.5% T/3% C) were prepared by mixing 12.5 ml Glycine lower gel buffer (pH 8.8) (0.75 M Tris, 0.007 M SDS), 12.5 ml Acrylamide stock solution (48.5% (w/v) Acrylamide, 1.5% (w/v) Bis-acrylamide), 60 µl TEMED, 120 µl of 10% (w/v) APS (prepared fresh each time) and 24.7 ml sterile dH_2O (final volume of 50 ml). The Glycine-SDS polyacrylamide stacking gels (7.5% T/3%C) were prepared by mixing 7.5 ml Glycine upper gel buffer (pH 8.8) (0.25 M Tris, 0.007 M SDS), 4.5 ml Acrylamide stock solution (48.5% (w/v) Acrylamide, 1.5% (w/v) Bis-acrylamide), 60 µl TEMED, 120 µl of 10% (w/v) APS (prepared fresh each time) and 17.7 ml sterile dH_2O (final volume of 30 ml).

The protein samples were denatured by addition of 2x sample application buffer (SAB) (6% (w/v) SDS, 10% (v/v) β-mercaptoethanol, 20% (v/v) Glycerol, 0.125 M Tris.Cl

(pH 6.8), 0.02% (w/v) Bromphenol blue) in a ratio of 1:1. The samples were incubated in a rapidly boiling water bath for 10 min to allow for complete protein denaturation. The denatured protein samples were placed on ice to cool and then loaded into the gel wells (1-100 μg protein). A peqGOLD prestained protein marker III (Peqlab Biotechnologie GmbH, Germany) was used to determine protein sizes. The samples were electrophoresed using 1x Running buffer (0.25 M Tris, 1.29 M Glycine, 0.035 M SDS) at a constant current of 20 mA until the samples reached the separating gel interface, after which, the current was increased to 40 mA.

2.3.3 Transfer of protein onto PVDF membrane and immunodetection

Following electrophoresis, the proteins were transferred onto PVDF membrane by semi-dry electrophoretic transfer, according to the manufacturer's recommendations (PVDF Western Blotting Membranes, Roche, Germany and Trans-Blot® SD Semi-Dry Electrophoretic Transfer Cell, Bio-Rad, USA).

Briefly, the gel, extra thick filter paper (BioRad, USA) and PVDF membrane were incubated in Bjerrum and Schafer-Nielsen transfer buffer (48 mM Tris, 39 mM Glycine, 20% (v/v) Methanol, 0.038% SDS) for 30 min. This was to ensure that the filter paper was completely soaked through and the gel and PVDF membrane were entirely equilibrated in transfer buffer. The transfer stack was set up according to the instructions in the Trans-Blot® SD Semi-Dry Electrophoretic Transfer Cell instruction manual. The voltage was set for 15 - 23 V and the transfer process allowed to proceed for 30 - 60 min. The current was maintained at approximately 80 - 234 mA throughout the transfer process. After the transfer was complete, the gel was stained in heated (90°C) Coomassie Brilliant Blue staining solution (0.025% (w/v) Coomassie Brilliant Blue R250, 10% (v/v) Acetic acid) for approximately 30 min. The gel was destained in 10% (v/v) Acetic acid O/N, to check if the protein transfer was sufficient (Westermeier and Marouga, 2005). Due to the extreme hydrophobicity of the PVDF membrane, it was placed in methanol for a few seconds (before and after the transfer process) to allow it to wet in aqueous solutions. Afterwards the membrane was quickly rinsed twice with dH_2O to remove any residual methanol.

Chemiluminescence detection was performed using the BM Chemiluminescence Western Blotting Kit (Mouse/Rabbit) (Roche, Germany) according to the manufacturer's recommendations. Briefly, after the transfer procedure, the membrane was incubated O/N in 1% (v/v) Blocking solution (10 ml of 10% (w/v) stock solution of BM Chemiluminescence Western Blotting Kit Blocking reagent in 1x TBS (50 mM Tris, 150 mM NaCl)), at 4°C while rotating. This was to ensure that non-specific binding sites were blocked, thereby preventing non-specific binding of antibody to the membrane. After blocking the membrane, the 1% (v/v) Blocking solution was discarded and the membrane incubated with primary antibody solution.

The polyclonal primary antibodies used were against β-actin, Bip and FADD (human specific) (Cell Signaling Technology®, Inc.), as well as the monoclonal GADD153 (CHOP) antibody (Santa Cruz Biotechnology Inc., USA). The Bip and FADD antibodies were diluted in a ratio of 1:500 in 0.5% (v/v) Blocking solution (5 ml of 10% (w/v) stock solution of BM Chemiluminescence Western Blotting Kit Blocking reagent in 1x TBS), whereas the β-actin antibody was diluted in a ratio of 1:1000. The GADD153 antibody was diluted for use at concentrations ranging from 0.4 - 8 µg/ml (antibody stock was supplied at 200 µg/ml) to find the optimal concentration required for CHOP detection. (In the final experiments (section 3.2.2), the GADD153 antibody was used at a concentration of 1 µg/ml.) All antibody stocks were diluted with 0.5% (v/v) Blocking solution for use. All primary antibodies were incubated with the membrane at 4°C O/N, while rotating, to allow antibody binding to the immobilized antigen. After incubation with primary antibody, the membrane was washed twice with Tris buffered saline plus Tween-20 (TBST) (0.1% (v/v) Tween 20® in 1 L TBS) for 10 min each, followed by two 10 min washes with 0.5% (v/v) Blocking solution.

The membrane was incubated in the horseradish peroxidase (POD)-conjugated secondary antibody (anti-mouse/rabbit IgG) solution for 30 min at room temperature with constant shaking (to allow binding to the primary antibody). The secondary antibody was used at a concentration of 40 mU/ml for β-actin, Bip and FADD and 40-160 mU/ml for the GADD153 antibody. (In the final experiments of section 3.2.2, 160 mU/ml secondary antibody was used for GADD153 immunodetection). Following this, the membrane was first rinsed with TBST and then washed four times for 15 min each in TBST. For membranes probed with GADD153 antibody and incubated in 80 - 160

mU/ml secondary antibody, the number of washes in TBST was increased to six times for 15 min each.

Afterwards, the membrane was incubated in detection reagent (BM Chemiluminescence Western Blotting Kit starting solution B added to substrate solution A in a 1:100 ratio) for 60 s. The membrane was placed between two transparent plastic sheets and exposed to X-ray film (Fuji Super RX Medical X-ray Film, Fuji Photo Film Co., Ltd., Japan). The film was exposed for different time intervals (1 - 60 min) depending on the strength of the signal obtained. The exposed films were immediately developed using fixer and replenisher solutions from Axim Africa X-ray Industrial & Medical (PTY) Ltd., RSA.

2.3.4 Determination of optimal protein concentration required for detection

Protein was extracted (section 2.3.1) from untreated HL60 cells, separated according to size via SDS-PAGE (section 2.3.2) and transferred onto PVDF membrane (section 2.3.3) (30 min transfer at 22-23 V). The optimal concentration of protein (1 - 100 μg) required for detection was determined by probing the membrane with β-actin antibody (1:1000) (section 2.3.3) after transfer.

2.3.5 Stripping and reprobing of membranes

After development of the X-ray film, the membrane was stripped and reprobed according to manufacturer's instructions (BM Chemiluminescence Western Blotting Kit (Mouse/Rabbit), Roche, Germany) with some modifications. Briefly, the membrane was incubated in stripping solution (0.7% (v/v) β-mercaptoethanol, 2% (w/v) SDS, 0.0625 M Tris.Cl (pH 6.7)) for 30 min at 50°C while shaking. The membrane was washed twice for 10 min each and twice for 5 min each with TBST at room temperature, after which, it was incubated O/N in 1% (v/v) Blocking solution (at 4°C while rotating). The membrane was subsequently reprobed with primary antibodies and exposed to film as described in section 2.3.3).

In the final experiments of (section 3.2.2) the membrane was first probed with GADD153 antibody and subsequently stripped and reprobed with Bip and FADD

antibodies (together). The membrane was stripped a second time and reprobed with β-actin antibody.

2.5.6 Densitometric analysis

Darker images of the western blots were shown in Figs. 46 A and 47 A (section 3.2.2) so that the lighter bands appear more visible, since the figures come out lighter when printed. However, only bands that fell within the linear range of exposure, and were neither underexposed nor overexposed, were used to obtain the densitometric data of section 3.2.2. The densitometric analysis was performed using UVIgeltec version 12.4 software (UVItec Limited, UK). Results were obtained from the two western blot analysis performed for all drugs (BFA, H_2O_2 and FasL), after normalisation with β-actin.

2.6 Caspase activity assays

Caspase activity was measured by fluorogenic detection of the enzymatically cleaved product, 7-Amino-4-methylcoumarin (AMC) (AnaSpec, Inc., USA) (Anaspec, 2007). AMC, a synthetic fluorogenic compound, acts as a reporter molecule for caspase activity after the hydrolysis of the peptide-AMC (caspase substrate) bond by the caspase enzyme. This cleavage releases AMC, thus resulting in an increase in fluorescence.

2.4.1 Preparation of cell lysates for caspase assays

Following drug treatment, cell lysates were prepared according to the method described by Proteus BioSciences Inc.© ZappaZyme™ Enzyme Activity Assay Protocol (2007). The cells were pelleted (10 min at 1500 RPM and room temperature), the supernatant discarded, the pellets washed with 1x PBS (10 min at room temperature and 1500 RPM), and the wash removed. The cell pellets were resuspended in 100 µl ice-cold Cell lysis buffer (10 mM HEPES (pH 7.4), 0.1% CHAPS, 5 mM DTT (added fresh each time), 2 mM EDTA) (with or without the addition of protease inhibitor cocktail) per 10^7 cells. The samples were mixed and incubated on ice for approximately 30 - 60 min for cell lysis to occur. The samples were vortexed every 10 - 15 min to promote cell lysis. After 30 min incubation, a small volume of sample was placed on a microscope slide

and viewed to assess cell lysis. Following complete cell lysis, the samples were centrifuged (Beckman GS-15R, Beckman Coulter, USA) at 4°C for 30 min and at 14000 RPM to pellet the cell debris. The supernatants were transferred to clean tubes and kept on ice while the protein concentration was determined.

Protein concentration was determined using a Qubit™ Fluorometer and the Qubit™ assay system for proteins (Invitrogen) according to manufacturer's instructions. The incubation time, to ensure that the assay samples reach the optimal fluorescence, was 15 min at room temperature. The assay is accurate for protein concentrations from 12.5 µg/ml - 5 mg/ml and exhibits low protein-to-protein variation. The lysates were stored at -80°C in aliquots to avoid freeze-thaw cycles.

2.4.2 Initial caspase assay optimisations

2.4.2.1 Initial caspase assay protocol

The caspase activity assays were performed in black 96-well plates (Nunc™, Apogent™, Denmark) and were set up as described in Table 2. The following caspase substrates (AnaSpec, Inc., USA) were used: Ac-D-M-Q-D-AMC for caspase-3, Ac-L-E-V-D-AMC for caspase-4, Ac-I-E-T-D-AMC for caspase-8 and Ac-L-E-H-D-AMC for caspase-9 (Köhler *et al*., 2002; Anaspec, 2007). These caspase substrates consist of peptides (with the specific amino acid residues recognized and cleaved by its specific caspase) that are labelled with AMC.

Table 2: Components of caspase assay per well

Sample:	**Caspase substrate (1mM stock):**	**Cell lysis buffer:**	**25x Caspase Reaction Buffer:**	**dH_2O:**	**Protein (cell lysate):**
Blank	12.5-75 µM	*x* µl *****	1x	Up to 200 µl ******	/
Experiment	12.5-75 µM	/	1x	Up to 200 µl ******	1-10 µg (*x* µl *****)

***** Cell lysis buffer was added in equal volume to blank wells as that of protein volume added to experimental wells

****** Total volume per well (and assay) was 200 µl

All assay components were equilibrated to room temperature before use and DTT was added fresh to the assay buffers before addition to the well plate. The 25x Caspase Reaction Buffer consisted of 250 mM PIPES (pH 7.4), 2.5% CHAPS, 125 mM DTT and 50 mM EDTA. Once all assay components were added, the well plate was mixed on a shaker for 30 s and incubated at 37°C for 60 - 120 min prior to reading on the fluorimeter.

2.4.2.2 Determination of optimal incubation time

To determine the optimal incubation time required for maximal fluorescence detection (Relative Fluorescence Units (RFU)), caspase activity (using 50 µM caspase-3 substrate per reaction) was established after different incubation times.

Cell lysates (1, 5 or 10 µg protein) from HL60 cells (passage number 32), treated with 2.5 µg/ml - 30 µg/ml BFA for 24 hrs were used in caspase activity assays (as described in Table 2). The assay samples were incubated at 37°C for 60 min. Sample readings were then taken at 5 min intervals (60-85 min), with the well plate placed at 37°C in between readings, and the RFU determined.

Caspase activity was also established after 120 min incubation at 37°C using BFA treated (30 µg/ml BFA; 24 hrs) HL60 cell (passage number 31-40) lysates (5 µg protein).

2.4.2.3 Optimal caspase substrate concentration

To determine the optimal caspase substrate concentration required, different concentrations of caspase-3 substrate (12.5 µM, 25 µM, 50 µM and 75 µM) were added to sample reactions (were set up as described in Table 2). Cell lysates (5 µg of protein) from HL60 cells (passage number 32-41), treated with 1.5 mM H_2O_2 for 24 hrs, were used. The samples were set up as described in Table 2 and analysed as described in section 2.4.3.

2.4.3 Fluorimeter settings

Sample fluorescence was detected by a Cary Eclipse fluorimeter (Varian, USA) with the excitation wavelength set at 354 nm and emission wavelength at 442 nm. The sample readings were given in Relative Fluorescence Units (RFUs) and were converted to AMC release (µM) by the standard curve obtained from the AMC standards (section 2.4.4).

Initially, to find the optimal fluorimeter settings, the instrument gain (PMT Voltage) was set to either medium or high and the excitation and emission slits were both set at either 5, 10 or 20 nm before taking sample readings. It was found that by setting both the excitation and emission slits at 20 nm and changing the instrument gain (PMT Voltage) to high (maximum) that increased fluorescence signals for the samples were produced. The average reading time per sample well was set at 0.1 seconds to avoid longer reading times. At these settings the RFU values of the samples could clearly be distinguished and analysed.

Initially an automatic blank setting was used for analysis, but this was found to be unreliable. Instead, blank readings were taken in triplicate and the average blank value was manually subtracted from the average value obtained for each sample, which was also prepared and analysed in triplicate.

2.4.4 AMC standard curve

For the AMC standard curve, decreasing concentrations of AMC (3.13 µM - 0.0975 µM) (Anaspec, 2007) were prepared by serially diluting the AMC stock solution (10 mM AMC in DMSO) with dH_2O. The AMC standard wells contained the components set out in Table 3.

Table 3: Components of AMC standards per well

Sample:	25x Caspase Reaction Buffer:	AMC working solution (12.5 µM):	dH_2O:
Blank	1x	0 µl	Up to 200 µl **
3.13 µM AMC	1x	50 µl	Up to 200 µl **
1.56 µM AMC	1x	25 µl	Up to 200 µl **
0.78 µM AMC	1x	12.5 µl	Up to 200 µl **
0.39 µM AMC	1x	6.25 µl	Up to 200 µl **
0.195 µM AMC	1x	3.13 µl	Up to 200 µl **
0.0975 µM AMC	1x	1.56 µl	Up to 200 µl **

** Total volume per well was 200 µl

AMC standards were prepared in triplicate for each caspase assay. The blank value was automatically subtracted from sample values by the fluorimeter machine. The RFU of the caspase assay samples were converted to AMC release (µM) using the AMC standard curve's equation.

2.4.5 Caspase assay for final experiments

For the final experiments, caspase activity assays were performed for all three apoptotic pathways after drug treatment (section 2.1.6). The experiments were performed twice for each drug (low and high concentrations) using all four caspase substrates. This was done to determine which caspase(s) was activated for the specific drug treatment/apoptosis pathway (section 3.2.3). One protein sample per drug concentration (untreated, low dose and high dose) was prepared (section 2.4.1) from each experiment (BFA, H_2O_2 or FasL) for analysis. Cell lysates from HL60 cells (passage number 17-19) treated with BFA (30 µg/ml, 24 hrs) were used as a positive control for caspase-3 activity in all experiments performed. All samples were prepared and analysed in triplicate (from one sample- either untreated, low dose or high dose). The assays were set up as described in Table 4.

Table 4: Components of final caspase assays per well

Sample:	**Caspase substrate (1mM stock):**	**Cell lysis buffer:**	**25x Caspase Reaction Buffer :**	**dH_2O:**	**Protein (cell lysate):**
Blank	50 µM	*x* µl *****	1x	Up to 200 µl ******	/
Experiment	50 µM	/	1x	Up to 200 µl ******	10 µg (*x* µl *****)

***** Cell lysis buffer was added in equal volume to blank wells as that of protein volume added to experimental wells
****** Total volume per well (and assay) was 200 µl

All assay components were equilibrated to room temperature before use and DTT was added fresh to the assay buffers before addition to the well plate. Once all assay components were added, the well plate was mixed on a shaker for 30 s and incubated at 37°C for 60 min prior to reading on the fluorimeter.

2.4.6 Statistical analysis for caspase assays

A t-Test (paired two sample for means) was performed to compare caspase activity (of each caspase) of the low drug doses to the high drug doses, for each experiment and drug (BFA, H_2O_2 or FasL). The mean differences were considered significant when the *p*-value was less than 0.05 (level of significance was 0.05).

2.7 Cytochrome *c* release immunohistochemistry assays

2.5.1 Preparation of cells for immunohistochemistry assays

The HL60 cells (untreated or treated with 1.5 mM H_2O_2 for 24 hrs) (passage number 13-45) were transferred from the culture dishes to microcentrifuge tubes and centrifuged (Beckman GS-15R, Beckman Coulter, USA) at room temperature for 10 min at 1500 RPM. The medium was removed and the cells washed with 1x PBS to remove culture medium and/or apoptosis inducing agents. The samples were centrifuged for 10 min at 1500 RPM and room temperature, after which the PBS wash was removed and the cells

resuspended in 1x PBS to 10^5 - 10^7 cells per ml. From each sample, 100 µl cell suspension (10^4 - 10^6 cells) was taken and placed in a cytospin (Shandon, USA). This concentrated the cells in a smaller area and removed excess liquid, thereby allowing the specimens on the microscope slides to dry faster. Following cytospin, the slides were allowed to dry for approximately 10 min, after which the cells were fixed to the slides.

2.5.2 Initial cytochrome *c* immunohistochemistry assay

The first immunohistochemistry procedure was performed according to manufacturer's recommendations (Santa Cruz Biotechnology, Inc., USA) with modifications. Briefly, the cells (10^4 - 10^6 cells per slide) were fixed with 1-3 drops of ice-cold methanol for 5 min and air-dried. The slides were briefly washed three times in 1x PBS to remove the methanol. The excess liquid was removed from the slides and the specimens were incubated in 1-3 drops of undiluted FBS for 20 min to block non-specific binding sites. The slides were rinsed with 1x PBS and the excess liquid removed. The samples were incubated for 2 hrs at room temperature with cytochrome *c* (6H2)-phycoerythrin (PE) labelled murine monoclonal antibody (0.4 µg/ml and 4 µg/ml) (Santa Cruz Biotechnology, Inc., USA), which was diluted for use with FBS. The cells were not incubated in the dark.

After incubation with the antibody, the slides were first rinsed, and then washed twice with 1x PBS for 5 min each on a stir plate. The excess liquid was removed from the slides and 1-2 drops of 1,4-Diazabicyclo-octane (DABCO) (Sigma®-Aldrich) mounting medium was placed over the specimen and covered with a glass coverslip. DABCO is a colourless antifade mounting medium, which prevents or minimizes photobleaching of the fluorescent dye conjugates when they are excited by UV light (required for visualization).

2.5.3 Cytochrome *c* immunohistochemistry assays using different cell permeabilization protocols to improve antibody labelling

Untreated HL60 cells (10^5 cells per slide) were either fixed and permeabilized using the IntraPrep™ kit (Immunotech, Coulter) or via methanol fixation and permeabilization, using permeabilization buffer.

Briefly, the cells were fixed with either 1-3 drops of ice-cold methanol or IntraPrep^{TM} fixation reagent (IntraPrep^{TM} Kit, Immunotech, Coulter) for 5 min and air-dried. The slides were briefly washed three times in 1x PBS to remove the fixatives. The excess liquid was removed from the slides and the specimens were either incubated in 1-3 drops of cold permeabilization buffer (0.2% Triton X-100 in 1x PBS) or IntraPrep^{TM} permeabilization reagent (IntraPrep^{TM} Kit, Immunotech, Coulter) for 15 min. The cells were blocked with 1-3 drops of 10% (v/v) Blocking solution (BM Chemiluminescence Western Blotting Kit Blocking reagent) for 20 min. The slides were rinsed with 1x PBS and the excess liquid removed.

The cells were either incubated with cytochrome *c* (6H2)-PE labelled murine monoclonal antibody (4 µg/ml) or 1.5% (v/v) Blocking solution (unstained, to test for auto-fluorescence) for 2 hrs at room temperature in the dark. After the cells were labelled, the slides were first rinsed, and then washed twice with 1x PBS for 5 min each on a stir plate. The excess liquid was removed from the slides and 1-2 drops of VECTASHIELD® (Vector Laboratories, USA) mounting medium was placed over the specimen and covered with a glass coverslip. VECTASHIELD® is also an antifade mounting medium but, unlike DABCO, it contains a counterstain. VECTASHIELD® mounting medium contains 4',6-diamidino-2-phenylindole (DAPI), which is a fluorescent dye that specifically stains the nuclei of cells by binding double-stranded DNA, thereby assisting in visualizing the cells.

2.5.4 Cytochrome *c* immunohistochemistry assay optimisation with higher antibody concentration

Untreated and H_2O_2 treated (1.5 mM H_2O_2 for 24 hrs) HL60 cells (10^5 cells per slide) were fixed with 1-3 drops of ice-cold methanol for 5 min and air-dried. The slides were briefly washed three times in 1x PBS to remove the fixative. The excess liquid was removed from the slides and the specimens were incubated in 1-3 drops of cold permeabilization buffer (0.2% Triton X-100 in 1x PBS) for 15 min. The excess liquid was removed and the cells blocked with 1-3 drops of 10% (v/v) Blocking solution (BM Chemiluminescence Western Blotting Kit Blocking reagent) for 20 min. The slides were rinsed with 1x PBS and the excess liquid removed.

The cells were either incubated with cytochrome *c* (6H2)-PE labelled antibody (8 µg/ml and 20 µg/ml), IgG1 (mouse)-PE conjugated monoclonal antibody (2.5 µg/ml) (IOTest®, Beckman Coulter) or 1.5% (v/v) Blocking solution (unstained) for 2 hrs in the dark at room temperature. The IOTest® IgG1 (mouse)-PE conjugated monoclonal antibody was used as an isotypic control to test for non-specific labelling and fluorescence (IOTest®, Beckman Coulter). After the cells were labelled, the slides were first rinsed, and then washed twice with 1x PBS for 5 min each on a stir plate. The excess liquid was removed from the slides and 1-2 drops of VECTASHIELD® (Vector Laboratories, USA) mounting medium was placed over the specimen and covered with a glass coverslip.

2.5.5 Immunohistochemistry assays to determine cell membrane permeability

Untreated and H_2O_2 treated (1.5 mM H_2O_2 for 24 hrs) HL60 cells (10^5 cells per slide) were fixed with 1-3 drops of ice-cold methanol for 5 min and air-dried. The slides were briefly washed three times in 1x PBS to remove the fixative. The excess liquid was removed from the slides and the specimens were either incubated with 1-3 drops of cold permeabilization buffer or 1x PBS (methanol-fixation only) for 15 min. The excess liquid was removed and the cells blocked with 1-3 drops of 10% (v/v) Blocking solution (BM Chemiluminescence Western Blotting Kit Blocking reagent) for 20 min. The slides were rinsed with 1x PBS and the excess liquid removed.

The cells were either incubated with 20 µl of CD45-FITC murine monoclonal antibody (Stem-Kit™ Reagents, Beckman Coulter) (diluted in 30 µl 1.5% (v/v) Blocking medium), 2.5 µg/µl PI (Annexin V-FITC Apoptosis detection kit, Beckman Coulter) or 1.5% (v/v) Blocking solution (unstained). The CD45-FITC antibody and PI were incubated in the dark at room temperature for 20 min and 15 min, respectively. The cells stained with PI (Annexin V-FITC Apoptosis detection kit, Beckman Coulter) served as a positive control for permeabilized cell membranes. The CD45-FITC murine monoclonal antibody (Stem-Kit™ Reagents, Beckman Coulter) was used as a positive control to determine cell viability, since it binds to the CD45 family of cell-surface markers of intact haematopoietic cells. After the cells were labelled, the slides were first rinsed, and then washed twice with 1x PBS for 5 min each on a stir plate. The excess

liquid was removed from the slides and 1-2 drops of VECTASHIELD® (Vector Laboratories, USA) mounting medium was placed over the specimen and covered with a glass coverslip.

2.5.6 Cleaved caspase-3 (Asp175) antibody immunohistochemistry assay to determine viability of assay protocol

Untreated and H_2O_2 treated (1.5 mM H_2O_2 for 24 hrs) HL60 cells (10^5 cells per slide) were fixed with 1-3 drops of ice-cold methanol for 5 min and air-dried. The slides were briefly washed three times in 1x PBS to remove the fixative. The excess liquid was removed from the slides and the specimens were permeabilized with 1-3 drops of cold permeabilization buffer for 15 min. The excess liquid was removed and the cells blocked with 1-3 drops of 10% (v/v) Blocking solution (BM Chemiluminescence Western Blotting Kit Blocking reagent) for 20 min. The slides were rinsed with 1x PBS and the excess liquid removed.

The cells were either incubated with cleaved caspase-3 (Asp175) polyclonal rabbit antibody (Alexa Fluor®488 (FITC) conjugate) (Cell Signaling Technology®, Inc.), IgG1 (mouse)-FITC conjugated monoclonal antibody (IOTest®, Beckman Coulter) (isotypic control to test for non-specific labelling) or 1.5% (v/v) Blocking solution (unstained). The cleaved caspase-3 antibody was diluted 1:10 for use (with 1.5% (v/v) Blocking solution) whereas the IgG1-FITC antibody was used at 2.5 µg/ml. The cells were incubated O/N in the dark at 4°C. After the cells were labelled, the slides were first rinsed, and then washed twice with 1x PBS for 5 min each on a stir plate. The excess liquid was removed from the slides and 1-2 drops of VECTASHIELD® (Vector Laboratories, USA) mounting medium was placed over the specimen and covered with a glass coverslip.

2.5.7 Immunohistochemistry assays without cell permeabilization for cytochrome *c* (6H2)-PE and cleaved caspase-3-FITC antibodies

Untreated and H_2O_2 treated (1.5 mM H_2O_2 for 24 hrs) HL60 cells (10^5 cells per slide) were fixed with 1-3 drops of ice-cold methanol for 5 min and air-dried. The slides were briefly washed three times in 1x PBS to remove the fixative. The excess liquid was

removed from the slides and the cells blocked with 1-3 drops of 10% (v/v) Blocking solution (BM Chemiluminescence Western Blotting Kit Blocking reagent) for 20 min. The slides were rinsed with 1x PBS and the excess liquid removed.

The cells were incubated with either cytochrome *c* (6H2)-PE antibody (8 µg/ml), cleaved caspase-3-FITC antibody (1:10 dilution), IgG1-PE antibody (2.5 µg/ml), IgG1-FITC antibody (2.5 µg/ml) or 1.5% (v/v) Blocking solution (unstained control). The cytochrome *c* (6H2)-PE and IgG1-PE antibodies (with the unstained controls) were incubated in the dark for 2 hrs at room temperature. The cleaved caspase-3 (Asp175) and IgG1-FITC antibodies (with the unstained controls) were incubated O/N in the dark at 4°C. After the cells were labelled, the slides were first rinsed, and then washed twice with 1x PBS for 5 min each on a stir plate. The excess liquid was removed from the slides and 1-2 drops of VECTASHIELD® (Vector Laboratories, USA) mounting medium was placed over the specimen and covered with a glass coverslip.

2.5.8 Different immunohistochemistry assay protocol for cytochrome *c* release

The second immunohistochemistry procedure was performed according to the method used by the Cardiovascular Research Unit (MRC/UCT Cape Heart Centre). Briefly, the cells were spun onto slides, as described in section 2.5.1, and fixed with ice-cold methanol for 5 min and air-dried. The slides were briefly washed three times in 1x TBS, pH 7.5 (50 mM Tris, 150 mM NaCl), to remove the methanol, and blocked for 20 min in 1-3 drops of 1% (w/v) BSA (1 g BSA in 100 ml 1x PBS), after which they were rinsed with 1x TBS.

The cells were incubated with either cytochrome *c* (6H2)-PE antibody (2 or 4 µg/ml), IgG1 (mouse)-PE antibody (2.5 µg/ml) or 1% (w/v) BSA (unstained control) for 2 hrs at 37°C in the dark. After incubation, the slides were first rinsed then washed twice with 1x TBS for 5 min each on a stir plate. The excess liquid was removed from the slides and 1 drop of VECTASHIELD® mounting medium was placed over the specimen and covered with a glass coverslip.

2.5.9 Visualization of cells

After covering the cells with mounting medium, the slides were viewed using a fluorescent Nikon Eclipse 90i microscope (Nikon, USA). The microscope was equipped with a colour camera (Nikon DXM 1200c) and NIS imaging software to analyse the specimens. The microscope had four channels, DAPI, FITC, Cy3 (PE) and DIA (triple band, able to visualize DAPI, FITC, and Cy3 simultaneously) that could detect specific fluorescence signals. The microscope was adjusted to a gamma setting of 0.45, exposure of 210 ms - 10 s and a gain setting of normal or high.

2.6 Detection of changes in mitochondrial transmembrane potential (MTP) during apoptosis induction

Induction of the mitochondrial-mediated apoptosis pathway causes changes in the membrane potential of the mitochondria (Dror, 2003; Skommer *et al*., 2007). The MitoCapture^{TM} apoptosis detection kit (BioVision Research Products, USA) uses a fluorescent-based technique that allows for the detection of changes in mitochondrial transmembrane potential (MTP) upon induction of apoptosis.

MitoCapture^{TM} is a cationic dye similar to JC-1 (5,5',6,6'-tetrachloro-1,1',3,3'-tetraethylbenzimidazolo-carbocyanine iodide), which changes conformation depending on the status of the cell it enters (Lugli *et al*., 2005; Chaoui *et al*., 2006). An interchange between the dye monomers (in the cytoplasm) and aggregates (inside the mitochondria) exist within the cell, depending on the MTP. The MTP will determine how much dye is taken up by the mitochondria or how much remains in the cytosol. In healthy, non-apoptotic cells, the dye accumulates and aggregates within the mitochondria, producing a bright red fluorescence that is detected in the PE (Em = 488/590 ± 42 nm) channel. However, the MitoCapture^{TM} dye molecules cannot be taken up by the mitochondria in apoptotic cells, as a result of the changed or disrupted MTP. It therefore resides in the cytosol in its monomer form, which produces a green fluorescence that is detected in the FITC (Em = 488/530 ± 30 nm) channel.

2.6.1 MitoCapture™ labelling procedure

The MitoCapture™ labelling protocol was performed according to manufacturer's recommendations (BioVision Research Products, USA). Briefly, after treatment the cells were collected at room temperature by centrifugation (Beckman GS-15R, Beckman, USA) for 10 min at 1500 RPM. The cell pellets were washed once with 1x PBS to remove culture medium and/or apoptosis inducing agents and centrifuged for 10 min at 1500 RPM and room temperature. Cell pellets were resuspended in MitoCapture™ solution (1 µl MitoCapture™ reagent diluted in 1 ml pre-warmed (37°C) MitoCapture™ Incubation buffer) to 10^6 cells per ml. The cells were incubated for 20 min at 37°C in a 5% CO_2 incubator, after which they were centrifuged at room temperature for 10 min at 1500 RPM and the supernatant discarded. The pellets were resuspended in 1 ml of pre-warmed MitoCapture™ Incubation buffer and transferred to flow cytometry tubes for analysis on the flow cytometer (FC 500, Beckman Coulter, USA).

2.6.2 MitoCapture™ flow cytometry analysis protocol

Firstly, a flow cytometry protocol for detecting changes in MTP was created. HL60 cells (passage number 33-41) were treated with 0.4 mM or 1 mM H_2O_2 for 24 hrs and labelled with MitoCapture™, to serve as positive controls for setting up the flow cytometry protocol. Untreated MitoCapture™-labelled HL60 cells were used as negative controls. Unlabelled (untreated and drug-treated) cells were used to test for auto-fluorescence. These controls were included to confirm that the protocol was set up and working correctly. All samples were prepared and analysed in triplicate.

The flow cytometry protocol was set up so that the cells would either fluoresce in the PE (FL2) channel or FITC (FL1) channel depending on their transmembrane potential. The voltages of the FL1 and FL2 channels were adjusted to obtain clear positive or negative peaks in each channel using the untreated and/or drug-treated cells. Colour-compensation was also performed to obtain distinct cell populations in the colour-coded density plots (FL2 Log vs. FL1 Log plots). The flow cytometer protocol used to analyse the cells incorporated the cytometer settings shown in Table 5. (Using this flow

cytometer protocol, no auto-fluorescence was noted for the untreated or drug-treated unlabelled cells in incubation buffer only.)

Table 5: MitoCapture™ assay protocol flow cytometer settings

	FS	**SS**	**FL1**	**FL2**	**FL3**	**FL4**	**FL5**	**AUX**
Voltage	189	663	313	340	402	450	577	300
Gain	2.0	5.0	1.0	1.0	1.0	1.0	1.0	1.0
	FS	**SS**	**FL1**	**FL2**	**FL3**	**FL4**	**FL5**	**AUX**
Discriminator	100	OFF	OFF	OFF	OFF	OFF	OFF	OFF
	FL1	**FL2**	**FL3**	**FL4**	**FL5**			
FL1		80.2	0	0	0			
FL2	73.6		0	0	0			
FL3	0	0		0	0			
FL4	0	0	0		0			
FL5	0	0	0	0				

2.6.3 Fluorescent microscopy of MitoCapture™ labelled cells

MitoCapture™ labelled cells were also visualised using a fluorescent microscope to verify and compare it to the flow cytometer results. A drop of MitoCapture™ labelled cells were placed on a microscope slide and covered with a coverslip. The cells were viewed under the Nikon Eclipse 90i fluorescent microscope (Nikon, USA) using the DIA (triple band), FITC and Cy3 (PE) channels, at a gamma setting of 0.45, exposure of 333 ms and a gain setting at high.

CHAPTER THREE

RESULTS

3.1 Development and optimisation of assays to monitor apoptosis pathways in cells

3.1.2 Analysis of the general apoptotic response to drug treatment

After drug treatment, the percentage of cells that were committed to and undergoing apoptosis was determined with AV/PI labelling using flow cytometry, as described in section 2.2.

3.1.1.1 AV and PI labelling flow cytometry analysis protocol

Fig. 11 shows the typical fluorescence results obtained from AV/PI labelled cells using the colour-compensated protocol established in section 2.2.2 (and cytometer settings shown in Table 1).

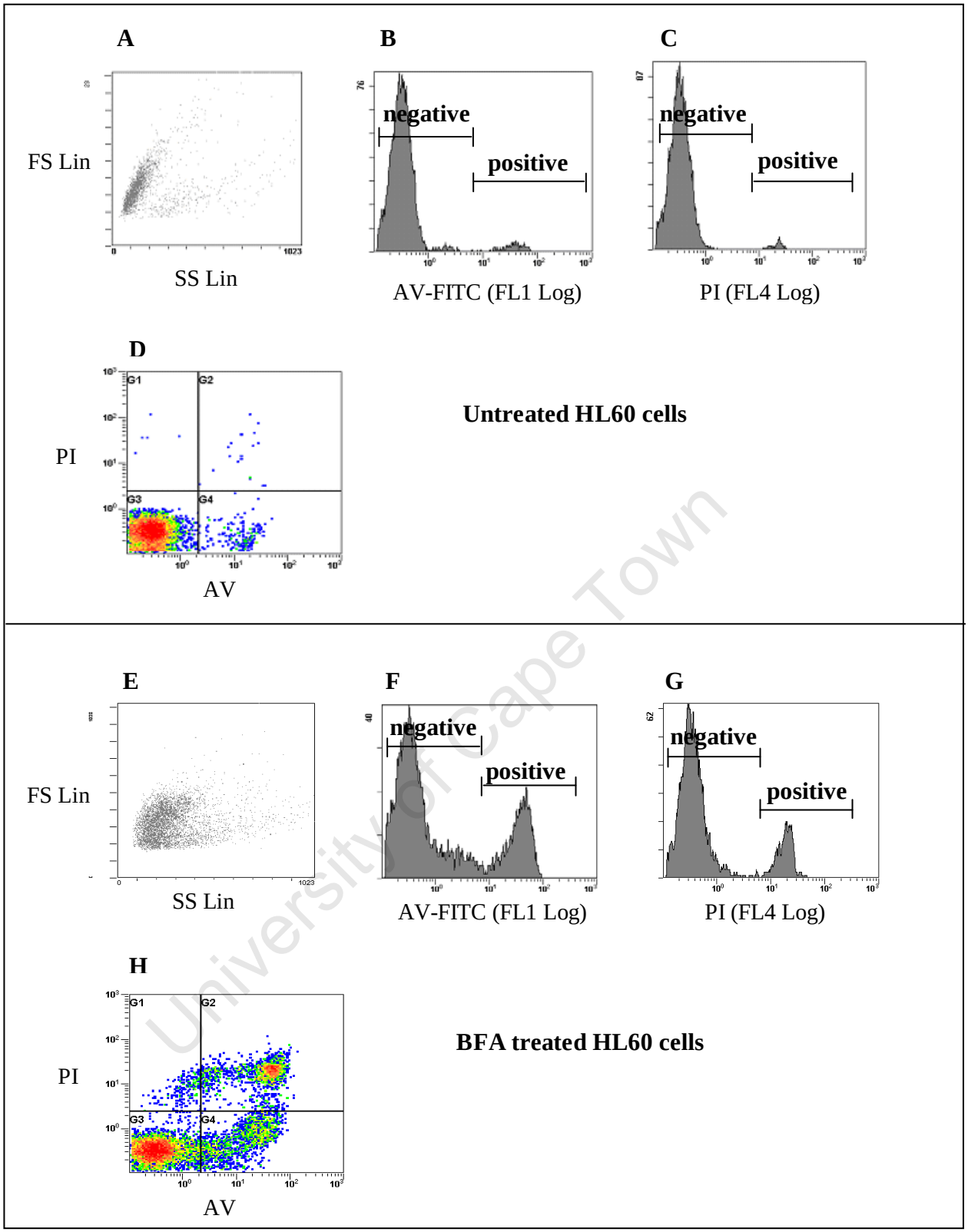

Fig. 11. Flow analysis of AV-FITC and PI labelled HL60 cells showing an increase in apoptosis after BFA treatment. HL60 cells were treated with 10 µg/ml BFA (24 hrs) (**E,F,G,H**) or untreated (**A,B,C,D**) and labelled with both AV and PI. The FS vs. SS plots for untreated (**A**) and drug-treated (**E**) cells show the different sizes and granularity of the cell population. The FL1-FITC histograms show the negative and positive peaks for AV-FITC labelling for untreated (**B**) and drug-treated (**F**) cells. The FL4 histograms show the negative and positive peaks for PI labelling for untreated (**C**) and drug-treated (**G**) cells. The colour-coded density plots (untreated (**D**) and drug-treated (**H**) cells) show the status of the apoptosing cells, either labelling with high PI and/or low AV (G1- mainly cellular debris containing DNA), both AV and PI (G2- late apoptosis), high AV and/or low PI (G4- early apoptosis) or low labelling cells (G3- viable cells). The different colours represent the number and density of cells in a specific area with red representing the most densely populated areas and blue the least dense.

The forward scatter (FS) setting indicates the sizes of the cells in the culture population, whereas the side-scatter (SS) shows the granularity of the cells (Fig. 11 A). A discriminator was set at 100 for the FS setting to eliminate most of the cellular debris, which was detected below 100 FS (Table 1).

The cells, untreated and drug-treated, were either labelled with AV or PI or both to obtain two defined peaks by altering the voltage settings on the flow cytometer. The two peaks that occur in the histograms in Figs. 11 B, C, F and G represent a negative population, which are non-fluorescing (non-labelled) cells and a positive population, which represent fluorescing (labelled) cells.

The colour-coded density plot of PI vs. AV shows the stages of the cells undergoing apoptosis (Figs. 11 D and H). This plot was used to colour-compensate the data, by changing the voltage settings on the flow cytometer. In so doing, the non-specific fluorescence that occurred due to the spectral overlap of the two fluorescent molecules, AV and PI, was removed. Depending on the stage of apoptosis the cells either label with:

1. High PI and/or low AV - represented by area G1, indicating mainly cellular debris and disintegrated cells containing DNA;
2. Both high AV and high PI - represented by area G2 and indicating late apoptosis with resultant cell lysis;
3. High AV and/or low PI - represented by area G4, indicating early apoptosis (cell membranes are intact but have lost asymmetry);
4. Low labelling cells - represented by area G3 and indicating viable cells.

The different colours of the colour-coded density plot represent the density of cells in a specific area (G1-4) with red being the most densely populated areas and blue the least dense.

Using this protocol, no auto-fluorescence was noted for untreated or drug-treated unlabelled cells and the DMSO solvent did not result in any apoptosis on its own (results not shown). The labelled drug-treated cells showed increased labelling with AV and PI as indicated by the histograms Figs. 11 F and G, compared to the untreated cells (Figs. 11 B and C). The colour-coded density plot for the BFA treated cells (Fig. 11 H) also showed an increase in the number of cells present in areas G1, 2 and 4 and a

decrease in the density of area G3, compared to the untreated cells (Fig. 11 D). The untreated cells had the highest density in area G3. This was all indicative of an increase in apoptosis within the drug-treated cell population compared to that of the untreated cell population, as expected, and demonstrated that the protocol was set up correctly.

3.1.1.2 Two populations represented by FS vs. SS plots

The cells in the HL60 cultures (passage number 8) were classified via May-Grünwald-Giemsa (MGG) staining (performed by the Haematology diagnostic laboratory, GSH) and identified as being a single population of predominantly undifferentiated promyelocytes. However, the FS vs. SS plots of drug-treated and untreated HL60 cells consistently showed what seemed to be two different populations of cells, with differences in size (FS) and granularity (SS) (Fig. 12).

To establish what the two cell populations in the FS vs. SS plots represented, untreated cells (in 1x PBS) were compared to cells that were either freshly thawed, drug-treated or heat-shocked. Prior to flow analysis (FS vs. SS only), the viability of the cells was determined by Trypan blue staining and compared to the flow results shown in Fig. 12.

The thawed cells (also resuspended in 1x PBS) showed similar cell populations to the untreated cells in Fig. 12 A (data not shown). The Trypan blue cell viabilities also corresponded with the population in area H, at approximately 90% viability.

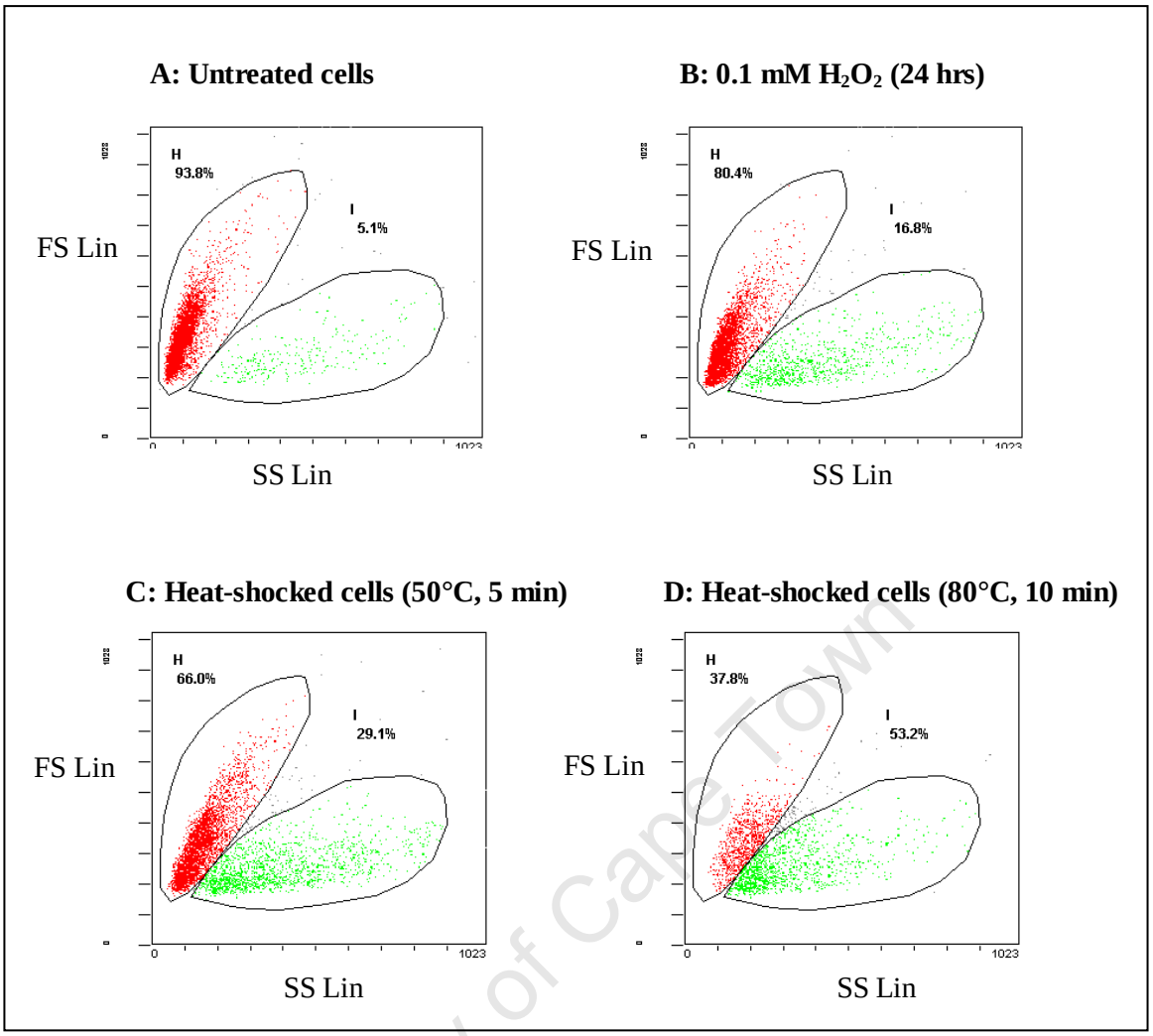

Fig.12. Two cell populations represented by FS vs. SS plot. HL60 cells were analysed on the flow cytometer to compare the FS vs. SS plots of untreated (**A**), drug-treated (**B**) and heat-shocked (**C-D**) cells. The cells were treated with 0.1 mM H_2O_2 for 24 hrs (**B**) and analysed, after which, the sample was heated at 50°C for 5 min and analysed again (**C**). The sample was once again heated at a higher temperature, 80°C, for 10 min (**D**) to observe the increase in cells moving from H to I.

The drug-treated cells (0.1 mM H_2O_2 for 24 hrs) (Fig. 12 B), compared to untreated cells (Fig. 12 A), showed an increase in population I (green) with a decrease in H (red). To determine if the populations were shifting with increasing apoptosis induction, the drug-treated sample was heated at 50°C for 5 min and analysed (Fig. 12 C), and heated again at 80°C for 10 min and once again analysed (Fig. 12 D).

The FS vs. SS plots for the drug-treated (Fig. 12 B) and heat-shocked cells (Figs. 12 C and D) show that the cell population in H (red) moved towards the population in I (green) as the level of apoptotic induction (heat treatment) was increased. The percentage viability for all the cells, as determined by AV and PI staining,

approximately corresponded with the percentage of the cells in H. The population in H could therefore be seen as the number of viable cells in the total cell population analysed, with I representing apoptotic cells.

To confirm the apoptotic status of these cells, untreated and drug-treated (0.5 mM H_2O_2 for 24 hrs) HL60 cells were labelled with AV and PI, analysed and the PI vs. AV plots gated on the areas H and I (Figs. 13 A and B).

The colour-coded density plots of PI vs. AV (Fig. 13) gated on population I, for both drug-treated and untreated cells, showed a spread of cells predominantly in areas G1, G2 and G4 representing apoptotic cells. The notable increase in population I upon drug treatment (Fig. 13 B), as well as the increase in cells fluorescing in areas G1, G2 and G4, clearly demonstrated the apoptotic nature of the cell population in I. These results confirmed that population H contained predominantly viable cells, whereas population I were mostly apoptotic cells. This analysis indicated that the untreated HL60 cells contained approximately 5 - 10% apoptotic cells, which had to be considered in the experiments to follow. This was also observed in the Jurkat cells (data not shown).

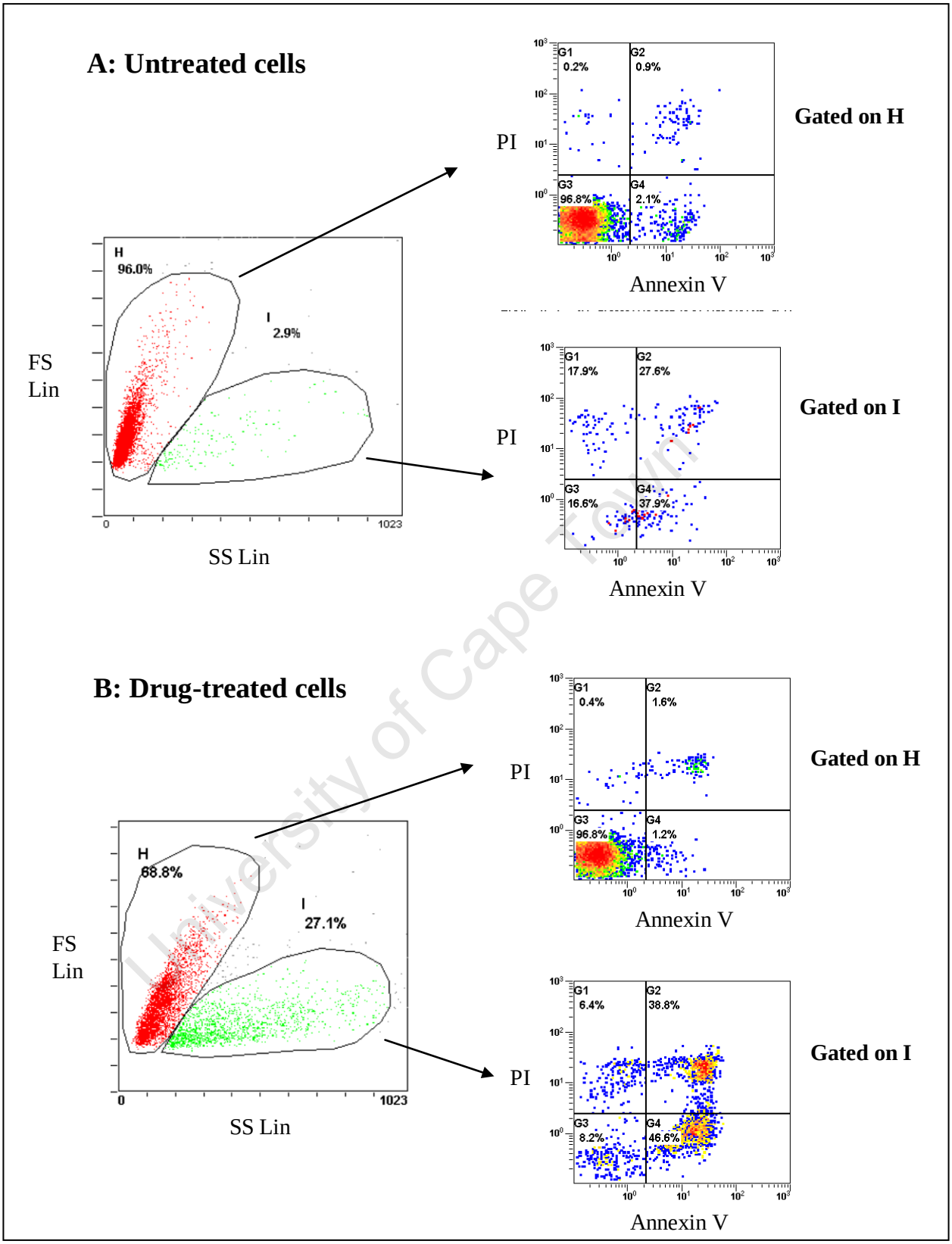

Fig. 13. The apoptotic status of the two cell populations. HL60 cells, untreated (**A**) and drug-treated (0.5 mM H_2O_2, 24 hrs) (**B**) were labelled with AV and PI and analysed on the flow cytometer to determine the stages of apoptosis of the two populations in areas H and I. In each case the colour-coded density plots were gated on either population H or I of the FS vs. SS plots to show the stages of apoptosis of the cells in H and I.

3.1.1.3 Determining appropriate drug concentrations and exposure times required to induce low and high levels of early apoptosis

The apoptotic response of the cells to drug treatment over time was determined after treatment with different concentrations of each specific drug. The aim was to determine the appropriate drug (BFA, H_2O_2 or FasL) concentrations to induce approximately 5 - 15% (low %) and 20 - 50% (high %) early apoptosis, above that of the untreated cells. The percentage apoptosis was quantified via AV/PI labelling and flow analysis. Area G4, of the respective PI vs. AV colour-coded density plots, was used to determine the percentage of early apoptotic cells after drug treatment. By using this quadrant only, it would exclude any non-apoptotic and/or necrotic cells, which could directly label with PI and fluoresce in areas G1 and/or G2. Therefore only cells that labelled with high AV and low PI (area G4) were considered to be early apoptotic and taken into account for this analysis.

3.1.1.3 A) BFA treatment of HL60 cells to induce the ER-stress induced apoptotic pathway

HL60 cells were treated with BFA (5 μg/ml - 30 μg/ml) for 24 hrs to induce the ER-stress induced apoptotic pathway (Guillemain and Exton, 1997; Liu *et al*., 1997; Li *et al*., 2006). The percentage of early apoptosis (% cells in area G4 of the colour-coded density plot) induced by BFA treatment after 24 hrs is shown in Fig. 14.

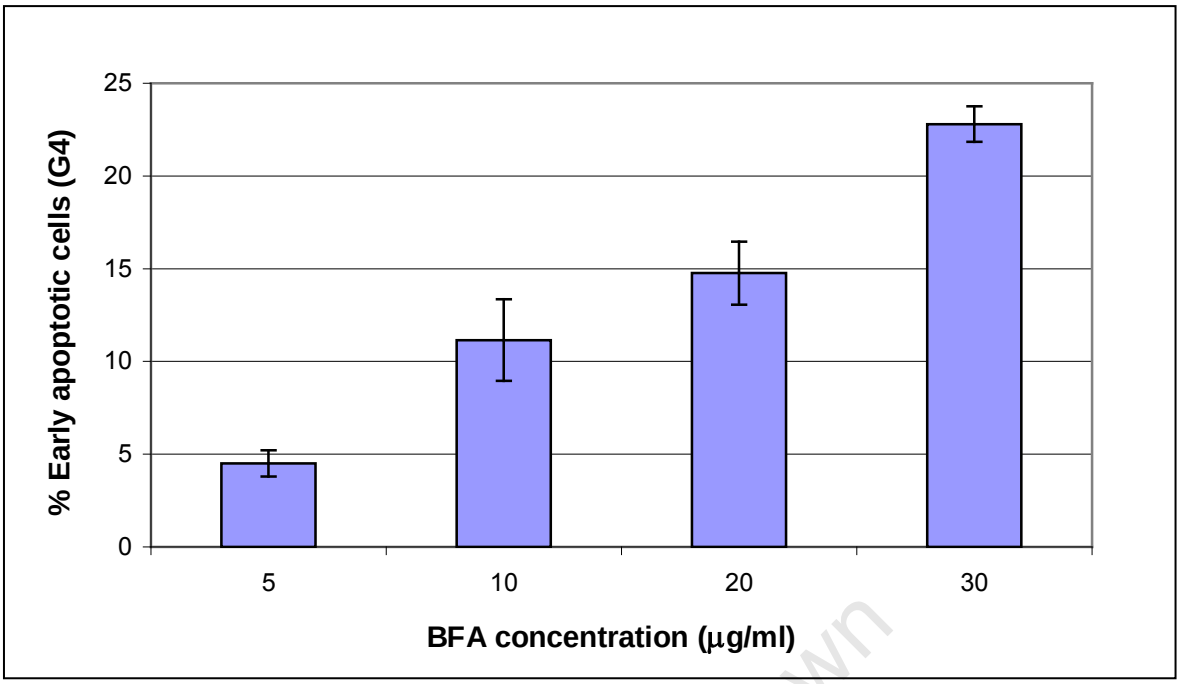

Fig. 14. Bar graph of % early apoptosis induced vs. different BFA concentrations after 24 hrs exposure. The graph shows the percentage early apoptosis induced by the different BFA concentrations after 24 hrs exposure. The samples were either prepared and analysed in duplicate or triplicate. The values were corrected for background apoptosis by subtracting the average %G4 for the untreated cells from the average %G4 for the BFA treated cells.

Fig. 14 shows that the 24 hr BFA treatment induced a linear increase in apoptotic response with increasing BFA concentrations. The HL60 cells were also treated with BFA (0.5 µg/ml - 10 µg/ml) for 6 and 48 hrs to determine the extent of apoptosis induced (data not shown). However, it was found that 6 hrs exposure time was insufficient to produce a significant increase in apoptosis and 48 hrs was too extensive, thereby producing an excessive amount of apoptosis. Other studies have found that at least 24 hrs incubation is needed to overcome the UPR and induce apoptosis through the ER-stress induced apoptotic pathway (Liu *et al.*, 1997; Rao *et al.*, 2002 b). Therefore, it was decided that 24 hrs exposure to BFA was optimal. Of the different BFA concentrations used, it was determined from Fig. 14 that 5 µg/ml induced approximately 5% (low level) and 30 µg/ml induced approximately 20% (high level) early apoptosis above that of the untreated cells.

Fig. 15 shows the representative PI vs. AV colour-coded density plots that were obtained for the low level (5%) and high level (20%) of early apoptosis (G4) induced by BFA over 24 hrs, after AV/PI labelling and flow analysis.

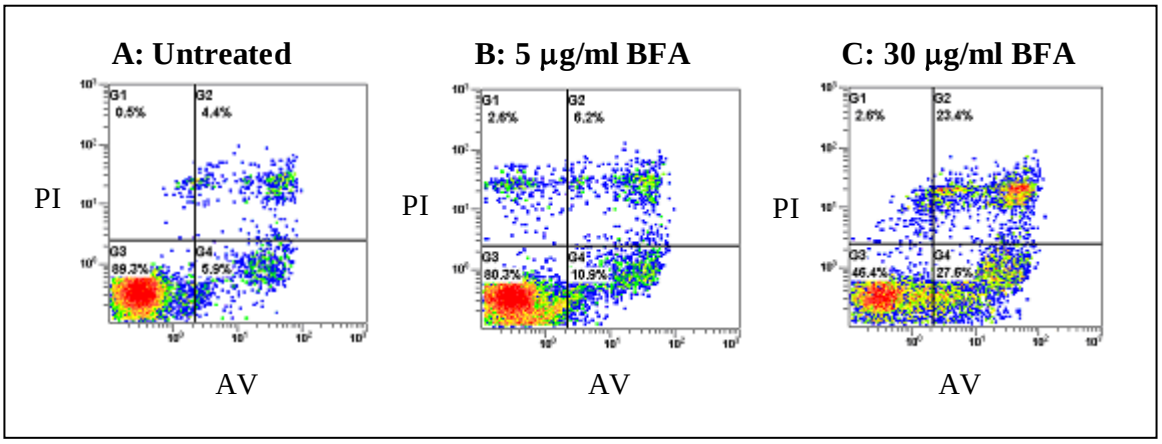

Fig. 15. PI vs. AV density plots of BFA treated HL60 cells. HL60 cells were treated with BFA and labelled with AV and PI and analysed via flow cytometry. The cells were treated for 24 hrs with (**B**) 5 µg/ml BFA to induce approximately 5% (low level) early apoptosis (G4) and (**C**) 30 µg/ml BFA to induce approximately 20% (high level) early apoptosis (G4) above that of the untreated cells (**A**).

3.1.1.3 B) H_2O_2 treatment of HL60 cells to induce the mitochondrial-mediated apoptosis pathway

HL60 cells were treated with H_2O_2 (0.005 mM - 2 mM) for 6, 15 and 24 hrs to induce the mitochondrial-mediated apoptotic pathway (Hosokawa *et al*., 2005). The percentage of early apoptosis (% cells in G4 of PI vs. AV colour-coded density plot) induced by the different H_2O_2 concentrations and exposure times are shown in Fig. 16.

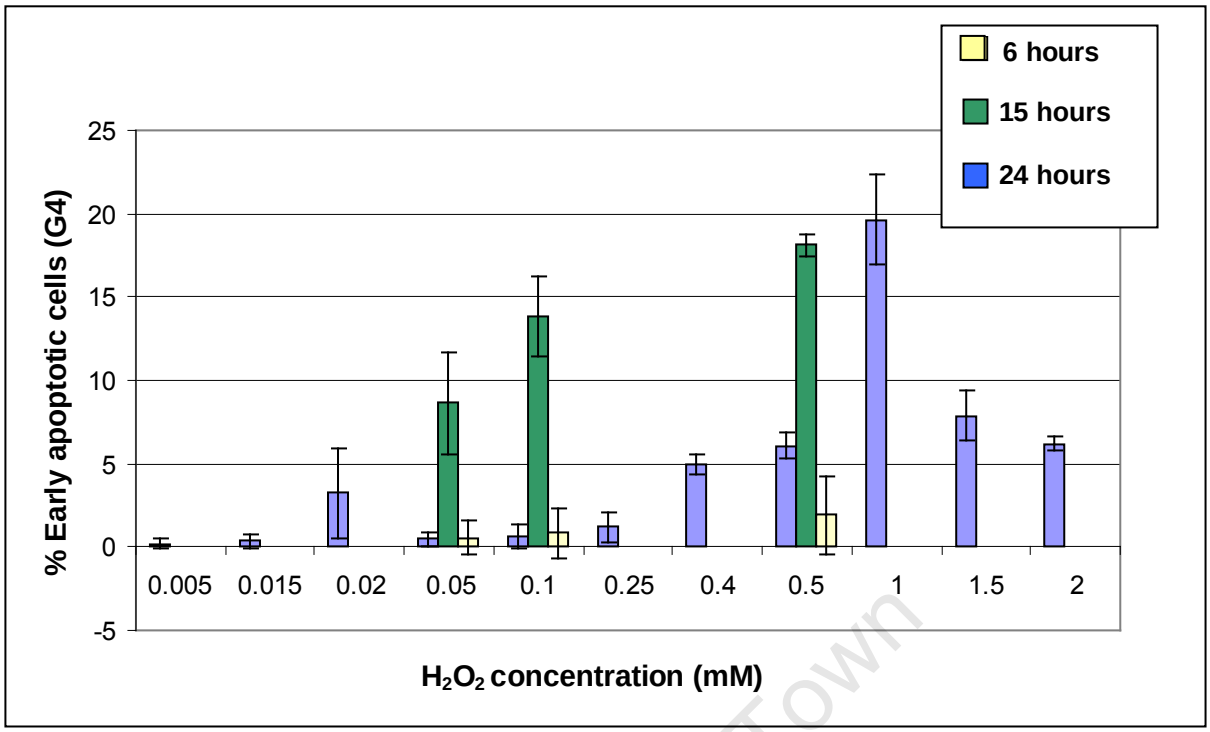

Fig. 16. Bar graph of % early apoptosis induced vs. different H_2O_2 concentrations for 6, 15 and 24 hours. The graph shows the percentage early apoptosis induced by the different H_2O_2 concentrations after 6 hrs (yellow), 15 hrs (green) and 24 hrs (blue) exposure times. The samples were prepared and analysed in triplicate. The values were corrected for background apoptosis by subtracting the average %G4 for the untreated cells from the average %G4 for the H_2O_2 treated cells.

Fig. 16 shows that 6 hrs exposure was not sufficient to produce a significant increase in apoptosis and would require higher H_2O_2 concentrations to produce the desired amount of apoptosis. At 15 hrs exposure, the results were inconclusive, since the lower H_2O_2 concentrations (0.05 mM and 0.1 mM) produced higher increases in apoptosis compared to 6 hr and 24 hr treated cells. Furthermore, different results were obtained for 15 hr 0.05 mM treated cells on different occasions (data not shown). This could be due to differences in viability (%G3) and % early apoptosis (%G4) of the untreated cells, which varied between experiments. It was therefore decided that 24 hrs exposure to H_2O_2 was more appropriate. It was determined from Fig. 16 that 0.4 mM H_2O_2 induced approximately 5% (low level) and 1 mM H_2O_2 induced approximately 20% (high level) early apoptosis above that of the untreated cells. Moreover, Fig. 16 also indicated that at H_2O_2 concentrations greater than 1 mM (24 hrs), there was a decrease in the number of early apoptotic cells (G4), since more cells were present in areas G2 and G1 (late apoptosis and/or necrosis). Therefore after 24 hrs exposure to 1 mM H_2O_2, the maximum percentage of cells appeared to be early apoptotic (G4).

Fig. 17 shows the representative PI vs. AV colour-coded density plots that were obtained for the low level (5%) and high level (20%) of early apoptosis (G4) induced by H_2O_2 after 24 hrs, following AV/PI labelling and flow analysis.

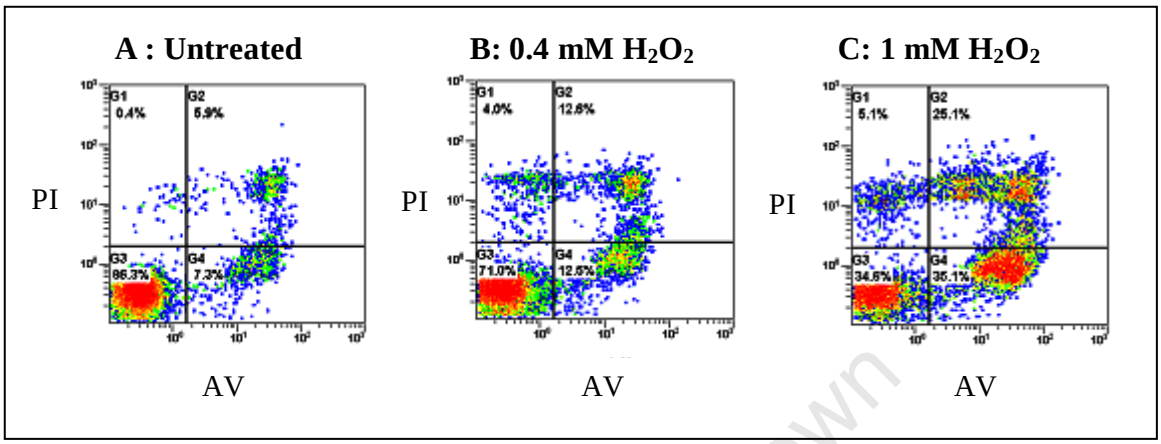

Fig. 17. PI vs. AV plots of H_2O_2 treated HL60 cells. HL60 cells were treated with H_2O_2, labelled with AV and PI and analysed via flow cytometry. The cells were treated for 24 hrs with (**B**) 0.4 mM H_2O_2 to induce approximately 5% (low level) early apoptosis (G4) and (**C**) 1 mM H_2O_2 to induce approximately 20% (high level) early apoptosis (G4) above that of the untreated cells (**A**).

3.1.1.3 C) FasL treatment of HL60 cells to induce the death receptor pathway

HL60 cells were treated with 0.5 - 500 ng/ml FLAG-tagged FasL, in the presence of 0.25 µg/ml or 0.5 µg/ml ANTI-FLAG® M2 antibody, for 4 and 24 hrs to induce the death receptor pathway via the Fas receptor (Li, W. *et al.*, 2006; Sigma®-Aldrich, 2008). The percentage of early apoptosis (% cells in area G4 of PI vs. AV colour-coded density plot) induced by FLAG-tagged FasL and ANTI-FLAG® M2 antibody is shown in Table 6.

Table 6: Percentage of early apoptosis in HL60 cells following treatment with FLAG-tagged FasL and ANTI-FLAG® M2 antibody after 4 and 24 hrs

Incubation time (hrs):	FLAG-tagged FasL concentration (ng/ml):	ANTI-FLAG® M2 antibody concentration (µg/ml):	Average % early apoptotic cells (Area G4) †:	Values corrected for background apoptosis ‡:
4	0 **	0	2.99 (±0.01)	0
	0.5 **	0.25	2.81 (±0.4)	-0.18 (±0.4)
	5 **	0.25	3.80 (±2.7)	0.81 (±2.7)
	50 **	0.25	4.29 (±0.2)	1.3 (±0.2)
	0 **	0	3.61 (±0.9)	0
	0 **	0.25	3.74 (±0.4)	0.13 (±0.4)
	0 ***	0.5	4.11	0.5
	50 ***	0.25	5.18	1.57
	50 ***	0.5	5.47	1.86
	200 ***	0.25	5.17	1.56
	200 ***	0.5	4.28	0.59
24	0 *	0	1.92 (±0.4)	0
	5 *	0.25	2.27 (±0.7)	0.35 (±0.7)
	50 *	0.25	1.67 (±0.1)	-0.25 (±0.1)
	200 *	0.25	2.59 (±0.6)	0.67 (±0.6)
	500 *	0.25	2.48 (±0.4)	0.56 (±0.4)

Different colours represent experimental sets performed on different days
* Values reflect the averages with standard deviation (n=3)
** Values reflect the averages with standard deviation (n=2)
*** n=1
† The average % early apoptotic cells were obtained from area G4 of the respective PI vs. AV density plots
‡ The values were corrected for background apoptosis by subtracting the average %G4 for the untreated cells from the average %G4 for the FasL treated cells (for each experimental set)

The combination of FLAG-tagged FasL and ANTI-FLAG® M2 antibody, over 4 and 24 hrs treatment, had very little affect on the HL60 cells as seen in Table 6. Less than 2% early apoptosis was induced above that of the untreated cells over the entire range tested.

To examine the effect of higher ANTI-FLAG® M2 antibody concentrations, and to see if it could induce apoptosis on its own, the cells were treated with 0.25 or 0.5 µg/ml

antibody and different concentrations of FasL (0-200 ng/ml) over 4 hrs. The results (Table 6) indicated that 0.25 μg/ml antibody alone did not induce a significant amount of apoptosis. Furthermore, 0.5 μg/ml antibody induced only 0.5% apoptosis, above that of the untreated cells. It was also found that even at the higher antibody concentration (0.5 μg/ml) (with FLAG-tagged FasL), there was not a significant difference in early apoptosis induced, compared to the values obtained with 0.25 μg/ml antibody.

The results in Table 6 therefore show that the FLAG-tagged FasL and ANTI-FLAG® M2 antibody set did not induce a significant percentage of apoptosis in HL60 cells. Due to this and the high expense of FasL, it was therefore decided to use a different cell line, which would require lower FasL concentrations to produce the required levels of apoptosis. The Jurkat cell line was therefore acquired to perform the FasL-death receptor pathway optimisation experiments.

3.1.1.3 D) FasL treatment of Jurkat cells to induce the death receptor pathway

Jurkat cells were treated with FLAG-tagged FasL (0.04 ng/ml – 5 ng/ml) for 4 hrs, in the presence of 0.25 μg/ml ANTI-FLAG® M2 antibody, to induce the death receptor pathway (Huang *et al.*, 1999; Sigma®-Aldrich, 2008). It was decided to use 4 hrs as the optimal incubation time, since this was the time used by the manufacturer in inducing apoptosis in Jurkat cells (Sigma®-Aldrich, 2008). The percentage of early apoptosis (% cells in area G4 of PI vs. AV colour-coded density plot) induced after treatment with FLAG-tagged FasL and ANTI-FLAG® M2 antibody (after 4 hrs exposure) is shown in Fig. 18.

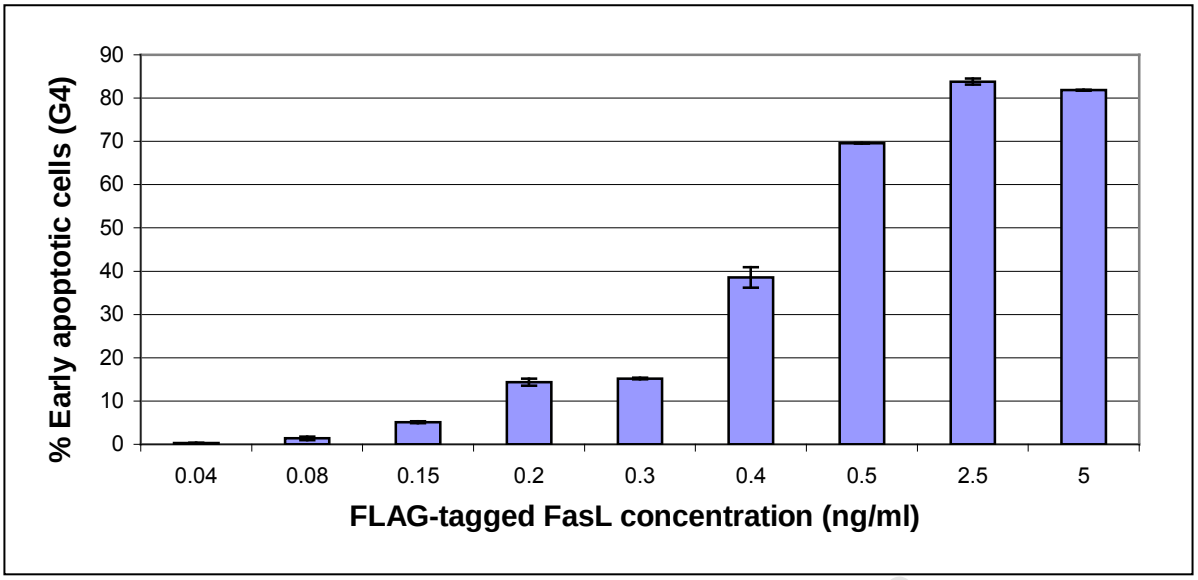

Fig. 18. Bar graph of % early apoptosis induced vs. different FLAG-tagged FasL concentrations (in the presence of ANTI-FLAG® M2 antibody) after 4 hrs exposure. Jurkat cells were exposed to different FLAG-tagged FasL concentrations in the presence of 0.25 µg/ml ANTI-FLAG® M2 antibody for 4 hrs. The samples were either prepared and analysed in duplicate or triplicate. The values were corrected for background apoptosis by subtracting the average %G4 for the untreated cells from the average %G4 for the FasL treated cells.

Fig. 18 shows an increase in the percentage of early apoptosis (area G4) induced in the FasL treated cells as the FLAG-tagged FasL concentrations were increased. It was determined from Fig. 18 that 0.2 ng/ml FLAG-tagged FasL together with 0.25 µg/ml ANTI-FLAG® M2 antibody induced approximately 15% (low level) early apoptosis, above that of the untreated cells. Given that 0.3 ng/ml FLAG-tagged FasL produced less than 20% apoptosis (G4), it was decided that 0.4 ng/ml FLAG-tagged FasL (with 0.25 µg/ml antibody) was more appropriate, since it induced approximately 40% (high level) apoptosis (G4) above that of the untreated cells (Fig. 18).

Fig. 19 shows the representative PI vs. AV colour-coded density plots that were obtained for the low level (15%) and high level (40%) of early apoptosis (G4) induced by FLAG-tagged FasL and 0.25 µg/ml ANTI-FLAG® M2 antibody after 4 hrs exposure, following AV/PI labelling and flow analysis.

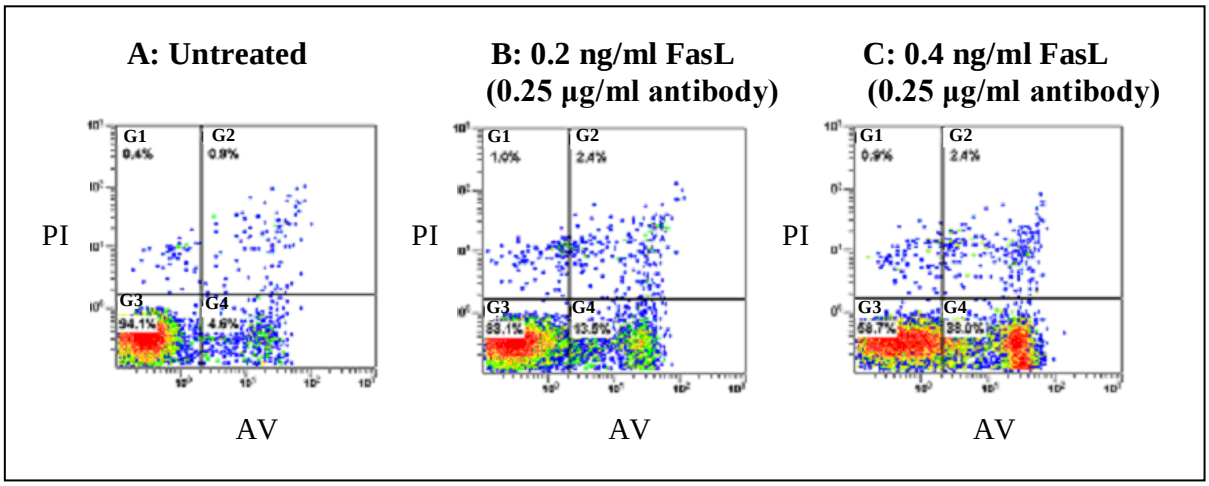

Fig. 19. PI vs. AV plots of FasL treated Jurkat cells. Jurkat cells were treated for 4 hrs with FLAG-tagged FasL and ANTI-FLAG® M2 antibody, labelled with AV and PI and analysed via flow cytometry. The cells were treated with (**B**) 0.2 ng/ml FLAG-tagged FasL and 0.25 µg/ml ANTI-FLAG® M2 antibody to induce approximately 15% apoptosis and (**C**) 0.4 ng/ml FLAG-tagged FasL and 0.25 µg/ml ANTI-FLAG® M2 antibody to induce approximately 40% apoptosis above that of the untreated cells (**A**).

3.1.2 Western blot analysis and optimisation

During the initial part of this study, the western blot assays were optimised to find the:

- Optimal transfer conditions required for maximal protein transfer
- Appropriate protein concentration needed for optimal detection by the antibody
- Optimal concentration of each antibody required for detection.

3.1.2.1 Optimisation of transfer conditions for western blot analysis

Initial western blot analyses, using β-actin antibody as probe, determined that 20-23 V was the maximum voltage that could be used with the Trans-Blot® SD Semi-Dry Electrophoretic Transfer Cell, since it had a voltage limit of 25 V. The current was maintained at approximately 80-234 mA to prevent over-heating. It was also found that 30-60 min transfer time was sufficient, depending on the size of the gel.

3.1.2.2 Optimisation of Bip western blot assay

To optimise the Bip western blot assay, the appropriate antibody concentration (required to detect Bip) was firstly determined. In previous experiments performed, it

was found that Bip (5 μg protein; extracted without protease inhibitors) was not detected at 1:1000 diluted Bip antibody (data not shown). It was therefore decided to repeat the western blot analysis, using higher antibody and protein (extracted with protease inhibitors) concentrations. Protein was extracted from untreated and BFA treated (30 μg/ml BFA; 24 hrs) HL60 cells (section 2.3.1). The western blot analysis was performed as described in sections 2.3.2 and 2.3.3. The membrane was probed with 1:500 diluted Bip antibody and subsequently developed (Fig. 20).

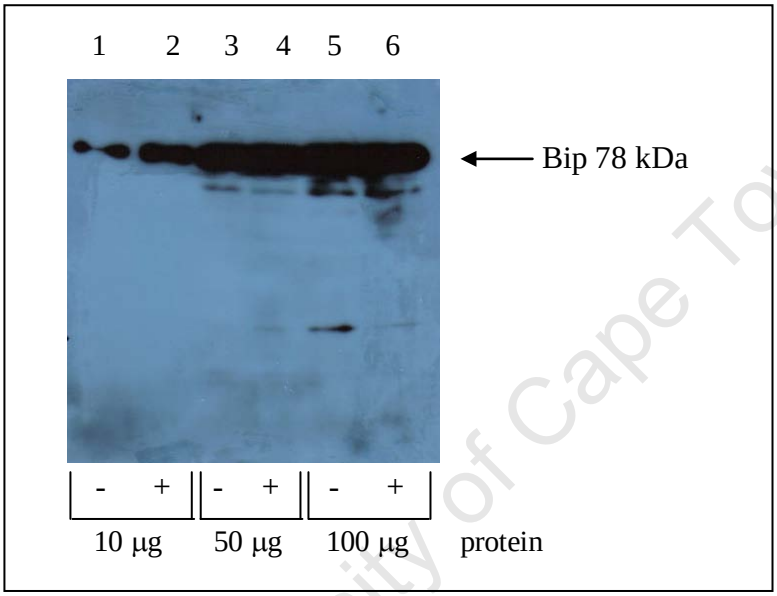

Fig. 20. Optimisation of Bip western blot assay. Protein lysates (10-100 μg) from untreated and BFA (30 μg/ml BFA; 24 hrs) treated HL60 cells were separated via SDS-PAGE and transferred onto PVDF membrane. The membrane was probed with Bip antibody (1:500) and developed. Lanes 1, 3 and 5 contained 10, 50, 100 μg of untreated HL60 cell protein, respectively. Lanes 2, 4 and 6 contained 10, 50, 100 μg of BFA treated HL60 cell protein, respectively.

Fig. 20 shows that Bip (78 kDa) was detected by the increased (1:500) Bip antibody concentration for both untreated and BFA treated HL60 lysates and at all the protein concentrations used. As indicated by Fig. 20, the band intensities also increased as the protein concentration was increased, as expected. The higher protein concentrations (50-100 μg) resulted in some non-specific bands directly below Bip and at approximately 20 kDa. Fig. 20 also shows an increase in Bip protein levels after BFA treatment (lane 2), compared to the untreated control (lane 1), at 10 ug protein. However, the other lanes (3-6) were too over-exposed to observe differences between untreated and BFA treated protein expression levels. This western blot analysis therefore indicated that as little as

10 ug protein could be used to detect changes in Bip protein expression (section 3.1.2.5). Moreover, the use of protease inhibitors in the RIPA buffer appeared to improve the detection of Bip. It was therefore decided to include protease inhibitors for all protein samples.

3.1.2.3 Optimisation of FADD western blot analysis

The western blot assay for FADD was optimised to determine the optimal FADD antibody concentration required for detection of the protein. Since the death receptor pathway drug-response (section 3.1.1.3 D) was optimised using Jurkat cells, protein (100 µg; extracted with protease inhibitors) from untreated Jurkat cells was used for this purpose. The western blot analysis was performed as described in section 2.3. Initially, the membrane was probed with 1:1000 diluted FADD antibody, however no signal was detected. Therefore, the membrane was stripped and reprobed (section 2.3.5) with 1:500 diluted FADD antibody, which was successful (data not shown).

To verify these results, the western blot assay was repeated with untreated Jurkat cell protein (50-100 µg; extracted with protease inhibitors). The membrane was probed with 1:500 diluted FADD antibody and 1:1000 β–actin antibody, as a positive control, and subsequently developed (Fig. 21).

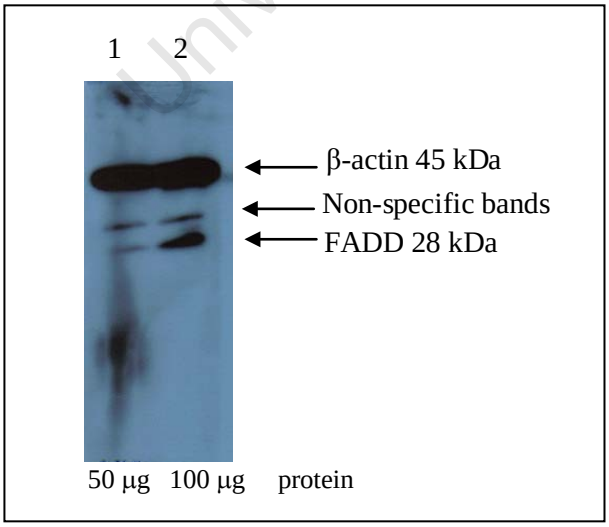

Fig. 21. FADD and β–actin western blot optimisation assay. Protein lysates (50-100 µg) from untreated Jurkat cells were separated via SDS-PAGE and transferred onto PVDF membrane. The membrane was probed with FADD (1:500) and β–actin (1:1000) antibodies and developed. Lane 1: 50 µg protein. Lane 2: 100 µg protein.

Fig. 21 shows that FADD (28 kDa) was detected by the increased (1:500) FADD antibody concentration at both protein concentrations (50 µg and 100 µg), however 100 µg protein produced a more intense signal. The β-actin (45 kDa) positive control was detected at both protein concentrations, as expected. Since both proteins (FADD and β-actin) were detected successfully, it indicated that the membrane could be incubated with both antibodies (for FADD and β-actin) simultaneously. This was important for the final experiments to follow (section 3.2.2), since it would minimise the stripping and re-probing steps required (hence, minimise loss of protein from the membrane between stripping steps).

The non-specific bands that were detected directly below β-actin (indicated on Fig. 21) appear to be due to the β-actin antibody, since another western blot, with β-actin only, produced the same bands (Fig. 22). The western blot assay was performed (as described in section 2.3) with protein (150 µg) extracted from untreated and BFA treated (30 µg/ml BFA; 24 hrs) HL60 cells. The membrane was probed with 1:1000 diluted β-actin antibody and subsequently developed (Fig. 22).

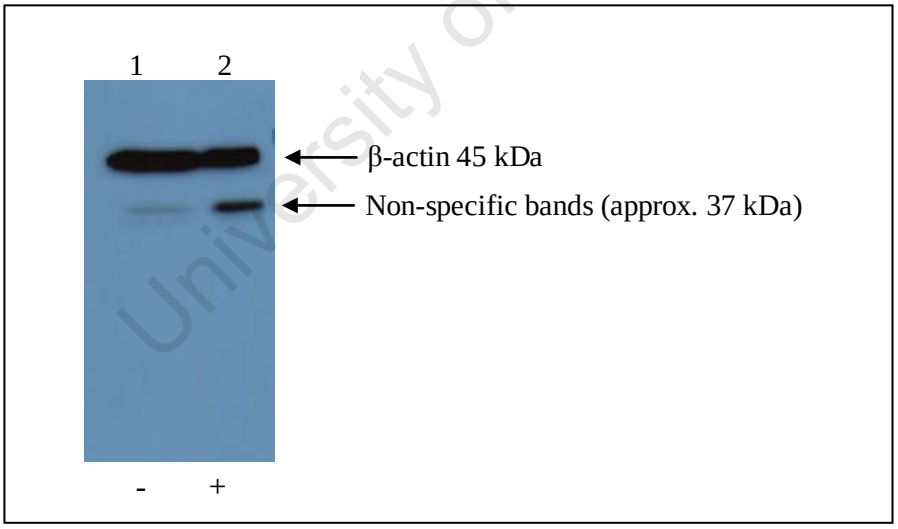

Fig. 22. β–actin western blot showing non-specific bands. Protein lysates (150 µg) from untreated and BFA (30 µg/ml BFA; 24 hrs) treated HL60 cells were separated via SDS-PAGE and transferred onto PVDF membrane. The membrane was probed with β-actin antibody (1:1000) and developed. Lane 1 contained 150 µg of untreated HL60 cell protein. Lane 2 contained 150 µg of BFA treated HL60 cell protein.

Fig. 22 shows that β-actin (45 kDa) was detected for untreated and BFA treated samples, as expected. Fig. 22 also shows two non-specific bands, which were detected

between 33 kDa and 40 kDa (at approximately 37 kDa). These non-specific bands were also detected in Fig. 21 (directly below β-actin), therefore confirming that these bands were due to the β-actin antibody and not FADD.

3.1.2.4 Optimisation of CHOP western blot analysis

The CHOP (GADD153) western blot assay was optimised to determine the optimal protein and antibody concentrations required for detection. The western blot analysis protocol (section 2.3.3) was also modified to improve on the results obtained. Protein isolated (with protease inhibitors) from untreated and BFA treated (30 μg/ml BFA for 24 hrs) HL60 cells was resolved through SDS-PAGE (section 2.3.2) and transferred onto PVDF membrane (section 2.3.3) for 30-60 min at 20-23 V.

For the initial experiments, 5 μg and 150 μg protein was used and the membrane was probed with 4 μg/ml GADD153 antibody. However, no bands were detected and a high background signal was present. To attempt to decrease the high background signal, experiments with lower protein concentrations (10 and 50 μg) were performed. The membranes were probed with different concentrations of GADD153 antibody (0.4 μg/ml, 2 μg/ml or 8 μg/ml), however no signal was detected. The experiment was repeated but instead, 1 μg/ml GADD153 antibody was used (Fig. 23).

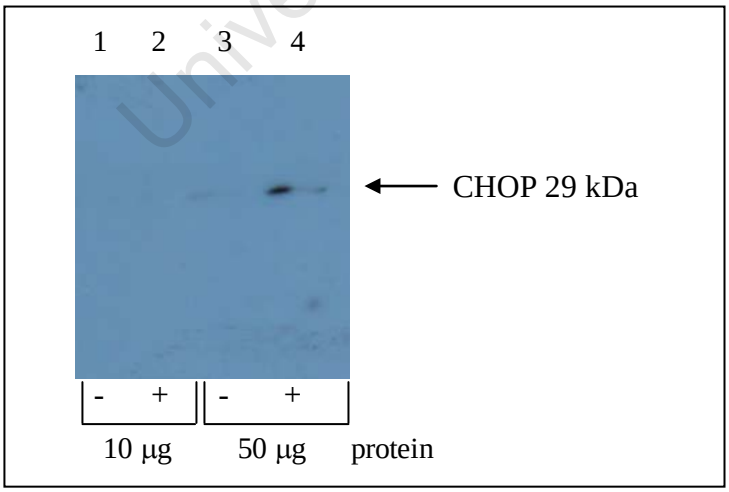

Fig. 23. Optimisation of CHOP western blot assay. Protein lysates (10-50 μg) from untreated and BFA treated (30 μg/ml BFA; 24 hrs) HL60 cells were separated via SDS-PAGE and transferred onto PVDF membrane. The membrane was probed with 1 μg/ml GADD153 antibody and developed. Lane 1: 10 μg of untreated HL60 cell protein. Lane 2: 10 μg of BFA treated HL60 cell protein. Lane 3: 50 μg of untreated HL60 cell protein. Lane 4: 50 μg of BFA treated HL60 cell protein.

Fig. 23 shows that a very faint signal was detected for CHOP (29 kDa) at 50 μg protein only (lanes 3-4). Fig. 23 also shows a slight increase in CHOP protein levels after BFA treatment (lane 4), compared to the untreated control (lane 3). In an attempt to improve the signal obtained in Fig. 23, the membrane was stripped and reprobed with higher GADD153 antibody concentration (8 μg/ml). However, no signal was obtained (data not shown). This could, in part, have been due to loss of some protein during the stripping and reprobing procedure.

To determine the affinity of the POD-conjugated secondary antibody for the β–actin, Bip, FADD and GADD153 antibodies, a "dot blot" experiment was performed. It was found that the secondary antibody's affinity for the GADD153 antibody was lower than for the other antibodies (data not shown). Therefore, it was decided to repeat the CHOP western blot analysis with increased POD-conjugated secondary antibody concentrations and increased subsequent washing steps (to minimize high background signal) (as described in section 2.3.3).

A western blot assay with 10 and 50 μg protein (isolated from untreated and BFA (30 μg/ml; 24 hrs) treated HL60 cells) was performed. The membrane was probed with 1 μg/ml GADD153 antibody and detected with 80 mU/ml POD-conjugated secondary antibody. There was a slight improvement in band detection for 50 μg protein only, however, the background signal was somewhat high and there were non-specific bands present (data not shown).

The experiment was repeated with the same protein and GADD153 antibody concentrations but using a higher POD-conjugated secondary antibody concentration (160 mU/ml) than before (Fig. 24).

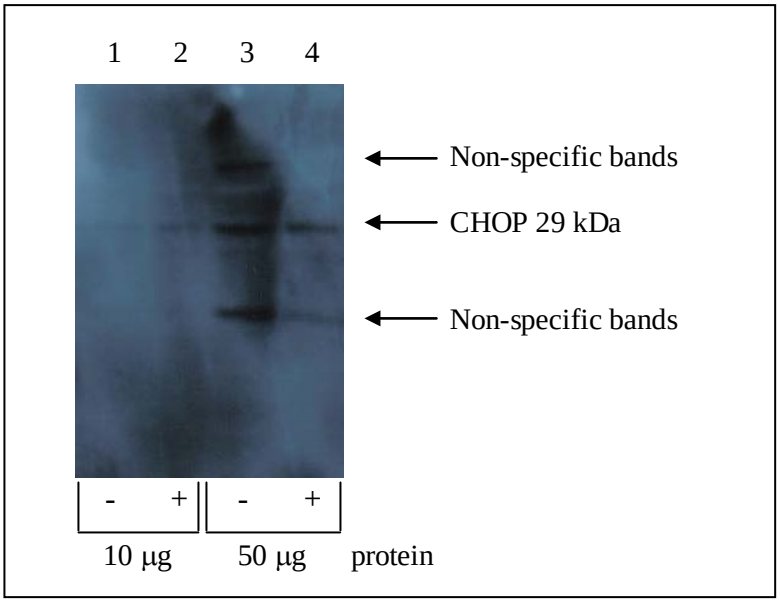

Fig. 24. CHOP western blot analysis with 160 mU/ml POD-conjugated secondary antibody. Protein lysates (10-50 μg) from untreated and BFA treated (30 μg/ml BFA for 24 hrs) HL60 cells were separated via SDS-PAGE and transferred onto PVDF membrane. The membrane was probed with 1 μg/ml GADD153 antibody and developed with 160 mU/ml POD-conjugated secondary antibody. Lane 1: 10 μg of untreated HL60 cell protein. Lane 2: 10 μg of BFA treated HL60 cell protein. Lane 3: 50 μg of untreated HL60 cell protein. Lane 4: 50 μg of BFA treated HL60 cell protein.

Fig. 24 shows that a signal for CHOP (29 kDa) was detected at 50 μg protein only (lanes 3-4) and the background signal had decreased significantly. However, there were still some non-specific bands present, which could not be improved upon. The requirements for detection of CHOP were therefore found to be: higher protein concentrations (greater or equal to 50 μg protein), an increased POD-conjugated secondary antibody concentration (160 mU/ml) (to increase its binding affinity to GADD153 antibody) and subsequent increased number of washing steps to minimize high background signal (section 2.3.3).

3.1.2.5 Determination of optimal protein concentration required for detection

Since the transfer apparatus used creates very strong fields during the transfer process, the amount of protein transferred onto the membrane may not always be quantitative. Therefore, the optimal protein concentration required for signal detection was determined. Since β-actin was used as a positive invariant control, it was expected to be present in both untreated and drug-treated samples, unlike the other genes (Bip, CHOP

and FADD), which could vary. It was therefore decided to use β-actin as reference for determining the optimal protein concentration required for detection.

A western blot assay with protein (1 - 100 μg) extracted from untreated HL60 cells was performed (as described in section 2.3.4) (Fig. 25).

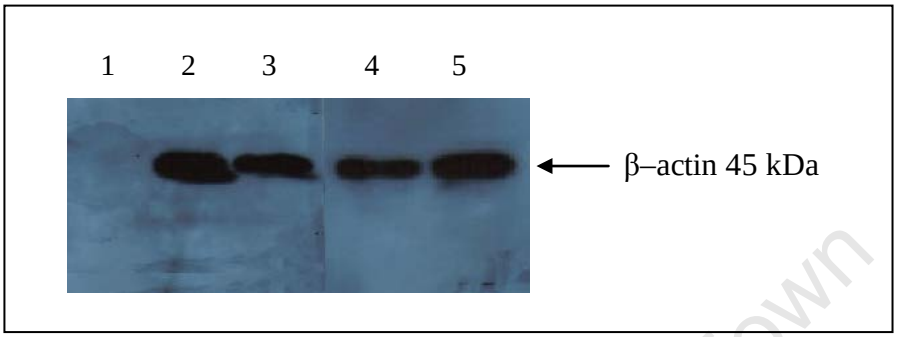

Fig. 25. Determination of optimal protein concentration required for detection of β–actin protein. SDS-PAGE was performed on untreated HL60 cell protein extracts (1-100 μg) after which the protein was transferred onto PVDF membrane and probed with β-actin antibody (1:1000). Lanes 1-5 contained 1, 5, 10, 50 and 100 μg protein, respectively.

Fig. 25 shows that the intensity of the detected protein (β-actin, 45 kDa) does not significantly differ with increasing protein concentrations (lanes 2-5). Since there was no band detected for 1 μg protein (lane 1), it can be concluded that it was not sufficient for transfer. Therefore, less than 5 μg protein would not be recommended. Previous results (Fig. 20) indicated that 10 ug protein was sufficient for quantitative differentiation of Bip between untreated and BFA treated samples. Therefore, it was concluded that as little as 10 ug protein could be used for western blot analysis. However, since the membranes were to be stripped and reprobed in the final experiments to follow (section 3.2.2), it was decided to use 100 μg protein. This would ensure that enough protein was transferred and would remain on the membrane after successive stripping and reprobing steps.

3.1.3 Caspase activity assays

Increases in caspase activity were monitored using fluorometric caspase activity assays, which were optimised to determine optimal assay conditions (Köhler *et al*., 2002). Since

a manufactured caspase activity assay kit was not used, it was necessary to confirm that the assay was working correctly and to optimise the parameters where necessary.

3.1.3.1 Determination of minimal protein concentration required for caspase activity

The minimal amount of protein that could be used to determine caspase activity was investigated using caspase-3 substrate (Anaspec, 2007). The assay was performed as described in section 2.4. The Relative Fluorescence Units (RFU) values obtained for the different protein concentrations are shown in Fig. 26.

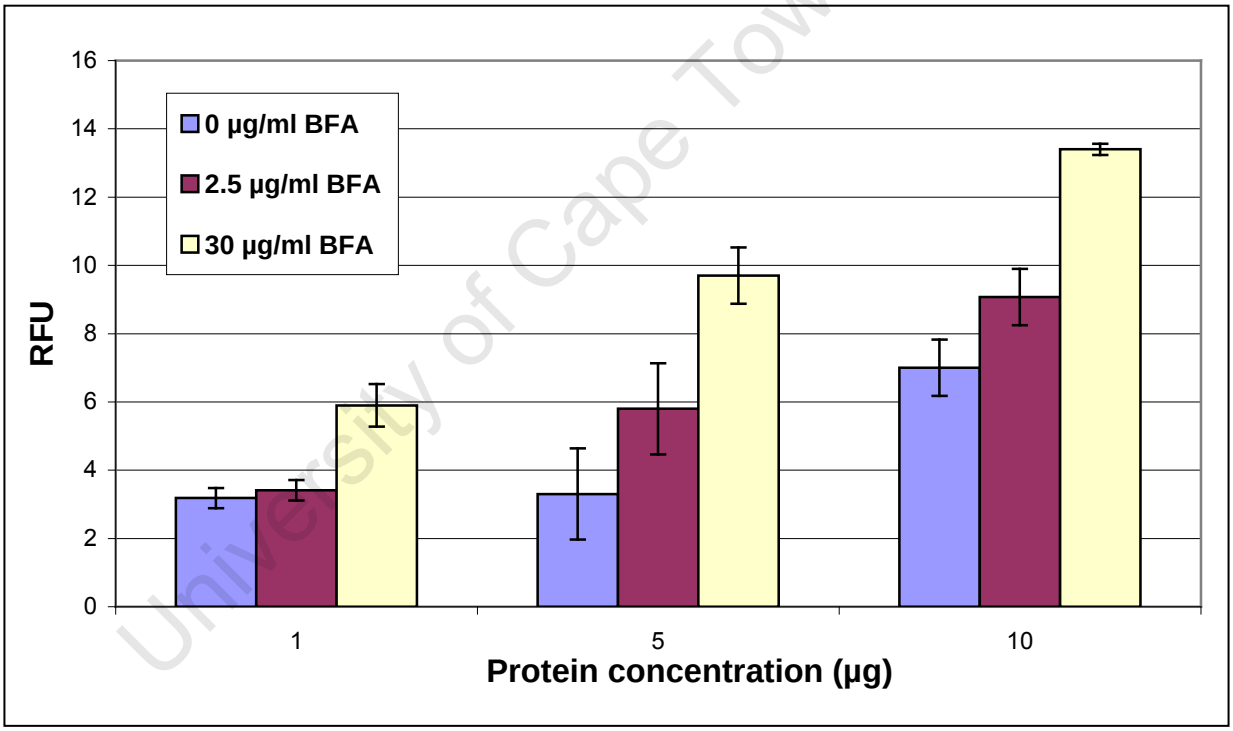

Fig. 26. Caspase-3 activity expressed as RFU for different protein concentrations. Different protein concentrations (1 - 10 µg) of BFA treated (0 µg/ml, 2.5 µg/ml and 30 µg/ml; 24 hrs) HL60 cell lysates were used in a caspase activity assay with caspase-3 substrate (50 µM) to determine the optimal protein concentration required to produce a satisfactory fluorescence signal. The assay components were incubated for 60 min at 37°C before readings were taken. Readings were taken at Ex/Em= 354/442 nm with Ex/Em slit= 20/20nm and PMT Voltage= medium. An automatic blank setting was used. Samples were prepared and analysed in triplicate and RFU values reflect averages with error bars representing the standard deviation.

Fig. 26 shows that the RFU values increased with higher protein concentrations, as well as higher drug concentrations, as expected. The BFA treated cells (30 µg/ml BFA for 24

hrs, which induced approximately 20% apoptosis) showed much greater caspase-3 activity compared to that of the 2.5 µg/ml BFA treated and untreated samples, as expected. The results indicated that the RFU values increased in proportion to the amount of protein added per caspase reaction. This can be seen in the linear increase in caspase activity from 5 - 10 µg protein and with increasing BFA concentration (Fig. 26).

The RFU values produced with 10 µg protein were the highest, although as little as 5 µg protein could be used at these assay conditions and fluorimeter settings (Fig. 26). The RFU values were, however, very low and therefore the caspase assay was optimised in terms of fluorimeter settings, incubation time and substrate concentration to try and increase the RFU signal and make the assay more robust.

3.1.3.3 Optimisation of caspase assay reaction conditions

3.1.3.2 A) Determination of optimal incubation time

Other studies have used a range of incubation times (60-120 min) to determine caspase activity (Juin *et al.*, 1998; Cardier and Erickson-Miller, 2002; Nagase *et al.*, 2002; Hosokawa *et al*., 2005; Karki *et al.*, 2007).

The optimal incubation time required for maximal RFU values and AMC release was determined as described in section 2.4.2.2. The results indicated that there was no significant difference between RFU values at extended incubation times. Furthermore, it was found that 60 min incubation time was sufficient for optimal caspase activity and AMC release (data not shown).

3.1.3.2 B) Optimal caspase substrate concentration

The optimal caspase substrate concentration required to produce adequate RFU readings was determined as described in section 2.4.2.3. It was found that the RFU values increased in proportion to increased substrate concentrations. It was also found that 50 µM of caspase-3 substrate was sufficient to produce adequate RFU signals that could be analysed and compared (data not shown).

3.1.3.2 C) Effect of protease inhibitors on caspase activity

Some research groups performed caspase assays with protein lysates that contained a protease inhibitor cocktail (DiPietrantonio *et al.*, 1999; Kim *et al.*, 1999; Doyle *et al.*, 2002; Huang *et al.*, 2004; Higuchi *et al.*, 2006). Since caspases are proteases and caspase activity was being investigated, it was important to establish the effect of protease inhibitors on caspase activity. Therefore, cell lysates isolated with or without protease inhibitor cocktail (section 2.4.1) were analysed using caspase-3 substrate (50 µM) (as described in sections 2.4.2 and 2.4.3). The RFU values obtained for these samples are shown in Fig. 27.

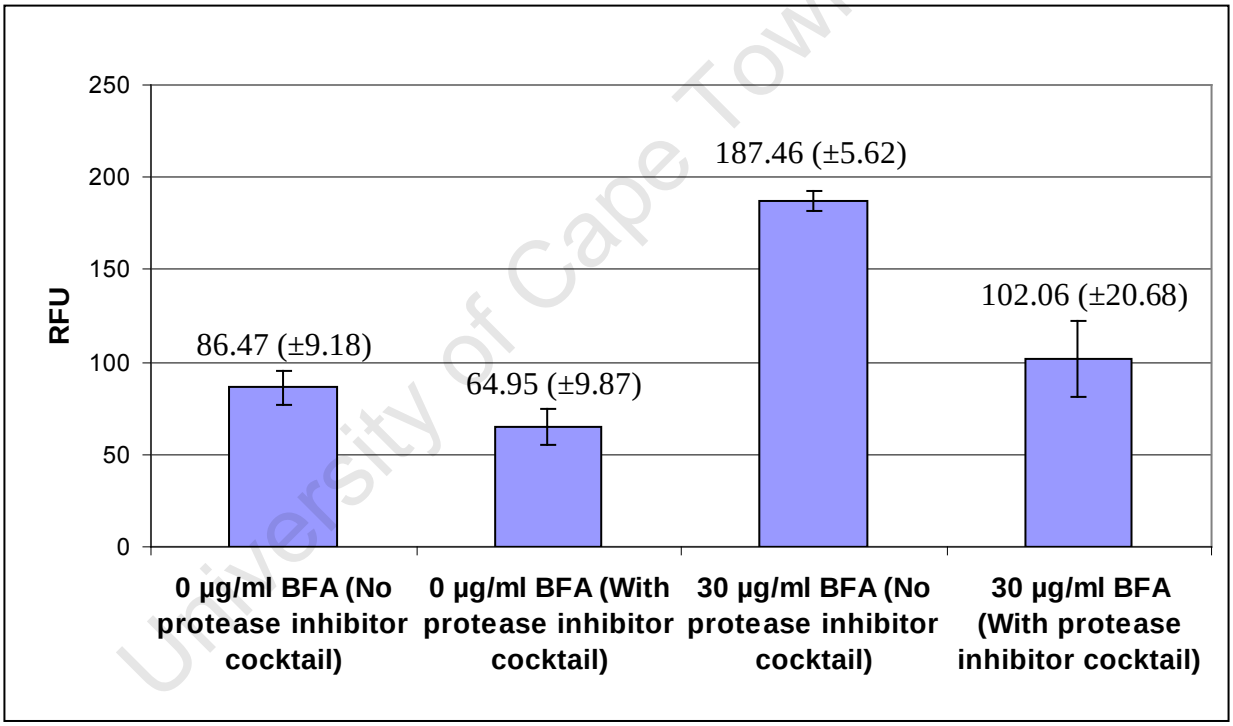

Fig. 27. RFU plot showing the effect of protease inhibitor cocktail on caspase-3 activity. Untreated and BFA treated (30 µg/ml, 24 hrs) HL60 cell lysates (5 µg protein), which were isolated with or without protease inhibitor cocktail, were used in a caspase activity assay with caspase-3 substrate (50 µM) to determine the effect of protease inhibitors on caspase activity. Samples were prepared and analysed in triplicate and RFU values (shown on graph) reflect averages with error bars representing the standard deviation.

It was found that the protease inhibitor cocktail did in fact significantly inhibit caspase-3 activity, as indicated by Fig. 27. Both the untreated and drug-treated (30 µg/ml BFA) samples that did not contain protease inhibitor cocktail had higher caspase-3 activity compared to the untreated and BFA treated samples with added protease inhibitor

cocktail. It was therefore decided not to include protease inhibitor cocktail when isolating protein for the caspase assays.

3.1.3.3 Caspase assay controls

Using the optimised conditions established (section 3.1.3.2), the following control assays were performed to determine if the caspase assay was working correctly and to understand the role of the various assay components in generating the fluorescent signal:

1. Heat inactivation of lysates (15 min in rapidly boiling water)
2. Cell lysates only (no caspase substrate)
3. Caspase substrate (50 µM per sample) with reaction buffer only
4. Caspase substrate (50 µM per sample) only
5. Reaction buffer only
6. Cell lysis buffer only

The RFU values obtained from these control assays are shown in Figs. 28 and 29.

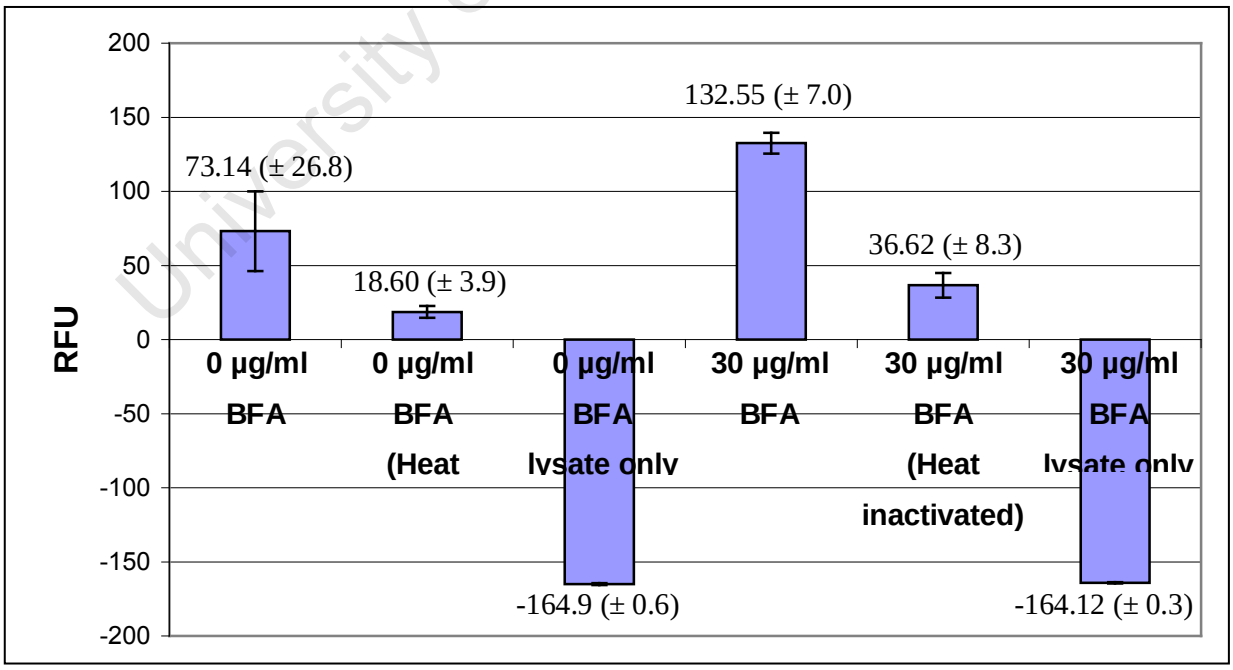

Fig. 28. The effect of the heat inactivation on caspase activity and cell lysates on the assay reaction. Caspase reactions were performed with untreated and drug-treated (30 µg/ml BFA, 24hrs) HL60 cell lysates (5µg protein; without protease inhibitor cocktail). The effect of heat inactivation on caspase activity as well as the effect of the cell lysates (without caspase substrate) was determined. Samples were prepared and analysed in triplicate and the average RFU values are shown on the graph with the error bars representing the standard deviation. An automatic blank setting was used to obtain RFU values.

Fig. 28 indicates that the untreated cell lysates contained a low level of caspase-3 activity, since approximately 5-10% of the cells were apoptotic (background level of apoptosis) (section 3.1.1.2), as expected. The BFA treated samples (approximately 20% early apoptosis) showed an increase in caspase-3 activity compared to the untreated samples, as expected. After heat inactivation (a basic means of inducing loss of enzymatic function through protein denaturation), the RFU values for both drug-treated and untreated samples significantly decreased. This indicated that the fluorescence signals were in fact due to enzyme (caspase) activity. Furthermore, the absence of a positive signal without addition of caspase-3 substrate (lysate only samples) indicated that the reaction was specific for caspase-3 activity and that samples did not auto-fluoresce.

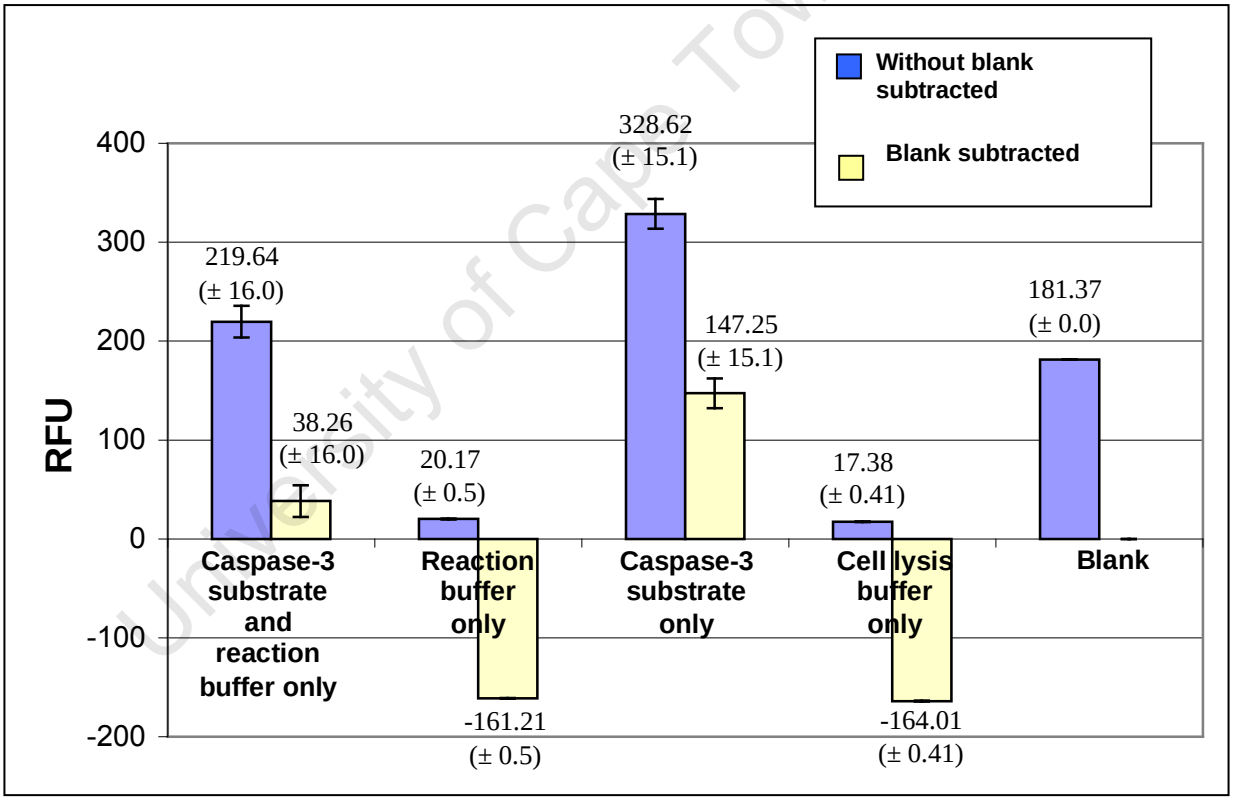

Fig. 29. The effects of the different assay components on the caspase assay reaction. Caspase assays were performed without any cell lysates and the effects of caspase-3 substrate, reaction buffer and cell lysis buffer were determined. Samples were prepared and analysed in triplicate and the average RFU values are shown on the graph with the error bars representing the standard deviation. Values on the graph represent samples without the blank subtracted (blue) and samples with the blank subtracted (yellow).

Fig. 29 indicated that the caspase-3 substrate (on its own) auto-fluoresces, however, this effect was reduced after addition of reaction buffer, which contains DTT. Fig. 29 also shows that the cell lysis buffer and reaction buffer did not auto-fluoresce. The blank

reaction, which contained all components (caspase substrate, reaction buffer and cell lysis buffer), had a greater RFU value than the cell lysis and reaction buffers on their own (Fig. 29 blue bars). Therefore, after the blank was subtracted, it resulted in large negative RFU values for both buffers (Fig. 29 yellow bars). In contrast, the caspase-3 substrate (only) reaction had a greater RFU value than the blank reaction (Fig. 29 blue bars). Therefore, it produced a positive RFU value after the blank was subtracted (Fig. 29 yellow bar).

3.1.3.4 AMC standard curve

Caspase activity was measured as an increase in fluorescence intensity, which occurred as a result of the cleavage of AMC molecules, and was expressed as RFU values. Since RFU values were not constant and can vary with each experiment, the sample RFU readings were converted to AMC release (µM) using the equation from a standard curve (Fig. 30). (The AMC standards were prepared as described in section 2.4.4 and Table 3.) Fig. 30 shows an example of an AMC standard curve obtained from the RFU values of the AMC standards.

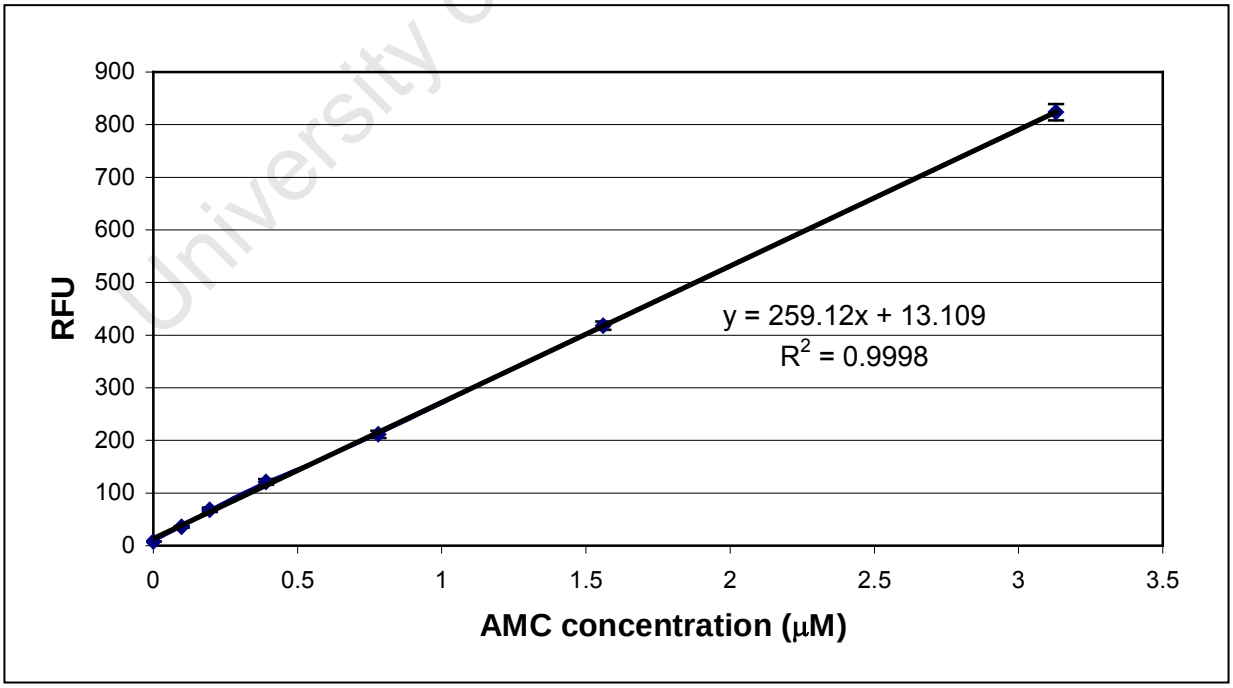

Fig. 30. Example of an AMC standard curve for caspase assays. AMC standards (3.13 µM - 0.0975 µM) were prepared by serially diluting 10 mM AMC stock solution with dH_2O. Sample RFU readings were converted to AMC release (µM) using the standard curve equation. The AMC standards were prepared and analysed in triplicate and the average RFU values are shown on the graph with the error bars representing the standard deviation. An automatic blank setting was used to obtain RFU values.

3.1.3.5 Caspase assay for all caspase substrates

After the optimisation experiments, the validity of the caspase assays for all caspase substrates (caspase-3, -4, -8 and -9) were confirmed using untreated and BFA treated (30 µg/ml BFA, 24 hrs) cell lysates. The aim was to see if the appropriate caspases would be activated after induction of the ER-stress induced apoptotic pathway (via BFA treatment).

The caspase assays were performed as described in section 2.4 (according to the optimised conditions determined). The AMC release for the samples is shown in Fig. 31.

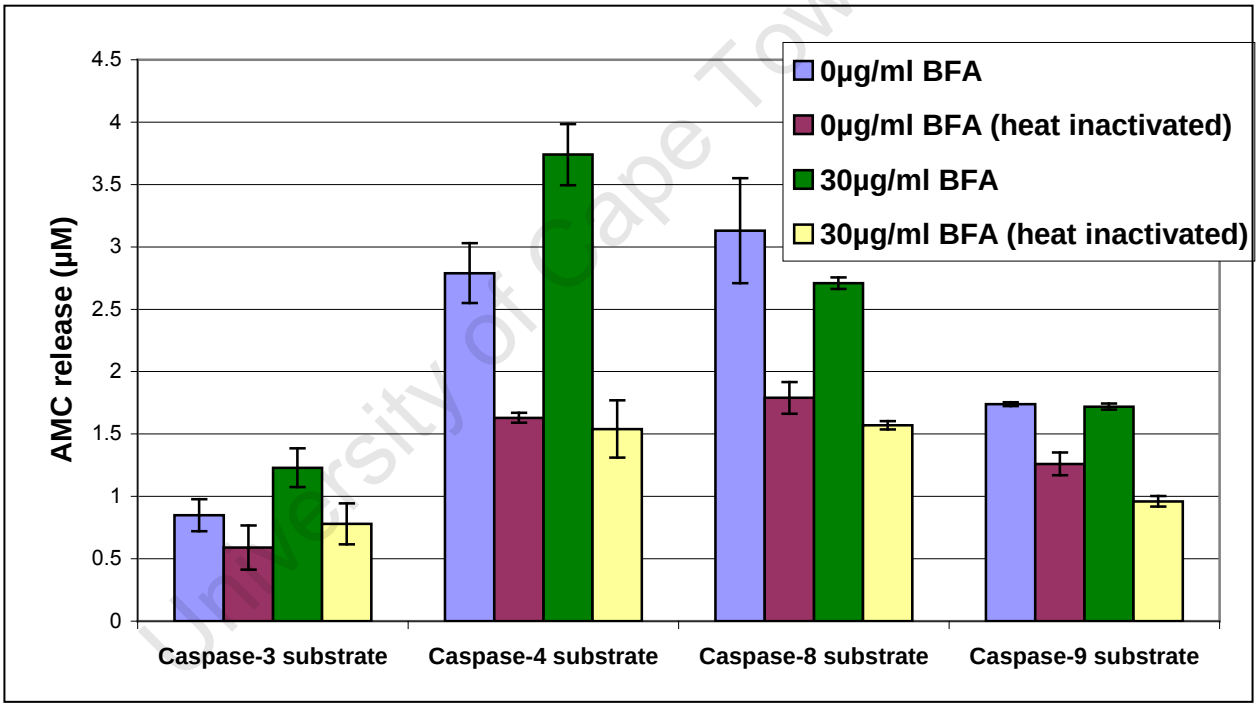

Fig. 31. AMC release for all caspase substrates using untreated and BFA lysates. BFA treated (30 µg/ml, 24 hrs) (green) and untreated (blue) HL60 cell lysates (10 µg protein) were analysed for caspase activity and compared to heat inactivated controls (purple- untreated heat inactivated cell lysates and yellow- BFA treated heat inactivated cell lysates). Samples were prepared and analysed in triplicate and AMC release reflects averages with standard deviation as indicated by error bars. The average RFU for the blank readings were subtracted from the average sample RFU values before the AMC release was calculated. Readings were taken at Ex/Em= 354/442 nm with Ex/Em slit= 20/20nm and PMT Voltage= High.

Fig. 31 shows that AMC release was reduced for all samples after heat inactivation, which indicated that enzyme activity was reduced. Any changes in AMC release were therefore due to changes in enzyme (caspase) activity. The untreated samples (0 µg/ml

BFA, 24 hrs) indicated that all four caspases were activated in the apoptotic cell population (approximately 5-10% cell death; section 3.1.1.2), with caspase-4 and -8 activity being greatest. As expected, there was an increase in caspase-3 and -4 activity for BFA treated cells (approximately 20% early apoptotic), since the ER-stress induced apoptotic pathway was activated. There was no increase in caspase-8 and -9 activity for BFA treated cells compared to their untreated values. The experiment therefore confirmed that the caspase assay could be performed for all four of the caspase substrates.

3.1.3.6 Use of alternative protein extraction buffer for caspase assay

Two different protein extraction buffers were used for the western blot analysis (RIPA buffer) and caspase assays (Cell lysis buffer). As a result, it was important to determine if one extraction buffer (RIPA), and therefore one protein sample, could be used for both assays (for the final experiments of section 3.2.3).

The caspase assay was performed as described in section 2.4 (according to the optimised conditions determined), except protein was extracted with RIPA buffer (without protease inhibitors) instead. The AMC release for all samples is shown in Fig. 32.

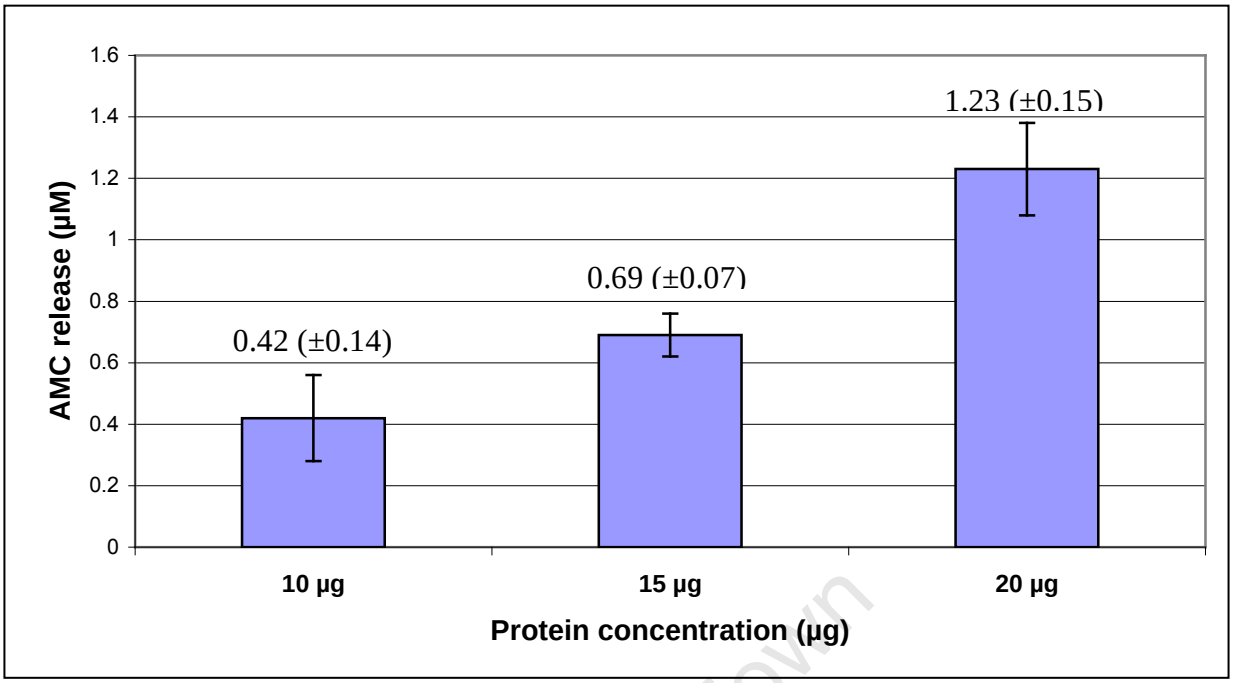

Fig. 32. AMC release for RIPA buffer extracted BFA treated HL60 cell lysates at different protein concentrations. HL60 cells were treated with BFA (30 µg/ml, 24 hrs) and protein was isolated with RIPA buffer. Caspase-3 activity (using 50 µM caspase-3 substrate per reaction) at different protein concentrations (10 - 20 µg) was determined at Ex/Em= 354/442 nm with Ex/Em slit= 20/20nm and PMT Voltage= High. Samples were prepared and analysed in triplicate and RFU values reflect averages with standard deviation. The average RFU for the blank readings were subtracted from the average sample RFU values. The RFU readings for the samples were converted to AMC release (µM) using the equation of the AMC standard curve.

Fig. 32 shows a linear increase in caspase-3 activity with increasing protein concentrations. RIPA buffer could therefore be used to determine caspase activity, however, the AMC release (for 10 µg protein) was significantly lower (0.42 (±0.14) µM) compared to that of the Cell lysis buffer lysates in Fig. 31, which was 0.78 (±0.17) µM. Moreover, protease inhibitors, which would reduce caspase activity and the sensitivity of the assay, have to be included in the protein extraction buffer for the western blot experiments. Therefore, the same protein sample cannot be used for both experiments.

3.1.4 Cytochrome *c* release immunohistochemistry assays

Immunohistochemistry assays were performed on untreated and H_2O_2 treated HL60 cells to investigate cytochrome *c* release from the mitochondria as described in section 2.5. Fig. 33 shows all the experiments conducted.

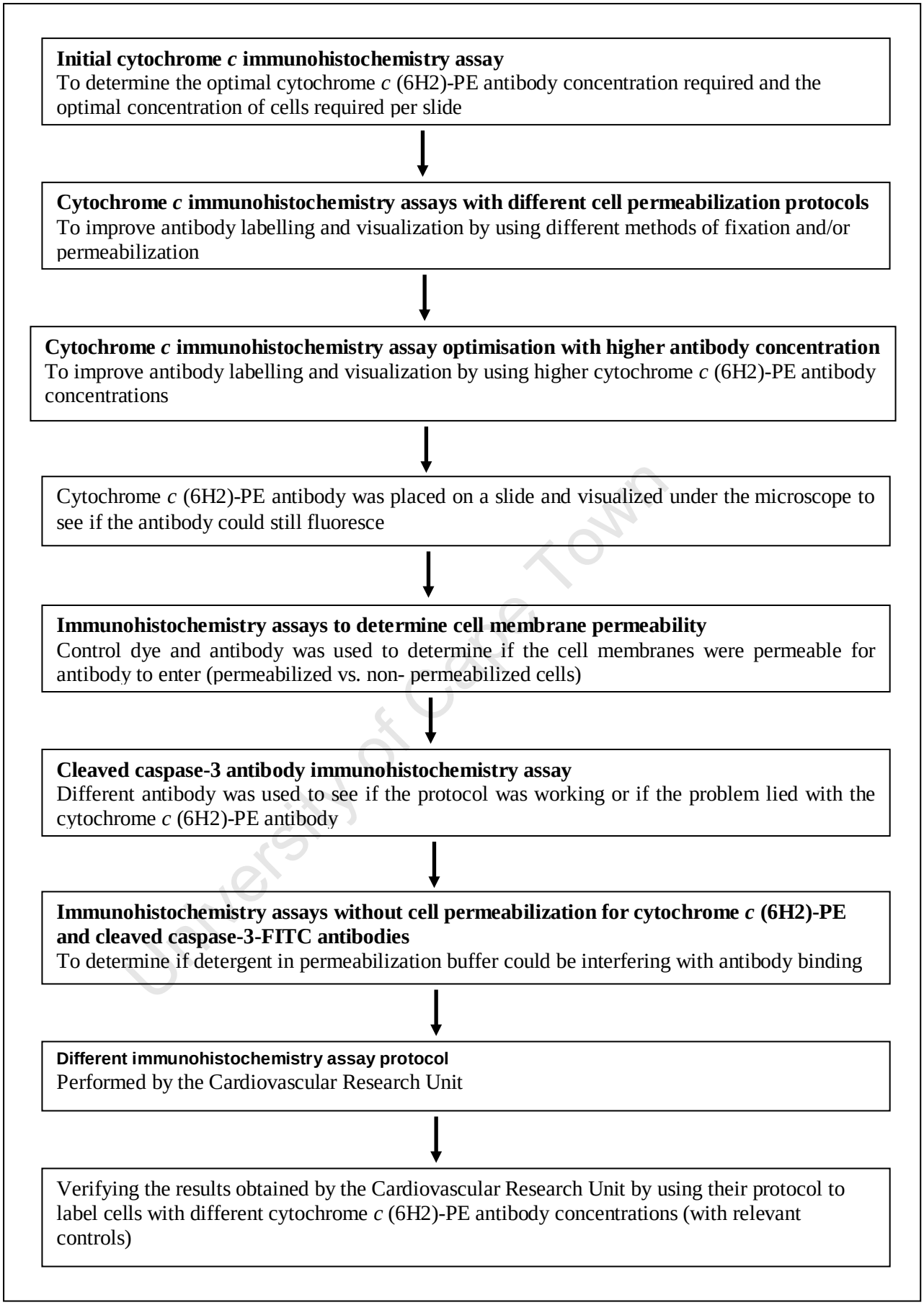

Fig. 33. Flow diagram that summarizes all the experiments conducted in this section.

3.1.4.1 Initial cytochrome *c* immunohistochemistry assay

Firstly, the optimal cytochrome *c* (6H2)-PE antibody concentration (required for visualization of cytochrome *c* release via fluorescent microscopy) and optimal concentration of cells required per slide was determined. The cells were treated as described in section 2.5.2.

It was found that 10^5 cells per slide and 4 µg/ml cytochrome *c* (6H2)-PE antibody was required for fluorescence detection, since higher cell numbers caused the background fluorescence to increase (data not shown). However, it was very difficult to find the cells at lower exposure times (less than 2 s exposure) and increasingly difficult to maintain focus on the cells at these high exposure times. Therefore, it could not be clearly distinguished, even at higher magnification, whether the labelled cytochrome *c* molecules were inside the mitochondria or being released into the cytoplasm of the cells.

3.1.4.2 Cytochrome *c* immunohistochemistry assays using different cell permeabilization protocols to improve antibody labelling

Since the cells were difficult to visualize, it was decided to modify the immunohistochemistry protocol to see if cell labelling and visibility could improve. Different methods for fixation were performed, as well as including a cell membrane permeabilization step to ensure that the antibody was able to enter the cells and label cytochrome *c* molecules. A different blocking solution, instead of FBS, was also used (as described in section 2.5.3) (Fig. 34).

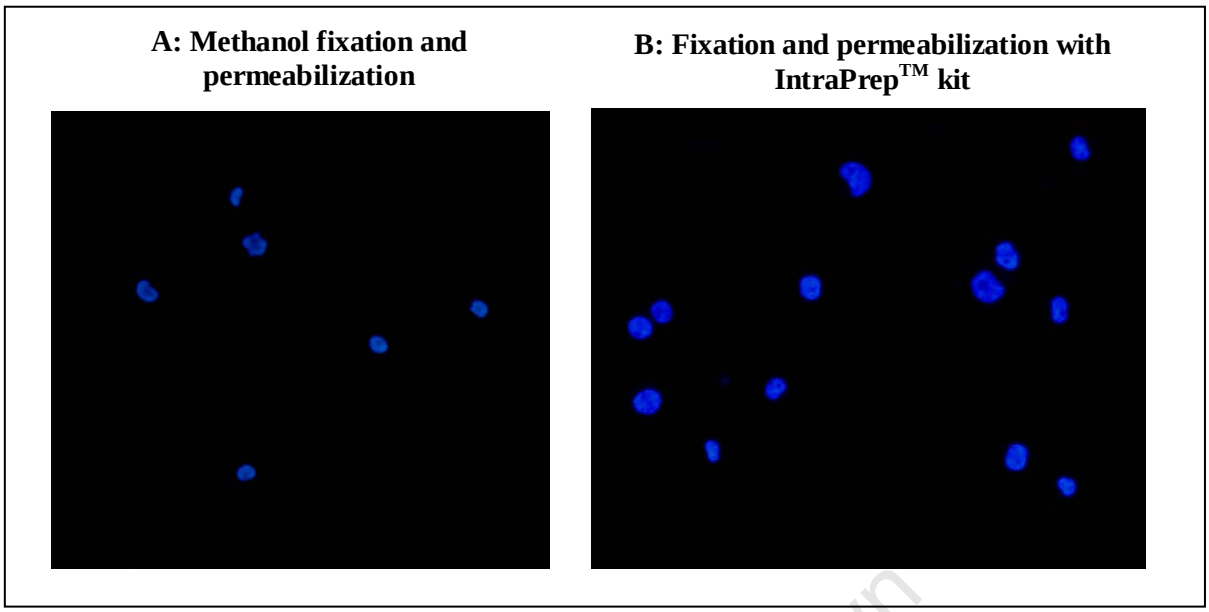

Fig. 34. Immunohistochemistry assay using different cell permeabilization protocols to improve cytochrome *c* labelling. Untreated HL60 cells (10^5 cells per slide) were either fixed and permeabilized using methanol and permeabilization buffer (**A**) or the IntraPrep™ kit (**B**) and labelled with cytochrome *c* (6H2)-PE labelled antibody (4 µg/ml). The cells were mounted with VECTASHIELD® mounting medium and visualized via a fluorescent microscope, using the DIA filter at 833 ms exposure time (gain=high; gamma=0.45) and 10x magnification.

There was no significant difference found between the two fixation and permeabilization methods (Fig. 34). The unstained cells did not produce any fluorescence signal in the Cy3 (PE) channel (833 ms exposure), therefore indicating that the cells did not auto-fluoresce. However, the cytochrome *c* (6H2)-PE labelled cells (for both methods) did not fluoresce in the Cy3 (PE) channel (833 ms - 8 s exposure) either. Only the cells mounted with VECTASHIELD® could be visualized under the microscope in either the DAPI or DIA channels (833 ms exposure) (Fig. 34 A and B). At exposure times of 5 - 10 s the resolution on the microscope's computer screen was considerably reduced and only static was visible without any cells.

3.1.4.3 Cytochrome *c* immunohistochemistry assay optimisation with higher antibody concentration

It was decided to repeat the assay using the methanol fixation and permeabilization method and a higher cytochrome *c* (6H2)-PE antibody concentration as described in section 2.5.4. An isotypic negative antibody was included as a control to check for non-

specific labelling. (Figures are not shown, since fluorescence was either too weak or there was no signal at all).

The untreated, unstained cells did not fluoresce in any channel (at 833 ms or 4 s exposure) therefore the cells did not auto-fluoresce. However, the H_2O_2 treated, unstained cells showed some faint green fluorescence in the FITC channel (833ms exposure) but not in the Cy3 (PE) channel. This indicated that perhaps the drug treatment caused some auto-fluorescence in the FITC, but not Cy3 (PE), channel.

There was no fluorescence signal detected for the untreated, 8 µg/ml or 20 µg/ml cytochrome *c* (6H2)-PE antibody labelled cells in the Cy3 (PE) channel, even at higher exposure times (4 s). The 20 µg/ml cytochrome *c* (6H2)-PE antibody labelled cells did, however, produce a non-specific green fluorescence signal in the FITC channel at 4 s exposure time. It therefore appeared that the untreated cells did not label with the cytochrome *c* (6H2)-PE antibody at both antibody concentrations.

The H_2O_2 treated, 20 µg/ml cytochrome *c* (6H2)-PE antibody labelled cells had no fluorescence signal in the Cy3 (PE) channel (833 ms or 4 s exposure), thus indicating that the cells had not labelled with the antibody. The H_2O_2 treated, 8 µg/ml cytochrome *c* (6H2)-PE antibody labelled cells had some faint fluorescent signal in the Cy3 (PE) channel at 4 s exposure. However, the signal at 833 ms exposure was significantly reduced. Therefore, these cells did not label properly with the cytochrome *c* (6H2)-PE antibody either. At both cytochrome *c* (6H2)-PE antibody concentrations (8 µg/ml and 20 µg/ml) the drug-treated cells did, however, fluoresce green in the FITC channel at 833 ms exposure time. This indicated that the drug treatment possibly caused some auto-fluorescence and/or non-specific fluorescence in the FITC, but not Cy3 (PE), channel.

The IgG-PE antibody labelled untreated cells (negative isotypic control) had no fluorescent signal in the Cy3 (PE) channel at 833 ms or 4 s exposure. This indicated that there was no non-specific labelling for the untreated cells. The IgG-PE antibody labelled drug-treated cells had a very faint fluorescent signal in the Cy3 (PE) channel at 4 s exposure but none was detected at 833 ms. These cells did, however, fluoresce green

in the FITC channel at 833ms exposure, indicating again that H_2O_2 treatment may have caused some auto-fluorescence in the FITC channel.

Since the IgG-PE antibody labelled cells (untreated and drug-treated) did not fluorescence in the FITC or Cy3 (PE) channels at 833 ms exposure, it was decided that this was sufficient to detect a true fluorescence signal. Higher exposure times caused non-specific fluorescence in the wrong channels, such as FITC.

Given that the cells did not label with cytochrome *c* (6H2)-PE antibody, a drop of the antibody was placed on a slide and visualized under the microscope. The different channels were used to see if the antibody could still fluoresce. It was also compared to the fluorescence of a drop of the cleaved caspase-3-FITC antibody. It was found that both antibodies did fluoresce (data not shown). The cytochrome *c* (6H2)-PE antibody fluoresced bright orange-red in the DIA, FITC and Cy3 (PE) channels at 833 ms exposure and only in the DIA and Cy3 (PE) channels at 72 ms exposure. The cleaved caspase-3-FITC antibody fluoresced bright green in the FITC and DIA channels at 833 ms exposure with no signal in the Cy3 (PE) channel. There was no signal for the cleaved caspase-3-FITC antibody at lower exposure times. It therefore appeared that high exposure times may have caused the cells to fluoresce in the wrong channels, and therefore did not reflect true fluorescence signals from antibody labelling.

3.1.4.4 Immunohistochemistry assays to determine cell membrane permeability

Given that the cells still did not have a fluorescence signal after cytochrome *c* (6H2)-PE antibody labelling, it was decided to determine their permeability status. Perhaps the cell membranes were not permeable to allow the antibody to enter and bind its target. Immunohistochemistry assays using CD45-FITC murine monoclonal antibody and propidium iodide (PI) as controls, to determine the cell permeability status, were performed as described in section 2.5.5 (Figs. 35 and 36).

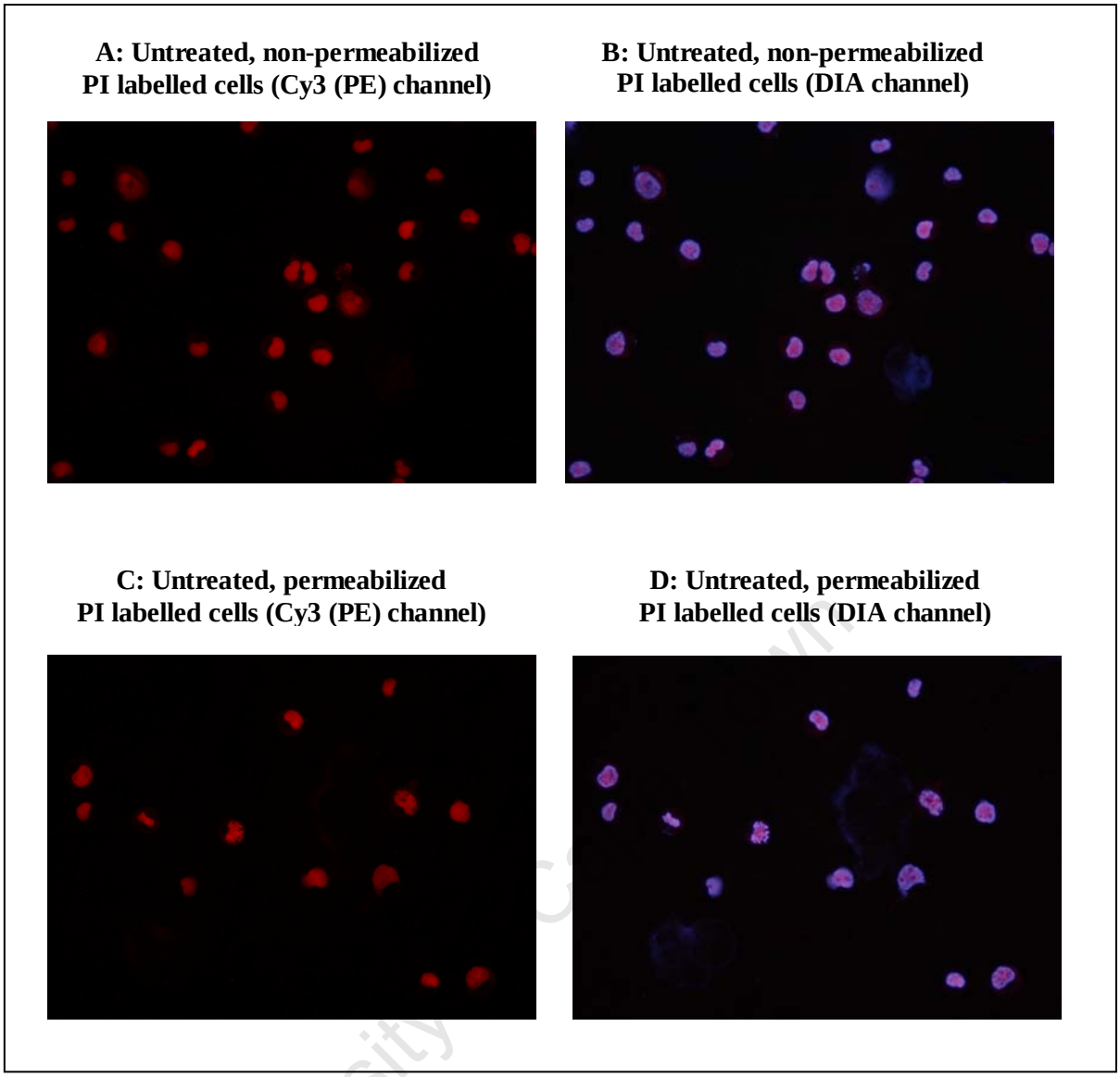

Fig. 35. Immunohistochemistry assay with PI labelling of non- permeabilized and permeabilized HL60 cells. Untreated HL60 cells (10^5 cells per slide) were fixated with methanol and either permeabilized with buffer (**C, D**) or not (**A, B**). The cells were labelled with PI, to determine if the permeabilization procedure worked, and mounted with VECTASHIELD® mounting medium. The cells were visualized via a fluorescent microscope using the Cy3 (PE) and DIA filters at 833ms exposure time and 20x magnification.

The unstained controls for both untreated and H_2O_2 treated cells (permeabilized and non-permeabilized) showed no fluorescence in the Cy3 (PE) or FITC channels at 833 ms exposure, indicating that the cells did not auto-fluoresce.

All PI labelled cells (untreated and drug-treated, both permeabilized and non-permeabilized) fluoresced in the Cy3 (PE) (red fluorescence for PI labelling) and DIA channels (Fig. 35). The DIA (triple) channel can detect and overlap the different colours from fluorescence signals in the FITC (green), Cy3 (PE) (red) and DAPI (blue) channels. The purple fluorescence seen in the DIA channel occurred as a result of the

overlap between the red fluorescence of the PI staining (in Cy3 (PE)) and the blue fluorescence of the DAPI stain (in the VECTASHIELD® mounting medium) (Figs. 35 B and D).

PI can only enter and stain the nuclei and DNA of permeabilized cells. Since all the cells (permeabilized and non-permeabilized) labelled with PI, it therefore indicated that all the cells were permeabilized. Therefore, the methanol fixation alone was sufficient to permeabilize the cell membranes to allow the cytochrome *c* (6H2)-PE antibody to enter and stain its target. The additional permeabilization step, with detergent buffer, would therefore not be necessary and the detergent could possibly hamper antibody-antigen binding.

Cells were also labelled with CD45-FITC antibody, which served as a positive control for non-permeabilized cell membranes (Fig. 36). The CD45-FITC antibody binds to the CD45 family of cell-surface markers of intact haematopoietic cells, therefore no fluorescence signal should be detected if the cell membranes were permeabilized.

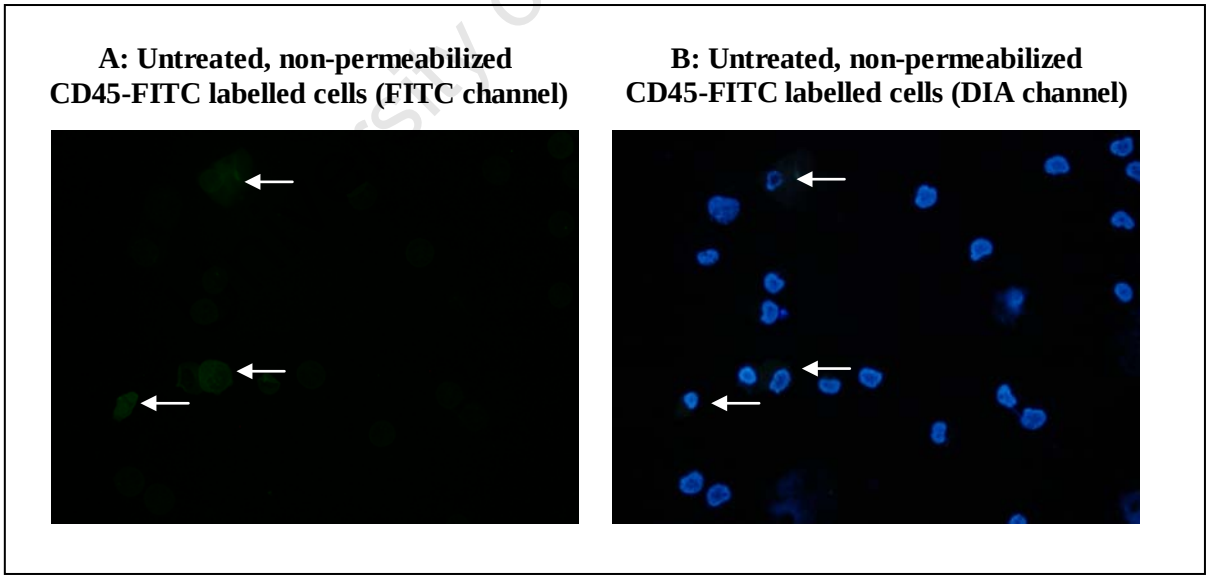

Fig. 36. Immunohistochemistry assay with CD45-FITC antibody labelling of non-permeabilized and permeabilized HL60 cells. Untreated HL60 cells (10^5 cells per slide) were fixated with methanol without permeabilization. The cells were labelled with CD45-FITC murine monoclonal antibody, to determine if the cell membranes were still intact, and mounted with VECTASHIELD® mounting medium. The cells were visualized via a fluorescent microscope using the FITC (**A**) and DIA (**B**) filters at 833ms exposure time and 20x magnification. The white arrows indicate the green fluorescing cell membranes labelled with antibody.

Fig. 36 shows the FITC (Fig. 36 A) and DIA channel (overlapping FITC and DAPI) (Fig. 36 B) for the untreated, non-permeabilized CD45-FITC labelled cells. Only the faint green outlines of some cells (indicated by the white arrows) were visible in both the DIA and FITC channels (833 ms exposure). This indicated that these cells' membranes were still intact. However, the remaining cells that did not fluoresce in the FITC channel (Fig. 36 A) but only in the DIA channel (Fig. 36 B), did not label with CD45-FITC antibody. These cells therefore had permeabilized membranes. Furthermore, the drug-treated, permeabilized CD45-FITC labelled cells also showed some fluorescence in the FITC channel, although it was significantly weaker compared to the results in Fig. 36 (data not shown). In contrast, the untreated, permeabilized and drug-treated, non-permeabilized CD45-FITC labelled cells did not have any fluorescence signal in the FITC channel (833 ms exposure). This indicated that their cell membranes had been permeabilized (data not shown).

It was therefore concluded that most cells (whether permeabilized with buffer or not) had permeablized membranes (due to the methanol fixation). This confirmed the previous results obtained from the PI labelled cells (Fig. 35). The protocol was therefore working, since the CD45-FITC antibody and PI could enter the cells and bind to their targets (whether the cells were incubated with permeabilization buffer or not). Furthermore, it indicated that the permeabilization buffer did not necessarily interfere with antibody-antigen binding properties, since the drug-treated, permeabilized (CD45-FITC labelled) cells fluoresced in the FITC channel, albeit weakly.

3.1.4.5 Cleaved caspase-3 (Asp175) antibody immunohistochemistry assay to determine viability of assay protocol

The viability of the immunohistochemistry protocol (with the permeabilization step) was determined by repeating the experiment using another antibody as a positive control (as described in section 2.5.6). Cleaved caspase-3 (Asp175) polyclonal rabbit antibody (Alexa Fluor®488 conjugate), which binds to caspase-3 molecules in cells undergoing apoptosis, was used for this purpose (Fig. 37). By using another antibody, it could be determined if it was the protocol that was ineffective or if the antibody (cytochrome *c* (6H2)-PE) had lost its binding specificity and/or affinity.

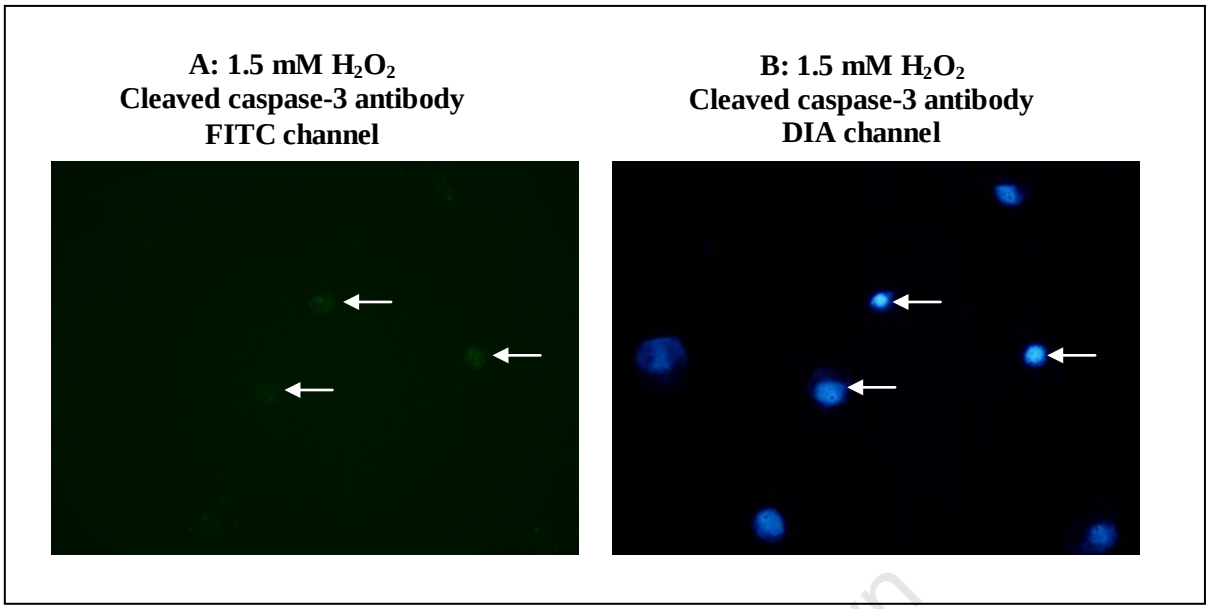

Fig. 37. Immunohistochemistry assay with cleaved caspase-3-FITC antibody to determine viability of labelling protocol. H_2O_2 treated (1.5 mM H_2O_2 for 24 hrs) HL60 cells (10^5 cells per slide) were fixated with methanol and permeabilized. The cells were labelled with cleaved caspase-3-FITC antibody, to determine if the assay protocol works, and mounted with VECTASHIELD® mounting medium. The cells were visualized via a fluorescent microscope using the FITC (**A**) and DIA (**B**) filters at 833ms exposure time and 20x magnification. The white arrows indicate the green fluorescing cleaved caspase-3 molecules labelled with antibody.

The unstained controls (for both untreated and drug-treated cells) did not fluoresce in the Cy3 (PE) or FITC channels at 833 ms exposure, therefore indicating that the cells did not auto-fluoresce. There was also no fluorescence signal detected for the isotypic control (IgG1-FITC) antibody labelled cells, therefore indicating that the cells were not labelling non-specifically. Furthermore, the untreated, cleaved caspase-3-FITC antibody labelled cells did not fluoresce in the FITC channel at 833 ms exposure either. However, this could be due to low levels of apoptosis in untreated cells with insufficient levels of cleaved (activated) caspase-3 molecules present.

The drug-treated (1.5 mM H_2O_2 for 24 hrs) cells successfully labelled with cleaved caspase-3-FITC antibody and produced a green fluorescence signal in the FITC and DIA channels at 833 ms exposure (Fig. 37). It was concluded from Fig. 37 that the immunohistochemistry assay protocol worked, since the cleaved caspase-3-FITC antibody could bind to its target and produce a fluorescence signal. It therefore appeared that something was wrong with the cytochrome *c* (6H2)-PE antibody and its ability to bind successfully to its target molecule and to produce a fluorescent signal.

3.1.4.6 Immunohistochemistry assays without cell permeabilization for cytochrome *c* (6H2)-PE and cleaved caspase-3-FITC antibodies

Since the previous experiment was successful, it was decided to repeat the assay using the cytochrome *c* (6H2)-PE and cleaved caspase-3-FITC antibodies without the permeabilization step (as described in section 2.5.7). The aim was to determine if the buffer detergent could be interfering with the cytochrome *c* (6H2)-PE antibody's ability to bind to its target antigen.

There was no fluorescence signal detected in the Cy3 (PE) or FITC channels (833 ms exposure) for the unstained cells or isotypic controls (IgG1-PE and IgG1-FITC labelled cells). This indicated that the cells did not auto-fluoresce or label non-specifically.

The untreated and drug-treated cells labelled with cytochrome *c* (6H2)-PE antibody did not fluoresce in the Cy3 (PE) channel (833 ms exposure). Furthermore, the untreated and drug-treated cells labelled with cleaved caspase-3-FITC antibody did not fluoresce in the FITC channel (833 ms exposure) either (data not shown). Therefore the experiment was unsuccessful, since both antibodies failed to label their target antigens. This again indicated that the permeabilization buffer did not appear to interfere with cytochrome *c* (6H2)-PE antibody binding affinity. Therefore, both the permeabilization and non-permeabilization protocols seemed to be ineffective for successful cytochrome *c* labelling.

3.1.4.7 Different immunohistochemistry assay protocol for cytochrome *c* release

Since the previous immunohistochemistry protocol was unsuccessful, it was decided to try another protocol. Untreated and H_2O_2 treated (1.5 mM H_2O_2 for 24 hrs) HL60 cells were fixed with methanol and the slides sent to the Cardiovascular Research Unit (MRC/UCT Cape Heart Centre) for labelling. The Cardiovascular Research Unit used their own method to label the cells with either cytochrome *c* (6H2)-PE (2 µg/ml) or cleaved caspase-3-FITC (1:10 dilution) antibodies. The cells were mounted with VECTASHIELD® and are shown in Figs. 38-39.

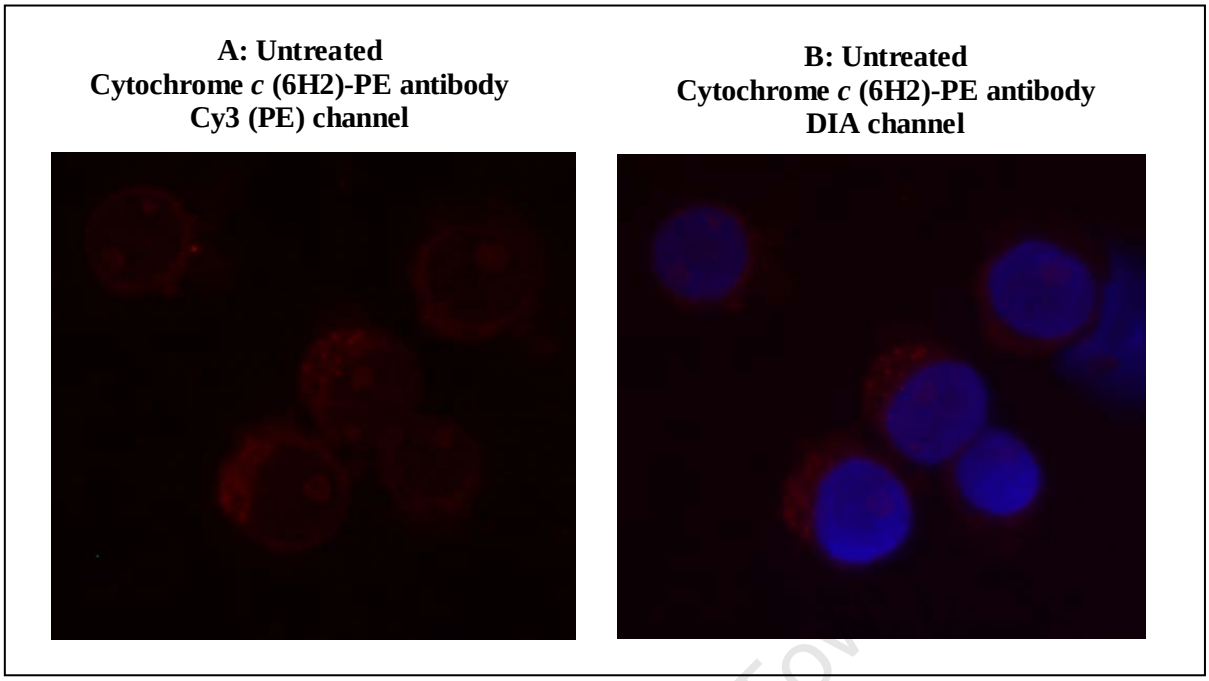

Fig. 38. Immunohistochemistry assay with cytochrome *c* (6H2)-PE antibody performed by the Cardiovascular Research Unit. Untreated HL60 cells (10^5 cells per slide) were fixated with methanol and labelled with cytochrome *c* (6H2)-PE antibody. The cells were mounted with VECTASHIELD® and visualized via a fluorescent microscope using the Cy3 (PE) (**A**) and DIA (**B**) filters at 1 s exposure time and 40x magnification.

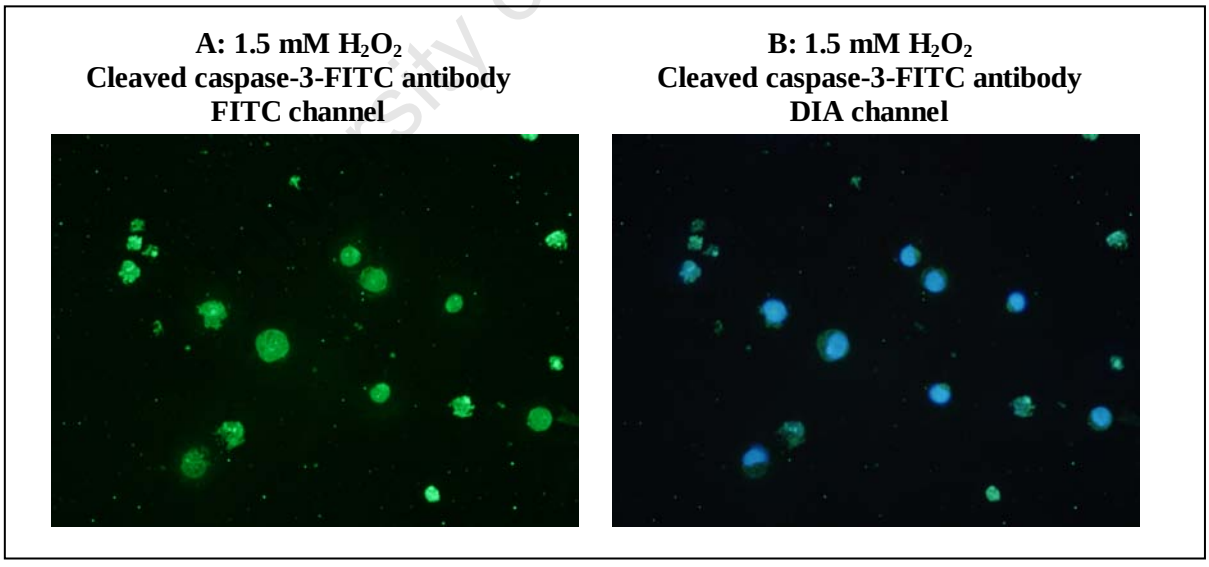

Fig. 39. Immunohistochemistry assay with cleaved caspase-3-FITC antibody performed by the Cardiovascular Research Unit. H_2O_2 treated (1.5 mM H_2O_2 for 24 hrs) HL60 cells (10^5 cells per slide) were fixated with methanol and labelled with cleaved caspase-3-FITC antibody. The cells were mounted with VECTASHIELD® and visualized via a fluorescent microscope using the FITC (**A**) and DIA (**B**) filters at 583 ms exposure time and 20x magnification.

Their immunohistochemistry labelling protocol was successful, since both the cytochrome *c* (6H2)-PE and cleaved caspase-3-FITC antibodies labelled the target antigens and produced a fluorescence signal (Figs. 38 and 39). However, the fluorescence intensity of the cytochrome *c* (6H2)-PE labelled cells (Fig. 38), at such a high exposure time (1 s), was not as bright or intense compared to that of the cleaved caspase-3-FITC labelled cells at 583 ms exposure (Fig. 39). The cytochrome *c* (6H2)-PE antibody therefore appeared to have some difficulty in labelling the cells.

The Cardiovascular Research Unit did not perform experiments with unstained and isotypic controls, to check for auto-fluorescence and/or non-specific labelling. Furthermore, they did not check all three channels (Cy3 (PE), FITC and DIA), for each specimen, to determine if there was non-specific fluorescence. Therefore, it was decided to verify their results by using their protocol to label the cells with different cytochrome *c* (6H2)-PE antibody concentrations and to include all the relevant controls (as described in section 2.5.8).

Fig. 40 shows the images obtained after using the Cardiovascular Research Unit's protocol.

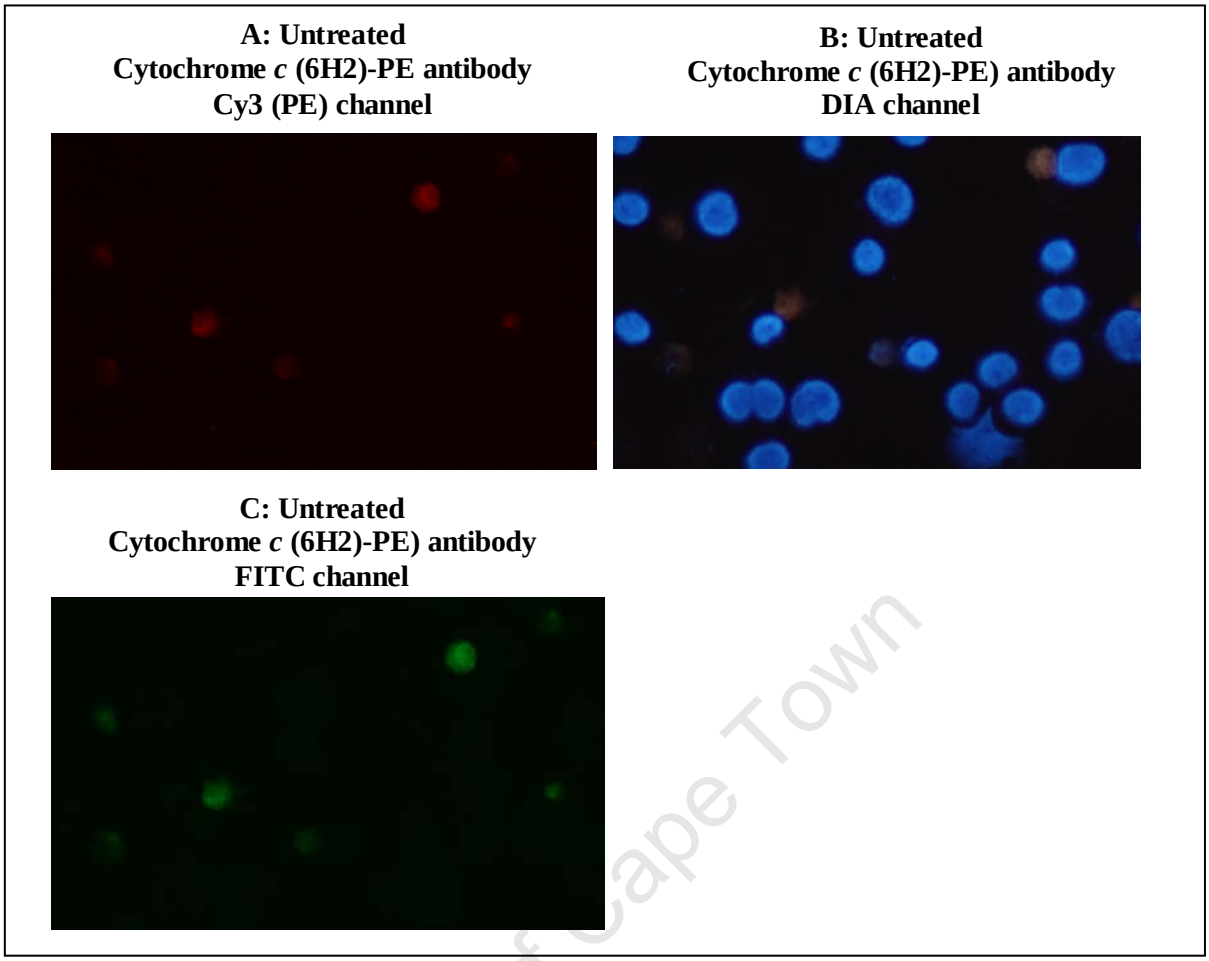

Fig. 40. Immunohistochemistry assay with new protocol using the cytochrome *c* (6H2)-PE antibody. Untreated HL60 cells (10^5 cells per slide) were labelled with cytochrome *c* (6H2)-PE labelled antibody (2 µg/ml), using the new immunohistochemistry protocol. The cells were mounted with VECTASHIELD® and visualized via a fluorescent microscope using the Cy3 (PE) (**A**), DIA (**B**) and FITC (**C**) filters at 833 ms exposure time and 20x magnification.

The results seen in Fig. 40, for the untreated cells labelled with 2 µg/ml cytochrome *c* (6H2)-PE antibody, were similar for all the different controls used in the experiment. It was found that all the cells (untreated and drug-treated) and controls (unstained and isotypic IgG1-PE labelled) fluoresced in all three channels at 833 ms exposure. This indicated that the cells auto-fluoresced and were labelling non-specifically and therefore the assay was unsuccessful. The results obtained by the Cardiovascular Research Unit (Figs. 38-39) could therefore be due to non-specific fluorescence. This could not be verified, since all the controls were not included in their experiment. It was decided to abandon the cytochrome *c* release immunohistochemistry assay and to focus on changes in MTP (section 3.1.5), before and after drug treatment, using flow cytometry.

3.1.5 Detection of changes in mitochondrial transmembrane potential (MTP) during apoptosis induction

After drug treatment, the changes in MTP of the cells were determined with MitoCapture™ labelling and flow cytometry as described in section 2.6. Fig. 41 shows the typical results obtained from drug-treated and untreated cells using the resultant colour-compensated protocol (section 2.6.2, Table 5).

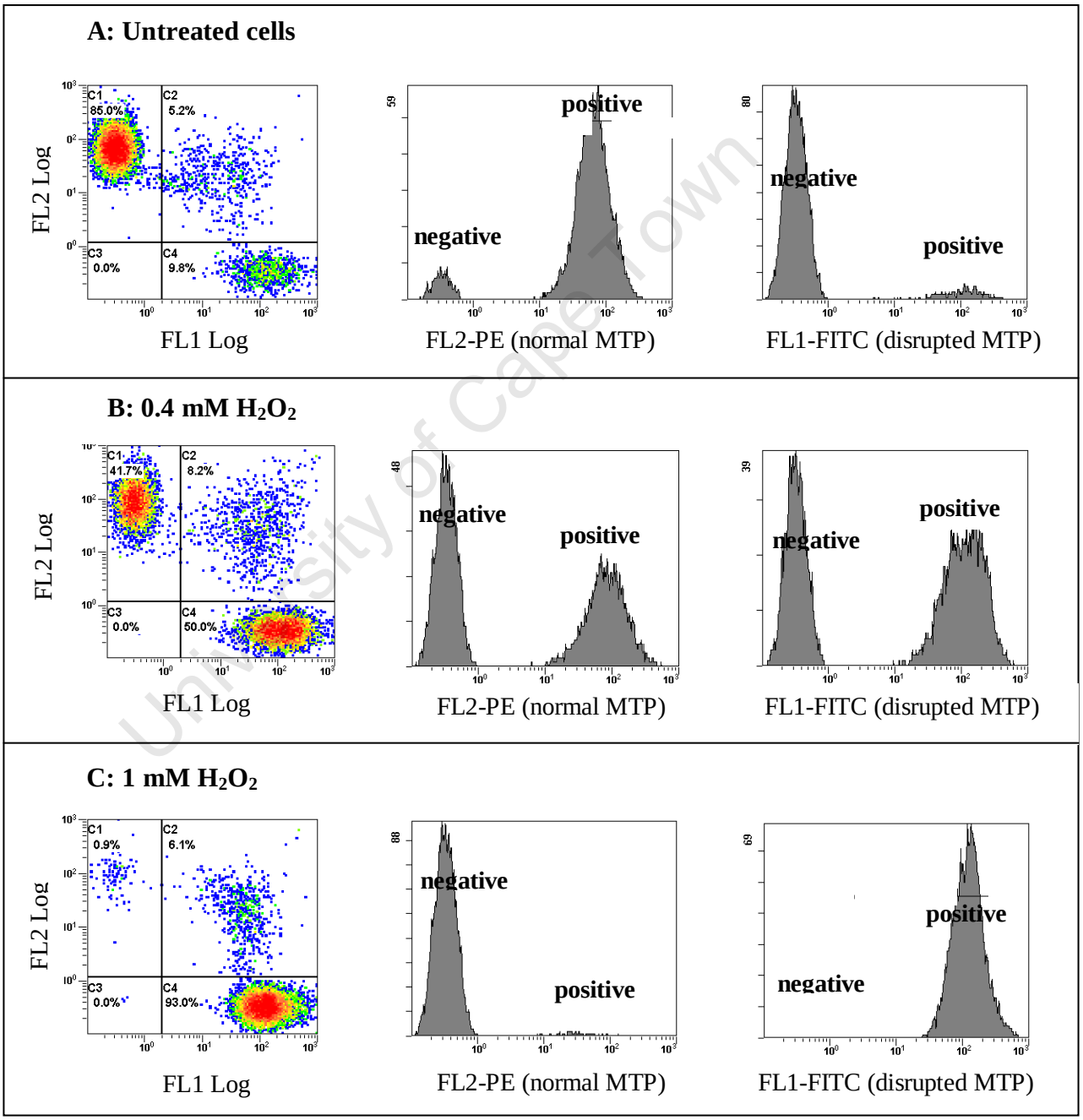

Fig. 41. Flow analysis of MitoCapture™ labelled HL60 cells showing differences in MTP with increasing drug concentrations. HL60 cells were treated with 0.4 mM (**B**) and 1 mM (**C**) H_2O_2 for 24 hrs and labelled with MitoCapture™ dye. The untreated (control) cells are shown in (**A**).

Fig. 41 shows FL2-PE histograms, which represent cells with normal/unaltered MTPs (red fluorescence) and FL1-FITC histograms, which represent cells with disrupted MTP (green fluorescence).

In the FL2-PE histogram, the "positive" peak represents normal functioning mitochondria with aggregated dye molecules, which fluoresce red in the FL2 channel. The "negative" peak represents dye molecules in the monomer state that have not been taken up by mitochondria (cells that do not fluoresce red).

In the FL1-FITC histogram, the "positive" peak represents apoptotic cells with disrupted MTP. Therefore, an increased number of dye molecules, which could not be taken up by the mitochondria, exist in the monomer state and fluoresce green in the FL1 channel. The "negative" peak represents cells that do not fluoresce green.

The colour-coded density plots (FL2 Log vs. FL1 Log) in Fig. 41 indicate the changes in MTP of the cells. Depending on the status of MTP, the cells either fluoresce:

1. Red – shown in area C1, representing cells that were non-apoptotic and had unaltered/normal MTP;
2. Green – shown in area C4, representing apoptotic cells with disrupted MTP;
3. Yellow-orange (both red and green) – shown in area C2, representing cells with both normal and disrupted MTP (intermediate MTP).

Since the majority of the untreated cells (approximately 90% viable) were non-apoptotic, most of the MitoCapture^{TM} dye was taken up by the mitochondria and therefore formed dye aggregates, which fluoresced red (Fig. 41 A, area C1). The untreated cells also had a greater percentage of red fluorescing cells in the FL2-PE histogram ("positive" peak) (Fig. 41 A) compared to that of the H_2O_2 treated cells (Figs. 41 B and 42 C).

After H_2O_2 treatment, the mitochondrial-mediated apoptotic pathway was initiated and resulted in disruption of MTP. Therefore, less dye molecules were taken up by the mitochondria, leaving it in the cytoplasm as monomers, which fluoresced green (Figs. 41 B and C, area C4). The drug-treated cells (0.4 mM and 1 mM H_2O_2 for 24 hrs) (Figs. 41 B and C) showed an increase in cells with disrupted MTP (areas C2 and C4)

compared to the untreated cells (Fig. 41 A), as expected. Furthermore, the drug-treated cells also had a greater percentage of green fluorescing cells in the FL1-FITC histograms ("positive" peaks) (Figs. 41 B and C) compared to that of the untreated cells (Fig. 41 A). Fig. 41 B also shows that approximately 50% of the 0.4 mM H_2O_2 treated cells (approximately 7% apoptosis induced) were undergoing mitochondrial-mediated apoptosis (area C4). As the drug concentration was increased to 1 mM H_2O_2 (approximately 20% apoptosis induced), this increased to 93% cells undergoing mitochondrial-mediated apoptosis (Fig. 41 C, area C4).

Some cells (untreated and drug-treated) contained both normal functioning mitochondria, as well as mitochondria with disrupted MTP. These cells had intermediate MTP and had not completely committed to cell death. The cells contained dye aggregates (inside the mitochondria), as well as dye monomers (in the cytoplasm) resulting in a yellow-orange fluorescence (Fig. 41, area C2). The untreated cells had 5.2% cells with intermediate MTP, whereas the 0.4 mM and 1 mM H_2O_2 treated cells had 8.2% and 6.1%, respectively (Fig. 41, area C2 of colour-coded density plots).

The results of the flow analysis were confirmed by visualizing the MitoCapture™ labelled cells using a fluorescent microscope (as described in section 2.6.3) (Fig. 42).

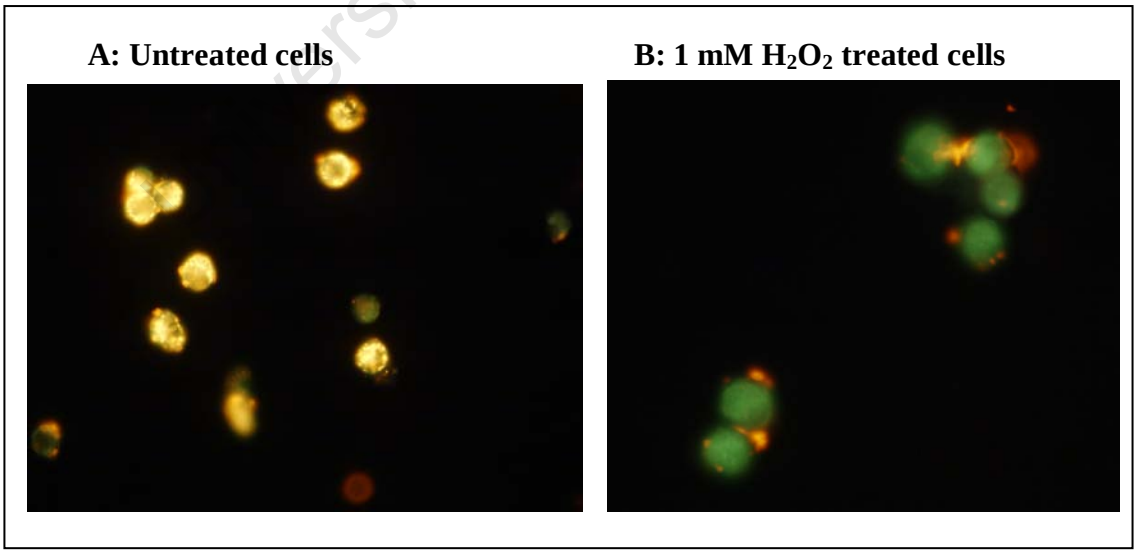

Fig. 42. Fluorescent microscopy results of H_2O_2 treated HL60 cells after MitoCapture™ labelling. HL60 cells were visualised at 40x magnification and 333 ms exposure time with a fluorescent microscope after labelling with MitoCapture™. Untreated (control) cells (**A**) and cells treated with 1 mM H_2O_2 (24 hrs) (**B**) were visualised in the DIA triple band channel.

The fluorescent microscopy results showed that the untreated cells (Fig. 42 A) had a greater amount of red fluorescence (normal/unaltered MTP) in the DIA triple-band channel, compared to the drug-treated cells (Fig. 42 B). The majority of drug-treated cells had disrupted MTP, since they contained high amounts of green fluorescing MitoCapture^{TM} dye monomers in the cytoplasm (Fig. 42 B). The fluorescent microscopy results therefore validated the results obtained via flow cytometry (Fig. 41 A and C).

3.2 Final experiments to analyse all three apoptotic pathways

The optimised conditions and techniques determined in section 3.1 were implemented in experiments to analyse all three apoptosis pathways. HL60 and Jurkat cells were treated with pathway-specific drugs as described in section 2.1.6. The cells were subsequently analysed for apoptotic response to drug treatment. The techniques included AV/PI labelling and flow cytometry, western blot analysis, caspase activity assays and detecting changes in MTP (MitoCapture^{TM} labelling and flow cytometry). These experiments were repeated for each drug (low and high dose) to compare results for each technique and determine if the results were reproducible and if the cell models are reliable.

3.2.1 Analysis of apoptotic response for all three apoptosis pathways

Cells were treated with pathway-specific drugs as described in section 2.1.6 and analysed as described in section 2.2. The experiments were performed twice for each drug and only one sample per drug concentration (untreated, low and high doses) was prepared per experiment (as shown in Table 7). The percentage of early apoptosis (% cells in area G4 of PI vs. AV colour-coded density plots) induced by all three drugs is shown in Tables 7 and 8. The values in Table 8 represent the average of the two experiments performed for each drug with the standard deviation.

Table 7: The percentage of early apoptosis induced by all three drugs for each experiment (as determined by AV/PI labelling and flow analysis)

Drug and	Experiment:	Incubation time	% Early apoptotic cells

concentration:		(hrs):	(Area G4) † :
0 μg/ml BFA	1	24	7.00
5 μg/ml BFA			12.98
30 μg/ml BFA			17.88
0 μg/ml BFA	2	24	2.10
5 μg/ml BFA			8.80
30 μg/ml BFA			22.60
0 mM H_2O_2	1	24	3.60
0.4 mM H_2O_2			10.20
1 mM H_2O_2			20.70
0 mM H_2O_2	2	24	5.00
0.4 mM H_2O_2			14.40
1 mM H_2O_2			28.30
0 ng/ml FasL	1	4	4.90
0.2 ng/ml FasL			13.50
0.4 ng/ml FasL			38.0
0 ng/ml FasL	2	4	4.60
0.2 ng/ml FasL			24.60
0.4 ng/ml FasL			57.50

† Values reflect the percentage of early apoptosis (%G4), obtained from each experiment, for each drug (n =1)

Table 7 shows the results obtained for all experiments (%G4 early apoptosis) and the variance of results between each experiment. Table 7 also shows that there was a greater variance in % early apoptosis of the untreated HL60 cells, compared to the Jurkat cells. However, this was also noted before in section 3.1.1.3 and is in accordance with the results obtained in section 3.1.1.2, which indicated that approximately 5-10% untreated cells were apoptotic.

Table 8: The average percentage of early apoptosis induced by all three drugs as determined by AV/PI labelling and flow analysis

Drug and concentration:	Incubation time (hrs):	Average % early apoptotic cells (Area G4) ‡:	Values corrected for background apoptosis †:
0 μg/ml BFA	24	4.55 (±3.5)	0
5 μg/ml BFA		10.89 (±3.0)	6.34 (±3.0)
30 μg/ml BFA		20.24 (±3.3)	15.69 (±3.3)
0 mM H_2O_2		4.3 (±1.0)	0
0.4 mM H_2O_2	24	12.3 (±3.0)	8.0 (±3.0)
1 mM H_2O_2		24.5 (±5.4)	20.2 (±5.4)
0 ng/ml FasL		4.75 (±0.2)	0
0.2 ng/ml FasL	4	19.05 (±7.9)	14.3 (±7.9)
0.4 ng/ml FasL		47.75 (±13.8)	43.00 (±13.8)

Values reflect the averages with standard deviation (*n* =2)
‡ The average % of early apoptotic cells were obtained from area G4 of the respective PI vs. AV density plots
†The average % of apoptosis of the untreated cells (for each time point) was subtracted from the average % of apoptosis obtained from the drug-treated cells

Tables 7 and 8 show that the cells treated with H_2O_2 fell within the desired range of apoptosis, with approximately 8% (low) and 20% (high) early apoptosis induced above that of the untreated cells. These results were also similar to those obtained in section 3.1.1.3 B.

Tables 7 and 8 show that the FasL treated cells had a great variation in % early apoptosis (%G4) induced between experiments. The second FasL experiment had higher %G4, at both drug concentrations, than expected (Table 7). However, as indicated by Table 7, the high dose FasL (0.4 ng/ml) induced approximately 53% early apoptosis (above that of the untreated cells), which was close to the desired range (20-50%). Values of the first FasL experiment fell within the desired range of apoptosis, with approximately 9% (low) and 33% (high) early apoptosis induced above that of the untreated cells (Table 7).

Tables 7 and 8 show that the cells treated with 5 μg/ml BFA, of both experiments, fell within the desired range of apoptosis, with approximately 6% (low) early apoptosis induced above that of the untreated cells. The 30 μg/ml BFA treated cells of the second

experiment also fell within the desired range of apoptosis, with approximately 20% (high) early apoptosis induced above that of the untreated cells (Table 7). These results were similar to those obtained in section 3.1.1.3 A for the low and high BFA concentrations. However, the 30 μg/ml BFA treated cells of the first BFA experiment, which were approximately 11% early apoptotic, had significantly less % early apoptosis induced than expected (20-50%) (Table 7).

Since the % early apoptosis induced by the 30 μg/ml BFA treated cells of the first experiment were very low, it was decided to repeat the experiments. Previously (section 3.1.1.3), only small volumes of cells (2-4 ml) (passage number 14-16) were treated to obtain the drug-response data. However, for these final experiments a larger number of cells were required for all the assays to be performed from one batch of cells per experimental condition (untreated and low and high drug doses). Therefore, larger volumes of cells were treated with drug. To determine if perhaps an increased volumetric error caused lower drug concentrations, thereby decreasing the percentage of apoptosis induced, the experiments were repeated in smaller volumes, as before (section 3.1.1.3). However, after numerous repeats there was no significant increase in apoptosis induced (above 10%) (data not shown). The quality of BFA had not been compromised, since new BFA was used. Therefore, it was decided to repeat the drug treatment with new cells that were thawed (passage number 11-13) to see if the results could improve. However, the results obtained in Table 8 could not be improved upon.

Figs. 43 - 45 show the representative PI vs. AV colour-coded density plots that were obtained for the low level (5-15%) and high level (20-50%) early apoptosis induced by BFA, H_2O_2 and FasL, respectively.

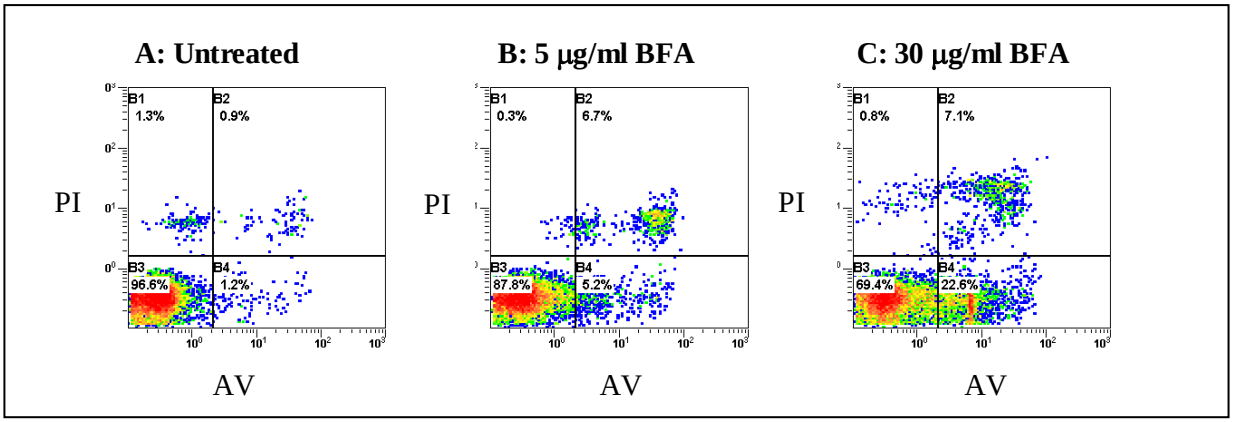

Fig. 43. PI vs. AV density plots of BFA treated HL60 cells. HL60 cells were treated for 24 hrs with (B) 5 µg/ml BFA to induce 5-15% (low level) apoptosis and (C) 30 µg/ml BFA to induce 20-50% (high level) apoptosis above that of the untreated cells (A). The cells were labelled with AV and PI and analysed via flow cytometry.

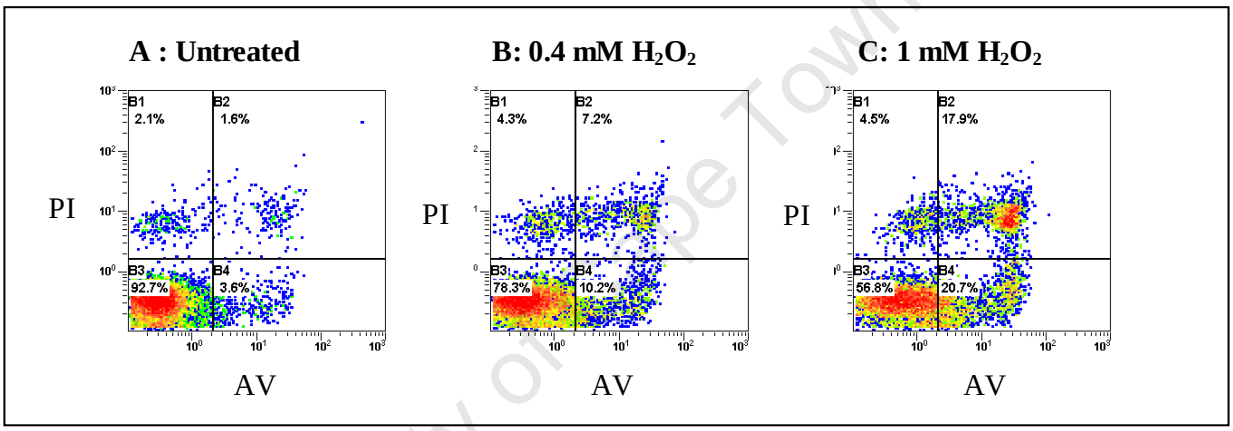

Fig. 44. PI vs. AV density plots of H_2O_2 treated HL60 cells. HL60 cells were treated for 24 hrs with (B) 0.4 mM H_2O_2 to induce 5-15% (low level) apoptosis and (C) 1 mM H_2O_2 to induce 20-50% (high level) apoptosis above that of the untreated cells (A). The cells were labelled with AV and PI and analysed via flow cytometry.

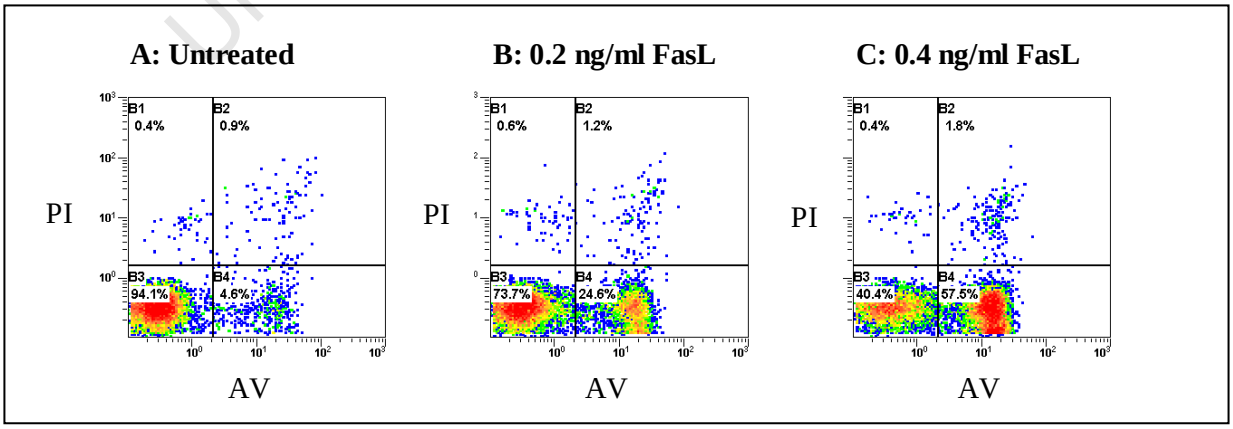

Fig. 45. PI vs. AV density plots of FasL treated Jurkat cells. Jurkat cells were treated for 4 hrs with (B) 0.2 ng/ml FLAG-tagged FasL (and 0.25 µg/ml ANTI-FLAG® antibody to induce 5-15% (low level) apoptosis and (C) 0.4 ng/ml FLAG-tagged FasL (and 0.25 µg/ml ANTI-FLAG® antibody to induce 20-50% (high level) apoptosis above that of the untreated cells (A). The cells were labelled with AV and PI and analysed via flow cytometry.

3.2.2 Western blot analysis for all three apoptotic pathways

In the final western blot assays, all three apoptotic pathways were analysed for FADD, Bip and CHOP expression (with β–actin as the invariant positive control). The cells were treated as described in section 2.1.6 and analysed via western blotting as described in section 2.3. The western blot assays were performed twice for each drug (BFA, H_2O_2 and FasL) using protein extracted from the two separate experiments for each drug as shown in Figs. 46 A and 47 A.

For the benefit of visibility, since the figures appear lighter when printed (and protein samples were transferred onto the same horizontal membrane strip), darker images/blots were shown in Figs. 46 A and 47 A (as described in section 2.3.6). However, only bands that fell within the linear range of exposure, and were neither underexposed nor overexposed, were used to obtain densitometric data. The densitometric data, after normalization (specific gene/β–actin ratio), for each drug is represented in the bar graphs (Figs. 46 B-C and 47 B-C).

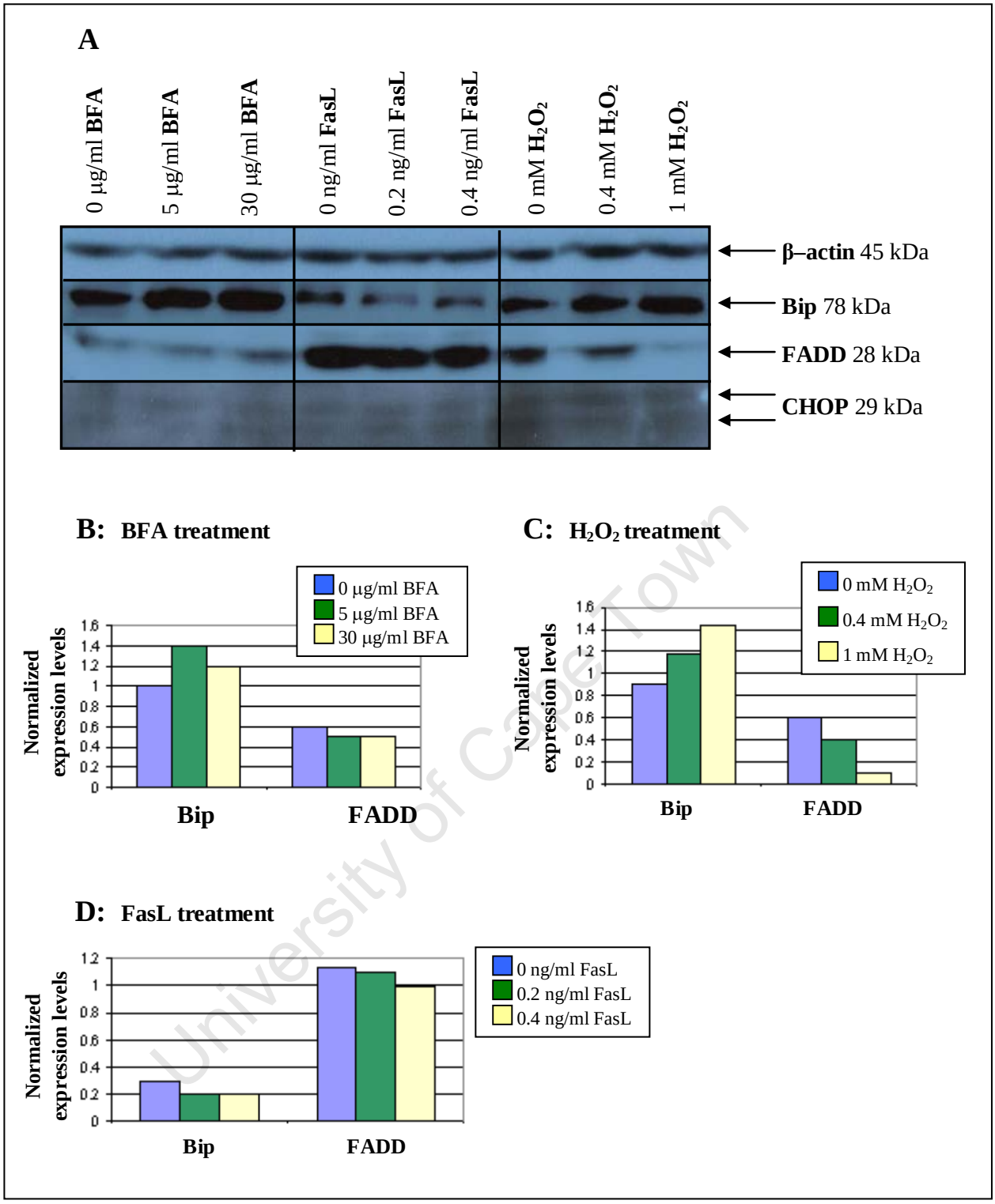

Fig. 46. Western blot analysis of Bip, FADD and CHOP protein levels for all drugs (first experiment). (**A**) HL60 cells were treated with BFA (5 µg/ml or 30 µg/ml) or H_2O_2 (0.4 mM or 1 mM) for 24 hrs and Jurkat cells were treated with FLAG-tagged FasL (0.2 ng/ml or 0.4 ng/ml) for 4 hrs, in the presence of 0.25 µg/ml ANTI-FLAG® M2 antibody. Protein (100 µg) isolated from untreated and drug-treated cells were separated via SDS-PAGE and transferred onto PVDF membrane. The membrane was probed with GADD153 (CHOP), Bip, FADD and β-actin antibodies (section 3.2.4.4) and developed accordingly. B-actin was used as an invariable control to confirm the equal loading of protein in each sample. Only bands that fell within the linear range of exposure, and were neither underexposed nor overexposed, were used to obtain densitometric data. After normalizing for the β-actin control, results from the densitometric analysis was used to measure changes in Bip and FADD protein levels between the different drugs, BFA (**B**), H_2O_2 (**C**) and FasL (**D**) and drug concentrations used.

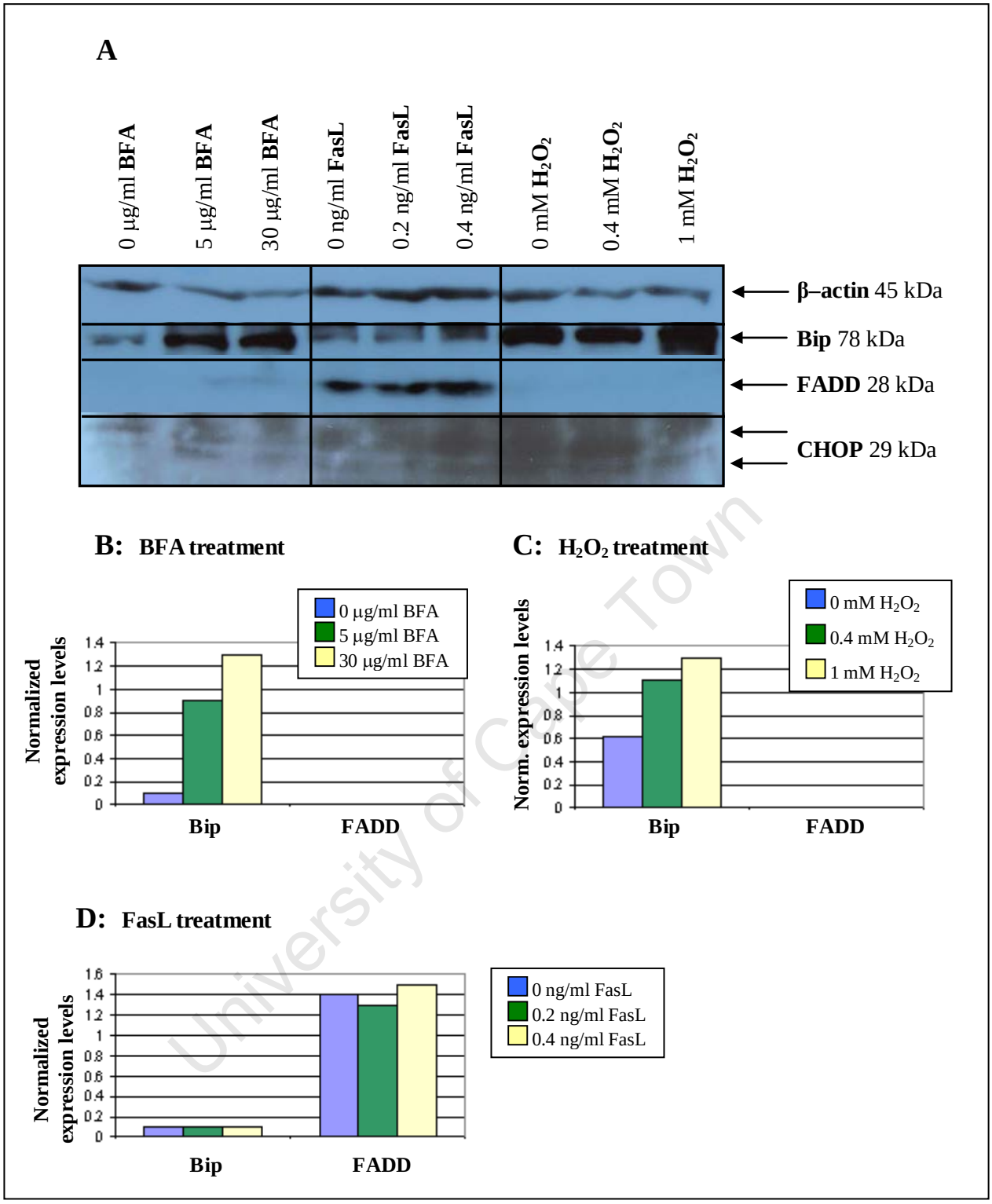

Fig. 47. Western blot analysis of Bip, FADD and CHOP protein levels for all drugs (second experiment). (**A**) HL60 cells were treated with BFA (5 µg/ml or 30 µg/ml) or H_2O_2 (0.4 mM or 1 mM) for 24 hrs and Jurkat cells were treated with FLAG-tagged FasL (0.2 ng/ml or 0.4 ng/ml) for 4 hrs, in the presence of 0.25 µg/ml ANTI-FLAG® M2 antibody. Protein (100 µg) isolated from untreated and drug-treated cells were separated via SDS-PAGE and transferred onto PVDF membrane. The membrane was probed with GADD153 (CHOP), Bip, FADD and β-actin antibodies (section 3.2.4.4) and developed accordingly. B-actin was used as an invariable control to confirm the equal loading of protein in each sample. Only bands that fell within the linear range of exposure, and were neither underexposed nor overexposed, were used to obtain densitometric data. After normalizing for the β-actin control, results from the densitometric analysis was used to measure changes in Bip and FADD protein levels between the different drugs, BFA (**B**), H_2O_2 (**C**) and FasL (**D**) and drug concentrations used.

Figs. 46 A and 47 A show that the western blot analysis for β–actin, Bip and FADD were successful. However, non-specific bands, as well as a high background signal were detected with the CHOP western blot assays, as before (section 3.1.2.4), therefore densitometric data could not be acquired for CHOP protein.

Figs. 46 B and 47 B show that Bip protein expression was upregulated after BFA treatment for both experiments. However, Bip protein levels were slightly higher for 5 μg/ml BFA treated cells compared to 30 μg/ml BFA in Fig. 46 B. The increase in Bip protein expression indicated that the UPR was activated, and the HL60 cells were experiencing ER-stress after BFA treatment.

Fig. 46 B shows that FADD protein levels were slightly decreased after BFA treatment, and were approximately equal at both BFA concentrations. However, the second BFA experiment (Fig. 47 B) shows that no FADD protein was detected in both untreated and BFA treated cells. Results of both experiments therefore indicated that there was no or limited death receptor pathway activity via FADD after BFA treatment of HL60 cells.

Figs. 46 C and 47 C show that Bip protein expression was upregulated after H_2O_2 treatment and Bip protein levels were higher for 1 mM H_2O_2 treated cells compared to 0.4 mM H_2O_2. The increase in Bip protein expression indicated that the UPR was activated, and the HL60 cells were experiencing ER-stress after H_2O_2 treatment.

Fig. 46 C shows that FADD protein levels were significantly decreased, after H_2O_2 treatment. Moreover, the second H_2O_2 experiment (Fig. 47 C) shows that no FADD protein was detected in both untreated or H_2O_2 treated cells. Results of both experiments therefore indicated that there was no or limited death receptor pathway activity via FADD after H_2O_2 treatment of HL60 cells.

Fig. 46 D shows that Bip protein levels were low in the untreated Jurkat cells and Bip protein expression was slightly downregulated after treatment with FLAG-tagged FasL and ANTI-FLAG® antibody. Furthermore, in the second FasL experiment, Bip protein levels were significantly low and remained unchanged after treatment with FLAG-tagged FasL and ANTI-FLAG® antibody (Fig.47 D).

Figs. 46 D and 47 D show that the untreated Jurkat cells had significantly high levels of FADD protein. Fig. 46 D shows that there was no significant increase or decrease in FADD protein levels after treatment with FLAG-tagged FasL and ANTI-FLAG® antibody. Fig. 47 D shows that FADD protein levels were slightly lower after treatment with 0.2 ng/ml FasL, however, 0.4 ng/ml FasL treated cells showed a slight increase in FADD protein levels. Both FasL experiments therefore indicated that there was possible death receptor pathway activity via FADD after the Jurkat cells were treated with FLAG-tagged FasL and ANTI-FLAG® antibody.

3.2.3 Caspase activity assays for all three apoptotic pathways

The cells were treated as described in section 2.1.6 and the activity of caspase-3, -4, -8 and -9, for each apoptotic pathway, was investigated (as described in section 2.4.5).

3.2.3.1 Caspase activity assays for BFA treated HL60 cells

The activity of caspase-3, -4, -8 and -9 as induced by 5 µg/ml and 30 µg/ml BFA (24 hrs), for both BFA experiments, are shown in Figs. 48 and 49. The average values obtained for the blank and untreated (0 µg/ml BFA) samples were subtracted from the drug-treated sample readings. Therefore values on the graphs reflect AMC release, after addition of caspase substrate, for drug treatment only.

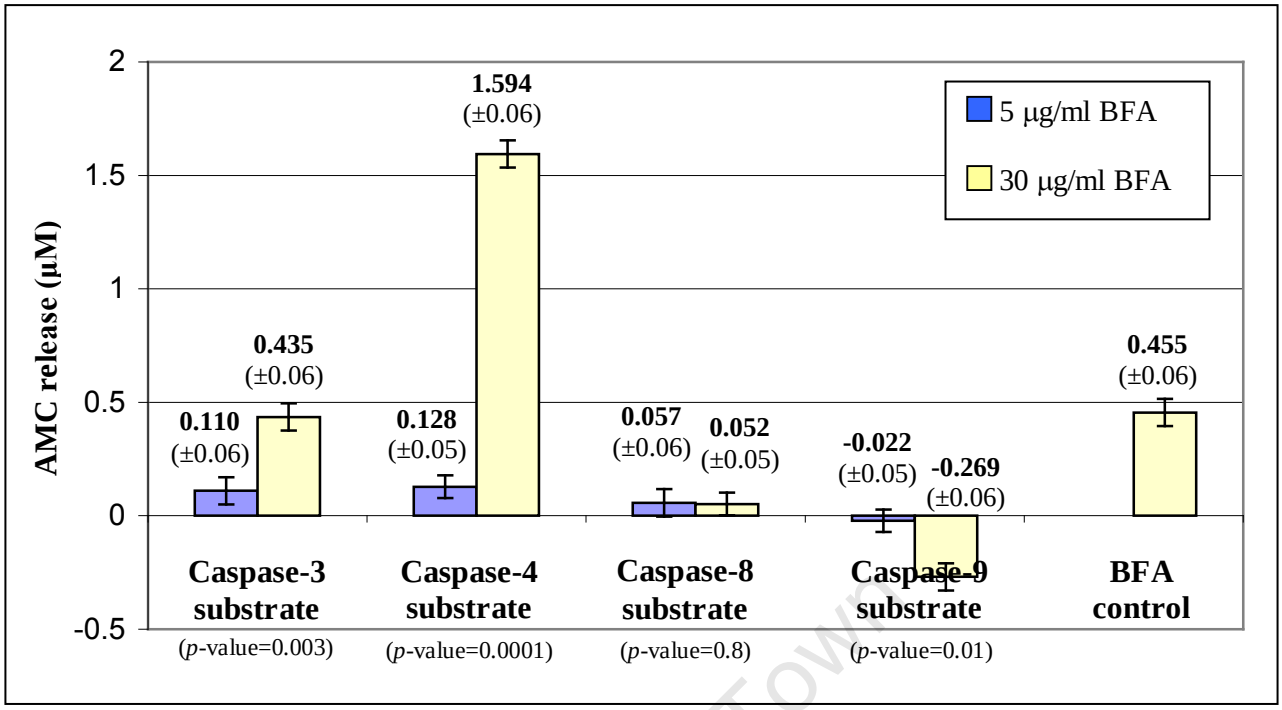

Fig. 48. AMC release of BFA treated HL60 cells for all caspase substrates (first experiment). HL60 cells were treated with 5 µg/ml BFA (blue) or 30 µg/ml BFA (yellow) for 24 hrs, after which protein was extracted. The HL60 cell lysates (10 µg protein) were analysed using caspase-3, -4, -8 and -9 substrates for caspase activity. BFA controls (30 µg/ml, 24 hrs) were included as a positive control for caspase-3 activity. Samples were prepared and analysed in triplicate and AMC release reflects averages (RFU readings for samples were converted to AMC release using the equation of the AMC standard curve) with standard deviation. A t-Test was performed for data obtained from the low and high drug doses for each caspase assay and the *p*-values are shown on the graph (level of significance was 0.05). The average RFU for the blank and untreated (0 µg/ml BFA) control readings were subtracted from the average sample (drug-treated) RFU values before the AMC release was calculated. Readings were taken at Ex/Em= 354/442 nm with Ex/Em slit= 20/20nm and PMT Voltage= High.

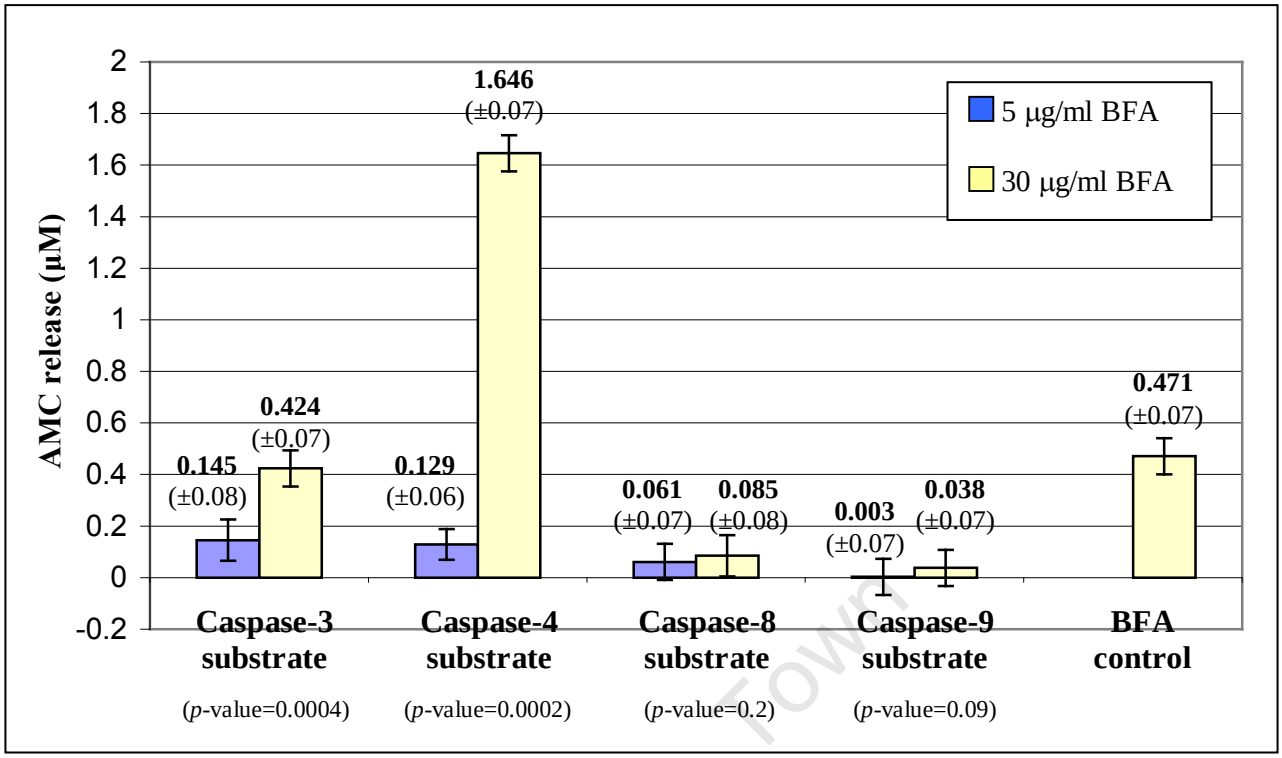

Fig. 49. AMC release of BFA treated HL60 cells for all caspase substrates (second experiment). HL60 cells were treated with 5 µg/ml BFA (blue) or 30 µg/ml BFA (yellow) for 24 hrs, after which protein was extracted. The HL60 cell lysates (10 µg protein) were analysed using caspase-3, -4, -8 and -9 substrates for caspase activity. BFA controls (30 µg/ml, 24 hrs) were included as a positive control for caspase-3 activity. Samples were prepared and analysed in triplicate and AMC release reflects averages (RFU readings for samples were converted to AMC release using the equation of the AMC standard curve) with standard deviation. A t-Test was performed for data obtained from the low and high drug doses for each caspase assay and the *p*-values are shown on the graph (level of significance was 0.05). The average RFU for the blank and untreated (0 µg/ml BFA) control readings were subtracted from the average sample (drug-treated) RFU values before the AMC release was calculated. Readings were taken at Ex/Em= 354/442 nm with Ex/Em slit= 20/20nm and PMT Voltage= High.

Figs. 48 and 49 show that BFA treatment, for both experiments, induced caspase-3 and caspase-4 activity but very little caspase-8 activity and no significant amount of caspase-9 activity. Fig. 48 shows negative values (graph) for the caspase-9 activity assay, since the blank and untreated values (AMC release) (which were higher) were subtracted from the drug-treated values (which were lower). Caspase-3 activity, in both experiments, was significantly higher for the 30 µg/ml BFA treated cells, compared to 5 µg/ml BFA, as expected (*p*-values considerably less than 0.05). Caspase-4 activity, in both experiments, was also significantly higher for the 30 µg/ml BFA treated cells, compared to 5 µg/ml BFA, as expected (*p*-values considerably less than 0.05). BFA treatment therefore seemed to activate mainly caspase-4, which is involved in the ER-stress induced apoptotic pathway, and caspase-3, which was used as a common

apoptotic marker to all three pathways. The BFA controls (separate experiment in which approximately 19% apoptosis was induced) were positive for caspase-3 activity, therefore demonstrating that the caspase-3 substrate and caspase assay worked as expected.

3.2.3.2 Caspase activity assays for FasL treated Jurkat cells

The activity of caspase-3, -4, -8 and -9 as induced by 0.2 ng/ml and 0.4 ng/ml FLAG-tagged FasL with 0.25 µg/ml ANTI-FLAG® M2 antibody (4 hrs), for both FasL experiments, are shown in Figs. 50 and 51. The average values obtained for the blank and untreated (0 µg/ml BFA) samples were subtracted from the drug-treated sample readings. Therefore values on the graphs reflect AMC release, after addition of caspase substrate, for drug treatment only.

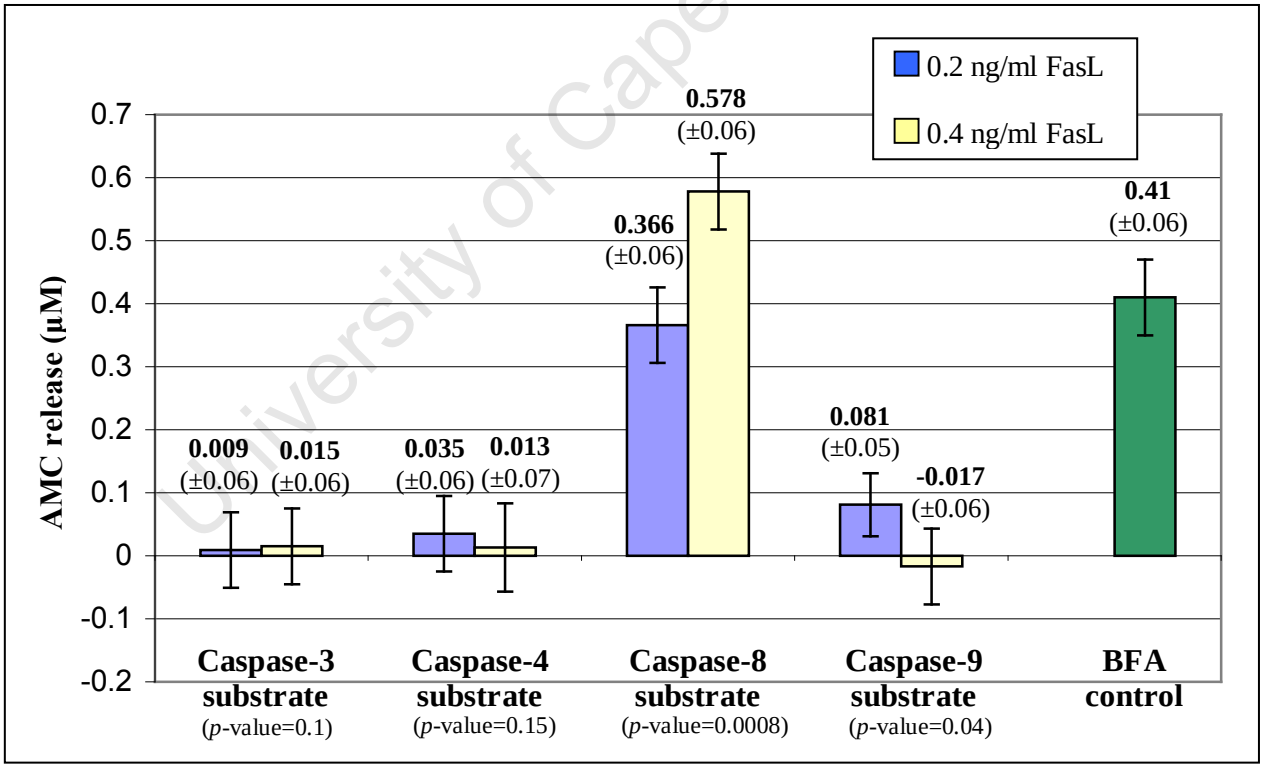

Fig. 50. AMC release of FasL treated Jurkat cells for all caspase substrates (first experiment). Jurkat cells were treated with FLAG-tagged FasL (0.2 ng/ml (blue) or 0.4 ng/ml (yellow)) and 0.25 µg/ml ANTI-FLAG® M2 antibody for 4 hrs, after which protein was extracted. The Jurkat cell lysates (10 µg protein) were analysed using caspase-3, -4, -8 and -9 substrates for caspase activity. BFA controls (30 µg/ml, 24 hrs) (green) were included as a positive control for caspase-3 activity. Samples were prepared and analysed in triplicate and AMC release reflects averages (RFU readings for samples were converted to AMC release using the equation of the AMC standard curve) with standard deviation. A t-Test was performed for data obtained from the low and high drug doses for each caspase assay and the *p*-values are shown on the graph. The average RFU for the blank and untreated control readings were subtracted from the average drug-treated sample RFU readings. Readings were taken at Ex/Em= 354/442 nm with Ex/Em slit= 20/20nm and PMT Voltage= High.

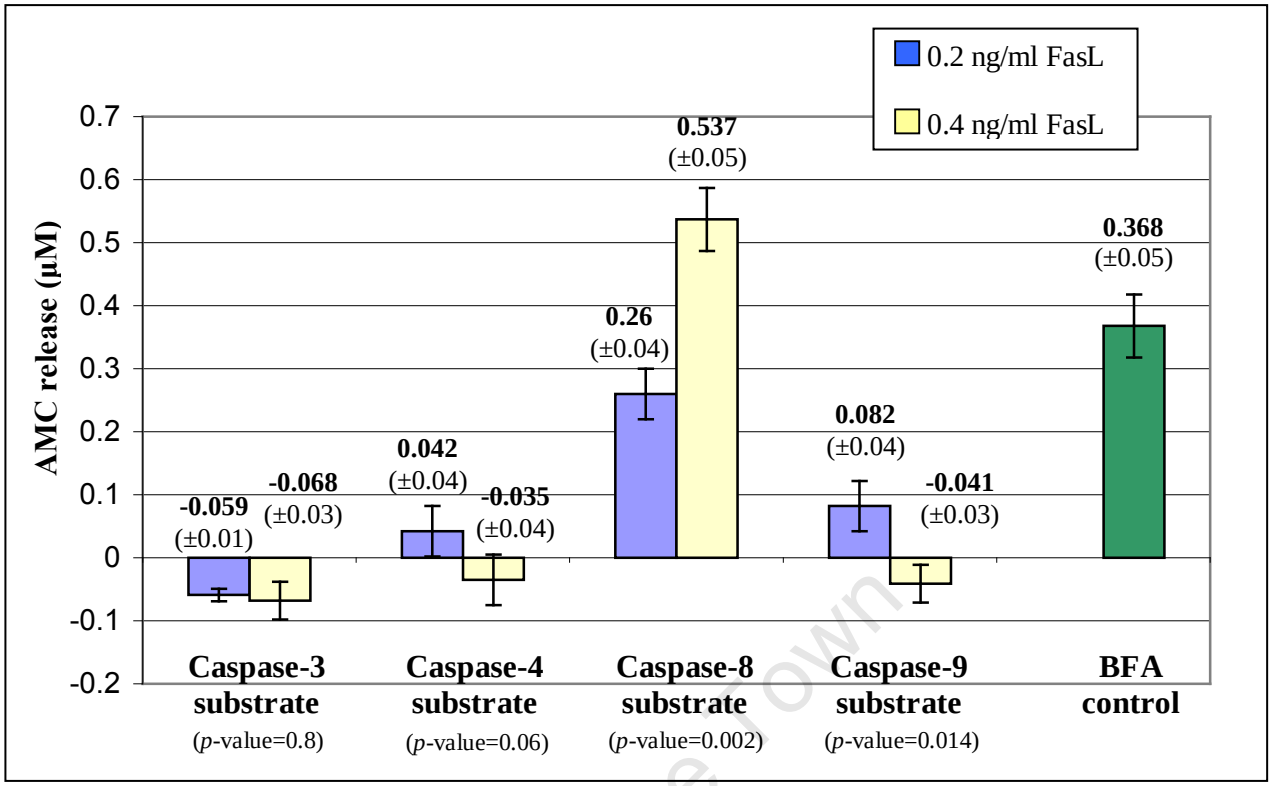

Fig. 51. AMC release of FasL treated Jurkat cells for all caspase substrates (second experiment). Jurkat cells were treated with FLAG-tagged FasL (0.2 ng/ml (blue) or 0.4 ng/ml (yellow)) and 0.25 µg/ml ANTI-FLAG® M2 antibody for 4 hrs, after which protein was extracted. The Jurkat cell lysates (10 µg protein) were analysed using caspase-3, -4, -8 and -9 substrates for caspase activity. BFA controls (30 µg/ml, 24 hrs) (green) were included as a positive control for caspase-3 activity. Samples were prepared and analysed in triplicate and AMC release reflects averages (RFU readings for samples were converted to AMC release using the equation of the AMC standard curve) with standard deviation. A t-Test was performed for data obtained from the low and high drug doses for each caspase assay and the *p*-values are shown on the graph (level of significance was 0.05). The average RFU for the blank and untreated (0 ng/ml FasL) control readings were subtracted from the average sample (drug-treated) RFU values before the AMC release was calculated. Readings were taken at Ex/Em= 354/442 nm with Ex/Em slit= 20/20nm and PMT Voltage= High.

Figs. 50 and 51 show that FasL treatment, for both experiments, induced caspase-8 activity, however, no significant amount of caspase-3 and -4 activity was detected. Low levels of caspase-9 activity were detected after treatment with 0.2 ng/ml FasL only (for both experiments). The negative values shown in Figs. 50 and 51 for caspase-3, -4 and -9 activity was due to the blank and untreated sample readings (which were higher) being subtracted from the drug-treated sample readings. In both experiments caspase-8 activity was significantly higher for 0.4 ng/ml FasL treated cells, compared to 0.2 ng/ml FasL, as expected (*p*-values considerably less than 0.05). Since there was no significant amount of caspase-3 activity detected, in both experiments, it could be deduced that very little cells were in the late stages of apoptosis, when the executioner caspases are activated. Treatment with FLAG-tagged FasL and ANTI-FLAG® antibody therefore

seemed to activate mainly caspase-8, which is specific to the death receptor apoptotic pathway. The BFA controls (approximately 19% apoptosis induced) were positive for caspase-3 activity, therefore demonstrating that the caspase-3 substrate and caspase assay worked as expected.

3.2.3.3 Caspase activity assays for H_2O_2 treated HL60 cells

The activity of caspase-3, -4, -8 and -9 as induced by 0.4 mM H_2O_2 and 1 mM H_2O_2 (24 hrs), for both H_2O_2 experiments, are shown in Figs. 52 and 53. The average values obtained for the blank and untreated (0 mM H_2O_2) samples were subtracted from the drug-treated sample readings. Therefore values on the graphs reflect AMC release, after addition of caspase substrate, for drug treatment only.

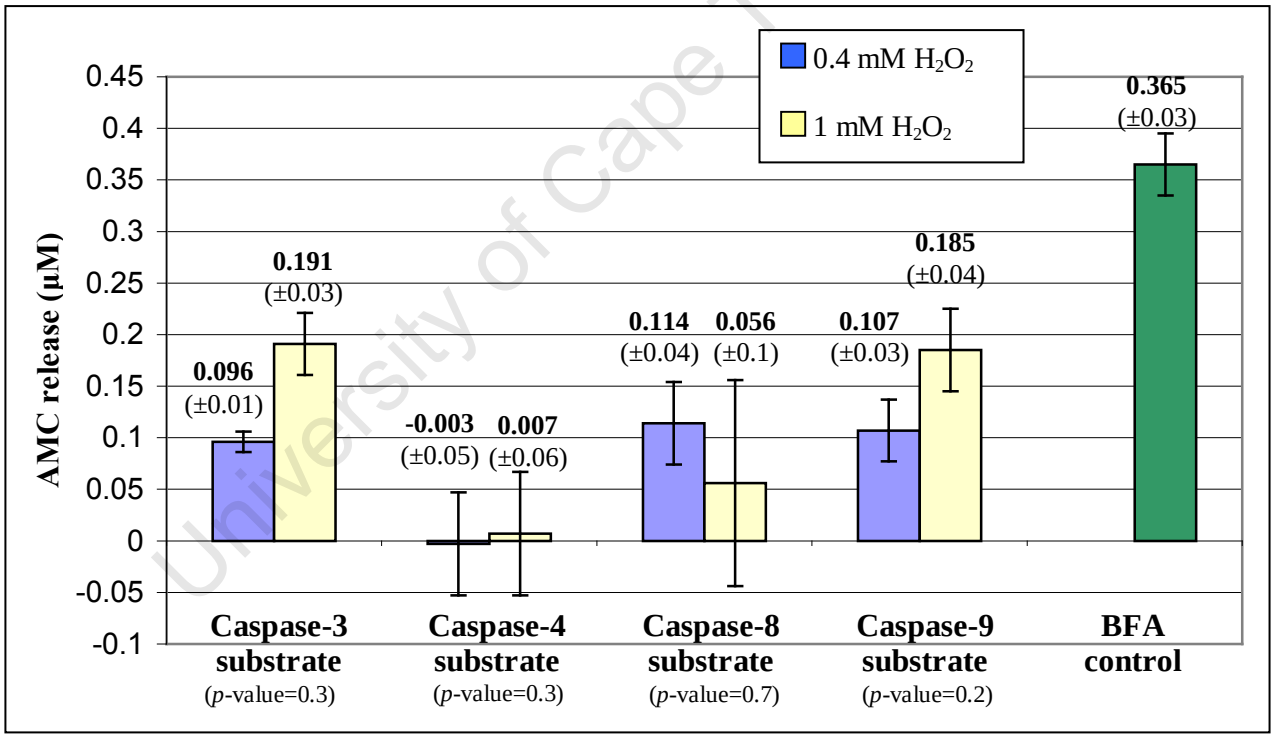

Fig. 52. AMC release of H_2O_2 treated HL60 cells for all caspase substrates (first experiment). HL60 cells were treated with 0.4 mM H_2O_2 (blue) and 1 mM H_2O_2 (yellow) for 24 hrs, after which protein was extracted. The HL60 cell lysates (10 µg protein) were analysed using caspase-3, -4, -8 and -9 substrates for caspase activity. BFA controls (30 µg/ml, 24 hrs) (green) were included as a positive control for caspase-3 activity. Samples were prepared and analysed in triplicate and AMC release reflects averages (RFU readings for samples were converted to AMC release using the equation of the AMC standard curve) with standard deviation. A t-Test was performed for data obtained from the low and high drug doses for each caspase assay and the *p*-values are shown on the graph (level of significance was 0.05). The average RFU for the blank and untreated (0 mM H_2O_2) control readings were subtracted from the average sample (drug-treated) RFU values before the AMC release was calculated. Readings were taken at Ex/Em= 354/442 nm with Ex/Em slit= 20/20nm and PMT Voltage= High.

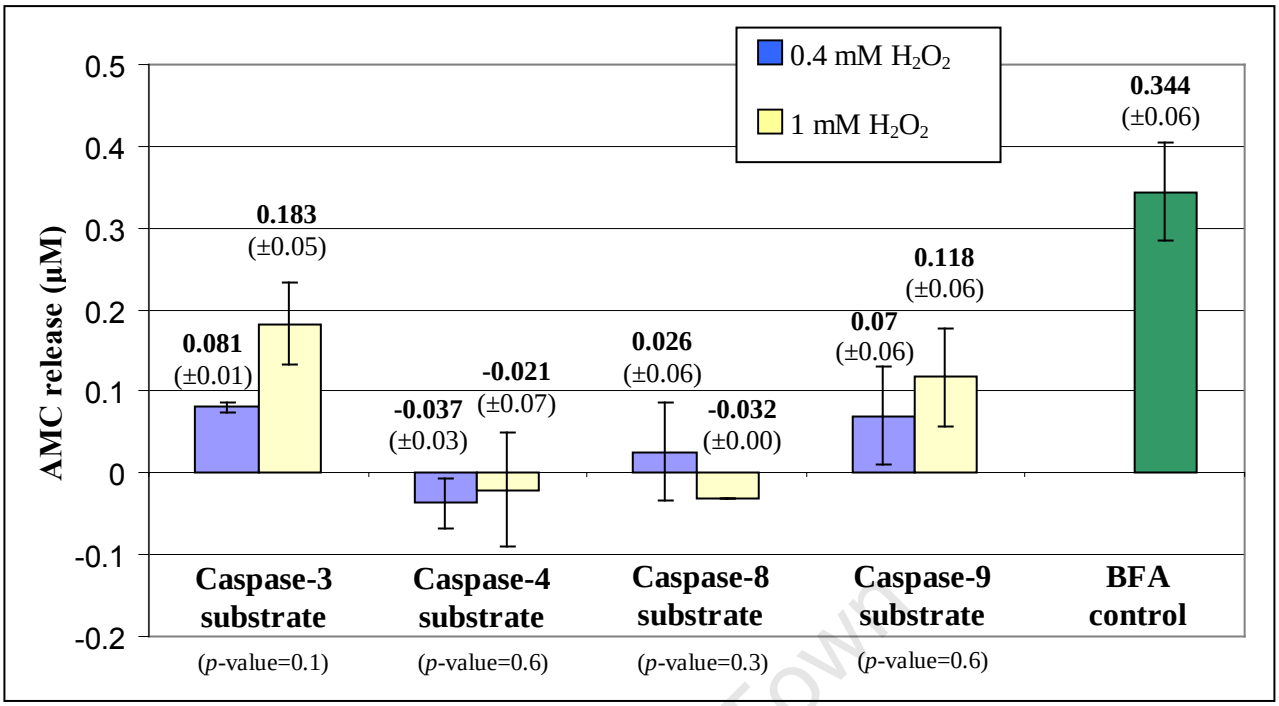

Fig. 53. AMC release of H_2O_2 treated HL60 cells for all caspase substrates (second experiment). HL60 cells were treated with 0.4 mM H_2O_2 (blue) and 1 mM H_2O_2 (yellow) for 24 hrs, after which protein was extracted. The HL60 cell lysates (10 µg protein) were analysed using caspase-3, -4, -8 and -9 substrates for caspase activity. BFA controls (30 µg/ml, 24 hrs) (green) were included as a positive control for caspase-3 activity. Samples were prepared and analysed in triplicate and AMC release reflects averages (RFU readings for samples were converted to AMC release using the equation of the AMC standard curve) with standard deviation. A t-Test was performed for data obtained from the low and high drug doses for each caspase assay and the *p*-values are shown on the graph (level of significance was 0.05). The average RFU for the blank and untreated (0 mM H_2O_2) control readings were subtracted from the average sample (drug-treated) RFU values before the AMC release was calculated. Readings were taken at Ex/Em= 354/442 nm with Ex/Em slit= 20/20nm and PMT Voltage= High.

Figs. 52 and 53 show that treatment with H_2O_2, for both experiments, induced caspase-3 and -9 activity but no activity was detected for caspase-4. Fig. 52 shows that caspase-8 activity was detected after treatment with 0.4 mM H_2O_2, however, there was not a significant difference between the low and high drug doses since the *p*-value was 0.7. Furthermore, Fig. 53 shows that there was not a significant increase in caspase-8 activity for both drug concentrations. Therefore, it could be concluded that after H_2O_2 treatment there was not a significant increase in caspase-8 activity for both experiments. There was no significant difference in caspase-9 activity levels between the low and high H_2O_2 concentrations (of both experiments), since the *p*-values were significantly greater than 0.05. Fig. 53 also indicated that caspase-9 activity (for both drug concentrations) was lower compared to Fig. 52. Furthermore, there was no significant difference in caspase-3 activity between the low and high H_2O_2 concentrations (of both

experiments), since the *p*-values were greater than 0.05. The levels of caspase activity of the H_2O_2 treated cells, of both experiments, were also lower than expected, even though the BFA controls demonstrated that the caspase-3 substrate and caspase assay worked as expected.

Since caspase-9 activity was lower than expected for both experiments (Figs. 52-53) and caspase-3 activity was lower compared to the BFA treated HL60 cells (Figs. 48-49), it was decided to determine if any residual H_2O_2 in the cell lysates could inhibit caspase activity. Untreated HL60 cell lysates (20 µg protein) were analysed for caspase-3 activity with or without the addition of 0.5 mM H_2O_2. Since the H_2O_2 treated cell lysates produced lower AMC release (caspase activity), compared to BFA and FasL treated cells, higher protein and substrate concentrations were used to try and increase the RFU signal obtained. As a basic means of measuring enzyme activity, a heat inactivated control was included for comparison (Fig. 54).

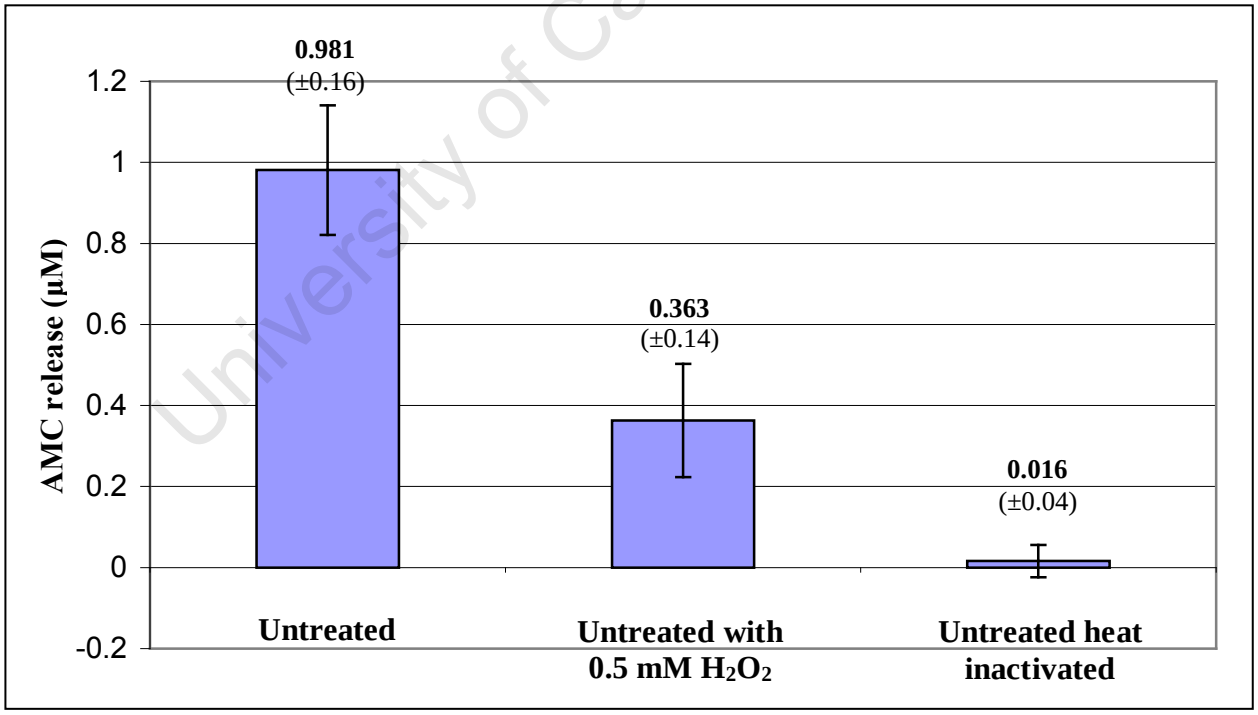

Fig. 54. The effect of 0.5 mM H_2O_2 on caspase-3 activity. Untreated HL60 cell lysates (20 µg protein) were analysed using caspase-3 substrate (75 µM) for caspase-3 activity. 0.5 mM H_2O_2 was added to untreated cell lysate prior to analysis. Heat inactivated controls were included as a negative control for caspase-3 activity. Samples were prepared and analysed in triplicate and AMC release reflects averages (RFU readings for samples were converted to AMC release using the equation of the AMC standard curve) with standard deviation. Readings were taken at Ex/Em= 354/442 nm with Ex/Em slit= 20/20nm and PMT Voltage= High.

Fig. 54 shows that the addition of H_2O_2 significantly reduced caspase-3 activity, even at higher protein and substrate concentrations. The activity of caspases in the H_2O_2 treated cell lysates could therefore be inhibited or reduced if there was residual H_2O_2 left in the preparation. This could account for the lower caspase-3 and -9 activity detected for H_2O_2 treated cells in Figs. 52-53.

3.2.4 Detection of changes in MTP during apoptosis induction for all three apoptotic pathways

After drug treatment (section 2.1.6), the changes in MTP were determined with MitoCapture™ labelling and flow cytometry as described in sections 2.6.1 and 2.6.2. The experiments were performed twice for each drug, although only one sample per drug concentration (untreated, low dose and high dose) was prepared per experiment for MitoCapture™ labelling. The changes in MTP of the cells after drug treatment (for all drugs) are shown in Table 9. The values represent the average of the two experiments performed for each drug with the standard deviation.

Table 9: The changes in MTP during apoptosis as determined by MitoCapture™ labelling and flow analysis

Drug and concentration:	Incubation time (hrs):	% Cells Area C1 (normal MTP):	% Cells Area C2 (intermediate MTP):	% Cells Area C4 (disrupted MTP):
0 µg/ml BFA	24	80.15 (±11.2)	13.8 (±5.8)	5.95 (±5.4)
5 µg/ml BFA		28.9 (±25.7)	21.5 (±12.7)	49.6 (±38.5)
30 µg/ml BFA		19.6 (±21.07)	22.2 (±19.2)	58.25 (±40.23)
0 mM H_2O_2	24	64.3 (±19.9)	22.3 (±17.5)	13.45 (±2.3)
0.4 mM H_2O_2		30.15 (±9.9)	29.65 (±2.9)	40.25 (±12.7)
1 mM H_2O_2		6.65 (±3.8)	18.25 (±9.4)	75.15 (±13.3)
0 ng/ml FasL	4	85.15 (±3.6)	8.8 (±3.8)	6.05 (±0.2)
0.2 ng/ml FasL		78.8 (±0)	9 (±0.1)	12.15 (±0.1)
0.4 ng/ml FasL		59.85 (±4.7)	12.25 (±2.5)	27.85 (±2.2)

Values reflect the averages with standard deviation (n =2)
Areas C1, C2 and C4 denote the areas of the colour-coded density plots shown in Figs. 55-57

Table 9 shows that the majority of untreated cells (for all experiments) fluoresced red (normal MTP) in area C1. Approximately 10-20% of the untreated cells had an intermediate MTP (area C2) and approximately 5-15% fluoresced green (disrupted MTP) in area C4. The cells induced with BFA, H_2O_2 and FasL treatment (low and high doses) showed decreased fluorescence and cell density in area C1 and increased fluorescence and density in areas C2 and C4, compared to the untreated cells, as expected. Approximately 65-85% cells underwent mitochondrial membrane depolarisation (area C4) upon H_2O_2 treatment (high dose) compared to 30-87% for 30 μg/ml BFA and 30% for 0.4 ng/ml FasL.

The results for BFA treatment varied the most between the two experiments, with 5 μg/ml BFA inducing 22% fluorescence in area C4 for the initial experiment and 76% for the second experiment (Table 9). For the initial high dose BFA experiment approximately 30% fluorescence was detected in area C4, compared to 87% for the last experiment. Therefore, the cells of the initial BFA experiment appeared to be dying via the ER-stress induced apoptotic pathway, with less mitochondrial activity (and changes in MTP) compared to the second experiment. In the second BFA experiment, the majority of cells seemed to be apoptosing via the mitochondrial-mediated apoptosis pathway.

For both high and low doses of H_2O_2 treated cells, the majority fluoresced green (area C4), indicating that the cells were undergoing apoptosis via the mitochondrial-mediated apoptotic pathway (Table 9) (also seen in Fig. 56). Furthermore, the 1 mM H_2O_2 treated cells showed a significant decrease in fluorescence in area C2 compared to the 0.4 mM H_2O_2 treated cells. This would suggest that at 1 mM H_2O_2 there was a decrease in the number of cells with intermediate MTP and most cells were committed to mitochondrial-mediated apoptosis.

The majority of cells treated with FasL (low and high dose) fluoresced red, with smaller increases in fluorescence in area C4, compared to the BFA and H_2O_2 treated cells (high and low doses) (Table 9). This indicated that most of the FasL treated cells did not undergo apoptosis via the mitochondrial-mediated apoptotic pathway (also seen in Fig. 57).

Figs. 55-57 shows the representative colour-coded density plots for the MitoCapture™ labelled cells after drug treatment.

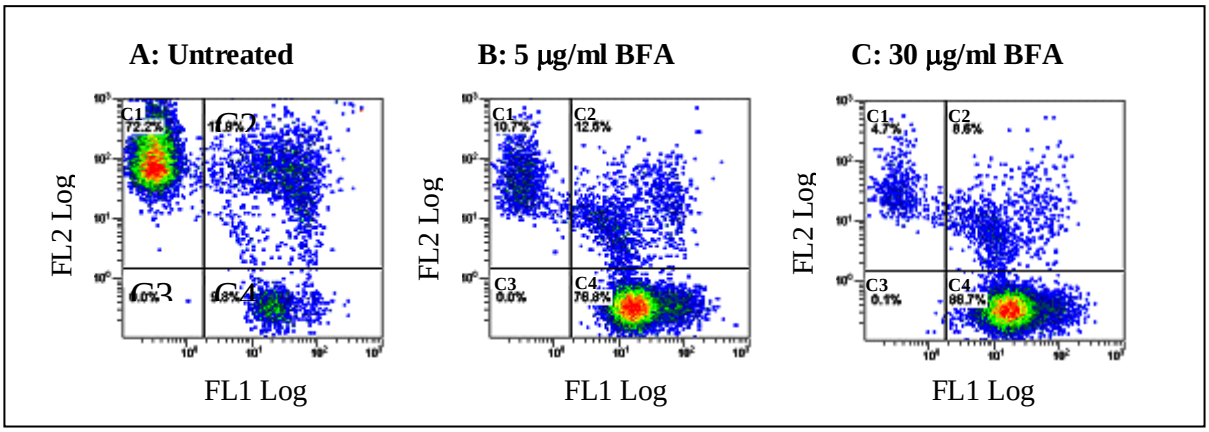

Fig. 55. Flow cytometry analysis of BFA treated HL60 cells after MitoCapture™ labelling. HL60 cells were treated with 5 µg/ml (**B**) and 30 µg/ml (**C**) BFA for 24 hrs and labelled with MitoCapture™ dye. The untreated (control) cells are shown in (**A**).

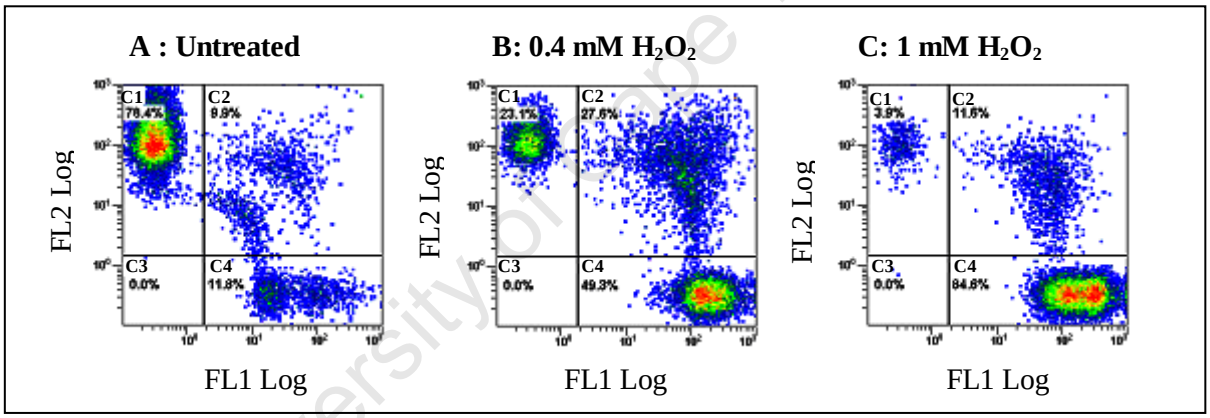

Fig. 56. Flow cytometry analysis of H_2O_2 treated HL60 cells after MitoCapture™ labelling. HL60 cells were treated with 0.4 mM (**B**) and 1 mM (**C**) H_2O_2 for 24 hrs and labelled with MitoCapture™ dye. The untreated (control) cells are shown in (**A**).

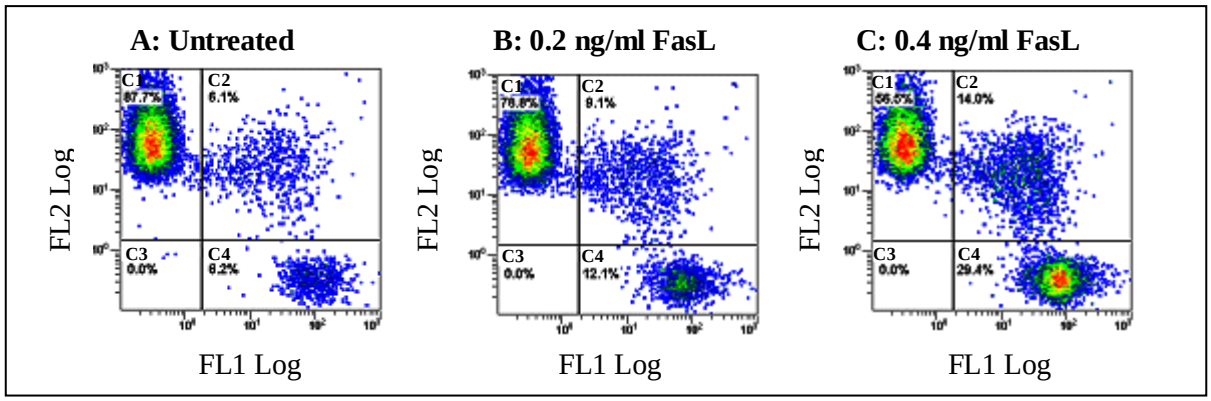

Fig. 57. Flow cytometry analysis of FasL treated Jurkat cells after MitoCapture™ labelling. Jurkat cells were treated with 0.2 ng/ml (**B**) and 0.4 ng/ml (**C**) FLAG-tagged FasL and 0.25 µg/ml ANTI-FLAG® antibody for 4 hrs and labelled with MitoCapture™ dye. The untreated (control) cells are shown in (**A**).

As the colour-coded density plots in Figs. 55-57 indicate, in untreated cells (Figs. 55-57 A) most of the MitoCapture^{TM} dye was taken up by the mitochondria and fluoresced red (area C1). Therefore the majority of the untreated cells had unaltered or normal MTP. Initiation of the mitochondrial-mediated apoptotic pathway, via drug treatment, resulted in the disruption of MTP, therefore leaving the green fluorescing dye monomers in the cytoplasm (area C4) (Figs. 55-57 B and C). Some cells (untreated and drug-treated) had intermediate MTP and therefore fluoresced yellow-orange (both red and green) (area C2) (Figs. 55 -57).

CHAPTER FOUR

DISCUSSION

4.1 Cell lines

The myelodysplastic syndromes and other haematological disorders are associated with apoptotic defects in the progenitor cells (Hellström-Lindberg, 2005). Therefore, reliable models to study three caspase-dependent apoptotic pathways in defined cell populations were established and the assay techniques involved for each pathway were optimised. The promyelocytic HL60 and T lymphocyte Jurkat cell lines were used as leukaemic cell models to examine the specific apoptotic pathways after pathway-specific drug treatment.

The Jurkat cell line is a continuous human T lymphocyte cell line, which was derived from the peripheral blood of a 14-year-old male with acute lymphoblastic T cell leukaemia (Schneider *et al.*, 1977). The Jurkat cell line also grows in suspension culture and maintains continued proliferation without the addition of exogenous inducers. Cell growth is entirely dependent on the presence of foetal bovine serum in the culture medium (ATCC: Cell Biology Collection, 2007).

The HL60 cell line is a continuous malignant human myeloid cell line, which was derived from the peripheral blood leukocytes of a patient diagnosed with acute myeloblastic leukaemia with maturation (Dalton *et al.*, 1988). The ultrastructure of HL60 cells reveals many similarities to that of early promyelocytes. The HL60 cell line grows in suspension and cell growth remains completely dependent on the presence of foetal bovine serum in the culture medium. The cells are capable of sustaining proliferation in the absence of an added source of conditioned medium and can continue to replicate and differentiate along myeloid lines. The predominant cell type in cultures is a neutrophilic promyelocyte. Up to 10% of cells in culture differentiate spontaneously beyond the promyelocyte stage into more mature cells of the monocytic and granulocytic lineages (Rovera *et al*., 1979; Trayner *et al*., 1998).

HL60 cells are capable of adapting to different culture mediums and the cells' morphology and sensitivity to chemical induction of differentiation remains unchanged through at least 85 passages (Gallagher *et al*., 1979). Leglise *et al*. (1988) have, however, found that HL60 cells have a wide variety of phenotypes and display an unstable phenotype when maintained in culture for a long period of time. When cultured in continuous/prolonged log phase (by subculturing twice a week) for 3-18 months, the cells underwent phenotypic drift. The cells developed drug resistance, oncogene amplification, loss of granulocyte and monocyte lineage markers and changes in cell growth parameters. The cells were found to develop from granulated promyelocytes to undifferentiated agranular blast-type cells. The loss of promyelocytic phenotype occurred within less than one month of culturing, after which the cells maintained a stable phenotype for a variable period. They suggested that the phenotypic drift resulted because the cells had lost their response to regulatory signals, which affected the cells' gene expression.

The cells in this study were subcultured twice or three times a week (for 1-3 months), however, the increase in passage number was not taken into account. Therefore, the HL60 cells were analysed and/or treated with drugs at different passage numbers. This could therefore have caused some inconsistency in the results obtained between experiments, since cells with different passage numbers would have different characteristics and/or gene expression. According to Leglise *et al*. (1988) the cells with higher passage number would also exhibit an unstable phenotype and drug resistance could occur, as discussed in section 4.3.1.

The three central apoptotic pathways studied in this investigation, were the death receptor pathway, the ER-stress induced apoptotic pathway and the mitochondrial-mediated apoptosis pathway. Each pathway was induced with a different drug known to be more specific to induce that particular pathway. The HL60 cell line was used to study the ER-stress induced and mitochondrial-mediated apoptosis pathways. The Jurkat cell line was used to investigate the death receptor pathway, since HL60 was found to be less responsive to apoptosis induction via FasL in this study. The assays used to detect the characteristic markers of each specific pathway, were optimised and tested for sensitivity and reproducibility.

4.2 Development and optimisation of assays to monitor apoptosis pathways

4.2.1 Analysis of the general apoptotic response to drug treatment

4.2.1.1 AV/PI labelling and flow cytometry analysis

The general apoptotic response of the two cell lines to drug treatment was determined via AV and PI labelling and flow cytometry. AV and PI are fluorescent dyes used for flow cytometry, since they bind to different components of the cell and allow for the monitoring of different characteristics of apoptotic cells. AV binds to phosphatidylserine molecules, which are exposed on the surface of cells during the early phase of apoptosis. Phosphatidylserine is a negatively charged phospholipid molecule that is exposed at the cell surface when the cell membrane is still intact but loses the asymmetry of its membrane phospholipids. PI intercalates DNA molecules, but can only do so when the cell membrane has become permeable. PI therefore labels cells that are in the advanced stages of apoptosis and have already lost their membrane integrity. PI can also label any cellular debris and/or apoptotic bodies that contain DNA fragments. However, PI cannot distinguish between apoptosis or other forms of cell death, such as necrosis (Mattes, 2007). Since this investigation was focussed on apoptosis, it was important to differentiate between necrosis and apoptosis. Cells that labelled with high PI, areas G2 and G1 of the PI vs. AV colour-coded density plots (section 3.1.1.1), were not necessarily apoptotic, since necrotic cells could directly label with PI. Therefore, only the percentage of cells that fluoresced in area G4 was analysed after drug treatment, since it represented early apoptotic cells that labelled with high AV and low PI (section 3.1.1.1).

The flow cytometry results also provided information on the morphology of the cells analysed. During apoptosis, cells shrink and therefore decrease in size (FS), as well as increase in granularity (SS) due to chromatin condensation and proteolytic breakdown of all cellular components (Kerr *et al.*, 1972). These changes could be seen in the FS vs. SS plots (section 3.1.1.2, Figs. 12 and 13) as the cells moved from population H to I (with increased apoptosis induction) due to decreased size (FS) and increased granularity (SS). This indicated that the FS vs. SS plots could be used as a quick basic measure of cell viability, without labelling, since the majority of viable cells would be

situated in population H (Fig. 13). An apoptotic population of approximately 5-10% cells were noted in the untreated cells (section 3.1.1.2). Therefore, care was taken to only analyse cells (HL60 and Jurkat), which were not more than 10% apoptotic prior to drug treatment.

4.2.1.3 Apoptotic response of cells to drug treatment

In the first part of this investigation, the appropriate drug concentrations and exposure times required to induce each pathway were established. One of the aims was to detect and examine apoptotic markers for each pathway during the initial (Bip and FADD), intermediate (changes in mitochondrial transmembrane potential) and later stages of apoptosis (CHOP, cytochrome *c* release and caspase activation). Therefore, it was not required to induce an overall high percentage of apoptosis. For these investigations it was necessary to have cells that were still intact, albeit apoptotic. Cells that label with AV (high AV, low PI), have lost their membrane asymmetry and have exposed phosphatidylserine molecules on the membrane surface, however, the cell membrane is still intact. Therefore, drug concentrations and exposure times required to induce approximately 20-50% and a lower level of approximately 5-15% early apoptosis was decided on. The low and high drug concentrations served to determine if there were any differences in detecting the apoptotic markers at lower and/or higher levels of apoptosis induced. The colour-coded density plots played an important role in determining the stage of apoptosis of the drug-treated cells with increasing drug concentrations (section 3.1.1.1).

4.2.1.2 A) Induction of the ER-stress induced apoptotic pathway by BFA treatment

HL60 cells were treated with Brefeldin A (BFA) to initiate the ER-stress induced apoptotic pathway. BFA blocks protein transport from the ER to the Golgi, therefore causing an accumulation of unprocessed proteins within the ER lumen. This leads to activation of the UPR, whereby ER chaperones like Bip, are employed to counteract protein aggregation, reduce protein translation and induce proteasome-mediated protein degradation of misfolded proteins (Guillemain and Exton, 1997; Li *et al*., 2006).

ER chaperone proteins have an extended half-life, therefore a longer period of exposure is required by apoptosis inducers to override the UPR and induce cell death. Studies

have found that at least 24 hrs exposure to inducers is needed to overcome the UPR and induce apoptosis through the ER-stress induced apoptotic pathway (Rao *et al.*, 2002 b). Similarly, in this present study, it was also found that 24 hrs exposure to BFA was optimal, since it produced a linear increase in apoptotic response with increasing BFA concentrations (Fig. 14). In contrast, another study achieved greater apoptosis induction in HL60 cells with less BFA (0.56 μg/ml) over a shorter exposure time (15 hrs) (Shao *et al.*, 1996). Comparatively, the HL60 cells used in this study (section 3.1.1.3 A) appeared to be less sensitive to induction of apoptosis by BFA. However, since very little research on apoptosis (and the ER-stress induced apoptotic pathway) induced by BFA in HL60 cells has been done to date, it was difficult to compare results obtained.

4.2.1.2 B) Induction of the mitochondrial-mediated apoptotic pathway by H_2O_2 treatment

H_2O_2 was used to induce the mitochondrial-mediated apoptotic pathway in HL60 cells. H_2O_2 generates reactive oxygen species, which oxidizes the cell's lipids, proteins and nucleic acids and augments the disruption of mitochondrial transmembrane potential. Mitochondrial functions are subsequently disrupted and the death signal is amplified, thereby reinforcing the cell's fate towards apoptosis (Skommer *et al.*, 2007).

Hosokawa *et al.* (2005) exposed HL60 cells to 0.05 mM and 0.5 mM H_2O_2 for 4 min, after which the cells were washed and re-incubated in growth medium for 24 hrs. After the re-incubation, the percentage of apoptosis was determined via Trypan blue staining. They found that approximately 10% apoptosis was induced with 0.05 mM H_2O_2 and approximately 50% apoptosis with 0.5 mM H_2O_2. DiPietrantonio *et al.* (1999) found that 3 hrs incubation with 50 μM H_2O_2 induced approximately 25% apoptosis, whereas 100 μM H_2O_2 induced approximately 80% apoptosis, as determined by Trypan blue staining. Since Trypan blue stains cells that have ruptured membranes, much like PI, it is not clear whether these cells were apoptotic or necrotic. However, in both studies, the cells were more susceptible to much lower H_2O_2 concentrations (and exposure times) than those that were established in this study (Fig. 16). Therefore, it appeared that the HL60 cells used in this study were less sensitive to induction of apoptosis by H_2O_2 (section 3.1.1.3 B), compared to the other two studies. This was also observed for the BFA treated HL60 cells as discussed in section 4.2.1.2 A.

4.2.1.2 C) FasL treatment of cells to induce the death receptor pathway

FLAG-tagged FasL binds to the Fas/CD95 receptor on the cell's surface, while the ANTI-FLAG® M2 antibody binds to the FLAG-tag, to induce trimerization and activation of the receptor. The activated trimeric death receptor recruits the adaptor protein FADD, thereby forming the death-inducing signalling complex. The death-inducing signalling complex recruits procaspase-8 molecules through FADD, resulting in autoproteolytic cleavage and cross-activation of caspase-8 molecules in close proximity. This generates a downstream caspase cascade leading to the activation of executioner caspases and ending in apoptosis (Lavrik *et al*., 2008).

FLAG-tagged FasL and ANTI-FLAG® M2 antibody treatment had very little affect on the HL60 cells (section 3.1.1.3 C). Li, W. *et al.* (2006) used FasL concentrations of 1.5 μg/ml - 50 μg/ml for 12 hrs (without anti-FLAG antibody) and found that approximately 6 μg/ml FasL was required to induce 50% apoptosis. Such high FasL concentrations were, however, not financially feasible in this study. Since the HL60 cell line appeared to be less sensitive to apoptosis induction, it was therefore decided to use the Jurkat cell line, which required lower concentrations of FasL to attain the required levels of apoptosis.

The Jurkat cells were found to be significantly more susceptible to apoptosis induced by FLAG-tagged FasL and ANTI-FLAG® M2 antibody (section 3.1.1.3 D), compared to the HL60 cells. Schneider *et al.* (1998) induced apoptosis in Jurkat cells with treatment of FLAG-tagged recombinant FasL and anti-FLAG monoclonal antibody over 16 hrs. They determined cell viability via chromium release and established that approximately 100 ng/ml FLAG-tagged FasL (with 1 μg/ml anti-FLAG antibody) induced almost 100% cell death. Huang *et al.* (1999) found that Jurkat cells had completely apoptosed after 24 hrs incubation with 100 ng/ml FLAG-tagged FasL (with 1 μg/ml anti-FLAG antibody), as determined via AV and PI labelling. However, in this present study, it was found that 5 ng/ml FLAG-tagged FasL (with 0.25 μg/ml ANTI-FLAG® antibody) induced approximately 80% early apoptosis after 4 hrs incubation only (section 3.1.1.3 D, Fig. 18). Therefore, the Jurkat cells used in this study required lower concentrations of FasL (and anti-FLAG antibody) and a shorter exposure time, compared to the other studies.

4.2.2 Western blot analysis

The western blot assays for Bip, FADD and CHOP were optimised to determine the optimal experimental conditions for immunodetection of the proteins, as described in section 3.1.2. Since the transfer apparatus used created very strong currents during the transfer process, the amount of protein transferred would not always be quantitative. Therefore, the β-actin antibody was used as an invariant positive control to normalize the results obtained for Bip, FADD and CHOP in the final experiments of section 3.2.2.

From the western blot analysis for Bip (section 3.1.2.2) it was found that the inclusion of protease inhibitors in the protein extraction buffer was essential to prevent any protein degradation. Higher antibody concentrations were also necessary for the detection of Bip and FADD (section 3.1.2.3).

Different protein and antibody concentrations were used to optimise the CHOP western blot assay, to ensure that there was sufficient protein and primary antibody for detection. However, it was difficult to detect a signal for CHOP since a high background signal was present, or in some experiments no signal at all. To determine if the primary and secondary antibodies were compatible, the affinity of the POD-conjugated secondary antibody for the GADD153 antibody was determined with a "dot blot" experiment. Since it was found that the secondary antibody's affinity for the GADD153 antibody was lower compared to the other antibodies, an increased secondary antibody concentration was required for detection of CHOP (section 3.1.2.4). The number of subsequent washing steps was also increased to minimise background signal due to the higher concentration of secondary antibody used (section 2.3.3). However, some non-specific bands were detected and could not be removed nor could these results be improved upon. A way of differentiating between specific and non-specific bands is the use of blocking peptides to block the specific bands, which disappear and leave the non-specific bands behind (Abcam®, 2008).

4.2.3 Caspase activity assays

The caspase activity assays for caspases-3, -4, -8 and -9 were optimised with respect to the protein concentration, optimal incubation time, machine settings and optimal caspase substrate concentrations required.

4.2.3.1 Minimal protein concentration required for caspase activity

Other studies have used different protein concentrations for their caspase activity assays. Sommer *et al*. (2005) used 1 µg protein per caspase activity assay, whereas Liu *et al.* (2000) used 100 µg protein. For this study, it was found that as little as 5 µg protein could be used, although 10 µg protein was preferred since it obtained higher RFU values (section 3.1.3.1).

RFU also increased with increasing concentrations of protein. Since high amounts of substrate could cause substrate saturation and slow down enzyme activity, an increase in enzyme (caspase) concentration would counteract this. Higher protein concentrations, which would include more caspase molecules, would therefore result in increased RFU, since caspase activity would be greater. Therefore, with higher protein concentrations, more caspases were available to proteolytically cleave substrate, thus resulting in increased RFU values (Berg *et al*., 2002).

4.2.3.2 Effect of protease inhibitors on caspase activity

It was also determined whether protease inhibitors should be added to the protein extraction (cell lysis) buffer or not. Some research groups performed caspase activity assays using protease inhibitors in their protein lysates (DiPietrantonio *et al.*, 1999; Kim *et al*., 1999; Doyle *et al.*, 2002; Huang *et al.*, 2004; Higuchi *et al.*, 2006). Since caspases are proteases, it was important to establish if protease inhibitors would in fact inhibit caspase activity. In this present study it was found that the protease inhibitors significantly reduced caspase-3 activity (section 3.1.3.2 C).

The caspase assay cell lysis buffer contains EDTA, which removes metal ions that are used as cofactors by certain proteases other than caspases, which are cysteine dependent

(Ebbing, 1996). Therefore, additional protease inhibitors are not required and only decreases caspase activity. It was therefore concluded that protease inhibitors should not be added to the cell lysis buffer when isolating protein for caspase assays.

4.2.3.3 Optimal fluorimeter settings

The fluorimeter settings were adjusted so as to acquire maximal fluorescence readings from the samples analysed. It was important to generate RFU values that were clearly distinguishable from any background fluorescence. Initially an automatic blank setting, which automatically subtracted the blank reading from all the sample readings, was used. However, this was found to be unreliable and instead the blank samples were analysed in triplicate, with the samples (also prepared and analysed in triplicate). The average blank RFU value calculated was manually subtracted from the average sample RFU values.

4.2.3.4 Determination of optimal incubation time

Some studies used different incubation times, to allow for caspase activity and proteolytic cleavage of the caspase substrate. Nagase *et al.* (2002) and Doyle *et al.* (2002) both incubated their caspase assay samples with substrate for 1 hr at 37°C, whereas Liu *et al.* (2000) incubated their assay samples for 2 hrs at 37°C. In this study, no significant difference between RFU values at extended incubation times was found (section 3.1.3.2 A). It was therefore decided that 60 min incubation time was sufficient for caspase activity and substrate cleavage (and AMC release).

4.2.3.5 Optimal caspase substrate concentration

Other research groups have used various caspase substrate concentrations for their caspase activity assays. Karki *et al.* (2002) used 10-500 µM substrate (AMC conjugated) concentration to measure caspase-2, -3/7, -6, -8, -9, and -4 activity. Sommer *et al.* (2005) measured cysteine protease activity using 15 µM of n-carbobenzoxyl-arginyl-arginyl-7-amido-4-methylcoumarin (Z-RR-AMC) as substrate. Liu *et al.* (2000) used 20 µM of caspase-3/7 (Ac-DEVD-AMC) substrate, whereas Juin *et al.* (1998) measured caspase-3 activity using 50 µM of caspase-3/7 (Ac-DEVD-AMC) substrate.

Nagase *et al*. (2002) determined caspase-3, -8 and -9 activity using 100 µM AMC conjugated caspase substrates and Doyle *et al*. (2002) measured caspase-3 and -9 activity using 20 mM of AMC conjugated caspase substrates. In this study it was found that 50 µM AMC conjugated caspase substrate was sufficient to obtain adequate RFU readings (section 3.1.3.2 B). It was also found that RFU increased as substrate concentration was increased. This could be due to increased caspase activity, since more substrate is available for proteolytic cleavage, and also because the substrate on its own fluoresced (section 3.1.3.3).

4.2.3.6 Caspase assay controls

To understand the roles of the various assay components in generating RFU, controls that consisted of heat inactivated lysates, lysates only (no caspase substrate), caspase substrate with reaction buffer only, caspase substrate only, reaction buffer only and cell lysis buffer only were performed.

Cell lysates were heat inactivated to denature proteins and induce loss of enzymatic function. Although the heat inactivation was not specific for caspase inhibition, it was only a basic method to determine enzyme activity. Heat inactivated controls could therefore verify whether the RFU values obtained for non-heat inactivated samples were due to enzyme (caspase) activity or some non-specific fluorescence signal. Since the heat inactivated samples had significantly lower RFU values, compared to the non-heat inactivated samples, it indicated that the RFU values obtained were in fact due to enzyme (caspase) activity (section 3.1.3.3).

It was found that the caspase-3 substrate (only) auto-fluoresced (section 3.1.3.3). This fluorescence signal was, however, reduced by the addition of reaction buffer, which contained dithiothreitol (DTT). The cell lysis buffer and reaction buffer did not auto-fluoresce. The reaction buffer consisted mainly of PIPES (1,4-piperazinediethanesulfonic acid) and the cell lysis buffer mainly of HEPES (N-(2-hydroxyethyl)piperazine-N'-(2- ethanesulfonic acid)), both of which contain sulphur groups. DTT maintains sulfhydryl (-SH) groups in the reduced state and reduces disulfide (-S-S-) groups (Cleland, 1964). Therefore, the buffers, together with DTT,

maintained a reduced environment, which quenched the caspase substrates and thus minimised auto-fluorescence.

AMC alone produced a significant fluorescence signal in the presence of reaction buffer and DTT (AMC standards in section 3.1.3.4). However, the caspase substrates, which are short peptide sequences covalently bonded to AMC, did not fluoresce to such an extent in the presence of reaction buffer and DTT (fluorescence was quenched). The caspase substrates therefore only produced a significant fluorescence signal (in the presence of reaction buffer and DTT) once AMC was cleaved from the AMC-peptide bond by an active caspase. Therefore, the increase in fluorescence intensity, which was measured in RFU, occurred as a result of the cleavage of AMC molecules due to caspase activity. AMC was therefore the reporter molecule for caspase activity (Anaspec, 2007).

4.2.3.7 Caspase assay for all caspase substrates

The reliability of the caspase assays for all caspase substrates were confirmed with BFA treated cell lysates, to determine if the appropriate caspases were activated upon induction of the ER-stress induced apoptotic pathway (section 3.1.3.5). It was found that BFA treatment induced an increase in caspase-3 and -4 activity only. This indicated that the ER-stress induced apoptosis pathway was activated after BFA treatment, since caspase-4 is specific to that pathway. Caspase-3 is an executioner caspase that is common to all three pathways, during the late stages of apoptosis. The experiment therefore established that the caspase assay could be performed, using all four caspase substrates, for all three apoptosis pathways after pathway-specific drug treatment.

4.2.3.8 Use of alternative protein extraction buffer for caspase assay

Caspase assays using RIPA buffer for protein extraction, instead of cell lysis buffer, were performed to determine if one extraction buffer (RIPA), and therefore one protein sample, could be used for both western blot analysis and caspase assays. Zapata *et al.* (1998) successfully used RIPA buffer lysates for their caspase assays, therefore it was important to establish if it could be reproduced in this study.

A linear increase in caspase activity, with increasing protein concentrations, was also obtained for the RIPA buffer lysates (section 3.1.3.6). However, the RIPA buffer lysates produced lower amounts of AMC release (caspase activity) compared to the cell lysis buffer lysates. Since it was also necessary to include protease inhibitors in the extraction buffer for the western blot analysis, it was therefore not practical to use RIPA buffer for the caspase assays.

4.2.4 Cytochrome *c* release immunohistochemistry assays

Cytochrome *c* release is a key event in the transmission of the death signal via the mitochondrial-mediated apoptotic pathway (as discussed in section 1.5.3). The aims of the cytochrome *c* immunohistochemistry assays were to visualize cytochrome *c* release via fluorescent microscopy, after intracellular labelling with cytochrome *c* (6H2)–PE antibody.

A great deal of difficulty was experienced with the labelling protocols in terms of detecting a fluorescence signal for the cytochrome *c* (6H2)–PE labelled cells. Furthermore, the fluorescent microscope did not reach a higher magnification than 40x and often at higher exposure times (greater than 1 s) the picture resolution was poor and it was difficult to visualize the cells. At lower exposure times (less than 833 ms) it was often difficult to see the labelled cells and it was increasingly difficult to maintain focus on the cells at higher exposure times. Due to these constraints, the finer detail, such as the individually labelled mitochondria (with cytochrome *c* (6H2)–PE antibody) and cytochrome *c* release into the cytoplasm, could not be visualized. It could not be clearly distinguished (even at 40x magnification) whether the labelled cytochrome *c* molecules were inside the mitochondria (punctated staining pattern) or released into the cytoplasm (diffuse staining pattern), since the entire cell would fluoresce red (PE).

To improve visibility and to assist in locating the cells, the samples were mounted with VECTASHIELD® mounting medium containing DAPI, which stained the cells' nuclei blue. In addition, different methods for fixation, as well as cell membrane permeabilization, were also performed, however, no significant difference was found between the two methods or permeabilized and non-permeabilized cells (sections 3.1.4.2 and 3.1.4.4).

Various other studies have successfully established cytochrome *c* release using fixation and permeabilization methods to label their cells. Goebel *et al.* (2001) fixed and permeabilized HL60 cells before labelling with mouse anti–cytochrome *c* monoclonal antibody. Their specimen was labelled with secondary Cy3-conjugated F(ab')2 fragments donkey anti-mouse IgG antibody to visualize cytochrome *c* release. Tehranchi *et al.* (2003) fixed and permeabilized hematopoietic stem cells before labelling the cells, first with anti–cytochrome *c* antibody and then with secondary FITC–conjugated goat anti–mouse antibody. Dror (2003) fixed and permeabilized marrow cells and lymphoblasts before labeling with monoclonal anti-cytochrome c antibody sheep anti-human antibody. A secondary FITC-conjugated rabbit-anti-sheep IgG antibody was also used to visualize cytochrome *c* release. However, Hirpara *et al.* (2000) used methanol and acetone fixation only, without permeabilization, to label their M14 melanoma cells with monoclonal anti-cytochrome *c* antibody. They also labelled their samples with secondary anti-mouse FITC-conjugated IgG antibody to analyse cytochrome *c* release.

These studies successfully labelled cytochrome *c* molecules and were able to visualise cytochrome *c* release. Cytochrome *c* that was released into the cytoplasm was seen as diffuse staining, whereas cytochrome *c* contained within the mitochondria produced a punctated staining pattern. These studies used unconjugated cytochrome *c* antibody and incubated with secondary Cy3 or FITC–conjugated antibody to obtain a fluorescence signal for cytochrome *c* molecules. In contrast, the cytochrome *c* antibody used in this study was already conjugated with PE (section 2.5.2). Perhaps the fluorescence signal would have been enhanced and/or visualisation of cytochrome *c* molecules better if an unconjugated antibody for cytochrome *c* was used together with a fluorochrome-conjugated secondary antibody.

Since the different immunohistochemistry assay protocol (used by the Cardiovascular Research Unit, section 3.1.4.7) could not be reproduced successfully, it was decided to abandon the cytochrome *c* release immunohistochemistry assay. Instead, it was decided to focus on changes in mitochondrial transmembrane potential, before and after drug treatment, using flow cytometry.

4.2.5 Detection of changes in mitochondrial transmembrane potential (MTP) during apoptosis induction

The changes in MTP of cells, upon induction of apoptosis, play an important role in the initiation of cytochrome *c* release (as discussed in section 1.5.2). These changes were examined using MitoCapture^{TM} labelling and flow cytometry analysis (section 3.1.5).

It was found that the majority of untreated cells fluoresced red, thus indicating that most of the MitoCapture^{TM} dye was taken up by the mitochondria and existed in its aggregated state. Therefore, the majority of untreated cells had mitochondria with unaltered/normal transmembrane potential. In comparison, the majority of drug-treated cells fluoresced green, indicating that most of the MitoCapture^{TM} dye was present in the cytoplasm, in its monomer form. The majority of drug-treated cells therefore had mitochondria with disrupted transmembrane potential. Other studies also found that cells with normal/unaltered MTP fluoresced red, whereas disruption of MTP (e.g. after induction of apoptosis) resulted in green fluorescence (Piccoli *et al.*, 2004; Lugli *et al*., 2005; Chaoui *et al.*, 2006).

It was also observed that a certain percentage of cells, untreated and drug-treated, fluoresced orange-yellow. This indicated that these cells contained some mitochondria with normal/unaltered MTP, as well as mitochondria with disrupted MTP. As a result, a transitional (intermediate) fluorescent signal between red and green was generated. These cells therefore presented with an intermediated MTP. Lugli *et al.* (2005) also found this phenomenon in HL60 cells. They found that the cells with an intermediate MTP were positive for AV labelling, however, most did not label with PI and were therefore considered to be early apoptotic. Since ATP is required for the formation of the apoptosome, it was proposed that these cells continued to produce ATP for caspase-9 activation, given that most of their mitochondrial membranes were still intact. Given the differences in MTP (normal and/or disrupted) of the mitochondria in these intermediate cells, it also indicated that different cells (untreated and drug-treated) were in different stages of apoptosis. The MitoCapture^{TM} results therefore gave an idea of the apoptotic status (non-apoptosing, intermediate or apoptosing) of the cells. These results can also be compared and used in conjunction with the AV/PI results to determine the stages of apoptosis within a cell population (Lugli *et al.*, 2005).

4.3 Final experiments to analyse all three apoptotic pathways

Large volumes of cells were treated with drug (either BFA, H_2O_2 or FasL) at the low and high doses to induce approximately 5-15% (low) and 20-50% (high) early apoptosis, as determined in section 3.1.1.3. From each batch of cells (untreated, low and high drug doses), cells were taken for AV/PI and MitoCapture^{TM} labelling and flow analysis, as well as protein extraction. The cells were subsequently analysed for apoptotic response to drug treatment (AV/PI labelling), changes in MTP (MitoCapture^{TM} labelling), activation of pathway-specific caspases and changes in Bip, CHOP and FADD expression via western blot analysis. These experiments were repeated for each drug (low and high dose) to compare results for each technique and determine if the results were sensitive and reproducible and if the cell models were reliable.

It was also important to determine which markers were activated (for each pathway) at the untreated, low and high drug doses. This would establish the apoptotic status of the cells and determine how the markers are regulated and/or activated under different levels of apoptosis induction. In addition, it was important to determine if each marker was specific to its pathway or if there was cross talk between the pathways.

4.3.1 BFA treatment experiments and ER-stress induced apoptosis pathway

The % early apoptosis induced by the 30 μg/ml BFA treated cells (passage number 11-13) of the first experiment was very low, compared to previous results obtained from cells with passage number 14-16 (section 3.1.1.3 A). The experiments were repeated, however, after numerous repeats (with cells at passage number 11-29) there was no significant increase in apoptosis induced (section 3.2.1). Leglise *et al.* (1988) have found that HL60 cells that were maintained in culture for a long time (3-18 months) underwent phenotypic drift and developed drug resistance. The cells in this study were maintained in culture for approximately 1-3 months. Therefore, the cells could have developed drug resistance, since Leglise *et al.* (1988) also found that the cells lost the promyelocytic phenotype within less than one month of culturing.

The HL60 cells of this study were classified via May-Grünwald-Giemsa staining and identified as being a single population of predominantly undifferentiated promyelocytes (section 3.1.1.2). However, these cells were freshly thawed and at passage number 8 (without culturing) when they were classified. Therefore, the cells maintained in culture could have undergone changes in phenotype, which could have contributed to drug resistance. The passage number of the cells in the second BFA experiment (passage 16-19). and the drug-optimisation experiments (section 3.1.1.3 A) were similar. However, the passage number of the cells treated with BFA in the first experiment was lower by comparison. Therefore, it is not clear whether these cells did in fact undergo phenotypic changes during culturing, however, the results suggested that the cells had become more resistant to apoptose after BFA treatment.

Results of both BFA experiments (section 3.2.1) indicated that a large population of BFA treated cells (low and high doses), which did not label with high AV (low PI) (% cells in area G4) did, however, have disrupted MTP. Since the majority of untreated (control) cells fluoresced red (normal/unaltered MTP), it indicated that the MitoCapture^{TM} assay was indeed reflecting changes in MTP after drug treatment (section 3.2.4). It can therefore be assumed that some BFA (low and high dose) treated cells had disrupted MTP but were negative for AV/PI labelling. This indicated that these cells did not have phosphatidylserine exposure (AV positive) and/or cell membrane lysis (PI positive) yet. It therefore appears that MTP disruption is an earlier event in the apoptosis pathway than phosphatidylserine exposure (positive AV labelling). This was also observed by Chaoui *et al*. (2006). They found that the average level of apoptotic cells were higher when measured via JC-1 (similar to MitoCapture^{TM}) than with AV/PI labelling. They proposed that this was due to the fact that changes in MTP (measured via JC-1 labelling) precede phosphatidylserine exposure (detected via AV labelling).

The BFA treated cells of the first experiment had a higher percentage of cells with intermediate MTP, compared to the second experiment. Since there was no significant amount of caspase-9 activity detected for both BFA experiments (section 3.2.3.1), it appears that these cells (with intermediate MTP) were not required for ATP production and apoptosome formation (for caspase-9 activation) as proposed by Lugli *et al*. (2005).

However, these cells could be in different stages of apoptosis, containing varying amounts of mitochondria with both normal and disrupted MTP (Lugli *et al*., 2005).

The MitoCapture^{TM} results indicated that there was interaction between the ER-stress induced and mitochondrial-mediated apoptosis pathways (and both can function simultaneously) at the level of the mitochondria, since BFA treatment induced changes in MTP. This is in accordance with other researchers' findings, which showed that activation of pro-apoptotic proteins, Bax and Bak, results in the transmission of the apoptotic signal from the ER to the mitochondria, where the death signal is amplified (Hacki *et al.,* 2000; Zong *et al.,* 2003). Wlodkowic *et al*. (2007) also found that BFA-induced cell death in the HF1A3, HF4.9 and HF28RA human follicular lymphoma cell lines was associated with ER stress, mitochondrial rupture and subsequent activation of the caspase cascade.

Disruption of MTP can lead to eventual rupture of the mitochondria and the subsequent release of pro-apoptotic molecules (such as cytochrome *c*) into the cytoplasm. Cytochrome *c* release results in caspase-9 activation via the apoptosome (Acehan *et al*., 2002). However, since no significant amount of caspase-9 activity was detected for both BFA experiments (at low and high concentrations), it could be assumed that the apoptosome pathway was not activated in this instance. Furthermore, the lack of caspase-9 activity also indicated that the BFA treated cells did not follow the entire mitochondrial-mediated apoptosis pathway to its end point of caspase-9 activation.

BFA treatment (both concentrations) induced mainly caspase-3 and -4 activity. The 5 μg/ml BFA treated cells of both experiments had lower caspase-4 and -3 activity compared to the 30 μg/ml BFA treated cells. This indicated that the cells treated with the lower drug dose, were still in the earlier stages of the apoptosis pathway with lower caspase activity, preceding the activation of the caspase cascade. Since caspase-3 and -4 activity was higher for the 30 μg/ml BFA treated cells (of both experiments), it indicated that the caspase cascade was activated via the ER-stress induced apoptosis pathway (caspase-4 activation). The high levels of caspase-3 activity also indicated that these cells were in the late stages of apoptosis with subsequent activation of executioner caspases, such as caspase-3. Hitomi *et al*. (2004) also found that caspase-4 is activated

in human cells during periods of severe or prolonged ER stress, followed by activation of downstream caspases, like caspase-3. However, the group of caspases linked or activated upon ER stress-induced apoptosis has not yet been fully elucidated (Rao *et al.*, 2002 a).

Very low levels of caspase-8 activity were detected for the BFA treated cells (of both experiments) (section 3.2.3.1). This was in contrast to the findings of Hu *et al.* (2006). They found that caspase-8 also mediates ER-stress induced apoptosis, since inhibition of caspase-8 activity was found to significantly decrease or prevent apoptosis induced by the ER stress inducers, thapsigargin and tunicamycin. They also found that inhibition of caspase-4 activity did not, however, prevent caspase-8 activity (and apoptosis induced by thapsigargin and tunicamycin). Hu *et al.* (2006) therefore proposed that caspase-4 and -8 are involved in separate apoptotic signalling pathways in response to ER stress. However, since no significant increase in caspase-8 activity was observed after BFA treatment (ER stress) in this present study, it could indicate that the caspase-4 mediated apoptotic pathway was induced rather than the caspase-8 mediated pathway. Furthermore, FADD protein levels (section 3.2.2) were also significantly low or not present at all after BFA treatment (both high and low concentrations). The lack of FADD protein expression and caspase-8 activity therefore indicated that there was no or limited death receptor pathway activity after BFA treatment.

Bip protein expression was upregulated after BFA treatment, at both high and low concentrations. The increase in Bip protein expression indicated that the UPR was activated and the cells were experiencing ER-stress after BFA treatment. Other studies have also found that Bip expression increases upon ER stress to prevent accumulation of misfolded proteins, since it acts as a chaperone by binding unfolded or misfolded proteins (Kozutsumi *et al.*, 1988; Dorner *et al.*, 1989; Flynn *et al.*, 1991).

4.3.2 H_2O_2 treatment experiments and mitochondrial-mediated apoptosis pathway

For both H_2O_2 experiments (high and low H_2O_2 concentrations), the percentage of cells with disrupted MTP was higher than the percentage of cells positive for AV/PI labelling (% early apoptosis induced). Since the majority of untreated (control) cells fluoresced red (normal MTP), it indicated that the MitoCapture^{TM} assay was successful and

reflected changes in MTP after H_2O_2 treatment (section 3.2.4). Therefore the cell population, which had disrupted MTP but were negative for AV/PI labelling, did not have phosphatidylserine exposure yet. Disruption of MTP therefore preceded phosphatidylserine exposure (positive AV labelling) (Chaoui *et al*., 2006). This was also found for the BFA treated cells (section 4.3.1).

Since the caspase activity was lower than expected for the H_2O_2 treated cells (of both experiments), it was determined if any residual H_2O_2 in the cell lysates could inhibit caspase activity. It was found that the addition of H_2O_2 significantly reduced caspase-3 activity (section 3.2.3.3). This could therefore account for the lower and varied (increased standard deviation) caspase activity obtained for the H_2O_2 experiments, compared to the BFA controls and experiments.

Both H_2O_2 experiments indicated that caspase-3 and -9 activity increased after H_2O_2 treatment (low and high concentrations). Furthermore, it was found that caspase-3 and -9 activity was higher for the 1 mM H_2O_2 treated cells, compared to the 0.4 mM H_2O_2 treated cells (of both H_2O_2 experiments). This indicated that the cells treated with 1 mM H_2O_2 were in the late stages of apoptosis with resultant activation of the caspase cascade and executioner caspases, like caspase-3. These results were in accordance with DiPietrantonio *et al*. (1999), who also found that caspase-3 was activated in HL60 cells after treatment with H_2O_2. Since caspase-9 was activated for all H_2O_2 treated cells, it indicated that the cells were undergoing apoptosis via the mitochondrial-mediated apoptotic pathway. Other studies have also found that caspase-9 is activated upon induction of the mitochondrial-mediated apoptosis pathway, after activation of the apoptosome pathway (Li, P *et al*., 1997; Zou *et al*., 1997; Cain *et al*., 1999).

There was no significant increase in caspase-8 activity observed for both H_2O_2 experiments (at low and high concentrations). Similarly, Dumont *et al*. (1999) found that H_2O_2 treatment of T-cells induced caspase-3 activation, however, it did not induce activation of caspase-8. In the same experiments they also found that H_2O_2 treatment induced changes in MTP, which lead to the release of cytochrome *c*. Moreover, FADD protein levels (section 3.2.2) were also significantly low or not present at all after H_2O_2 treatment (both low and high concentrations). This, and since no significant amount of caspase-8 activity was detected, indicated that the death receptor pathway was not

activated after treatment with H_2O_2. Similarly, Dumont *et al.* (1999) found that the CD95 (Fas) death receptor pathway was not required for H_2O_2-induced apoptosis. They also found that caspase-8 was only activated by CD95/Fas ligation (and formation of the death-inducing signalling complex, as described in section 1.3) and not by H_2O_2 treatment.

The results of the two H_2O_2 experiments, in particular the MitoCapture^{TM} and caspase assays, indicated that mainly the mitochondrial-mediated apoptosis pathway was activated after treatment with H_2O_2. However, the western blot analysis showed that Bip protein expression was upregulated after treatment with H_2O_2 (at both low and high doses) (section 3.2.2). This indicated that the UPR, and possibly the ER-stress induced apoptosis pathway, was activated and H_2O_2 treatment caused some extent of ER-stress in HL60 cells. However, caspase-4 activity did not increase after H_2O_2 treatment demonstrating that the ER-stress induced apoptosis pathway was not activated to the extent of ER-caspase activation.

4.3.3 FasL treatment experiments and death receptor apoptosis pathway

The percentage of cells with disrupted MTP was lower than the percentage of cells positive for AV/PI labelling (% early apoptosis induced) for both FasL experiments (low and high FasL concentrations). Since the majority of untreated (control) cells fluoresced red (normal MTP), it indicated that the MitoCapture^{TM} assays reflected accurate changes in MTP after FasL treatment. Therefore, the FasL treated cells had phosphatidylserine exposure and loss of cell membrane asymmetry, without corresponding changes in MTP. Only some of the cells that had phosphatidylserine exposure (early apoptotic) also had disrupted MTP. Furthermore, the majority of cells treated with FasL (low and high dose of both experiments) fluoresced red (normal MTP), indicating that most of these cells did not undergo apoptosis via the mitochondrial-mediated apoptotic pathway. These cells may have bypassed the mitochondrial pathway and perhaps directly induced cell death via DISC formation, caspase-8 activation and subsequent activation of the caspase cascade. However, Jurkat cells are Type II cells and therefore rely on amplification of the death signal by the mitochondria (Scaffidi *et al.*, 1999). Therefore, perhaps there was simultaneous

activation of the death receptor and mitochondrial-mediated apoptotic pathways in FasL treated Jurkat cells.

FasL treatment, for both experiments, induced caspase-8 activity, indicating that the death receptor apoptotic pathway was activated. Moreover, caspase-8 activity was significantly higher for 0.4 ng/ml FasL treated cells, compared to 0.2 ng/ml FasL, indicating that these cells were in the later stages of apoptosis. However, no significant amount of caspase-3 activity was detected after FasL treatment for both experiments. Therefore, it appeared that these cells were not in the advanced stages of apoptosis, with subsequent activation of executioner caspases, like caspase-3. Since Jurkat cells are Type II cells, the activation of the caspase cascade is significantly delayed because the cells rely on amplification of the apoptotic signal by the mitochondria (Scaffidi *et al.*, 1998). Therefore, the shorter exposure time to FasL (4 hrs), compared to the longer exposure time of the other drugs (24 hrs), could have been insufficient to allow for caspase-3 activity, either directly or via the mitochondrial-mediated apoptosis pathway (Type II cells).

Low levels of caspase-9 activity were detected after treatment with 0.2 ng/ml FasL only (for both experiments), indicating that the mitochondrial-mediated apoptosis pathway was activated to some extent. However, no significant amount of caspase-9 activity was observed for the 0.4 ng/ml FasL treated cells of both experiments. Furthermore, no caspase-4 was detected for all FasL treated cells (both experiments), indicating that the ER-stress induced apoptosis pathway was not activated to the extent of caspase activation. This was in accordance with the western blot analysis, which showed that Bip protein levels were significantly low after FasL treatment (low and high concentrations) in both experiments, compared to the other drugs.

The western blot analysis also showed that the untreated Jurkat cells had significantly high levels of FADD protein, compared to the HL60 cells. Furthermore, FADD protein levels remained more or less unchanged after treatment with FasL (low and high concentrations) in both experiments. This could indicate that the death receptor pathway was activated, since FADD protein was present (in high levels) and recruited, upon induction of apoptosis, rather than upregulated. Hennio *et al.* (2000) found that high levels of FADD and procaspase-8 are constitutively expressed in virgin B cells. They

also found that FADD and procaspase-8 were not significantly upregulated after induction of death receptor-mediated apoptosis. Since the untreated HL60 cells contained significantly lower (or no) levels of FADD (compared to the untreated Jurkat cells), it could perhaps explain why the HL60 cells also had reduced sensitivity to apoptose after treatment with FasL (section 3.1.1.3 C).

4.4 Comparison of apoptotic markers between pathways

The MitoCapture^{TM} assays indicated that all drugs (BFA, H_2O_2 and FasL) induced changes in the MTP of the treated cells. This demonstrated that the mitochondrial-mediated apoptotic pathway was involved, to some extent, in all three apoptosis pathways. The changes in MTP were greatest for cells treated with BFA and H_2O_2, compared to the FasL treated cells, since the majority of BFA and H_2O_2 treated cells had disrupted MTP. Since HL60 and Jurkat cells are both Type II cells, it can be concluded that the mitochondria play important roles in relaying and amplifying the apoptotic signal, for all three pathways (Scaffidi *et al*., 1998).

The results of the caspase activity assays indicated that the caspases were specifically activated for each pathway and caspase activity was higher for cells treated with the higher drug concentrations, for all three pathways.

The western blot analysis for β-actin, Bip and FADD were successful. However, non-specific bands, as well as a high background signal were detected with the CHOP western blot analysis and therefore densitometric data could not be acquired for CHOP. Guérardel *et al*. (2005) performed a western blot analysis on untreated and tunicamycin treated RIN-1027-B2 cells and also detected a multiple band pattern for CHOP. To determine which band was CHOP, they compared untreated cells with tunicamycin treated cells, which enhanced CHOP expression. They found that a 27 kDa band increased in intensity after tunicamycin treatment and concluded that this was CHOP. The bands obtained for the CHOP western blot analysis in this present investigation (section 3.2.2) were, however, indistinct and amidst a high background signal. Therefore, a clear increase or decrease in band intensity, after BFA treatment, could not be determined. The CHOP western blot analysis could therefore not be used to determine induction of the ER-stress induced apoptosis pathway after BFA treatment.

Bip protein expression was upregulated after treatment with BFA and H_2O_2, at both high and low drug concentrations. This indicated that there was some interaction between the ER-stress induced and mitochondrial-mediated apoptosis pathways. Furthermore, H_2O_2 can possibly induce ER stress, which results in the apoptotic signal being transmitted to the mitochondria, in addition to acting directly to induce the mitochondrial-mediated apoptosis pathway. CHOP, JNK and the Bcl-2 family of proteins regulate both the ER-stress induced- and mitochondrial-mediated apoptosis pathways. Therefore, the apoptotic signal can be passed on from the ER to the mitochondria (Hacki *et al.*, 2000; Boya *et al.*, 2002). There was no significant increase in Bip protein expression for the FasL treated cells. In addition, FADD protein levels were significantly lower (or absent) in BFA and H_2O_2 treated cells, compared to FasL treated cells. However, this could be due to the lower FADD levels observed in the untreated HL60 cells, compared to the Jurkat cells (untreated and FasL-treated). Since FADD protein levels were significantly higher in the Jurkat cells, it appears that these cells contained the necessary levels of FADD protein required for apoptosis via the death receptor pathway. It therefore appears that FADD is recruited rather than upregulated, since FADD protein levels remained relatively unchanged after treatment with FasL, after induction of the death receptor pathway.

4.5 Conclusions and future investigations

BFA treatment mainly activated the ER-stress induced apoptosis pathway with subsequent activation of caspase-4 and upregulation of Bip. Treatment with H_2O_2 mainly induced the mitochondrial-mediated apoptosis pathway with subsequent activation of caspase-9 and induction of changes in MTP, as well as upregulation of Bip. FasL treatment mainly activated the death receptor pathway with subsequent activation of caspase-8.

The results indicated that the flow cytometry assays were reproducible and sensitive to detect changes within the cells after induction of apoptosis with drug treatment. The apoptotic status of the cells could be determined using both AV/PI and MitoCapture^{TM} assays. The MitoCapture^{TM} results demonstrated that the mitochondria play important roles in apoptosis signalling after all three drug treatments. All three pathways

interacted with the mitochondrial-mediated apoptosis pathway, as demonstrated by the MitoCapture^{TM} results, therefore indicating that it was not pathway specific.

The western blot assays were not quantitatively reproducible for each experiment and not as sensitive as preferred, since a large amount of protein was required. Furthermore, Bip protein expression was increased after treatment with BFA and H_2O_2, therefore indicating that it was not a pathway-specific marker. Since FADD protein levels remained relatively unchanged after FasL treatment, it would not be suitable as a marker to indicate induction of the death receptor pathway.

The caspase activity assays were sensitive, reproducible and pathway specific. Caspase activity could therefore be used to determine pathway-specific induction, with different caspases to differentiate which pathways were activated. H_2O_2 treatment, however, appeared to inhibit some caspase activity and was therefore not ideal. Perhaps another inducer/drug could be used to induce the mitochondrial-mediated apoptosis pathway, in future studies.

This work provides a useful insight into the apoptosis pathways in the two cell lines studied. Future studies could include monitoring the three apoptosis pathways in CD34+ progenitors and establishing which pathway-specific markers are best suited for analysis in these cells. Eventually, apoptosis induction in individual cell types of bone marrow stroma (both normal and MDS) could be analysed to determine which apoptosis pathways are affected in MDS. This knowledge would assist in the diagnosis and treatment of MDS.

REFERENCES

Abcam® (2008) Western blotting tips. http://www.abcam.com/index.html?pageconfig=resource&rid=11352 http://www.abcam.com/ps/pdf/protocols/abcam_troubleshooting_tips_WB.pdf (last visited website on: 21/10/09) (website updated: 2009).

Acehan, D., Jiang, X., Morgan, D.G., Heuser, J.E., Wang, X., Akey, C.W. (2002) Three-dimensional structure of the apoptosome: implications for assembly, procaspase-9 binding and activation. *Mol Cell* **9**(2): 423-432.

Adler, H.T., Chinery, R., Wu, D.Y., Kussick, S.J., Payne, J.M., Fornace, A.J., Tkachuk, D.C. (1999) Leukemic HRX fusion proteins inhibit GADD34-induced apoptosis and associate with the GADD34 and hSNF5/INI1 proteins. *Mol Cell Biol* **19**: 7050–7060.

Alnemri, E.S., Livingston, D.J., Nicholson, D.W., Salvesen, G., Thornberry, N.A., Wong, W.W., Yuan, J. (1996) Human ICE/CED-3 protease nomenclature. *Cell* **87**: 171.

Anaspec (2007) Enzolyte™ AMC Caspase profiling Kit information sheet. http://search.cosmobio.co.jp/cosmo_search_p/search_gate2/docs/ASI_/71120.20060124.pdf (last visited on: 21/10/2009).

Annexin V-FITC Apoptosis detection kit, Beckman Coulter PN IM3546 http://www.bc-cytometry.com/DataSheetPDF/IM3546.pdf (last visited on: 21/10/2009).

Antonsson, B., Conti, F., Ciavatta, A., Montessuit, S., Lewis, S., Martinou, I., Bernasconi, L., Bernard, A., Mermod, J.J., Mazzei, G., Maundrell, K., Gambale, F., Sadoul, R., Martinou, J.C. (1997) Inhibition of Bax channel-forming activity by Bcl-2. *Science* **277**: 370-372.

Ashkenazi, A., Dixit, V. M. (1998) Death receptors: Signaling and modulation. *Science* **281**: 1305-1308.

ATCC protocol for HL60 cell line (ATCC: Cell Biology Collection, 2007) http://www.atcc.org/ATCCAdvancedCatalogSearch/ProductDetails/tabid/452/Default.aspx?ATCCNum=CCL-240&Template=cellBiology (last visited website on: 21/10/2009) (website last updated: 2009).

ATCC protocol for Jurkat, clone E6-1 cell line (ATCC: Cell Biology Collection, 2007) http://www.atcc.org/ATCCAdvancedCatalogSearch/ProductDetails/tabid/452/Default.aspx?ATCCNum=TIB-152&Template=cellBiology (last visited website on: 21/10/2009) (website last updated: 2009).

Banner, D.W., D'Arcy, A., Janes, W., Gentz, R., Schoenfeld, H-J., Broger, C., Loetscher, H., Lesslauer, W. (1993) Crystal structure of the soluble human 55 kd TNF receptor-human TNFβ complex: implication for TNF receptor activation. *Cell* **73**(3): 431-445.

Barnhart, B.C., Alappat, E.C., Peter, M.E. (2003) The CD95 Type I/Type II model. *Sem Immunol*, *15*, 185-193.

Bassik, M.C., Scorrano, L., Oakes, S.A., Pozzan, T., Korsmeyer, S.J. (2004) Phosphorylation of BCL-2 regulates ER Ca^{2+} homeostasis and apoptosis. *EMBO J* **23**: 1207–1216.

Bauer, M.K., Schubert, A., Rocks, O., Grimm, S. (1999) Adenine nucleotide translocase-1, a component of the permeability transition pore, can dominantly induce apoptosis. *J Cell Biol* **147**(7): 1493-502.

Berg, J.M., Tymoczko, J.L., Stryer, L. (editors) (2002) Biochemistry, 5th edition. W.H. Freeman and Company, USA.

Bernardi, P., Petronilli, V. (1996) The permeability transition pore as a mitochondrial calcium release channel: a critical appraisal. *J Bioenerg Biomembr* **28**: 131-138.

Bertolotti, A., Zhang, Y., Hendershot, L.M., Harding, H.P., Ron, D. (2000) Dynamic interaction of BiP and ER stress transducers in the unfolded-protein response. *Nat Cell Biol* 2(6): 326-332.

Beutler, B., Cerami, A. (1986) Cachectin and tumour necrosis factor as two sides of the same biological coin. *Nature* **320**: 584-588.

Beutner, G., Ruck, A., Riede, B., Brdiczka, D. (1998) Complexes between porin, hexokinase, mitochondrial creatine kinase and adenylate translocator display properties of the permeability transition pore. Implication for regulation of permeability transition by the kinases. *Biochim Biophys Acta* **1368**(1): 7-18.

Boldin, M.P., Goncharov, T.M., Goltsev, Y.V., Wallach, D. (1996) Involvement of MACH, a novel MORT1/FADD-interacting protease, in Fas/APO-1- and TNF receptor-induced cell death. *Cell* **85**: 803-815.

Borner, C. (2003) The Bcl-2 protein family: sensors and checkpoints for life-or-death decisions. *Mol Immunol* **39**(11): 615-47.

Boya, P., Cohen, I., Zamzami, N., Vieira, H.L., Kroemer, G. (2002) Endoplasmic reticulum stress-induced cell death requires mitochondrial membrane permeabilization. *Cell Death Differ* **9:** 465–467.

Bras, M., Queenan, B., Susin, S.A. (2005) Programmed cell death via mitochondria: Different modes of dying. *Biochemistry (Moscow)* **70**(2): 231-239.

Bredesen, D.E., Rao, R.V., Mehlen, P. (2006) Cell death in the nervous system. *Nature* **443**: 796-802.

Brewer, J.W., Cleveland, J.L., Hendershot, L.M. (1997) A pathway distinct from the mammalian unfolded protein response regulates expression of endoplasmic reticulum chaperones in non-stressed cells. *EMBO J* **16**(23): 7207-7216.

Brush, M.H., Weiser, D.C., Shenolikar, S. (2003) Growth arrest and DNA damage-inducible protein GADD34 targets protein phosphatase 1 alpha to the endoplasmic reticulum and promotes dephosphorylation of the alpha unit of eukaryotic translation initiation factor 2. *Mol Cell Biol* **23**(4): 1292-1303.

Budihardjo, I., Oliver, H., Lutter, M., Luo, X., Wang, X. (1999) Biochemical pathways of caspase activation during apoptosis. *Annu Rev Cell Dev Biol* **15**: 269–290.

Cain, K., Bratton, S.B., Langlais, C., Walker, G., Brown, D.G., Sun, X-M., Cohen, G.M. (2000) Apaf-1 oligomerizes into biologically active approximately 700-kDa and inactive approximately 1. 4-MDa apoptosome complexes. *J Biol Chem* **275**: 6067–6070.

Cain, K., Brown, D.G., Langlais, C., Cohen, G. M. (1999) Caspase activation involves the formation of the aposome, a large (approximately 700 kDa) caspase-activating complex. *J Biol Chem* **274**: 22686–22692.

Cardier, J.E., Erickson-Miller, C.L. (2002) Fas (CD95)- and Tumor Necrosis Factor-mediated apoptosis in liver endothelial cells: Role of caspase-3 and the p38 MAPK. *Microvas Res* **63**: 10-18.

Carlson, S.G., Fawcett, T.W., Bartlett, J.D., Bernier, M., Holbrook, N.J. (1993) Regulation of the C/EBP-related gene gadd153 by glucose deprivation. *Mol Cell Biol* **13**: 4736-4744.

Chang, S.C., Erwin, A.E., Lee, A.S. (1989) Glucose-regulated protein (GRP94 and GRP78) genes share common regulatory domains and are co-ordinately regulated by common trans-acting factors. *Mol Cell Biol* **13**: 4736-4744.

Chaoui, D., Faussat, A., Majdak, P., Tang, R., Perrot, J., Pasco, S., Klein, C., Marie, J., Legrand, O. (2006) JC-1, a sensitive probe for a simultaneous detection of P-glycoprotein activity and apoptosis in leukemic cells. *Cytometry Part B (Clinical Cytometry)* **70B**: 189–196.

Chowdhury, I., Tharakan, B., Bhat, G.K. (2008) Caspases – An update. *Comp Biochem Physiol Part B: Biochem Mol Biol* **151**(1): 10-27.

Cleland, W. W. (1964) Dithiothreitol, a new protective reagent for SH groups. *Biochemistry* **3**(4): 480-482.

Cohen, G.M. (1997) Caspases: The executioners of apoptosis. *Biochem J* **326**: 1-6.

Connor, J.H., Weiser, D.C., Li, S., Hallenbeck, J.M., Shenolikar, S. (2001) Growth arrest and DNA damage-inducible protein GADD34 assembles a novel signalling complex containing protein phosphatase 1 and inhibitor 1. *Mol Cell Biol* **21**(20): 6841-6850.

Cory, S., Adams, J.M. (2002) The Bcl2 family: regulators of the cellular life-or-death switch. *Nat Rev Cancer* **2**(9): 647-56.

Crompton, M. (1999) The mitochondrial permeability transition pore and its role in cell death. *Biochem. J*. **341**(2): 233–249.

Cullinan, S.B., Diehl, J.A. (2006) Coordination of ER and oxidative stress signalling: The PERK/Nrf2 signaling pathway. *Int J Biochem Cell Biol* **38**: 317-332.

Dalton, W.T., Ahearn, M.J., McCredie, K.B., Freireich, E.J., Stass, S.A., Trujillo, J.M. (1988) HL-60 cell line was derived from a patient with FAB-M2 and not FAB-M3. *Blood* **71**(1): 242-247.

Deveraux, Q. L., Takahashi, R., Salvesen, G. S., Reed, J. C. (1997) X-linked IAP is a direct inhibitor of cell-death proteases. *Nature* **388**: 300–304.

Dhein, J., Daniel, P.T., Trauth, B.C., Oehm, A., Moller, P., Krammer, P.H. (1992) Induction of apoptosis by monoclonal antibody anti-APO-1 class switch variants is dependent on cross-linking of APO-1 cell surface antigens. *J Immunol* **149**: 3166-3173.

DiPietrantonio, A.M., Hsieh, T., Wu, J.M. (1999) Activation of caspase 3 in HL-60 cells exposed to hydrogen peroxide. *Biochem Biophys Res Comm* **255**: 477-482.

Dorner, A.J., Wasley, L.C., Bole, D.G., Kaufman, R.J. (1989) Increased synthesis of secreted proteins induces expression of glucose regulated proteins in butyrate treated CHO cells. *J Biol Chem* **264**: 20602-20607.

Doyle, A., Griffiths, J.B., Newell, D.G. (1998) Cell and Tissue culture: Laboratory procedures. Part 4 C: 1.1-1.7. John Wiley and Sons, Ltd., USA.

Doyle, B.T., O'Neill, A.J., Newsholme, P., Fitzpatrick, J.M., Watson, R.W.G. (2002) The loss of IAP expression during HL-60 cell differentiation is caspase-dependent. *J Leukocyte Biol* **71**: 247-254.

Dror, Y. (2003) The role of mitochondrial-mediated apoptosis in a myelodysplastic syndrome secondary to congenital deletion of the short arm of chromosome 4. *Exp Hematol* **31**: 211-217.

Du, C., Fang, M., Li, Y., Li, L., Wang, X. (2000) Smac, a mitochondrial protein that promotes cytochrome c-dependent caspase activation by eliminating IAP inhibition. *Cell* **102**: 33–42.

Dumont, A., Hehner, S.P., Hofmann, T.G., Ueffing, M., Dröge, W., Schmitz, M.L (1999) Hydrogen peroxide-induced apoptosis is CD95-independent, requires the release of mitochondria-derived reactive oxygen species and the activation of NFκ-B. *Oncogene* **18**: 747-757.

Earnshaw, W.C., Martins, L.M., Kaufmann, S.H. (1999) Mammalian caspases: structure, activation, substrates, and functions during apoptosis. *Annu Rev Biochem* **68**: 383–424.

Ebbing, D.D. (1996) General chemistry (5th edition). Houghton Mifflin Company, USA.

Faris, M., Kokot, N., Latinis, K., Kasibhatla, S., Green, D.R., Koretzky, G.A., Nel, A. (1998) The c-Jun N-terminal kinase cascade plays a role in stress-induced apoptosis in Jurkat cells by up-regulating Fas ligand expression. *J Immunol* **160**(1): 134-144.

Fischer, H., Koenig, U., Eckhart, L., Tschachler, E. (2002) Human caspase 12 has acquired deleterious mutations. *Biochem Biophys Res Commun* **293**: 722-726.

Flynn, G.C., Pohl, J., Flocco, M.T., Rothman, J.E. (1991) Peptide-binding specificity of the molecular chaperone BiP. *Nature* **353**: 726-730.

Forman, M.S., Lee, V.M., Trojanowski, J.Q. (2003) 'Unfolding' pathways in neurodegenerative disease. *Trends Neurosci* **26**(8): 407-410.

Gallagher, R., Collins, S., Trujillo, J., McCredie, K., Ahearn, M., Tsai, S., Metzgar, R., Aulakh, G., Ting, R., Ruscetti, F., Gallo, R. (1979) Characterization of the continuous differentiating myeloid cell line (HL-60) from a patient with acute promyelocytic leukemia. *Blood* **54**(3): 713-733.

Gaut, J.R., Hendershot, L.M. (1993) The modification and assembly of proteins in the endoplasmic reticulum. *Curr Opin Cell Biol* **5**: 589–595.

Gewies, A. (2003) ApoReview-Introduction to apoptosis. 1-26. http://www.celldeath.de/encyclo/aporev/apointro.pdf or http://www.ihcworld.com/_books/apointro.pdf (last visited on: 02/02/09).

Giorgi, C., De Stefani, D., Bononi, A., Rizzuto, R., Pinton, P. (2009) Structural and functional link between the mitochondrial network and the endoplasmic reticulum. *Int J Biochem Cell Biol* **41**(10): 1817-1827.

Goebel, S., Gross, U., Lüder, C.G.K. (2001) Inhibition of host cell apoptosis by *Toxoplasma gondii* is accompanied by reduced activation of the caspase cascade and alterations of poly(ADP-ribose) polymerase expression. *J Cell Sci* **114**: 3495-3505.

Greenberg, P.L. (1998) Apoptosis and its role in the myelodysplastic syndromes: implications for disease natural history and treatment. *Leuk Res* **22**: 1123-1136.

Gross, A., McDonnell, J.M., Korsmeyer, S.J. (1999) BCL-2 family members and the mitochondria in apoptosis. *Genes Dev*. **13**: 1899–1911.

Guérardel, A., Barat-Houari, B., Vasseur, F., Dina, C., Vatin, V., Clément, K., Eberlé, D., Vasseur-Delannoy, V., Bell, C.G., Galan, P., Hercberg, S., Helbecque, N., Potoczna, N., Horber, F.F., Boutin, P., Froguel, P. (2005) Analysis of sequence variability in the *CART* gene in relation to obesity in a Caucasian population. *BMC Genetics* **6**:19 (doi:10.1186/1471-2156-6-19).

Guillemain, I., Exton, J.H. (1997) Effects of Brefeldin A on phosphatidylcholine phospholipase D and inositolphospholipid metabolism in HL-60 cells. *Eur J Biochem* **249**:812-819.

Haas, I.G., Wabl, M. (1983) Immunoglobulin heavy chain binding protein. *Nature* **306**: 387-389.

Hacki, J., Egger, L., Monney, L., Conus, S., Rosse, T., Fellay, I., Borner, C. (2000) Apoptotic crosstalk between the endoplasmic reticulum and mitochondria controlled by Bcl-2. *Oncogene* **19**: 2286–2295.

Harding, H.P., Calfon, M., Urano, F., Novoa, I., Ron, D. (2002) Transcriptional and translational control in the mammalian unfolded protein response. *Annu Rev Cell Dev Biol* **18**: 575–599.

Harding, H.P., Novoa, I., Zhang, Y., Zeng, H., Wek, R., Schapira, M., Ron, D. (2000 a) Regulated translation initiation controls stress-induced gene expression in mammalian cells. *Mol. Cell* **6**(5): 1099–1108.

Harding, H.P., Zhang, Y., Bertolotti, A., Zeng, H., Ron, D. (2000 b) Perk is essential for translational regulation and cell survival during the unfolded protein response. *Mol Cell* **5:** 897–904.

Harding, H.P., Zhang Y., Ron, D. (1999) Protein translation and folding are coupled by an endoplasmic-reticulum-resident kinase. *Nature* **397**(6716): 271-274.

Harding, H.P., Zhang Y., Zeng, H., Novoa, I., Lu, P.D., Calfon, M., Sadri, N., Yun, C., Popko, B., Paules, R., Stojdl, D.F., Bell, J.C., Hettmann, T., Leiden, J.M., Ron, D. (2003) An integrated stress response regulates amino acid metabolism and resistance to oxidative stress. *Mol Cell* **11**(3): 619–633.

Harris, M.H., Thompson, C.B. (2000) The role of the Bcl-2 family in the regulation of outer mitochondrial membrane permeability. *Cell Death Differ* **7**: 1182-1191.

Haze, K., Yoshida, H., Yanagi, H., Yura, T., Mori, K. (1999) Mammalian transcription factor ATF6 is synthesized as a transmembrane protein and activated by proteolysis in response to endoplasmic reticulum stress. *Mol Biol Cell* **10**(11): 3787-3799.

Hellström-Lindberg, E. (2005) Strategies for biology- and molecular-based treatment of Myelodysplastic syndromes. *Curr Drug Targets* **6**: 713-725.

Hengartner, M.O. (2000) The biochemistry of apoptosis. *Nature* **407**: 770-776.

Hennio, A., Berard, M., Casamayor-Pallejà, M., Krammer, P.H., Defrance, T. (2000) Regulation of the Fas death pathway by FLICE-Inhibitory protein in primary human B cells. *J Immunol* **165**: 3023-3030.

Higuchi, A., Shimmura, S., Takeuchi, T., Suematsu, M., Tsubota, K. (2006) Elucidation of apoptosis induced by serum deprivation in cultured conjunctival epithelial cells. *Br J Ophthalmol* **90**: 760-764.

Hirata, H., Takahashi, A., Kobayashi, S., Yonehara, S., Sawai, H., Okazaki, T., Yamamoto, K., Sasada, M. (1998) Caspases are activated in a branched protease cascade and control distinct downstream processes in Fas-induced apoptosis. *J Exp Med* **187**: 587-600.

Hirpara, J.L., Seyed, M.A., Loh, K.W., Dong, H., Kini, R.M., Pervaiz, S. (2000) Induction of mitochondrial permeability transition and cytochrome C release in the absence of caspase activation is insufficient for effective apoptosis in human leukemia cells. *Blood* **95**(5): 1773-1780.

Hitomi, J., Katayama, T., Eguchi, Y., Kudo, T., Taniguchi, M., Koyama, Y., Manabe, T., Yamagishi, S., Bando, Y., Imaizumi, K., Tsujimoto, Y., Tohyama, M. (2004) Involvement of caspase-4 in endoplasmic reticulum stress-induced apoptosis and Aβ – induced cell death. *J Cell Biol* **165**(3): 347-356.

Hosokawa, Y., Sakakura, Y., Tanaka, L., Okumura, K., Yajima, T., Kaneko, M. (2005) Radiation-induced apoptosis is dependent of caspase-8 but dependent on cytochrome c and the caspase-9 cascade in human leukemia HL60 cells. *J Radiat Res* **46**: 293-303.

Hu, P., Han, Z., Couvillion, A.D., Kaufman, R.J., Exton, J.H. (2006) Autocrine tumor necrosis factor alpha links endoplasmic reticulum stress to the membrane death receptor pathway through IRE1α-mediated NF-κB activation and down-regulation of TRAF2 expression. *Mol Cell Biol* **26**(8): 3071-3084.

Huang, D.C.S., Hahne, M., Schroeter, M., Frei, K., Fontana, A., Villunger, A., Newton, K., Tschopp, J., Strasser, A. (1999) Activation of Fas by FasL induces apoptosis by a mechanism that cannot be blocked by Bcl-2 or Bcl-x_L. *PNAS* **96**(26): 14871-14876.

Huang, H., Joazeiro, C.A., Bonfoco, E., Kamada, S., Leverson, J.D., Hunter, T. (2000) The inhibitor of apoptosis, cIAP2, functions as a ubiquitin-protein ligase and promotes in vitro monoubiquitination of caspases 3 and 7. *J Biol Chem* **275**(35): 26661-26664.

Huang, S-T., Yang, R-C., Chen, M-Y., Pang, J-H. S. (2004) *Phyllanthus urinaria* induces the Fas receptor/ligand expression and ceramide-mediated apoptosis in HL-60 cells. *Life Sciences* **75**: 339-351.

Huang, Y., Park, Y.C., Rich, R.L., Segal, D.., Myszka, DG., Wu, H. (2001) Structural basis of caspase inhibition by XIAP: differential roles of the linker versus the BIR domain. *Cell* **104**(5): 781-90.

Ichas, F., Jouaville, L.S., Mazat, J.P. (1997) Mitochondria are excitable organelles capable of generating and conveying electrical and calcium signals. *Cell* **89**(7): 1145-53.

Imaizumi, K., Miyoshi, K., Katayama, T., Yoneda, T., Taniguchi, M., Kudo, T., Tohyama, M. (2001) The unfolded protein response and Alzheimer's disease. *Biochim Biophys Acta* **1536**: 85-96.

Irmler, M., Thome, M., Hahne, M., Schneider, P., Hofmann, K., Steiner, V., Bodmer, J-L., Schröter, M., Burns, K., Mattmann, C., Rimoldi, D., French, L.E., Tschopp, J. (1997) Inhibition of death receptor signals by cellular FLIP. *Nature* **388**: 190-195.

Itoh, N., Nagata, S. (1993) A novel protein domain required for apoptosis: mutational analysis of human Fas antigen. *J Biol Chem* **268**: 10932-10937.

Itoh, N., Yonehara, S., Ishii, A., Yonehara, M., Mizushima, S., Sameshima, M., Hase, A., Seto, Y., Nagata, S. (1991) The polypeptide encoded by the cDNA for human cell surface antigen Fas can mediate apoptosis. *Cell* **66**: 233-243.

Juin, P., Pelletier, M., Oliver, L., Tremblais, K., Grégoire, M., Meflah, K., Vallette, F.M. (1998) Induction of a caspase-3-like activity by calcium in normal cytosolic extracts triggers nuclear apoptosis in a cell-free system. *J Biol Chem* **273**(28): 17559-17564.

Kantrow, S.P., Piantadosi, C.A. (1997) Release of cytochrome *c* from liver mitochondria during permeability transition. *Biochem Biophys Res Commun* **232**: 669-671.

Karki, P., Dahal, G.R., Park, I. (2007) Both dimerization and interdomain processing are essential for caspase-4 activation. *Biochem Biophys Res Comm* **356**: 1056-1061.

Kaufman, R.J. (2002) Orchestrating the unfolded protein response in health and disease. *J Clin Invest* **110:** 1389–1398.

Kayagaki, N., Kawasaki, A., Ebata, T., Ohmoto, H., Ikeda, S., Inoue, S., Yoshino, K., Okumura, K., Yagita, H. (1995) Metalloproteinase-mediated release of human Fas ligand. *J Exp Med* **182**(6): 1777-1783.

Kerr, J. F., Wyllie, A. H., Currie, A. R. (1972) Apoptosis: a basic biological phenomenon with wide-ranging implications in tissue kinetics. *Br J Cancer* **26**: 239-257.

Kim, Y-M., Chung, H-T., Kim, S-S., Han, J-A., Yoo, Y-M., Kim, K-M., Lee, G-H., Yun, H-Y, Green, A., Li, J., Simmons, R.L., Billiar, T.R. (1999) Nitric oxide protects PC12 cells from serum deprivation-induced apoptosis bt cGMP-dependent inhibition of caspase signalling. *J Neurosci* **19**(16): 6740-6747.

Kimball, S.R., Jefferson, L.S. (1992) Regulation of protein synthesis by modulation of intracellular calcium in rat liver. *Am J Physiol* **263**(5 Pt 1): E958-E964.

Kischkel, F.C., Hellbardt, S., Behrmann, I., Germer, M., Pawlita, M., Krammer, P.H., Peter, M.E. (1995) Cytotoxicity-dependent APO-1 (Fas/CD95)-associated proteins from a death-inducing signaling complex (DISC) with the receptor. *EMBO J* **14**: 5579-5588.

Köhler, C., Orrenius, S., Zhivotovsky, B. (2002) Evaluation of caspase activity in apoptotic cells. *J Immunol Met* **265**: 97-110.

Kozutsumi, Y., Segal, M., Normington, K., Gething, M.J., Sambrook, J. (1988) The presence of malfolded proteins in the endoplasmic reticulum signals the induction of glucose-regulated proteins. *Nature* **332**(6163): 462-464.

Krajewski, S., Tanaka, S., Takayama, S., Schibler, M.J., Fenton, W., Reed, J.C. (1993) Investigation of the subcellular distribution of the bcl-2 oncoprotein: residence in the nuclear envelope, endoplasmic reticulum, and outer mitochondrial membranes. *Cancer Res* **53**: 4701-4714.

Kroemer, G., Zamzami, N., Susin, S.A. (1997) Mitochondrial control of apoptosis. *Immunol Today* **18**(1): 44-51.

Kuwana, T., Mackey, M.R., Perkins, G., Ellisman, M.H., Latterich, M., Schneiter, R., Green, D.R., Newmeyer, D.D. (2002) Bid, Bax, and lipids cooperate to form supramolecular openings in the outer mitochondrial membrane. *Cell* **111**: 331–342.

Kuwana, T., Smith, J.J., Muzio, M., Dixit, V., Newmeyer, D.D., Kornbluth, S. (1998) Apoptosis induction by caspase-8 is amplifies through the mitochondrial release of cytochrome c. *J Biol Chem* **273**: 16589-16594.

Laemmli, U.K. (1970) Cleavage of structural proteins during the assembly of the head of bacteriophage T4. *Nature* **227**(5259): 680-685.

Lavrik, I.N., Mock, T., Golks, A., Hoffmann, J.C., Baumann, S., Krammer, P.H. (2008) CD95 stimulation results in the formation of a novel death effector domain protein-containing complex. *J Biol Chem* **283** (39): 26401–26408.

Lee, A.H., Iwakoshi, N.N., Glimcher, L.H. (2003) XBP-1 regulates a subset of endoplasmic reticulum resident chaperone genes in the unfolded protein response. *Mol Cell Biol* **23:** 7448–7459.

Lee, A.S. (1992) Mammalian stress response: induction of the glucose-regulated protein family. *Curr Opin Cell Biol* **4**: 267-273.

Leglise, M.C., Dent, G.A., Ayscue, L.H., Ross, D.W. (1988) Leukemic cell maturation: Phenotypic variability and oncogene expression in HL60 cells: a review. *Blood Cells* **13**: 319-337.

Lei, K., Davis, R.J. (2003) JNK phosphorylation of Bim-related members of the Bcl2 family induces Bax-dependent apoptosis. *Proc Natl Acad Sci USA* **100:** 2432–2437.

Leppa, S., Bohmann, D. (1999) Diverse functions of JNK signalling and c-Jun in stress response and apoptosis. *Oncogene* **18**: 6158-6162.

Li, H., Zhu, H., Xu, C.J., Yuan, J. (1998) Cleavage of BID by caspase 8 mediates the mitochondrial damage in the Fas pathway of apoptosis. *Cell* **94**: 491-501.

Li, J., Lee, B., Lee, A.S. (2006) Endoplasmic reticulum stress-induced apoptosis: multiple pathways and activation of p53-up-regulated modulator of apoptosis (PUMA) and NOXA by p53. *J Biol Chem* **281**(11): 7260-7270.

Li, L.Y., Luo, X., Wang, X. (2001) Endonuclease G is an apoptotic DNase when released from mitochondria. *Nature* **412**: 95-99.

Li, M., Baumeister, P., Roy, B., Phan, T., Foti, D., Luo, S., Lee, A.S. (2000) AFT6 as a transcription activator of the endoplasmic reticulum stress element: Thapsigargin stress-induced changes and synergistic interactions with NF-Y and YY1. *Mol Cell Biol* **20**(14): 5096-5106.

Li, P., Nijhawan, D., Budihardjo, I., Srinivasula, S.M., Ahmad, M., Alnemri, E.S., Wang, X. (1997) Cytochrome *c* and dATP-dependent formation of Apaf-1/caspase-9 complex initiates an apoptotic protease cascade. *Cell* **91**(4): 479–489.

Li, W.W., Hsiung, Y., Zhou, Y., Roy, B., Lee, A.S. (1997) Induction of the mammalian GRP78/BiP gene by Ca^{2+} depletion and formation of aberrant proteins: activation of the conserved stress-inducible grp core promoter element by the human nuclear factor YY1. *Mol Cell Biol* **17**: 54-60.

Li, W.W., Sistonen, L., Morimoto, R.I., Lee, A.S. (1994) Stress induction of the mammalian GRP78/BiP protein gene: *in vivo* genomic footprinting and identification of p70CORE from human nuclear extract as a DNA-binding component specific to the stress regulatory element. *Mol Cell Biol* **14**: 5533-5546.

Li, W., Wang, S., Chen, C., Zhuang, G. (2006) Induction of tumor cell apoptosis via Fas/DR5. *Cell & Mol Immunol* **3**(6): 467-471.

Liesveld, J.L., Jordan, C.T., Phillips, G.L. (2004) The hematopoietic stem cell in myelodysplasia. *Stem Cells* **22**: 590-599.

Liu, H., Bowes, R.C., van de Water, B., Sillence, C., Nagelkerke, J.F., Stevens, J.L. (1997) Endoplasmic reticulum chaperones GRP78 and calreticulin prevent oxidative stress, Ca2+ disturbances, and cell death in renal epithelial cells. *J Biol Chem* **272**(35): 21751-21759.

Liu, H., Chang, D.W., Yang, X. (2005) Interdimer processing and linearity of procaspase-3 activation. A unifying mechanism for the activation of initiator and effector caspases. *J Biol Chem* **280**(12): 11578–11582.

Liu, X., Kim, C.N., Yang, J., Jemmerson, R., Wang, X. (1996) Induction of apoptotic program in cell-free extracts: requirement for dATP and cytochrome c. *Cell* **86**: 147-157.

Liu, X-B., Masago, R., Kong, L., Zhang, B-X., Masago, S., Vela-Roch, N., Katz, M.S., Yeh, C-K., Zhang, G.H., Talal, N., Dang, H. (2000) G-protein signalling abnormalities mediated by CD95 in salivary epithelial cells. *Cell Death & Differentiation* **7**: 1119-1126.

Loeffler, M., Kroemer, G. (2000) The mitochondrion in cell death control: certainties and incognita. *Exp Cell Res* **256**: 19–26.

Lohret, T.A., Murphy, R.C., Drgoñ, T., Kinnally, K.W. (1996). Activity of the Mitochondrial Multiple Conductance Channel Is Independent of the Adenine Nucleotide Translocator. *J Biol Chem* **271**: 4846-4849.

Lugli, E., Troiano, L., Ferraresi, R., Roat, E., Prada, N., Nasi, M., Pinti, M., Cooper, E.L., Cossarizza, A. (2005) Characterization of cells with different mitochondrial membrane potential during apoptosis. *Cytometry Part A* **68A**: 28–35.

Luo, X., Budihardjo, I., Zou, H., Slaughter, C., Wang, X. (1998) Bid, a Bcl2 interacting protein, mediates cytochrome c release from mitochondria in response to activation of cell surface death receptors. *Cell* **94**: 481-490.

Ma, K., Vattem, K.M., Wek, R.C. (2002 a) Dimerization and release of molecular chaperone inhibition facilitate activation of eukaryotic initiation factor-2 kinase in response to endoplasmic reticulum stress. *J Biol Chem* **277**(21): 18728-18735.

Ma, Y., Brewer, J.W., Diehl, J.A., Hendershot, L.M. (2002 b) Two distinct stress signalling pathways converge upon the CHOP promoter during the mammalian unfolded protein response. *J Mol Biol* **318**(5): 1351-1365.

Ma, Y., Hendershot, L.M. (2003) Delineation of a negative feedback regulatory loop that controls protein translation during endoplasmic reticulum stress. *J Biol Chem* **278**(37): 34864-34873.

Marchetti, P., Castedo, M., Susin, S.A., Zamzami, N., Hirsch, T., Macho, A., Haeffner, A., Hirsch, F., Geuskens, M., Kroemer, G. (1996) Mitochondrial permeability transition is a central coordinating event of apoptosis. *J Exp Med* **184**: 1155-1160.

Marchetti, P., Decaudin, D., Macho, A., Zamzami, N., Hirsch, T., Susin, S.A., Kroemer, G. (1997) Redox regulation of apoptosis: impact of thiol oxidation status on mitochondrial function. *Eur J Immunol* **27**(1): 289-96.

Marciniak, S.J., Yun, C.Y., Oyadomari, S., Novoa, I., Zhang, Y., Jungreis, R., Nagata, K., Harding, H.P., Ron, D. (2004) CHOP induces death by promoting protein synthesis and oxidation in the stressed endoplasmic reticulum. *Genes Dev* **18**: 3066–3077.

Martin, D.A., Siegel, R.M., Zheng, L., Lenardo, M.J. (1998) Membrane oligomerization and cleavage activates the caspase-8 (FLICE/MACHalpha1) death signal. *J Biol Chem* **273**: 4345-4349.

Marzo, I., Brenner, C., Zamzami, N., Jürgensmeier, J.M., Susin, S.A., Vieira, H.L., Prévost, M.C., Xie, Z., Matsuyama, S., Reed, J.C., Kroemer, G. (1998) Bax and adenine nucleotide translocator cooperate in the mitochondrial control of apoptosis. *Science* **281**(5385): 2027-2031.

Mattes, M.J. (2007) Apoptosis assays with lymphoma cell lines: problems and pitfalls. *Br J Cancer* **96**(6): 928-936.

McCullough, K.D., Martindale, J.L., Klotz, L., Aw, T., Holbrook, N. (2001) Gadd153 sensitizes cells to endoplasmic reticulum stress by down-regulating Bcl2 and perturbing the cellular redox state. *Mol Cell Biol* **21**(4): 1249-1259.

Miller, L. K. (1999) An exegesis of IAPs: salvation and surprises from BIR motifs. *Trends Cell Biol* **9**: 323–328.

Miller, P.F., Hinnebusch, A.G. (1990) *cis*-Acting sequences involved in the translational control of GCN4 expression. *Biochim Biophys Acta* **1050**(1-3): 151-154.

Morishima, N., Nakanishi, K., Takenouchi, H., Shibata, T., Yasuhiko, Y. (2002) An endoplasmic reticulum stress-specific caspase cascade in apoptosis. Cytochrome c-independent activation of caspase-9 by caspase-12. *J Biol Chem* **277**: 34287–34294.

Morishima, N., Nakanishi, K., Tsuchiya, K., Shibata, T., Seiwa, E. (2004) Translocation of Bim to the endoplasmic reticulum (ER) mediates ER stress signaling for activation of caspase-12 during ER stress-induced apoptosis. *J Biol Chem* **279**: 50375–50381.

Muchmore, S.W., Sattler, M., Liang, H., Meadows, R.P., Harlan, J.E., Yoon, H.S., Nettesheim, D., Chang, B.S., Thompson, C.B., Wong, S.L., Ng, S.L., Fesik, S.W. (1996) X-ray and NMR structure of human Bcl-xL, an inhibitor of programmed cell death. *Nature* **381**: 335-341.

Mundle, S.D. (2003) Lingering biologic dilemmas about the status of the progenitor cells in myelodysplasia. *Arch Med Res* **34**: 515-519.

Munro, S., Pelham, H.R.B. (1986) An Hsp 70-like protein in the ER: Identity with the 78 Kd glucose-regulated protein and immunoglobulin heavy chain binding protein. *Cell* **46**: 291-300.

Muzio, M., Stockwell, B. R., Stennicke, H. R., Salvesen, G. S., Dixit, V. M. (1998) An induced proximity model for caspase-8 activation. *J Biol Chem* **273,** 2926–2930.

Nagase, M., Shiota, T., Tsushima, A., Alam, M.M., Fukuoka, S., Yoshizawa, T., Sakato, N. (2002) Molecular mechanisms of satratoxin-induced apoptosis in HL-60 cells: activation of caspase –8 and caspase-9 is involved in activation of caspase-3. *Immunol Lett* **84**: 23-27.

Nagata, S. (1999) Fas Ligand-induced apoptosis. *Annu Rev Genet* **33**: 29-55.

Nakagawa, T., Yuan, J. (2000) Cross-talk between two cysteine protease families: Activation of caspase-12 by calpain in apoptosis. *J Cell Biol* **150**(4): 887-894.

Nakagawa, T., Zhu, H., Morishima, N., Li, E., Xu, J., Yankner, B.A., Yuan, J. (2000) Caspase-12 mediates endoplasmic-reticulum-specific apoptosis and cytotoxicity by amyloid-beta. *Nature* **403**(6765): 98–103.

Nicholson, D.W., Thornberry, N.A. (1997) Caspases: killer proteases. *Trends Biochem Sci* **22**: 299-306.

Nishitoh, H., Matsuzawa, A., Tobiume, K., Saegusa, K., Takeda, K., Inoue, K., Hori, S., Kakizuka, A., Ichijo, H. (2002) ASK1 is essential for endoplasmic reticulum stress-induced neuronal cell death triggered by expanded polyglutamine repeats. *Genes Dev* **16**: 1345-1355.

Nishitoh, H., Saitoh, M., Mochida, Y., Takeda, K., Nakano, H., Rothe, M., Miyazono, K., Ichijo, H. (1998) ASK1 is essential for JNK/SAPK activation by TRAF2. *Mol Cell* **2**: 389–395.

Novoa, I., Zeng, H., Harding, H.P., Ron, D. (2001) Feedback inhibition of the unfolded protein response by GADD34-mediated dephosphorylation of eIF2alpha. *J Cell Biol* **153**(5): 1011-1022.

Ohoka, N., Yoshii, S., Hattori, T., Onozaki, K., Hayashi, H. (2005) TRB3, a novel ER stress-inducible gene, is induced via ATF4–CHOP pathway and is involved in cell death. *EMBO J* **24**: 1243–1255.

Okada, T., Yoshida, H., Akazawa, R., Negishi, M., Mori, K. (2002) Distinct roles of activating transcription factor 6 (ATF6) and double-stranded RNA-activated protein kinase-like endoplasmic reticulum kinase (PERK) in transcription during the mammalian unfolded protein response. *Biochem J* **366**(Pt. 2): 585-594.

Old, L.J. (1985) Tumor necrosis factor (TNF). *Science* **230**(4726): 630-632.

Oono, K., Yoneda, T., Manabe, T., Yamagishi, S., Matsuda, S., Hitomi, J., Miyata, S., Mizuno, T., Imaizumi, K., Katayama, T., Tohyama, M. (2004) JAB1 participates in unfolded protein responses by association and dissociation with IRE1. *Neurochem Int* **45**: 765–772.

Oshimi, Y., Oda, S., Honda, Y., Nagata, S., Miyazaki, S. (1996) Involvement of Fas ligand- and Fas-mediated pathway in the cytotoxicity of human natural killer cells. *J Immunol* **157**: 2909-2915.

Oyadomari, S., Koizumi, A., Takeda, K., Gotoh, T., Akira, S., Araki, E., Mori, M. (2002) Targeted disruption of the Chop gene delays endoplasmic reticulum stress-mediated diabetes. *J Clin Invest* **109**: 525–532.

Pae, H.-O., Jeong, S.-O., Jeong, G.-S., Kim, K.M., Kim, H.S., Kim, S.-A., Kim,Y.-C., Kang, S.-D., Kim, B.-N., Chung, H.-T. (2007) Curcumin induces pro-apoptotic endoplasmic reticulum stress in human leukemia HL60 cells. *Biochem Biophys Res Comm* **353**: 1040-1045.

Parker, J.E. Mufti, G.J., Rasool, F., Mijovic, A., Devereux, S., Pagliuca, A. (2000) The role of apoptosis, proliferation and the Bcl-2-related proteins in the myelodysplastic syndromes and acute myeloid leukemia secondary to MDS. *Blood* **96**: 3932-3938.

Petit, P.X., Goubern, M., Diolez, P., Susin, S.A., Zamzami, N., Kroemer, G. (1998) Disruption of the outer mitochondrial membrane as a result of large amplitude swelling: the impact of irreversible permeability transition. *FEBS Letters* **426**: 111-116.

Piccoli, C., Boffoli, D., Capitanio, N. (2004) Comparative analysis of mitochondria selective dyes in different cell types detected by confocal laser scanning microscopy: methods and applications. Formatex current issues on multidisciplinary microscopy research and education: 130-139.
http://www.formatex.org/microscopy2/papers/130-139.pdf
(last visited on 21/10/2009).

Pitti, R.M., Marsters, S.A., Lawrence, D.A., Roy, M., Kishkel, F.C., Dowd, P., Huang, A., Donahue, C.J., Sherwood, S.W., Baldwin, D.T., Godowski, P.J., Wood, W.I., Gurney, A.L., Hillan, K.J., Cohen, R.L., Goddard, A.D., Botstein, D., Ashkenazi, A. (1999) Genomic amplification of a decoy receptor for Fas ligand in lung and colon cancer. *Nature* **396**(6712): 699-703.

Proteus BioSciences Inc.© (2007) ZappaZyme™ Enzyme Activity Assay Protocol http://www.proteus-biosciences.com/Products/Enzyme-Activity-Assays.aspx (last visited website on: 22/10/2007).

Rao, L., Perez, D., White, E. (1996) Lamin proteolysis facilitates nuclear events during apoptosis. *J Cell Biol* **135**(6 Pt 1): 1441–1455.

Rao, R.V., Castro-Obregon, S., Frankowski, H., Schuler, M., Stoka, V., del Rio, G., Bredesen, D.E., Ellerby, H.M. (2002 a) Coupling endoplasmic reticulum stress to the cell death program. An Apaf-1-independent intrinsic pathway. *J Biol Chem* **277**: 21836–21842.

Rao, R.V., Hermel, E., Castro-Obregon, S., del Rio, G., Ellerby, L.M., Ellerby, H.M., Bredesen, D.E. (2001) Coupling endoplasmic reticulum stress to the cell death program: Mechanism of caspase activation. *J Biol Chem* **276**(36): 33869-33874.

Rao, R.V., Peel, A., Logvinova, A., del Rio, G., Hermel, E., Yokota, T., Goldsmith, P.C., Ellerby, L.M., Ellerby, H.M., Bredesen, D.E. (2002 b) Coupling endoplasmic reticulum stress to the cell death program: role of the ER chaperone GRP78. *FEBS letters* **514**: 122-128.

Ricci, J.E., Gottlieb, R.A., Green, D.R. (2003) Caspase-mediated loss of mitochondrial function and generation of reactive oxygen species during apoptosis. *J Cell Biol* **160**: 65-75.

Rodriguez, J., Lazebnik, Y. (1999) Caspase-9 and APAF-1 form an active holoenzyme. *Genes Dev*. **13**: 3179–3184.

Ron, D., Habener, J.F. (1992) CHOP, a novel developmentally regulated nuclear protein that dimerizes with transcription factors C/EBP and LAP and functions as a dominant-negative inhibitor of gene transcription. *Genes & Dev* **6**(3): 439-453.

Rosse, T., Olivier, R., Monney, L., Rager, M., Conus, S., Fellay, I., Jansen, B., Borner, C. (1998) Bcl-2 prolongs cell survival after Bax-induced release of cytochrome *c*. *Nature* **391**: 496-499.

Rovera, G., Santoli, D., Damsky, C. (1979) Human promyelocytic leukemia cells in culture differentiate into macrophage-like cells when treated with a phorbol diester. *Proc Natl Acad Sci USA* **76**(6): 2779-2783.

Salvesen, G. S., Dixit, V. M. (1999) Caspase activation: the induced-proximity model. *Proc Natl Acad Sci USA* **96**: 10964–10967.

Scaffidi, C., Fulda, S., Srinivasan, A., Friesen, C., Li, F., Tomaselli, K.J., Debatin, K., Krammer, P.H., Peter, M.E. (1998) Two CD95 (APO-1/Fas) signaling pathways. *EMBO J* **17**(6): 1675-1687.

Scaffidi, C., Schmitz, I., Zha, J., Korsmeyer, S.J., Krammer, P.H., Peter, M.E. (1999) Differential modulation of apoptosis sensitivity in CD95 Type I and Type II cells. *J Biol Chem* **274**(32): 22532-22538.

Schneider, P., Holler, N., Bodmer, J.L., Hahne, M., Frei, K., Fontana, A., Tschopp, J. (1998) Conversion of membrane-bound Fas (CD95) ligand to its soluble form is associated with downregulation of its proapoptotic activity and loss of liver toxicity. *J Exp Med* **187**(8): 1205-1213.

Schneider, U., Schwenk, H.U., Bornkamm, G. (1977) Characterization of EBV-genome negative "null" and "T" cell lines derived from children with acute lymphoblastic leukemia and leukemic transformed non-Hodgkin lymphoma. *Int J Cancer* **19**(5): 621-626.

Shao, R-G., Shimizu, T., Pommier, Y. (1996) Brefeldin A is a potent inducer of apoptosis in human cancer cells independently of p53. *Exp Cell Res* **227**: 190-196.

Shen, J., Prywes, R. (2005) ER stress signaling by regulated proteolysis of ATF6. *Methods* **35**: 382-389.

Shi, Y., Vattem, K.M., Sood, R., An, J., Liang, J., Stramm, L., Wek, R.C. (1998) Identification and characterization of pancreatic eukaryotic initiation factor-2alpha-subunit kinase, PEK, involved in translational control. *Mol Cell Biol* **18**(12): 7499-7509.

Shimizu, S., Narita, M., Tsujimoto, Y. (1999) Bcl-2 family proteins regulate the release of apoptogenic cytochrome *c* by the mitochondrial channel VDAC. *Nature* **399**: 483–487.

Shu, H.B., Halpin, D.R., Goeddel, D.V. (1997) Casper is a FADD- and caspase-related inducer of apoptosis. *Immunity* **6**(6): 751-763.

Sigma® - Aldrich (2008) Fas ligand set Technical bulletin. http://www.sigmaaldrich.com/sigma/bulletin/F4428bul.pdf (last visited on: 07/07/08).

Skommer, J., Wlodkowic, D., Deptala, A. (2007) Larger than life: Mitochondria and the Bcl-2 family. *Leuk Res* **31**: 277–286.

Slee, E.A., Harte, M.Y., Kluck, R.M., Wolf, B.B., Casiano, C.A., Newmeyer, D.D., Wang, H.G., Reed, J.C., Nicholson, D.W., Alnemri, E.S., Green, D.R., Martin, S.J. (1999) Ordering the Cytochrome c –initiated caspase cascade: Hierarchical activation of caspases-2, -3, -6, -7, -8, and –10 in a caspase-9-dependent manner. *J Cell Biol* **144**(2): 281-292.

Solomon, E.P., Berg, L.R., Martin, D.W. (editors) (1999) Biology, 5th edition. Saunders college publishing, USA.

Sommer, U., Costello, C.E., Hayes, G.R., Beach, D.H., Gilbert, O., Lucas, J.J., Singh, B.N. (2005) Identification of *Trichomonas vaginalis* cysteine proteases that induce apoptosis in human vaginal epithelial cells. *J Biol Chem* **280**(25): 23853-23860.

Sood, R., Porter, A.C., Ma, K., Quilliam, L.A., Wek, R.C. (2000) Pancreatic eukaryotic initiation factor-2alpha kinase (PEK) homologues in humans, *Drosophila melanogaster*

and *Caenorhabditis elegans* that mediate translational control in response to endoplasmic reticulum stress. *Biochem J* **346**(Pt 2): 281-293.

Srinivasula, S.M., Hegde, R., Saleh, A., Datta, P., Shiozaki, E., Chai, J., Lee, R.A., Robbins, P.D., Fernandes-Alnemri, T., Shi, Y., Alnemri, E.S. (2001) A conserved XIAP-interaction motif in caspase-9 and Smac/DIABLO regulates caspase activity and apoptosis. *Nature* **410**(6824): 112-6.

Stennicke, H. R., Deveraux, Q.L., Humke, E.W., Reed, J.C., Dixit, V.M., Salvesen, G.S. (1999) Caspase-9 can be activated without proteolytic processing. *J Biol Chem* **274**(13): 8359–8362.

Strasser, A., Harris, A., Huang, D., Kramer, P., Cory, S. (1995) Bcl-2 and Fas/APO-1 regulate distinct pathways to lymphocyte apoptosis. *EMBO J* **14**: 6136-6147.

Stroh, C., Schulze-Osthoff, K. (1998) Death by a thousand cuts: an ever increasing list of caspase substrates. *Cell Death Differ* **5**: 997-1000.

Suda, T., Hashimoto, H., Tanaka, M., Ochi, T., Nagata, S. (1997) Membrane Fas ligand kills human peripheral blood T lymphocytes, and soluble Fas ligand blocks the killing. *J Exp Med* **186**(12): 2045-2050.

Suda, T., Okazaki, T., Naito, Y., Yokota, T., Arai, N., Ozaki, S., Nakao, K., Nagata, S. (1995) Expression of the Fas ligand in T-cell-lineage. *J Immunol* **154**(8): 3806-3813.

Suda, T., Takahashi, T., Golstein, P., Nagata, S. (1993) Molecular cloning and expression of the Fas ligand: a novel member of the tumor necrosis factor family. *Cell* **75**: 1169-1178.

Susin, S.A., Lorenzo, H.K., Zamzami, N., Marzo, I., Snow, B.E., Brothers, G.M., Mangion, J., Jacotot, E., Costantini, P., Loeffler, M., Larochette, N., Goodlett, D.R., Aebersold, R., Siderovski, D.P., Penninger, J.M., Kroemer, G. (1999) Molecular characterization of mitochondrial apoptosis-inducing factor. *Nature* **397**(6718): 441-446.

Szegezdi, E., Logue, S.E., Gorman, A.M., Samali, A. (2006) Mediators of endoplasmic reticulum stress-induced apoptosis. *EMBO reports* **7**: 880-885.

Tanaka, M., Itai, T., Adachi, M., Nagata, S. (1998) Downregulation of Fas ligand by shedding. *Nat Med* **4**(1): 31-36.

Tanaka, M., Suda, T., Haze, K., Nakamura, N., Sato, K., Kimura, F., Motoyoshi, K., Mizuki, M., Tagawa, S., Ohga, S., Hatake, K., Drummond, A.H., Nagata, S. (1996) Fas ligand in human serum. *Nat Med* **2**(3): 317-322.

Takahashi, R., Deveraux, Q., Tamm, I., Welsh, K., Assa-Munt, N., Salvesen, G.S., Reed, J.C. (1998) A single BIR domain of XIAP sufficient for inhibiting caspases. *J Biol Chem* **273**(14): 7787-7790.

Takahashi, T., Tanaka, M., Ogasawara, J., Suda, T., Murakami, H., Nagata, S. (1996) Swapping between Fas and G-CSF receptor. *J Biol Chem* **271**: 17555-17560.

Tartaglia, L.A., Ayres, T.M., Wong, G.H.W., Goeddel, D.V. (1993) A novel domain within the 55 kd TNF receptor signals cell death. *Cell* **74**: 845-853.

Tehranchi, R., Fadeel, B., Forsblom, A., Christensson, B., Samuelsson, J., Zhivotovsky, B., Hellstrom-Lindberg, E. (2003) Granulocyte colony-stimulating factor inhibits spontaneous cytochrome c release and mitochondria-dependant apoptosis of MDS hematopoetic progenitors. *Blood* **101**:1080-1086.

Thornberry, N.A., Lazebnik, Y. (1998) Caspases: Enemies within. *Science* **281**: 1312-1316.

Thornberry, N. A., Rano, T.A., Peterson, E.P., Rasper, D.M., Timkey, T., Garcia-Calvo, M., Houtzager, V.M., Nordstrom, P.A., Roy, S., Vaillancourt, J.P., Chapman, K.T., Nicholson, D.W. (1997) A combinatorial approach defines specificities of members of the caspase family and granzyme B. Functional relationships established for key mediators of apoptosis. *J Biol Chem* **272**(9): 17907–17911.

Tirasphon, W., Welihinda, A.A., Kaufman, R.J. (1998) A stress response pathway from the endoplasmic reticulum to the nucleus requires a novel bifunctional protein kinase/endoribonuclease (Ire1p) in mammalian cells. *Genes Dev* **12**(12): 1812-1824.

Trauth, B.C., Klas, C., Peters, A.M., Matzku, S., Moller, P., Falk, W., Debatin, K.M., Krammer, P.H. (1989) Monoclonal antibody-mediated tumor regression by induction of apoptosis. *Science* **245**(4915): 301-305.

Trayner, I.D., Bustorff, T., Etches, A.E., Mufti, G.J., Foss, Y., Farzaneh, F. (1998) Changes in antigen expression on differentiating HL60 cells treated with dimethylsulphoxide, all-*trans* retinoic acid, α1,25-dihydroxyvitamin D_3 or 12-*O*-tetradecanoyl phorbol-13-acetate. *Leuk Res* **22**: 537-547.

Urano F, Wang X, Bertolotti A, Zhang Y, Chung P, Harding HP, Ron D (2000) Coupling of stress in the ER to activation of JNK protein kinases by transmembrane protein kinase IRE1. *Science* **287**: 664–666.

Uren, A.G., Coulson, E.J., Vaux, D.L. (1999) Conservation of baculovirus inhibitor of apoptosis repeat proteins (BIRPs) in viruses, nematodes, vertebrates and yeasts. *Trends Biochem Sci* **23**(5): 159–162.

van Huizen, R., Martindale, J.L., Gorospe, M., Holbrook, N.J. (2003) P58IPK, a novel endoplasmic reticulum stress-inducible protein and potential negative regulator of eIF2α signaling. *J Biol Chem* **278**: 15558–15564.

Vaux, D.L., Cory, S., Adams, J.M. (1988) Bcl-2 gene promotes haemopoietic cell survival and cooperates with c-myc to immortalize pre-B cells. *Nature* **335**(6189): 440-442.

Verhagen, A.M., Ekert, P.G., Pakusch, M., Silke, J., Connolly, L.M., Reid, G.E., Moritz, R.L., Simpson, R.J., Vaux, D.L. (2000) Identification of DIABLO, a mammalian protein that promotes apoptosis by binding to and antagonizing IAP proteins. *Cell* **102**(1): 43-53.

Verhagen, A.M., Silke, J., Ekert, P.G., Pakusch, M., Kaufmann, H., Connolly, L.M., Day, C.L., Tikoo, A., Burke, R., Wrobel, C., Moritz, R.L., Simpson, R.J., Vaux, D.L. (2002) HtrA2 promotes cell death through its serine protease activity and its ability to antagonize inhibitor of apoptosis proteins. *J Biol Chem* **277**(1): 445-454.

Wang, X.Z., Harding, H.P., Zhang, Y., Jolicoeur, E.M., Kuroda, M., Ron, D. (1998) Cloning of mammalian Ire1 reveals diversity in the ER stress responses. *EMBO J* **17**(19): 5708-5717.

Wang, X.Z., Lawson, B., Brewer, J.W., Zinszner, H., Sanjay, A., Mi, L.J., Boorstein, R., Kreibich, G., Hendershot, L.M., Ron, D. (1996) Signals from the stressed endoplasmic reticulum induce C/EBP-homologous protein (CHOP/GADD153). *Mol Cell Biol* **16**: 4273-4280.

Wei, M.C., Zong, W.X., Cheng, E.H., Lindsten, T., Panoutsakopoulou, V., Ross, A.J., Roth, K.A., MacGregor, G.R., Thompson, C.B., Korsmeyer, S.J. (2001) Proapoptotic BAX and BAK: a requisite gateway to mitochondrial dysfunction and death. *Science* **292**: 727–730.

Westermeier, R., Marouga, R. (2005) Protein detection methods in proteomics research. *Bioscience Reports* **25** (1/2): 19-32.

Willis, S.N., Adams, J.M. (2005) Life in the balance: how BH3-only proteins induce apoptosis. *Curr Opin Cell Biol* **17**: 617-625.

Wlodkowic. D., Skommer, J., Pelkonen, J. (2007) Brefeldin A triggers apoptosis associated with mitochondrial breach and enhances HA14-1- and anti-Fas-mediated cell killing in follicular lymphoma cells. *Leuk Res* **31**: 1687–1700.

Wu, J., Kaufman, R.J. (2006) From acute ER stress to physiological roles of the Unfolded Protein Response. *Cell Death Diff* **13**: 374-384.

Yan, W., Frank, C.L., Korth, M.J., Sopher, B.L., Novoa, I., Ron, D., Katze, M.G. (2002) Control of PERK eIF2α kinase activity by the endoplasmic reticulum stress-induced molecular chaperone P58IPK. *Proc Natl Acad Sci USA* **99**: 15920–15925.

Yang, X., Chang, H.Y., Baltimore, D. (1998) Autoproteolytic activation of procaspases by oligomerization. *Mol Cell* **1**: 319-325.

Yang, Y., Fang, S., Jensen, J.P., Weissman, A.M., Ashwell, J.D. (2000) Ubiquitin protein ligase activity of IAPs and their degradation in proteasomes in response to apoptotic stimuli. *Science* **288**(5467): 874-877.

Ye, J., Rawson, R.B., Komuro, R., Chen, X., Dave, U.P., Prywes, R., Brown, M.S., Goldstein, J.L. (2000) ER stress induces cleavage of membrane-bound ATF6 by the same proteases that process SREBPs. *Mol Cell* **6**: 1355-1364.

Yeh, W.C., Pompa, J.L., McCurrach, M.E., Shu, H.B., Elia, A.J., Shahinian, A., Ng, M., Wakeham, A., Khoo, W., Mitchell, K., El-Deiry, W.S., Lowe, S.W., Goeddel, D.V.,

Mak, T.W. (1998) FADD: essential for embryo development and signalling from some, but not all, inducers of apoptosis. *Science* **279**(5358): 1954-1958.

Yoneda, T., Imaizumi, K., Oono, K., Yui, D., Gomi, F., Katayama, T., Tohyama, M. (2001) Activation of caspase-12, an endoplasmic reticulum (ER) resident caspase, through Tumor Necrosis Factor Receptor-associated Factor-2-dependent mechanism in response to ER stress. *J Biol Chem* **276**(17): 13935-13940.

Yonehara, S., Ishii, A., Yonehara, M. (1989) A cell-killing monoclonal antibody (anti-Fas) to a cell surface antigen co-downregulated with the receptor of Tumor Necrosis Factor. *J Exp Med* **169**: 1747-1756.

Yoshida, H., Matsui, T., Yamamoto, A., Okada, T., Mori, K. (2001) XBP1 mRNA is induced by ATF6 and spliced by IRE1 in response to ER stress to produce a highly active transcription factor. *Cell* **107**: 881–891.

Zamzami, N., Susin, S.A., Marchetti, P., Hirsch, T., Gómez-Monterrey, I., Castedo, M., Kroemer, G. (1996) Mitochondrial control of nuclear apoptosis. *J Exp Med* **183**(4): 1533-1544.

Zapata, J.M., Takahasi, R., Salvesen, G.S., Reed, J.C. (1998) Granzyme release and caspase activation in activated human T-lymphocytes. *J Biol Chem* **273**(12): 6916-6920.

Zhang, J., Cado, D., Chen, A., Kabra, N.H., Winoto, A. (1998) Fas-mediated apoptosis and activation-induced T-cell proliferation are defective in mice lacking FADD/Mort1. *Nature* **392**: 296-300.

Zhang, X., Chen, Y., Jenkins, L.W., Kochanek, P.M., Clark, R.S.B. (2005) Bench-to-bedside review: Apoptosis/programmed cell death triggered by traumatic brain injury. *Critical Care* **9**: 66-75.

Zinszner, H., Kuroda, M., Wang, X., Batchvarova, N., Lightfoot, R.T., Remotti, H., Stevens, J.L., Ron, D. (1998) CHOP is implicated in programmed cell death in response to impaired function of the endoplasmic reticulum. *Genes Dev* **12**: 982-995.

Zong, W.X., Li, C., Hatzivassiliou, G., Lindsten, T., Yu, Q.C., Yuan, J., Thompson, C.B. (2003) Bax and Bak can localize to the endoplasmic reticulum to initiate apoptosis. *J Cell Biol* **162**: 59–69.

Zoratti, M., Szabò, I. (1995) The mitochondrial permeability transition. *Biochim Biophys Acta* **1241**(2): 139–176.

Zou, H., Henzel, W.J., Liu, X., Lutschg, A., Wang, X. (1997) Apaf-1, a human protein homologous to *C. elegans* CED-4, participates in cytochrome c-dependent activation of caspase-3. *Cell* **90**: 405–413.